

**Development of a Modular Recombinant  
Fungal toolkit for gene expression in  
*Ustilago maydis***



**Dissertation zur Erlangung des Doktorgrades**  
Der Mathematisch-Naturwissenschaftlichen Fakultät der  
Universität zu Köln

Vorgelegt von

**Dipl. Microbiologin Anna.I Hempel geb. Rybecky**

Argentinien

Köln, 2023



**Development of a Modular Recombinant  
Fungal toolkit for gene expression in  
*Ustilago maydis***

**Dissertation zur Erlangung des Doktorgrades**

Der Mathematisch-Naturwissenschaftlichen Fakultät der  
Universität zu Köln

Vorgelegt von

**Dipl. Microbiologin Anna.I Hempel geb. Rybecky**

Argentinien

Köln, 2023

Die Untersuchungen zur vorliegenden Arbeit wurden von März 2019 bis Januar 2023 am Lehrstuhl für Terrestrische Mikrobiologie an der Universität zu Köln unter der Betreuung von Herrn Prof. Dr. Gunther Doehlemann durchgeführt.

**Erstgutachter:** Prof. Dr. Gunther Doehlemann

**Zweitgutachter:** Prof. Dr. Stanislav Kopriva

**Tag der mündlichen Prüfung:** 06.12.2023

*Al andar se hace camino, y al volver la vista atrás se ve la senda que nunca se ha de volver a pisar. Caminante no hay camino, se hace camino al andar.*

*Wenn du gehst, bahnst du einen Weg, und wenn du zurückblickst, siehst du den Weg, den Du nie wieder beschreiten wirst. Wanderer, es gibt keinen Weg, der Weg entsteht durch Gehen.*

Cantares, Joan Manuel Serrat



## Summary

In recent years, the development of tools for manipulating gene expression has significantly advanced. These tools have been applied to model organisms, including mammalian cells, plants, bacteria, and fungi, to unravel complex cellular mechanisms and natural interactions.

This study focuses on the model organism *Ustilago maydis*, a biotrophic fungal plant pathogen that produces corn smut disease in maize (*Zea mays*). *U. maydis* is amenable to reverse genetic engineering, is easy to manipulate in laboratory conditions, has a sequenced genome and well-defined interactions with its host maize. One of the most relevant fields of research carried out in *U. maydis* is the study of its effector genes and their functions in virulence.

Various techniques have been used in *U. maydis* to functionally characterize its effector genes. However, there are still limitations due to their functional redundancy, or the indispensability of certain genes for the development of the disease, making knockout approaches ineffective.

In this study, new genetic tools to enhance recombinant gene expression in *U. maydis* are introduced. This dissertation describes a novel methodology called “Modular Recombinant Fungal toolkit for gene expression”, or “MoRFunG toolkit”, which leverages the Golden Gate and Molecular Cloning systems.

As a proof of concept, tailor-made transcript units were constructed and tested in *U. maydis*, to show the capacity of the technique to complement large genomic deletions. Additionally, steps towards standardization of the method were taken, in order to establish a group of promoters available to be used for differential gene expression during the infection process. Furthermore, experimental development was carried out to incorporate this system in the routinely cloning genetic locations already established and well-defined in *U. maydis*. Moreover, novel optogenetic tools were evaluated for potential implementation in *U. maydis* as a methodology to control the expression of effector genes.

Thusly, this study summarizes a series of experiments that serve to introduce a new high throughput cloning methodology, allowing systematic, user-friendly, and time-saving options for the manipulation of gene expression in the *U. maydis* system.

## List of Abbreviations

AG	Arbeitsgemeinschaft
Approx.	Approximately
ATP	Adenosine triphosphate
Bp	Base pair
BR	Biological replicate
°C	Degree Celsius
C	Complementation
Carb	Carbenicillin
Cbx	Carboxin
cDNA	Complementary DNA
CFP	Cyan fluorescent proteins
CRISPR	Clustered regularly interspaced short palindromic repeats
Ct	Cycle threshold
ddH <sub>2</sub> O	Double distilled water
DNA	Deoxyribonucleic acid
dNTP	Deoxynucleoside triphosphates
DMSO	Dimethylsulfoxid
Dpi	Days post infection
EDTA	Ethylenediaminetetraacetic acid



EtOH	Ethanol
FAO	Food and Agriculture Organization of the United Nations
Fig.	Figure
FLuc	F Luciferin
G	Gram
GFP	Green fluorescent protein
Hpi	Hours post inoculation
HCL	Hydrogen chloride
Ip	Iron-sulphur protein subunit of succinate dehydrogenase
Kan	Kanamycin
Kb	Kilobase
kDa	Kilo Dalton
KO	Knockout
LOV	Light oxygen voltage
MegNs	Meganucleases
mM	Micro molar
MgCl <sub>2</sub> .	Magnesium chloride
Min	Minute (s)
ml	Milliliter
MoClo	Molecular cloning

## List of abbreviations

mRNA	Messenger RNA
N°	Number
N	Nucleotide
NaCl	Sodium chloride
NaOH	Sodium hydroxide
NaPO <sub>4</sub>	Trisodium phosphate
Ng	Nanogram
Nm	Nanometre(s)
NosT	Nos terminator
O/N	Over night
OD	Optical density
ORF	Open reading frame
PAM	Protospacer adjacent motif
PAMP	Pathogen-associated molecular pattern
P <sub>CONS</sub>	Constitutive promoter
PCR	Polymerase chain reaction
PD	Potato dextrose
PDA	Potato dextrose agar
PEG	Polyethylenglycol
Pep1	Protein essential during penetration 1
pH	Potential of hydrogen

Pit2	Protein involved in tumor 2
pL0M	Plasmid level 0 module
pL1M	Plasmid level 1 module
pL2M	Plasmid level 2 module
P <sub>MIN</sub>	Minimal promoter
PU	Promoter and untranslated region
Prof.	Professor
qRT-PCR	Quantitative real-time polymerase chain reaction
RNA	Ribonucleic acid
RNA-seq	Ribonucleic acid sequencing
Rpm	Rounds per minute
RT	Room temperature
S	Seconds
See1	Seedling efficient effector 1
sgRNA	Single guide ribonucleic acid
SLIC	Sequence and Ligation Independent Cloning
Spp	Species
TAE	Tris-acetate + Na <sub>2</sub> -EDTA
TALENs	Transcription activator like effector nuclease
Tin2	Tumor inducing 2
TU	Terminator and untranslated regions

## List of abbreviations

Tpm	Transcripts per million
v/v	Volume/Volume
w/v	Weight/Volume
x g	Gravitational acceleration on earth (9.81m/s <sup>2</sup> )
μg	Microgram
μl	Microliter
μm	Micrometer
μM	Micromolar
ZFNs	Zink Finger Nucleases

## Table of content

<b>1</b>	<b>Introduction .....</b>	<b>1</b>
1.1	Synthetic biology .....	1
1.2	Manipulation of gene expression .....	1
1.2.1	Reverse genetics: the CRISPR-Cas system.....	2
1.2.2	Golden Gate and Molecular cloning .....	3
1.3	Synthetic Biology and model organisms.....	4
1.4	Fungal plant pathogens and their way of interaction with their host .....	4
1.5	<i>Ustilago maydis</i> as a model organism.....	6
1.6	<i>Ustilago maydis</i> as a plant pathogen.....	6
1.6.1	Effector genes .....	8
1.6.2	Approaches to functional characterize <i>Ustilago maydis</i> effector genes.....	10
1.7	Optogenetics as a tool for gene manipulation in <i>Ustilago maydis</i> .....	11
1.8	Objectives of this study.....	12
<b>2</b>	<b>Results.....</b>	<b>13</b>
2.1	Set up of the MoRFunG toolkit in <i>Ustilago maydis</i> .....	13
2.1.1	<i>Ustilago maydis</i> cluster 6A deletion and its impact on virulence .....	13
2.1.2	<i>Ustilago maydis</i> cluster 6A two steps complementation.....	16
2.1.3	Gene expression in the MoRFunG cluster 6A .....	19
2.2	Elucidation of relevant genes within the cluster 6A using the MoRFunG toolkit.....	21
2.2.1	Cluster 6A of <i>Ustilago maydis</i> : single and multiple gene knockouts .....	21
2.2.2	Identification of relevant genes within the virulence cluster 6A of <i>Ustilago maydis</i> using the MoRFunG toolkit.....	25
2.3	Endogenous promoters from <i>Ustilago maydis</i> included in the MoRFunG toolkit.....	28
2.3.1	Evaluation of endogenous promoter's activity in ectopic simultaneous multi-gene integration without insertion of resistance cassettes.....	31
2.3.2	Multi-tag ectopic integration.....	33
2.3.3	MoRFunG mediated $\Delta pep1$ combined complementation .....	37
2.4	New technologies for manipulation of gene expression, applied to <i>Ustilago maydis</i> .....	43
2.4.1	Optogenetics blue-on and blue-off systems in <i>Ustilago maydis</i> strains.....	44
2.4.2	Stable light regulated <i>see1FLuc</i> expression and secretion of the See1FLuc complex in absence of the host.....	44
2.4.3	<i>Ustilago maydis</i> optogenetic fungal strains and the maintenance of the biotrophic interaction with its host.....	46
2.4.4	Natural light exposure of maize leaves does not inadvertently affect the optogenetic light-regulated expression of <i>see1</i> in <i>U. maydis</i> during the infection process.....	47

<b>3</b>	<b>Discussion .....</b>	<b>49</b>
3.1	Proof of concept: the use of MoRFunG toolkit in <i>Ustilago maydis</i> and its ability to functionally complement large genomic deletions .....	49
3.2	Functional gene redundancy within the cluster 6A of <i>Ustilago maydis</i> , and the role of MoRFunG toolkit .....	51
3.3	MoRFunG's exchangeable modules, tailor-made transcript units and their activity in <i>Ustilago maydis</i> .....	55
3.3.1	Characterization of endogenous promoters using reporter genes: Multi-tag ectopic integration with the MoRFunG toolkit.....	55
3.3.2	<i>Ustilago maydis</i> $\Delta pep1$ tailored complementation using the MoRFunG toolkit .....	56
3.4	New technologies for gene expression and gene manipulation applied to <i>Ustilago maydis</i> .....	59
3.5	Overview and future perspectives.....	60
<b>4</b>	<b>Materials and methodologies.....</b>	<b>63</b>
4.1	Materials and suppliers .....	63
4.1.1	Chemicals, media components, and additional materials.....	63
4.1.2	Sterilization for buffers and solutions .....	63
4.1.3	Enzymes, antibiotics, and markers.....	63
4.2	Commercial kits .....	64
4.3	Media and growing conditions.....	65
4.3.1	Media for <i>Escherichia coli</i> .....	65
4.3.2	Cultivation of <i>Escherichia coli</i> .....	65
4.3.3	Media for <i>Ustilago maydis</i> .....	65
4.3.4	Cultivation of <i>Ustilago maydis</i> .....	66
4.3.5	Determination of cell density .....	66
4.3.6	Maize cultivation conditions .....	66
4.4	Virulence assay of <i>Ustilago maydis</i> in maize .....	66
4.5	Microbiological standard methods.....	67
4.5.1	Competent <i>Escherichia coli</i> cells production .....	67
4.5.2	Heat-shock transformation of <i>Escherichia coli</i> .....	68
4.5.3	<i>Ustilago maydis</i> protoplast.....	69
4.5.4	Transformation of <i>Ustilago maydis</i> .....	69
4.6	Molecular biology methods .....	70
4.6.1	Plasmids.....	70
4.6.2	Gibson Assembly .....	70
4.6.3	CIRSPR-CAS9 vectors .....	70

4.6.4	P-MiniT cloning.....	71
4.6.5	Golden Gate Molecular Cloning .....	71
4.6.6	<i>U. maydis</i> gDNA isolation protocol.....	75
4.6.7	Total RNA extraction from infected maize tissue.....	76
4.6.8	DNase treatment after RNA isolation from plant material.....	77
4.6.9	cDNA synthesis .....	77
4.6.10	Quantification of nucleic acids .....	77
4.6.11	Amplification of DNA by Polymerase chain reaction (PCR) .....	78
4.6.12	Quantitative real-time PCR (qRT-PCR) .....	78
4.6.13	DNA digest .....	79
4.6.14	Agarose gel .....	79
4.6.15	Southern blot.....	80
4.6.16	DNA purification .....	83
4.6.17	Sequencing.....	83
4.7	Microscopy .....	83
4.7.1	Confocal laser-scanning microscopy .....	83
4.8	Optogenetics .....	84
4.8.1	Determination of FLuc expression in maize leaves .....	84
<b>5</b>	<b>Bibliography.....</b>	<b>86</b>
<b>6</b>	<b>Supplementary.....</b>	<b>98</b>
6.1	Bacterial strains used in this study .....	98
6.2	Bacterial strains containing MoRFunG modules .....	101
6.3	Technical information of the optogenetic plasmids .....	104
6.4	Fungal strains used in this study .....	105
6.5	<i>Ustilago maydis</i> strains belonging to the optogenetic system.....	110
6.6	Cluster 6A deletion and complementation: genetic confirmation .....	111
6.7	Expression pattern of effector genes of the cluster 6A .....	114
6.8	Supporting experimental data for ectopic simultaneous multi-gene integration without insertion of resistance cassettes. ....	115
6.8.1	CRISPR mediated integration of a multi-gene construct. ....	115
6.8.2	Multi-Tag ectopic integration using the MoRFunG toolkit and homologous recombination .....	117
6.8.3	Complementation of $\Delta pep1$ using MoRFunG toolkit under the control of different promoters ....	118
6.9	Technical supporting information for the Optogenetic experiments.....	121
6.10	Oligonucleotides .....	122
6.10.1	Primers.....	122

6.10.2	sgRNAs.....	134
6.11	Figure licenses .....	137



# 1 Introduction

## 1.1 Synthetic biology

Synthetic biology is a rather new discipline that bridges engineering and life science (Braguy & Zurbruggen, 2016; Andres *et al.*, 2019). Nevertheless, there has not yet been a unanimous definition (Cameron, *et al.*, 2014). Even though the origins of the synthetic biology concept can be traced to more than 50 years ago, the range and scope increased significantly in the mid-2000s, when experts from multiple disciplines came together fusing ideas from contemporary engineering into molecular biology (Cameron *et al.*, 2014).

Synthetic biology as a discipline aims to construct tailor-made systems by combining engineering and molecular biology techniques (Kuruma *et al.*, 2009). The goal is to develop tools that rewire and reprogram organisms (Khalil & Collins, 2010), by applying engineering principles to a modular and combinatorial assembly of biological parts into higher structures (Andres *et al.*, 2019). Synthetic biology harnesses the modular architecture of biological systems (Andres *et al.*, 2019), while also providing the characteristics of standardization and application of construction principles (Purnick & Weiss, 2009). Modularity allows the independence of the parts with predictable behaviors. Standardization translates into consistency, and in practical terms can be understood as robustness. Lastly, the application of construction principles, in which these independent parts can be combined as a whole, recreating biological processes with targeted modifications.

## 1.2 Manipulation of gene expression

In recent years, many molecular tools applicable to synthetic biology have been developed. Gene manipulation at a single-gene scale and whole-genome scale aims to introduce precisely designed changes, to explore emergent phenotypes and/or introduce new functionalities, elucidating causal links between genotypes and phenotypes (Haimovich *et al.*, 2015). These designed changes can refer for example, to gene deletions, gene up- and down- regulation, and selective transcriptional activation. Another example is the manipulation of single or multiple genes, not only to observe their phenotypical behavior under specific experimental conditions, but also to predict them.

### 1.2.1 Reverse genetics: the CRISPR-Cas system

Genetic research aims to identify specific genes that contribute to specific phenotypes. In order to do this, there are two different approaches: forward genetic screens and hypothesis-driven reverse genetic methods (Shalem *et al.*, 2015). In forward genetics, massive gene modifications are done, and the sampled cells/organisms are selected based on their phenotype for the analysis of the originally unknown mutation/s. Conversely, reverse genetics uses previous knowledge to test specific perturbations and their causal consequences (Shalem *et al.*, 2015). In other words, while in forward genetics specific genotypes are selected based on observed phenotypes, in reverse genetics the genotypes are previously known.

Over the recent past, reverse genetics' techniques have improved dramatically. In consequence, numerous questions that in the past have been addressed using forward genetics, can now also be approached with reverse genetics. A remarkable first step in genome editing was the incorporation of DNA into a host genome using homologous recombination (Capecchi, 1989; van der Oost & Patinios, 2020). The homologous recombination was later improved with the incorporation of artificial endonucleases. One of the advantages of using endonucleases is the increased efficiency shown in homologous recombination, and non-homologous end joining, when a double break in the DNA was produced (Cohen-Tannoudji *et al.*, 1998; van der Oost & Patinios, 2020). Another benefit of the usage of external endonucleases was increased specificity of the mutations due to the specific recognition sites of the enzymes used. Amongst the modern technologies used for site specific gene editing, are the Mega Nucleases (MegNs), Zinc Finger Nucleases (ZFNs), Transcription Activator-Like Effector Nuclease (TALENs) and Clustered Regularly Interspaced Short Palindromic Repeats (CRISPR) (van der Oost & Patinios, 2020). The CRISPR technology is one of the most disruptive technologies in the area of reverse genetics (Hille & Charpentier, 2016). This system was first discovered as a part of a bacterial immune system in *Streptococcus pyogenes* (Barrangou *et al.*, 2007). By now the use of the CRISPR- Cas system has been successfully adapted to many organisms.

There are different classes of CRISPR systems, based on the occurrence of effector Cas proteins (Makarova *et al.*, 2015; Shmakov *et al.*, 2015; Hille & Charpentier, 2016). One of those classes, the CRISPR- associated RNA-guided Cas9 endonuclease, has been applied to a wide range of species (Wright *et al.*, 2016; Leisen *et al.*, 2020). The system is characterized for a double strand break of the DNA that occurs by the recognition of complementary

sequences of a single guide RNA leading the endonuclease to the target region (Leisen *et al.*, 2020).

The CRISPR-Cas9 system requires an additional sequence known as PAM (protospacer adjacent motif) and a NGG located in the 3' extreme of the target region (Sternberg *et al.*, 2014; Leisen *et al.*, 2020). After the double strand DNA breaks, the cell repairs the damage, either through small deletions or insertions. Alternatively, major modifications can be done by providing donor DNA containing flanking regions to the targeted area, resulting in large deletions or insertions by CRISPR-Cas9 mediated homologous recombination.

### **1.2.2 Golden Gate and Molecular cloning**

One of the most ambitious approaches of geneticists has been the endeavor to manipulate the behavior of cells or even complete organisms. Nowadays, several methodologies provide the option to achieve this. Some approaches consist of the deletion of specific gene/s, incorporation of specific mutations, generation of artificial transcripts and selective transcriptional activation.

In recent years, new high-throughput methodologies have been developed to facilitate the integration of foreign transcripts into a genome. Advances such as TA cloning and GC cloning have significantly improved the efficiency of conventional cloning (Ashwini *et al.*, 2016) by simplifying the cloning process, reducing the number of required steps, and enhancing recombination efficiency, among other benefits. Additionally, methodologies like Gateway cloning, and SLIC (Sequence and Ligation Independent Cloning) further streamline the cloning process by making it easier to generate recombination events and increasing the number of fragments that can be inserted into a host cell.

A method capable of assembling up to nine DNA fragments in one single step of cloning, without the requirement of long homology ends, has been developed (Engler *et al.*, 2008, 2009; Engler & Marillonnet, 2014). This system is known as Golden Gate cloning, and it is based on the mechanism of action of type IIS restriction enzymes *BpiI* and *BsaI*. The recognition sites of these enzymes get automatically eliminated of the ligated fragments, not being available to re-digestion in the restriction-ligation one pot reaction as explained by (Engler & Marillonnet, 2014). The type IIS restriction enzymes have a distinct mechanism of action characterized by their ability to cut the DNA outside of their recognition sequence,

generating defined, non-palindromic overhangs, which increases the overall efficiency of the Golden Gate cloning process.

Taking as a base the Golden Gate cloning methodology, a modular cloning system (MoClo), was engineered with the aim to facilitate the construction of complex genetic inserts (Weber *et al.*, 2011). The MoClo system comprises a standardized library of level 0 modules with the capacity to contain different genetic elements. In a higher hierarchy of cloning, different level 0 modules can be assembled into a construct that works as a single transcript unit (level 1 modules). On an even higher level, multigene constructs can be then constructed from a combination of these transcript units (level 2 modules) (Engler & Marillonnet, 2014).

### **1.3 Synthetic Biology and model organisms**

The application of new methodologies to control cellular behaviors, allows scientists to engineer cells with practical application in areas like bioremediation, biosensing, biofuel production and even medical therapies (Gilbert *et al.*, 2003; Khosla & Keasling, 2003; Anderson *et al.*, 2006; Rajendran & Ellington, 2008; Steen *et al.*, 2008; Mukherji & Van Oudenaarden, 2009; Waks & Silver, 2009). This type of research is typically developed in model organisms. In the past, the term model organism has been applied to those species whose traits facilitate their experimental manipulation due to their small size and short generation time. With the increase of whole-genome sequencing, this definition has broadened, for example by the inclusion of organisms with agronomic and economic importance (Hedges, 2002). The research focused on these organisms has contributed to the core of biological knowledge, applied to animals, plants, prokaryotes, protists, and fungi.

### **1.4 Fungal plant pathogens and their way of interaction with their host**

Fungal plant pathogens likely represent the group with the most diversified traits in ecological and economic terms (Doehlemann *et al.*, 2017). Since ancient times, fungal diseases of crops have been reported to produce massive yield losses, resulting in substantial social and economic impacts. The incidence of fungal diseases in global crop production can be indirectly estimated, for instance, by examining the usage of fungicides in recent years. According to the Food and Agriculture Organization of the United Nations (FAO) database, the consumption of fungicides and bactericides with agricultural application worldwide has

increased in the period between 1990 and 2020 (Figure 1).

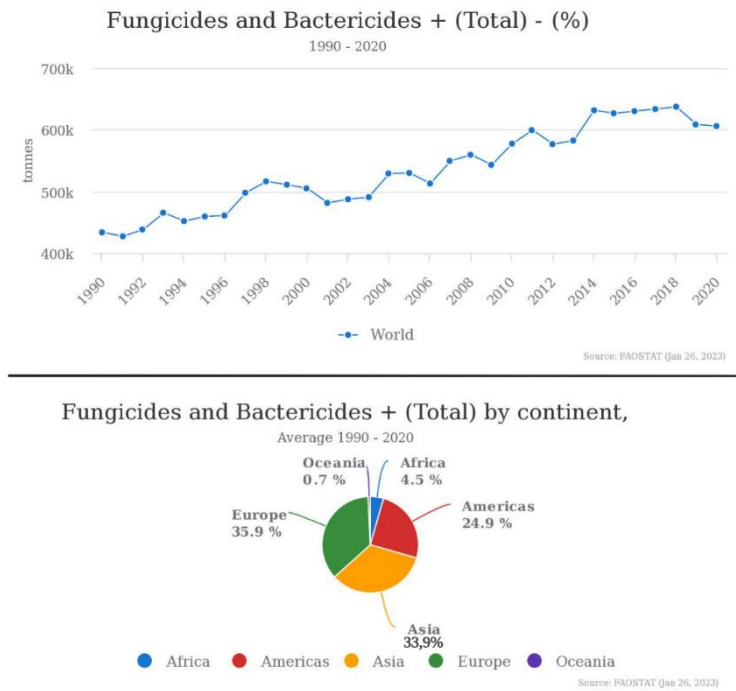


**Figure 1: Total usage of fungicides and bactericides worldwide from 1990 until 2020.** Data and figures were obtained on the official webpage Food and Agricultural Organization of the United Nations on Jan 26<sup>th</sup>. 2023. <https://www.fao.org/faostat/en/#data/RP/visualize>. Figure created with BioRender.com.

Fungal plant pathogens can be categorized into three primary groups based on their lifestyle and interaction with their plant hosts: biotrophic, necrotrophic, and hemi-biotrophic pathogens. The first group is characterized by the establishment of intimate interaction with plants, in which the fungus utilizes the nutrients from living host tissue to complete their pathogenic life cycle. In contrast, necrotrophic pathogens kill host tissue to extract nutrients (Doehlemann *et al.*, 2017). The third group consists of certain fungal plant pathogens known as hemi-biotrophs. These organisms exhibit both biotrophic and necrotrophic stages in their life cycle (Perfect *et al.*, 1998; Yi & Valent, 2013; Doehlemann *et al.*, 2017). Despite the seemingly mild overall symptoms caused by biotrophic pathogens, these fungi are responsible for the most devastating plant diseases (Doehlemann *et al.*, 2017). For instance, rust diseases produced by *Puccinia spp*, rank third in the list of top 10 fungal pathogens, based on their scientific and economic importance (Dean *et al.*, 2012).

### **1.5 *Ustilago maydis* as a model organism**

The fungi *Ustilago maydis* belongs to the Ustilaginales and serves as a well-defined model organism for the study of molecular plant-pathogen interactions (Brefort et al., 2009). Some of the advantages of using *U. maydis* as a model include its accessible and completely sequenced genome, an efficient transformation system, accessibility to dominant selection markers (Gold et al., 1994; Keon et al., 1991; Kojic & Holloman, 2000; Steinberg, 2004; Wang et al., 1988), and a well-established plant-pathogen system among others. Furthermore, *U. maydis* has contributed to the elucidation of several cellular processes, such as long-distance transport, mitosis, and motor-based microtubule organization in higher eukaryotes (Steinberg & Perez-martin, 2007). The *U. maydis* system has also been used for the analysis of DNA recombination and for cell biology studies (Holliday, 1964; Feldbrügge et al., 2004; Matei & Doehlemann, 2016). Moreover, the creation of the haploid solo-pathogenic strain has simplified its manipulation under laboratory conditions (Bölker et al., 1995) as it eliminates the need for mating to produce filamentous infectious strains.

Additional techniques that have been adapted in this organism include for example: PCR-based gene replacement (Kämper, 2004; Steinberg et al., 2004), the possibility to monitor gene expression during axenic growth and pathogenic development via marker genes such as  $\beta$ -glucuronidase and GFP (Genet & Urban, 1996; Spellig & Bottin, 1996; Basse et al., 2000; Steinberg, 2004), inducible promoter systems to enable controlled gene expression (Spellig & Bottin, 1996; Brachmann & Weinzierl, 2001; Straube et al., 2001; Steinberg, 2004), and the highly efficient CRISPR-Cas9 gene editing system (Schuster et al., 2016; Zuo et al., 2020).

While many important advances have been made in *U. maydis*, more techniques are being developed that can be adapted and applied to this pathosystem. These techniques are oriented to manipulate the behavior of its effector genes during different stages in the infection process to facilitate their functional characterization.

### **1.6 *Ustilago maydis* as a plant pathogen**

*Ustilago maydis* is a fungal plant pathogen capable of infecting maize (*Zea mays*) plants. *U. maydis* induces tumor formation in all aerial parts of its host-plant including leaves, tassel, and ears (Doehlemann et al., 2008; Matei & Doehlemann, 2016). In Mexico, the tumors produced by *U. maydis* are called “huitlacoche” and is considered a culinary delicacy (Lu,

1998) , although this pathogen can cause severe yield losses, since all the corn cub can be replaced by tumors.

The biotroph *U. maydis* has a biphasic lifecycle that involves a saprophytic stage and a pathogenic one (Doehlemann *et al.*, 2017). The transition from the saprophytic to the pathogenic stage occurs on the host surface with the germination of the haploid sporidia. When two compatible mating types of haploid sporidia come across, they fuse and form a dikaryotic infectious filament. This filament can directly penetrate the host cell through appressorium formation. During colonization, the hyphae are mostly intracellular and surrounded by the host plasma membrane. The area between the hyphal cell membrane and the host cell membrane is known as biotrophic interface, and is the area of exchange of nutrients, signals, and effector secretion (Brefort *et al.*, 2009; Doehlemann *et al.*, 2009; Lanver *et al.*, 2017). Subsequently, the infectious fungal hyphae reaches the bundle sheath cells (Matei & Doehlemann, 2016) where it manipulates the host to develop tumors, involving plant cell enlargement as well as increasing cell division (Doehlemann *et al.*, 2008; Matei *et al.*, 2018). Later during the infection process, within the dikaryotic fungal cells, karyogamy occurs and teliospores are formed from the fragmented hyphal cells. Teliospores accumulate in the tumors and disperse the fungal inoculum in the environment (Banuett & Herskowitz, 1996; Begerow *et al.*, 2006) to start a new pathogenic life cycle. The life cycle and pathogenic development of *U. maydis* is schematized in Figure 2.

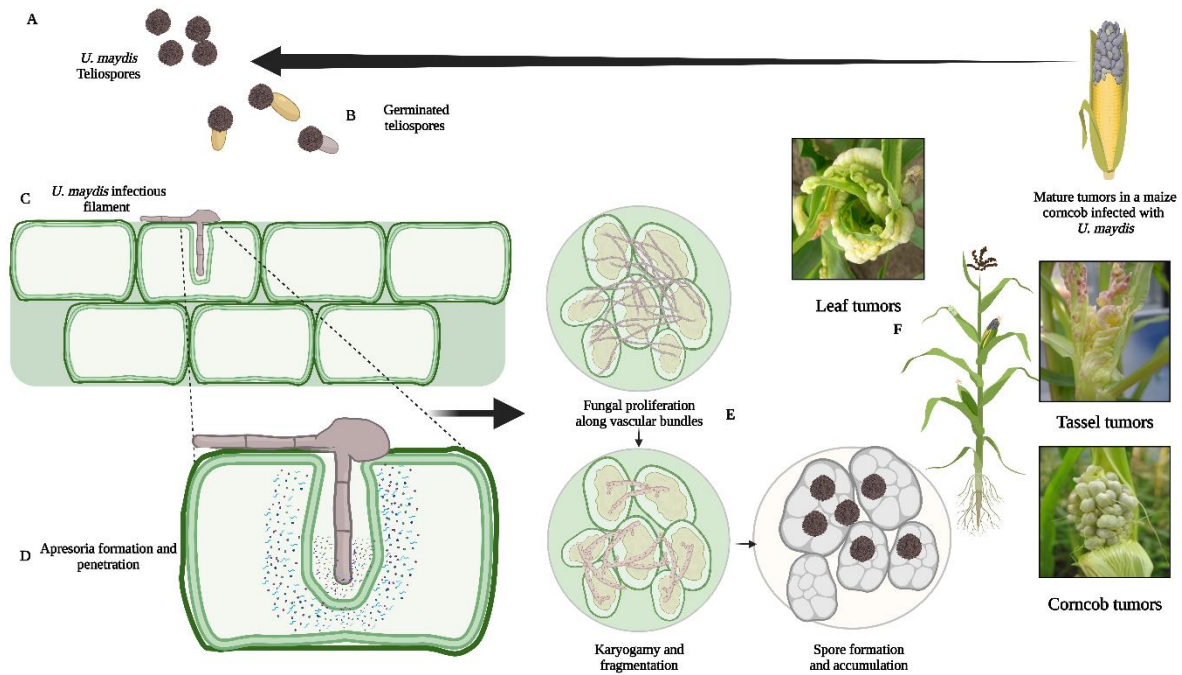


**Figure 2: Life cycle and pathogenic development of *U. maydis*.** This biotrophic fungus has a dimorphic life cycle, a yeast-like saprophytic phase, and a filamentous, pathogenic biotrophic stage. **A.** The teliospores from *U. maydis* are in the environment in a latent stage. **B.** Under specific conditions, those spores can germinate acquiring a yeast-like cellular form. **C.** When compatible yeast-like *U. maydis* cells meet on the surface of maize leaves, they can mate and form a dikaryotic infectious filament. The filament can penetrate the plant surface and initiate the infection process. **D.** Upon penetration the hyphae develop mostly intracellularly, surrounded by the plant plasma membrane. In between the fungus and the plant, an interaction zone is formed. This interaction is necessary for the establishment of a successful biotrophy. **E.** In advanced stages of the infection, *U. maydis* hyphae can develop intercellularly reaching deeper cellular levels inside the plant. After karyogamy hyphae fragmentation occurs, and teliospores are formed. **F.** Teliospores are accumulated in tumors. The tumors can develop in all aerial parts of the maize plants, for example leaf, tassel, and corn cobs. Pictures from leaf, tassel and corn cob tumors were done by Dr. Amey Redkar. Figure created with BioRender.com.

### 1.6.1 Effector genes

As a biotroph pathogen, *U. maydis* keeps its host cell alive during the infection process. In this context, *U. maydis* secretes effector proteins to manipulate the host metabolism and suppress the immune system. These effector proteins enable *U. maydis* to successfully establish the biotrophy, without induction of any defense-mediated, programmed cell death (Djamei & Kahmann, 2012; Lo Presti *et al.*, 2015; Matei & Doehlemann, 2016; Djamei *et al.*, 2023).

Within the genome of *U. maydis*, approximately 553 genes are predicted to encode for secreted effector proteins, many of those with unknown function or lack of defined functional or structural domains (Dutheil *et al.*, 2016; Schuster *et al.*, 2018). Several effector genes are co-located in genomic clusters, likely originated from gene duplication events for effector



diversification (Kämper et al, 2006). Sequences encoding predicted effector proteins are usually found in genomic regions with low sequence conservation. This genetic variation is consistent with an evolutionary perspective, reflecting co-evolution between the pathogen's effector race with its host targets for efficient defense suppression (Schirawski *et al.*, 2010).

Effector proteins can be functionally grouped in relation to the infection stage in which they are most required (Matei & Doehlemann., 2016) to guarantee a normal disease progression. Some proteins of *U. maydis* are defined as “core” effectors. These effector proteins are essential to colonize and infect the host tissue. Their activity is associated with the evasion of the plant’s first barrier of defense. A fitting example is the essential effector protein Pep1. This effector suppresses the plants immune reaction by inhibiting peroxidase activity in maize (Hemetsberger *et al.*, 2012, 2015; Matei & Doehlemann, 2016).

For a successful pathogenic development of *U. maydis*, it is crucial to establish and maintain biotrophy throughout the various stages of infection(Skibbe *et al.*, 2010; Schilling *et al.*, 2014; Matei & Doehlemann, 2016). Biotrophy is maintained, for example, through the secretion of the effector Pit2, which suppresses host immunity by inhibition of the maize cysteine proteases(Mueller *et al.*, 2013; Matei & Doehlemann, 2016). Another example is the effector Pep1, which is not only required for establishment of biotrophy, but also for its maintenance throughout the entire infection process. Without this effector, *U. maydis* cannot complete its sexual cycle (Brefort *et al.*, 2009; Doehlemann *et al.*, 2009; Hemetsberger *et al.*, 2012). Another example is the Cmu1 effector (secreted fungal chorismite mutase) which is one of the most highly upregulated effectors during plant colonization. It is taken up by the host cells, altering their metabolic status trough metabolic priming (Osorio *et al.*, 2011). Additionally, the effector protein Tin2, which modifies the lignin biosynthesis path in favor of the disease progression (Tanaka *et al.*, 2014; Matei & Doehlemann., 2016).

Alternatively, there are effectors that function in an organ/tissue specific manner. One example is the effector protein See1. This effector promotes the tumor formation in leaves by reinitiating cell division in vegetative tissue (Redkar *et al.*, 2015; Matei & Doehlemann, 2016). Another effector directly related to tumorigenesis is Sts2 (small tumor on seedlings 2), which was identified as a leaf-specific effector. (Schilling *et al.*, 2014; Djamei *et al.*, 2023).

### 1.6.2 Approaches to functional characterize *Ustilago maydis* effector genes

The interaction between plants and their pathogens often is described as a co-evolutionary “arms race”(Lanver *et al.*, 2017). This arms race is a three steps process. In a first step, the plant is attacked by a pathogen. The plant’s fitness is reduced, and in consequence novel defenses are selected and spread among the plant population. Subsequently, effectively defended plants decrease the pathogen’s fitness. As third step, a selection of a pathogen’s genotype, with effector genes that can overcome the plant defenses is spread across the pathogen population (Jones., 2006).

The relatively small and well annotated genome of *U. maydis*, along with its efficient transformation system, positions this model organism as one of the few eukaryotic plant pathogens in which effector proteins can be studied at a functional level (Dean *et al.*, 2012; Stotz *et al.*, 2014; Lanver *et al.*, 2017). New bioinformatic tools, including Effector P (Sperschneider *et al.*, 2016) Effector P 2.0 (Sperschneider *et al.*, 2018), Effector P 3.0 (Sperschneider & Dodds, 2022), Effector Hunter (Carreón-Anguiano *et al.*, 2020),and Wide Effector Hunter (Gisel *et al.*, 2022) among others, have enabled scientists to narrow down the number of genes that meet the requirements to be defined as “effector” in *U. maydis*. These criteria include the presence of a secretory signal, specific motifs, small size, a high cysteine residue content, expression during pathogenic development, and the absence of known structural functional domains (Win *et al.*, 2012; Lanver *et al.*, 2017).

Without this preselection, a genome-wide knockout approach would be necessary (Lanver *et al.*, 2017). However, such an approach is not feasible because virulence is often unaffected by the deletion of single genes, presumably due to functional gene redundancy (Saitoh *et al.*, 2012; Giraldo & Valent, 2013; Ali *et al.*, 2014; Lanver *et al.*, 2017). Furthermore, effector genes can contribute to the pathogenicity in a host-lineage-specific manner or under specific circumstances (Depotter & Doehlemann, 2020; Depotter *et al.*, 2021; Schurack *et al.*, 2021)

Bioinformatical tools together with a wide range of approaches from the areas of biochemistry, genetics, and cell biology together with high throughput cloning methods, functional genomics, and phylogenetic assays, have made it possible to identify and functionally characterize many effector proteins of *U. maydis*. As (Lanver *et al.*, 2017) discussed, a major task is to group effector genes based on their expression profile, to define

time-dependent and/or space dependent mechanisms of actions. This could increase the recognition of for example co-regulated transcription factors, enabling those regulatory networks to different stages of infection.

### **1.7 Optogenetics as a tool for gene manipulation in *Ustilago maydis***

Synthetic biology systems rationally assemble components present in biological systems and apply them in other organisms. Light is a common environmental element essential not only for photosynthetic but also non-photosynthetic organisms, which during evolution have evolved numerous mechanisms to sense and respond to light stimuli (Müller & Weber, 2013). Synthetic biologists have adapted the components of such systems and transferred them to adaptable toolboxes to control specific processes, having the advantages of a high temporal and spatial resolution (Müller & Weber, 2013). One of the most used light-responsive systems in eukaryotes is based on LOV domains. The blue light sensing light-oxygen-voltage (LOV) proteins are approximately 125 kDa, and are usually found in prokaryotes (Losi, 2004), fungi and plants (Müller & Weber, 2013). These proteins respond to light by undergoing conformational changes or dimerization upon illumination with blue light in a reversible manner (Müller & Weber, 2013).

The PhD dissertation of Lisa Cristin Hüsemann; AG Zurbriggen at the University Düsseldorf, describes the establishment and quantitative characterization of a LOV<sub>pep</sub>/ePDZ-based blue light inducible gene expression system in *U. maydis*. has the potential to enable spatial-temporal gene regulation in the *U. maydis*-maize pathosystem through the utilization of different wavelengths. In this study, the vectors systems for the blue-on and blue-off, originally described, has been modified to control the expression of the organ-specific effector gene, *see1*, as depicted in Figure 3 This modification was undertaken to evaluate the possibility of using light as a regulatory factor for the real-time expression of effector genes during biotrophy of *U. maydis*.

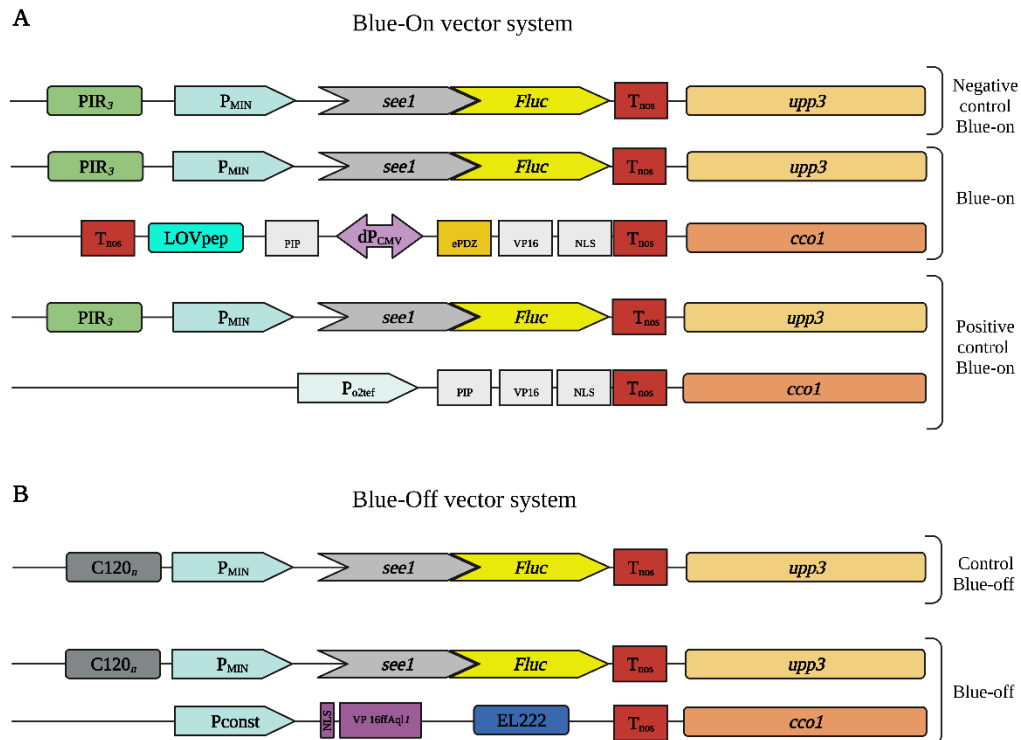


**Figure 3: Blue-on and Blue-off vectors adapted for the expression of *see1*.** **A. The blue-on system:** Reporter plasmid containing the firefly luciferase (FLuc) in frame with the effector gene *see1* and an operating sequence (PIR3) upstream of a minimal promoter. Additionally, the blue-on plasmid has a bi-directional promoter that control the expression of a light-sensitive protein (LOVpep), an ePDZZ fused with a trans activator and a nuclear localization sequence. The PIP-LOVpep fusion protein binds to the operating sequence (PIR3), after illumination with blue-light, this protein suffers a conformational change that leads to the uncaging of a peptide tag that is accessible to the ePDZ domain, bringing the trans activator near the minimal promoter, inducing in this way the expression of *see1FLuc*. **B. The blue-off system:** Two vector design of an EL222-based blue light-controllable gene expression system in *U. maydis*. The reporter plasmid has a firefly luciferase (FLuc) as a reporter in frame with the effector gene *see1* and several repeats of the EL222 operating sequence (C120) upstream of a minimal promoter (Pmin). The second vector counts with a constitutive promoter (Pconst) controlling the expression of an EL222 with a N-terminally fused *U. maydis-derived Sql1* repressor (and a nuclear localization sequence (NLS). In presence of blue light, the protein EL222 dimerizes and binds to the DNA in the C120n region, this interaction brings the repressor close to the minimal promoter repressing the expression of *see1FLuc*. Technical information about the strains in supplementary section 6.9. Figure created with BioRender.com.

## 1.8 Objectives of this study

The major aim of this study was to construct and test genetic tools that facilitate the functional characterization of effector genes in *U. maydis*. In order to do this, a standardized cloning methodology named MoRFunG toolkit (**M**odular **R**ecombinant **F**ungal toolkit for **G**ene expression) was developed. Accordingly, the main objectives were to:

1. Develop a standardized cloning methodology adapted to *U. maydis* that allows the systematic study of effector genes and their impact on virulence using the Golden Gate and the MoClo technologies.
2. Generate defined modular cloning units integrated in the MoRFunG toolkit to provide the system with independence as well as predictability.
3. Generate transcript units able to recreate the behavior of the wild-type effector genes in terms of expression pattern and impact on virulence of *U. maydis*.
4. Use the MorFunGtoolkit as a high throughput cloning methodology that allows the functional complementation of large genomic deletions.
5. Identify effector genes with relevant functions within the virulence cluster 6A of *U. maydis* as a proof of concept.
6. Manipulate the expression pattern of relevant effector genes by using tailor-made transcript units with the exchange of promoter regions.
7. Achieve ectopic integration by homologous recombination without major modifications of the genetic background.

In addition to these main objectives, a trial study was done to evaluate the utilization of optogenetic systems for manipulation of the expression of effector genes in the *U. maydis*-maize pathosystem.

## 2 Results

### 2.1 Set up of the MoRFunG toolkit in *Ustilago maydis*

#### 2.1.1 *Ustilago maydis* cluster 6A deletion and its impact on virulence

The 18,6% of all the genes encoding secreted proteins in *U. maydis* are organized in physical clusters in the genome (Kämper et al., 2006), and deletions of five of those clusters had an impact on the virulence performance of this biotrophic pathogen (Kämper et al., 2006). In this study, the cluster 6A, which is required for full virulence of *U. maydis* (Kämper et al., 2006), was selected as a starting point for the setup of the MoRFunG toolkit as a high throughput cloning methodology. This decision was made based on several factors. Firstly, the cluster deletion exhibited a virulence defect (Kämper et al., 2006). Secondly, there is a lack of knowledge regarding specific virulence functions of individual genes within the cluster. Finally, previous attempts at complementation using established cloning methodologies have been highly challenging and unsuccessful until now.

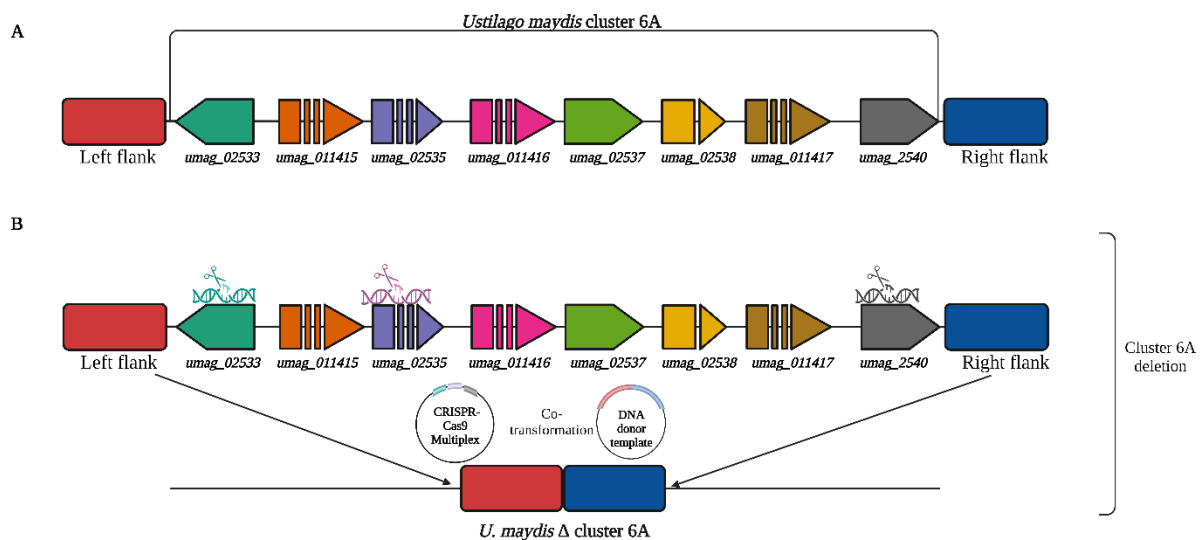


**Figure 4: Deletion of Cluster 6A of *U. maydis*.** **A:** The cluster 6A of *U. maydis* consist in 8 genes predicted to be effector proteins. In this representation the genes are represented for arrowed shapes. Each arrowed shape in a specific color represents one gene. Completed arrows are genes that contain only one exon. In interrupted arrows the interruption represents introns. In the left and right extremes of the figure, squared shapes (red and blue) represent 1Kb flanking regions of the cluster. **B:** Scheme of the deletion of cluster 6A in a co-approach using CRISPR-Cas9 mediated homologous recombination to generate a genetic scar composed by the left and right flanks together. Scissors cutting double-strand DNA represent the targets of the CRISPR multiplex used for the generation of the cluster deletion. Figure created with BioRender.com.

For this study, deletion mutants of the cluster 6A (Figure 4), which includes the genes *umag\_02533*, *umag\_11415*, *umag\_02535*, *umag\_11416*, *umag\_02537*, *umag\_02538*, *umag\_11417* and *umag\_02540*, were created in the *U. maydis* SG200 solo-pathogenic genetic background. The deletion was performed using the CRISPR-Cas9 gene editing system in combination with homologous recombination. This approach allowed the creation of deletion strains without the introduction of resistance cassettes. A CRISPR-Cas9 multiplex plasmid (#2307-*pCas9Hfl\_02533\_02535\_02540*) containing sgRNAs targeting 3 out of the 8 genes of the cluster (*umag\_02533*, *umag\_02535* and *umag\_02540*) was used to generate double strand breaks in the DNA. Together with the CRISPR plasmid, a donor template containing the left and right flanking genomic regions of the cluster was co-transformed (#2305-*pGAM1311Lb-Rb*). This led to a CRISPR-Cas mediated homologous recombination that resulted in a complete deletion of the cluster 6A. The flanking regions were assembled by a Gibson Isothermal reaction (Gibson *et al.*, 2009; Gibson, 2011) and transformed into *U. maydis* as a circular vector, shortening the cloning steps previous to the mutant generation, since plasmid linearization and clean-up was not required. The mutants were selected based on carboxin resistance conferred by the CRISPR vector. The cluster deletion and the generation of the genetic scar of the generated strain were confirmed by southern blot analysis, PCR, and sequencing (supplementary section 6.6) Three independent mutants were selected, and their virulence was evaluated in maize infection assays.

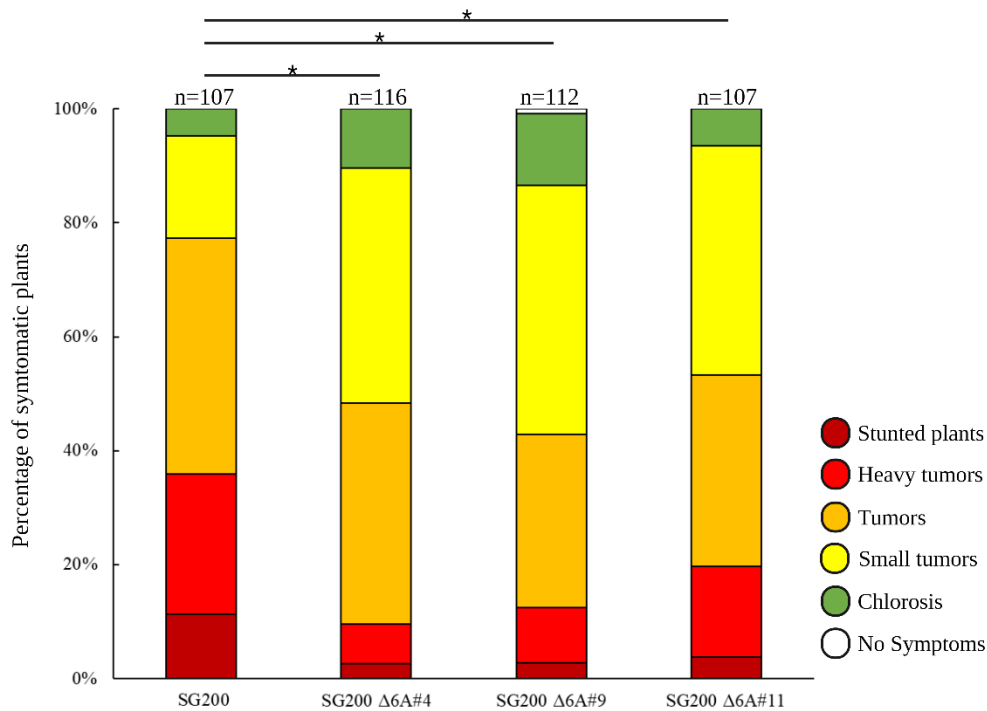


**Figure 5: Virulence assay *U. maydis* SG200 Δ6A:** Virulence assays including *U. maydis* SG200 and three independent mutants for the cluster 6A deletion strains (SG200 Δ6A) in Golden Bantam (GB)maize leaves. The scoring was performed at 12 days post inoculation (dpi). Disease rates are given as a percentage of the total number of infected plants. Three biological replicates were carried out. “n” represents the number of infected maize seedlings. Significant differences between strains were analyzed by unpaired Student’s t-test analysis (\*:  $P \leq 0.05$ , \*\* $P \leq 0.01$ ).

The results revealed that all the 3 independent mutants with deletion of cluster 6A had a reduced virulence phenotype when compared with the *U. maydis* SG200 control (Figure 5). The impaired virulence phenotype was in all cases characterized by a reduction in the size and amount of tumor formation. These results re-confirmed the relevance of the effector cluster 6A for a normal *U. maydis* SG200 disease development in maize as shown by ( Kämper et al., 2006).

The combination of CRISPR-Cas9 together with homologous recombination, allowed to generate a “genetic scar” without resistance cassettes in the mutation zone. The dispensability of the resistance cassettes in this methodology makes all the available selection markers accessible for future experiments, without the need of eliminating the cassette in an extra cloning step. The “genetic scar” generated by the flanking regions, in the cluster deletion, served as clear genetic background for the subsequent cluster complementation using the MoRFunG toolkit.



### 2.1.2 *Ustilago maydis* cluster 6A two steps complementation

The complementation of large genomic deletions is a challenging approach, mainly due to the technical difficulties of assembling large DNA fragments as functional units. In this study, a cluster 6A complementation strain was created using MoRFunG toolkit modules. This complementation process was carried out in two steps, employing both CRISPR-Cas9 and homologous recombination methods simultaneously.

In the first step, the CRISPR vector (#2456-*pCas\_9Hfl\_1<sup>st</sup>Comp 6A*) targeted the middle of the genetic scar (in the right flanking region). With the aim of inducing homologous recombination, a donor DNA vector template (#2511-*pL2M<sup>1/2</sup> 6A:R1: R6Short*) was co-transformed together with the CRISPR vector in the *U. maydis* SG 200Δ6A genetic background. The donor DNA was a MoRFunG Level 2 plasmid containing clustered arranged transcript units (*umag\_02533*, *umag\_11415*, *umag\_02535* and *umag\_11416*) and the flanking sequences of the cluster used in the genetic scar (the left flank and a shortened right flank, without the recognition sequence found in the CRISPR vector to prevent plasmid linearization during transformation). The outcome of this first step transformation resulted in mutant strains with an insertion in the cluster 6A loci, containing half of the genes of the cluster 6A (SG 200 Δ6A:: *02533/11415/02535/11416*) (Figure 6B), shortly designated “SG200Δ6A/C1” in the virulence assays.

In the second complementation step, the CRISPR vector (#2457-*pCas\_9Hfl\_2<sup>nd</sup>C6A*) targeted an artificial DNA sequence generated by MoClo in between the *umag\_11416* and the right flank. The donor template (MoRFunG Level 2 module #2453-*pL2-F1:R6A2<sup>nd</sup>C6A*) included the gene *umag\_11416* (serving as a left flank for homologous recombination) followed by the transcript units *umag\_02537*, *umag\_02538*, *umag\_11417*, *umag\_02540* and the right flank, in its full extension, as depicted in Figure 6C. The resultant strain contained a complete cluster complementation done with the MoRFunG toolkit (SG200 Δ6A:: *02533/11415/02535/11416/02537/02538/11417/02540*) shortly designated “SG200Δ6A/C2” in the virulence assays.

For the cluster 6A complementation, a total of 24 level 0 modules, 8 level 1 transcript units, three flanking regions in level 1 and two level 2 vectors each of them containing 6 tandemly arrange level 1 constructs were generated.

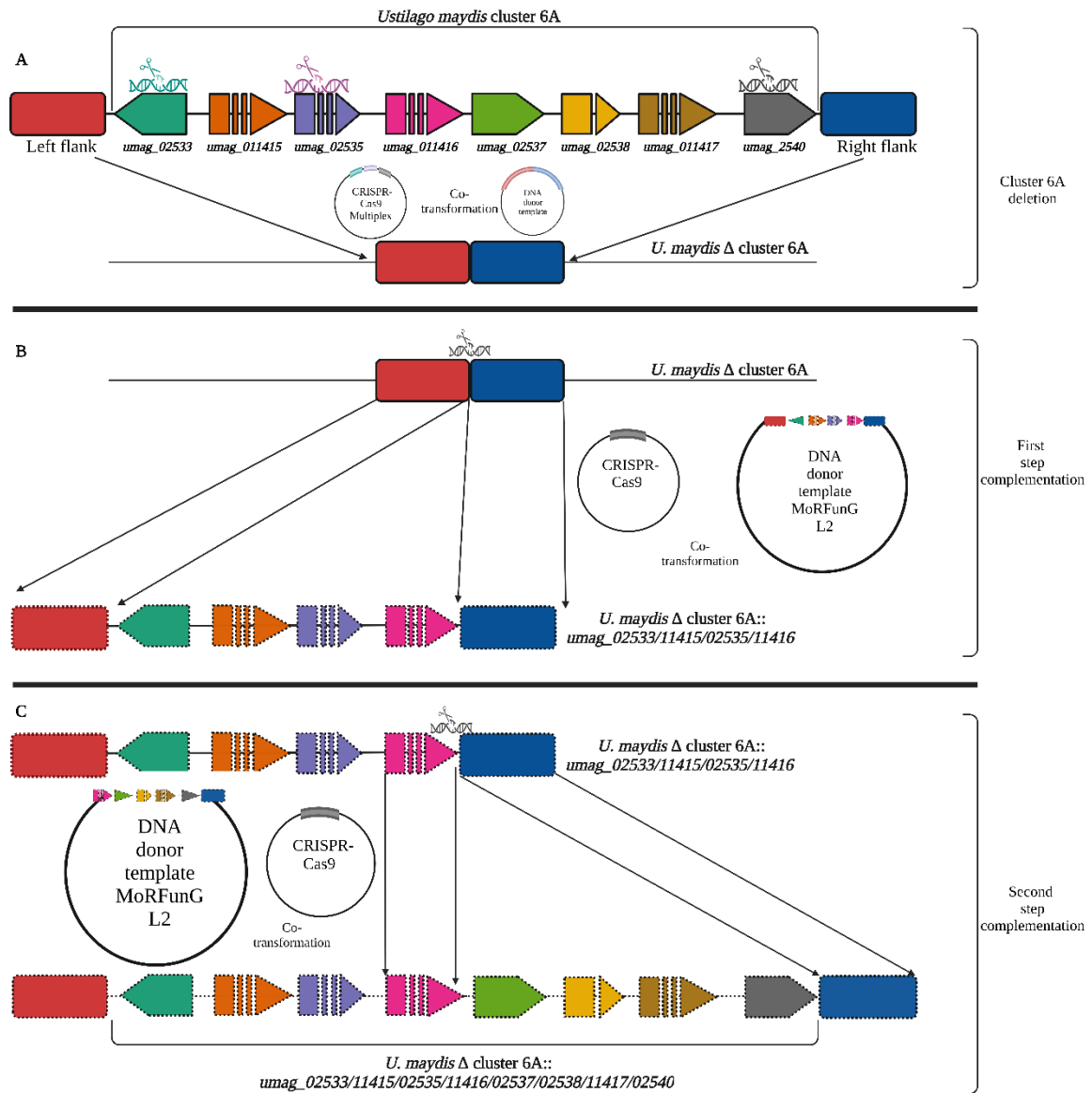


**Figure 6: Virulence cluster 6A deletion and complementation scheme:** Rectangles represent flanking regions. The arrow-shaped figures represent genes. Each fragment in the arrow shaped figures represents an exon. Dashed outlines of the shapes represent modules of the MoRFunG toolkit. Non-dashed shapes represent the genes in the *U. maydis* wild type strain. CRISPR targets are represented by scissors cutting double-stranded DNA. **A.** *U. maydis* cluster 6A deletion. Co-transformation using a CRISPR-Cas9 vector multiplexing 3 genes of the cluster in the SG200 genetic background. The donor template contains the left flank of the cluster (red) and right flank (blue) to generate a genetic scar. **B.** First step complementation (SG200 Δ6A genetic background): Introduction of the genes *umag\_02533*, *umag\_11415*, *umag\_02535*, and *umag\_11416* together with the flanking regions in a MoRFunG level 2 vector. The mutagenesis was directed in loci using a CRISPR-Cas9 vector targeting a sequence at the beginning of the right flank. **C.** Second step complementation (SG200 Δ6A/C1 genetic background). The donor DNA carried in a L2 MoRFunG vector contains the genes *umag\_11416*, *umag\_02537*, *umag\_02538*, *umag\_11417* and *umag\_02540* together with the right flank. The mutagenesis was directed in locus using a sgRNA carried in the CRISPR vector that targeted an artificial sequence in between *umag\_11416* and the right flank in the first complementation. Figure created with BioRender.com.

The complementation strains were confirmed by southern blot analysis (Supplementary Section 6.6). All the strains were able to form filament on charcoal plates (not shown). The virulence performance of one selected strain for each complementation was evaluated in

maize infection assays using the *U. maydis* SG200 and the SG200  $\Delta$ 6A as controls.

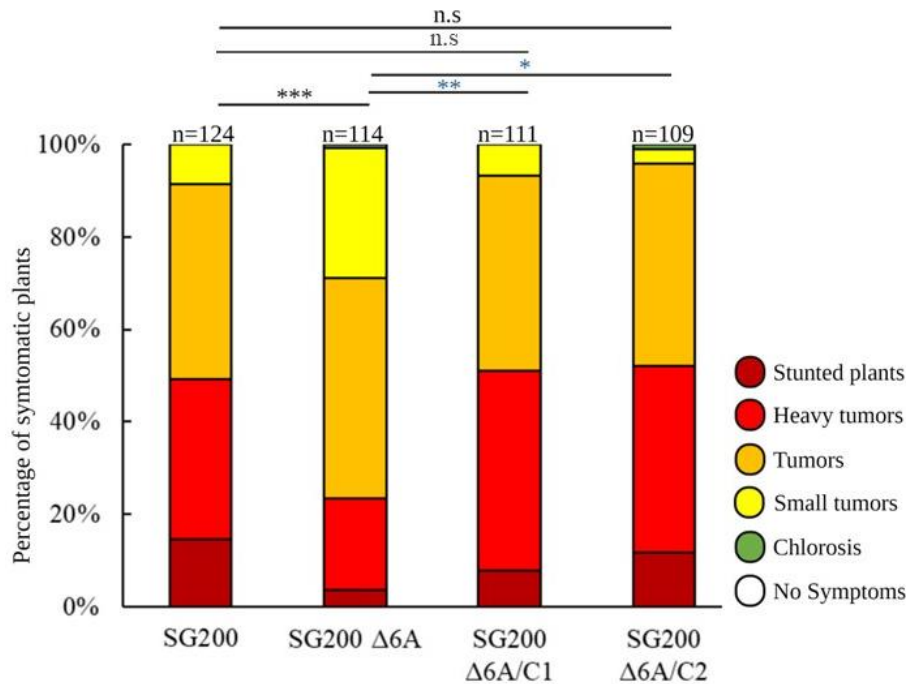


**Figure 7: Virulence assay of cluster 6A deletion and complementation:** SG200, SG200  $\Delta$ 6A, half cluster complementation (SG200  $\Delta$ 6A/C1) and complete cluster complementation (SG200  $\Delta$ 6A/C2) virulence assay on Golden Bantam (GB)maize leaves. The scoring was done at 12 days post inoculation (12 dpi). Disease rates are given as a percentage of the total number of infected plants. Three biological replicates were carried out. “n” represents the number of infected maize seedlings. Significant differences between strains were analyzed by unpaired Student’s t-test analysis (\*:  $P \leq 0.05$ , \*\*:  $P \leq 0.01$ , \*\*\* $P \leq 0.005$  n.s = no significance). **SG200 $\Delta$ 6A/C1** contains the genes *umag\_02533*, *11415*, *02535* and *11416*. **SG200 $\Delta$ 6A/C2** contains the genes *umag\_02533*, *11415*, *02535*, *11416*, *02537*, *02538*, *11417* and *02540*. Modification of a Figure created with BioRender.com.

The disease assay performed with SG200, SG200  $\Delta$ 6A and complementation mutants revealed that both complementation strains constructed with the MoRFunG toolkit fully recovered the virulence defect of the cluster 6A deletion (Figure 7). There were not statistical differences between the disease rate of the first complementation strain (SG200  $\Delta$ 6A/C1) and the complete cluster complementation (SG200  $\Delta$ 6A/C2) in relation to the SG200 strain. These results indicate that, potentially one or a combination of genes included in C1 (*umag\_02533*, *umag\_02535*, *umag\_11415* and/or *umag\_11416*) hold the most important virulence functions necessary for a full virulence performance.

### 2.1.3 Gene expression in the MoRFunG cluster 6A

After successful genetic and functional complementation of the cluster 6A, the gene expression level between the genes of the artificial cluster was compared to the wild type (positive control) and cluster deletion (negative control and genetic background) by performing qRT-PCRs. The samples analyzed were total RNA extracted from infected maize leaves. The samples were taken at 4 dpi. At this specific time point all the effector genes showed up-regulation based on RNA seq data (Lanver *et al.*, 2018b) as shown in supplementary section 6.7.

The qRT-PCRs performed for SG200  $\Delta$ 6A mutant showed the absence of gene expression for the cluster 6A genes. The first half complementation strain (red bars) showed detection of the first 4 genes of the cluster (genes mentioned in the left column) while the strain containing complete cluster 6A (grey bar) shows expression for all the eight genes (Figure 8). Analysis of qRT-PCRs demonstrated that the expression level of *umag\_02533/11415/02535* and *11416* genes were comparable between SG200  $\Delta$ 6A/C1 and SG200  $\Delta$ 6A/C2, and in both cases equivalent with the gene expression exhibited for the SG200. The student's t-test of the qRT-PCRs results showed that only *umag\_02535* exhibited a significant difference between the complementation strains (SG200  $\Delta$ 6A/C1 and SG200  $\Delta$ 6A/C2) when compared to the SG200.

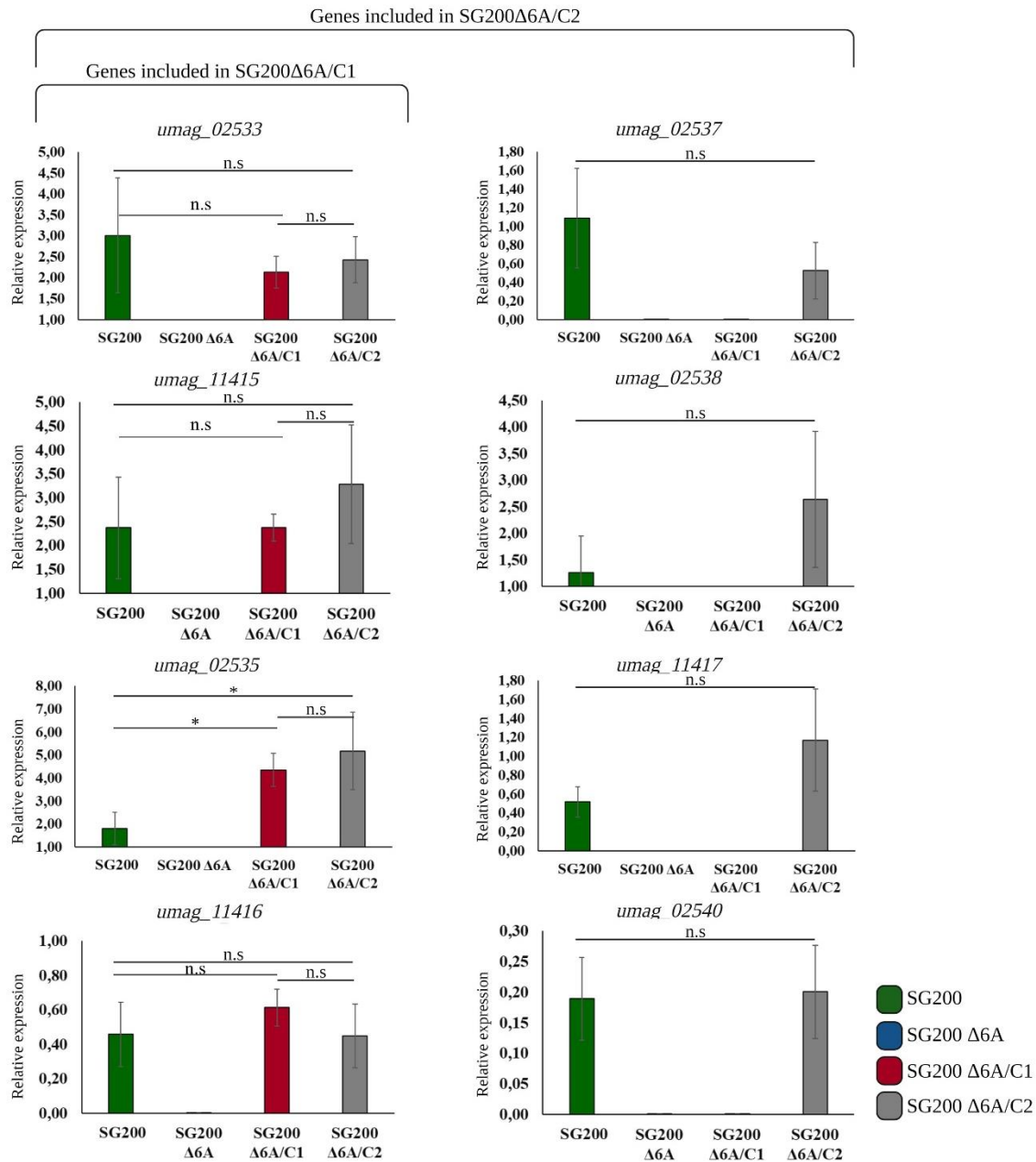


**Figure 8: qRT-PCR genes cluster 6A:** qRT-PCR from each gene of cluster 6A in the different strains generated during the cluster 6A complementation. All the expression data was normalized against the housekeeping gene *ppi*. Three biological replicates infected maize plants and two technical replicates for the cDNA were analyzed by qRT-PCR for each treatment, The bars indicate the average expression of the genes from 3 independent biological replicates, in ratio to *ppi* ( $2^{-\Delta C_t}$ ). Significant differences between strains were analyzed by unpaired Student's t-test analysis (\*:  $P \leq 0.05$ , \*\* $P \leq 0.01$ , n.s. = no significance). Modification of a Figure, originally created with BioRender.com.

The results proved that the MoRFunG cluster complementation recovered the virulence performance and the expression of the majority the genes of the cluster 6A in comparable levels to the SG200 under the experimental conditions used in this study. The expression level of the genes *umag\_02533*, *umag\_02535*, *umag\_11415* and *umag\_11416* did not exhibited statistical differences between SG200 Δ6A/C1 and SG200 Δ6A/C2 at 4 dpi, indicating that

successive transformation rounds did not affect the expression of the adjacent genes.

## **2.2 Elucidation of relevant genes within the cluster 6A using the MoRFunG toolkit**

Some of the effector genes of *U. maydis* are co-localized in clusters of virulence (Kämper et al., 2006), making it feasible to delete them simultaneously and evaluate the impact of the cluster on virulence performance. However, identifying the function of relevant genes within a virulence cluster, or understanding the relationship between the genes of a cluster, remains technically challenging due to potential transcriptional co-regulation or overlapping functions. This section provides a summary of the experiments conducted to gain insights into the significance of the genes within cluster 6A. Throughout this section, the results from knockouts, as well as experiments using the novel MoRFunG toolkit to understand the relation between the effector of the cluster 6A, are depicted.

### **2.2.1 Cluster 6A of *Ustilago maydis*: single and multiple gene knockouts**

Some of the greatest difficulties when characterizing effector genes of *U. maydis* are their large number in the genome and their functional redundancy (Khrunyk et al., 2010; Zuo et al., 2020). To understand the relation between the genes included in the virulence cluster 6A, single and multiple knockouts were done using CRISPR-Cas9 (Zuo et al., 2020), and their virulence performance compared to *U. maydis* SG200. In this study, strains which names contain the “Δ” symbol, refer to strains in which the complete sequence of the gene/s has been deleted of the genome. Alternatively, strains named KO (knockout) apply to strain in which a mutation (frameshift or premature stop-codon) was introduced into the ORF using CRISPR-Cas9, leading to the loss of functionality of the transcript.

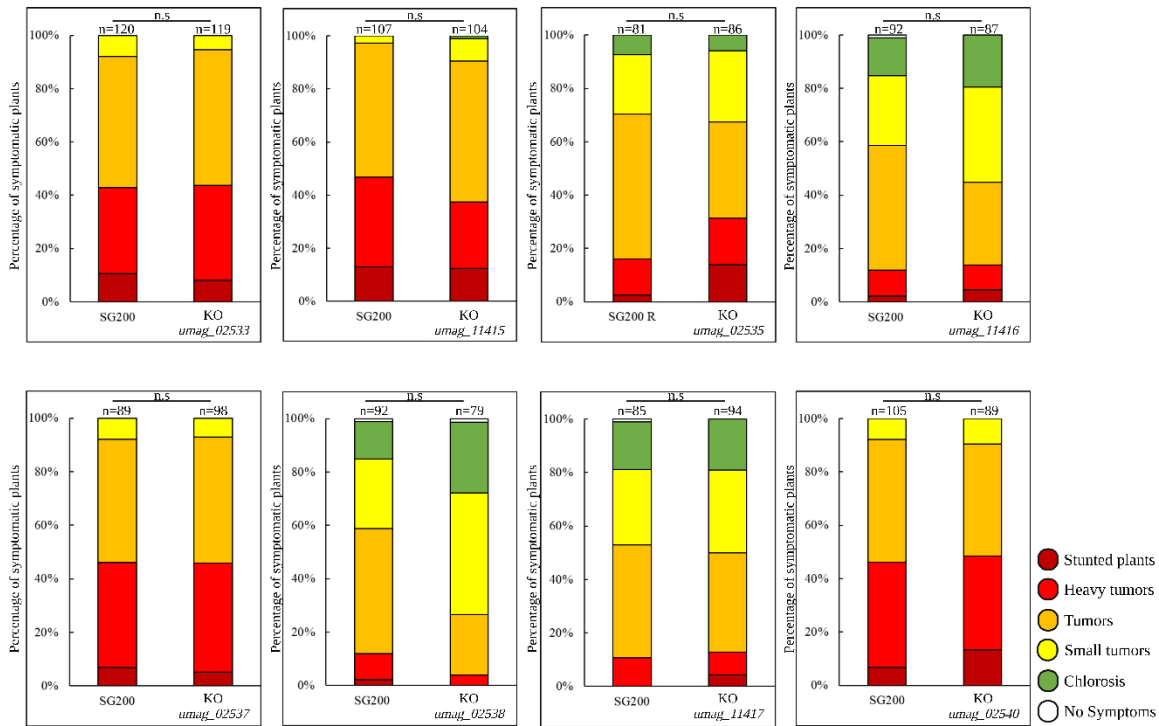


**Figure 9: Virulence assay of single KO of the genes of the cluster 6A:** Virulence assay performed for all single Knockouts (KO) of the genes from cluster 6A in Golden Bantam maize seedlings. The scoring was done at 12 days post inoculation (12 dpi). Disease rates are given as a percentage of the total number of infected plants. Three biological replicates were carried out. “n” represents the number of infected maize seedlings. Significant differences between strains were analyzed by unpaired Student’s t-test analysis (\*:  $P \leq 0.05$ , \*\*:  $P \leq 0.01$ , \*\*\*:  $P \leq 0.005$  n.s = no significance). Figure created with BioRender.com.

The results for the single gene knockout in a cluster context showed that none of the gene knockouts exhibited a virulence reduction when compared to the SG200 (Figure 9). These results indicate that the individual genes are dispensable for virulence when the rest of the cluster is present. Double knockouts of genes from the cluster 6A that showed a differential up regulation in different maize lines observed by Dr. Selma Schurack (*umag\_02533* and *umag\_02535*, as well as the knockout of *umag\_02533* together with *umag\_02540*), did not show any virulence reduction when compared to the SG200. Contrastingly, the triple knockout of the genes *umag\_02533*, *umag\_02535* and *umag\_02540* showed a significant reduction in the virulence performance in relation to the SG200 control (Figure 10).

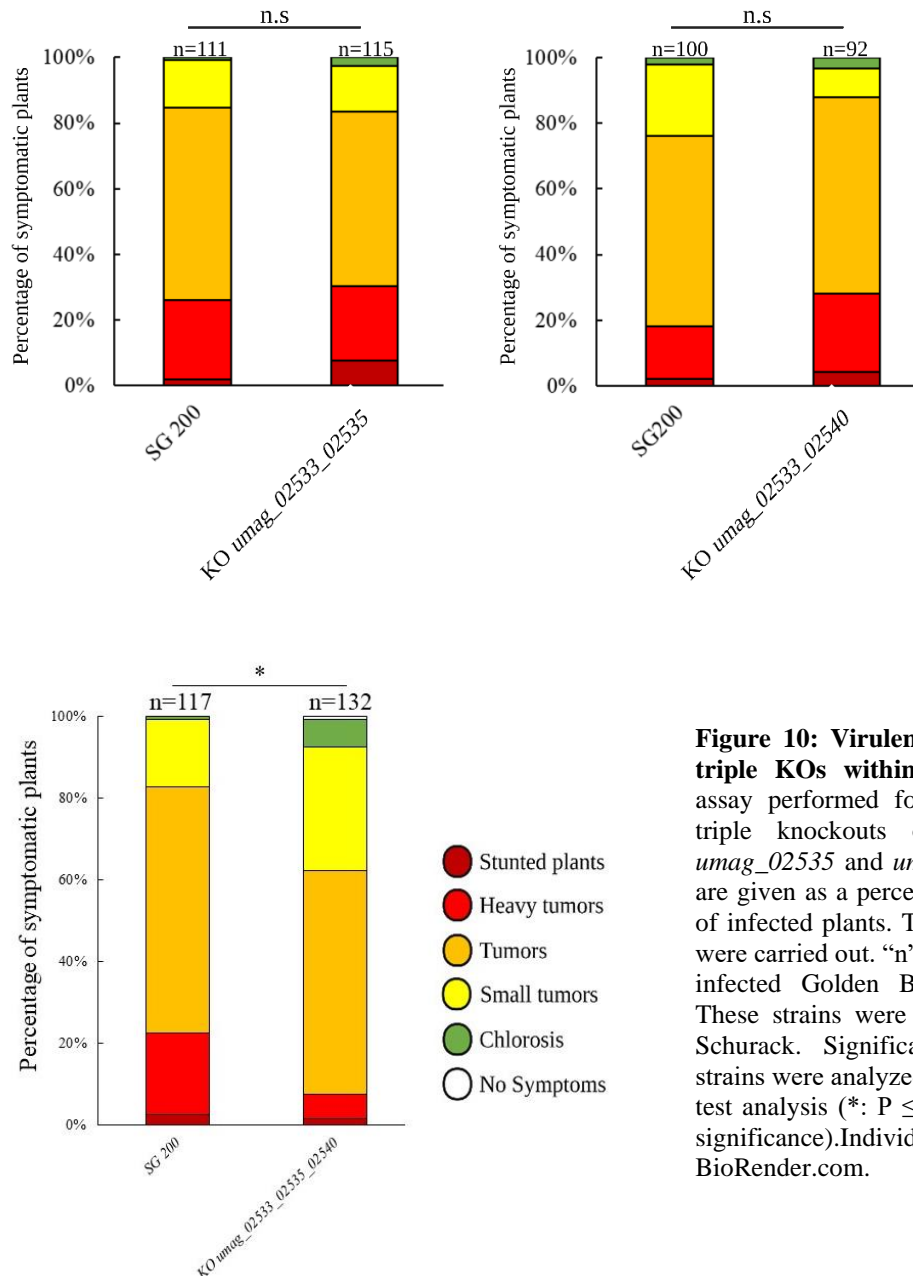


**Figure 10: Virulence assay of double and triple KOs within cluster 6A:** Virulence assay performed for double knockouts and triple knockouts of genes *umag\_02533*, *umag\_02535* and *umag\_02540*. Disease rates are given as a percentage of the total number of infected plants. Three biological replicates were carried out. “n” represents the number of infected Golden Bantam maize seedlings. These strains were generated by Dr. Selma Schurack. Significant differences between strains were analyzed by unpaired Student’s t-test analysis (\*:  $P \leq 0.05$ , \*\* $P \leq 0.01$ , n.s = no significance). Individual graphics created with BioRender.com.

Some of the genes included in the cluster 6A were previously identified as Tips (TOPLESS interactor proteins) (Bindics *et al.*, 2022). These genes were shown to induce auxin signaling in maize plants, contributing in this way to the virulence of *U. maydis*. The genes *umag\_11415*, *umag\_02535*, *umag\_02537*, *umag\_02538* and *umag\_11417* were then defined as Tip1- Tip5, respectively. In order to test, whether the Tips interactors had a direct impact on the virulence performance of *U. maydis*, a deletion strain of all the genes of cluster 6A except for *umag\_02533*, *umag\_11416* and *umag\_02540* was generated by Dr. Mamoona Khan from Crop Science and Resource Conservation (INRES), University of Bonn, and their



virulence performance evaluated in this study.

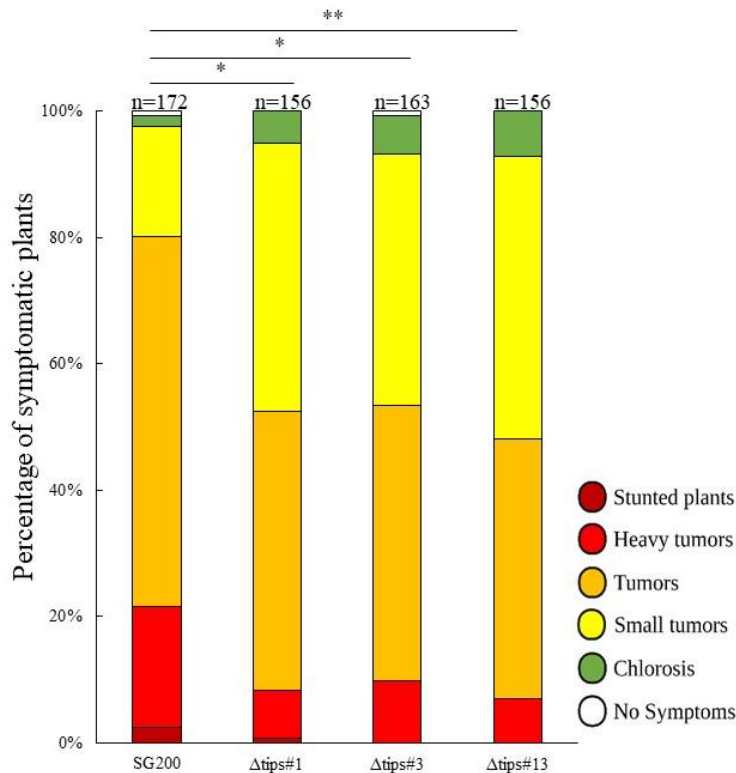


**Figure 11: Virulence assay deletion of Tips in the cluster 6A** Virulence assay performed for the deletion of the Tips genes of the cluster 6A (*umag\_02535*, *umag\_11415*, *umag\_02537*, *umag\_02538*, and *umag\_11417*) Disease rates are given as a percentage of the total number of infected plants. Four biological replicates were carried out. “n” represents the number of infected Golden Bantam maize seedlings. These strains were generated by Dr. Mamoonah Kahn. Significant differences between strains were analyzed by unpaired Student’s t-test analysis (\*:  $P \leq 0.05$ , \*\* $P \leq 0.01$ ).

The deletion of the Tips showed a reduced virulence phenotype compared to the SG200 strains (Figure 11). A potential hypothesis from this result indicates that one or more of the Tips interactors could potentially be essential for a fully virulence performance of *U. maydis*. A holistic analysis of all the knockout strains provided evidence indicating that not all the genes of the cluster are required to achieve a fully virulent performance. The combination between single double and multiple KOs/ deletions suggests that the genes *umag\_02533*, *umag\_11416* and *umag\_02540* are in principle dispensable for the normal development of the pathogenicity of *U. maydis*. Nevertheless, based on these results, is not possible to draw conclusions about the relevance of the rest of the effector genes from the cluster. In this context, questions related to the potential interactions between the cluster’s genes remain unclear. This constitutes a clear example of the limitations of gene deletion approaches for the understanding of tightly interconnected genes.

### **2.2.2 Identification of relevant genes within the virulence cluster 6A of *Ustilago maydis* using the MoRFunG toolkit**

Identifying genes with relevant functions for *U. maydis* can be challenging, especially when genes are clustered and co-regulated, or when they have functional homologs in the genome. The experimental data obtained from the gene deletions/knockouts supports the hypothesis that the genes of cluster 6A have functional redundancy. In this section, the modules of the MoRFunG toolkit used in the cluster complementation (Section 2.1.2) were used to generate “single gene complementation strains” with individual modular transcript units, in the SG200  $\Delta 6A$  genetic background as schematized in Figure 12. The goal was to identify, if there exist one or more effectors from this cluster that could individually recover the virulence defect from the cluster deletion in absence of the rest of the cluster. The use of the MoRFunG toolkit for this experiment had the advantage of a rapid assembly of the transcript units, inserted in locus without introduction of resistance cassette, by using CRISPR-Cas mediated homologous recombination.

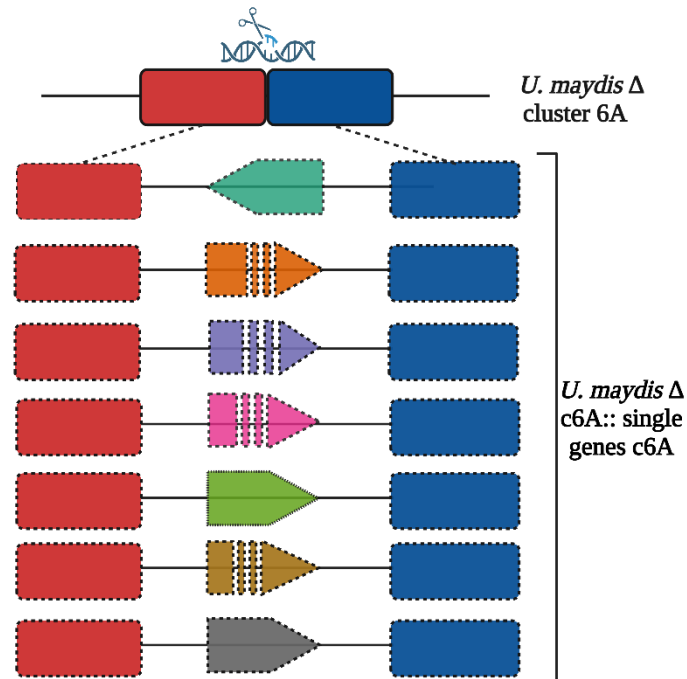


**Figure 12: Scheme of the single gene cluster complementation strains.** Dashed shapes represent genetic constructs done with the MoRFunG toolkit. The CRISPR target is represented with a cut DNA molecule. Each donor template contained the two flanking regions (squares red and blue) with single transcript units from cluster 6A (arrows). The insertions were done in locus in the genomic location for cluster 6A. Figure created with BioRender.com.

The virulence performances of the strains SG200Δ6A/02533, SG200Δ6A/02535, SG200Δ6A/11415, SG200Δ6A/02537 and SG200Δ6A/02538 were evaluated. The SG200 and SG200Δ6A strains were used as controls.

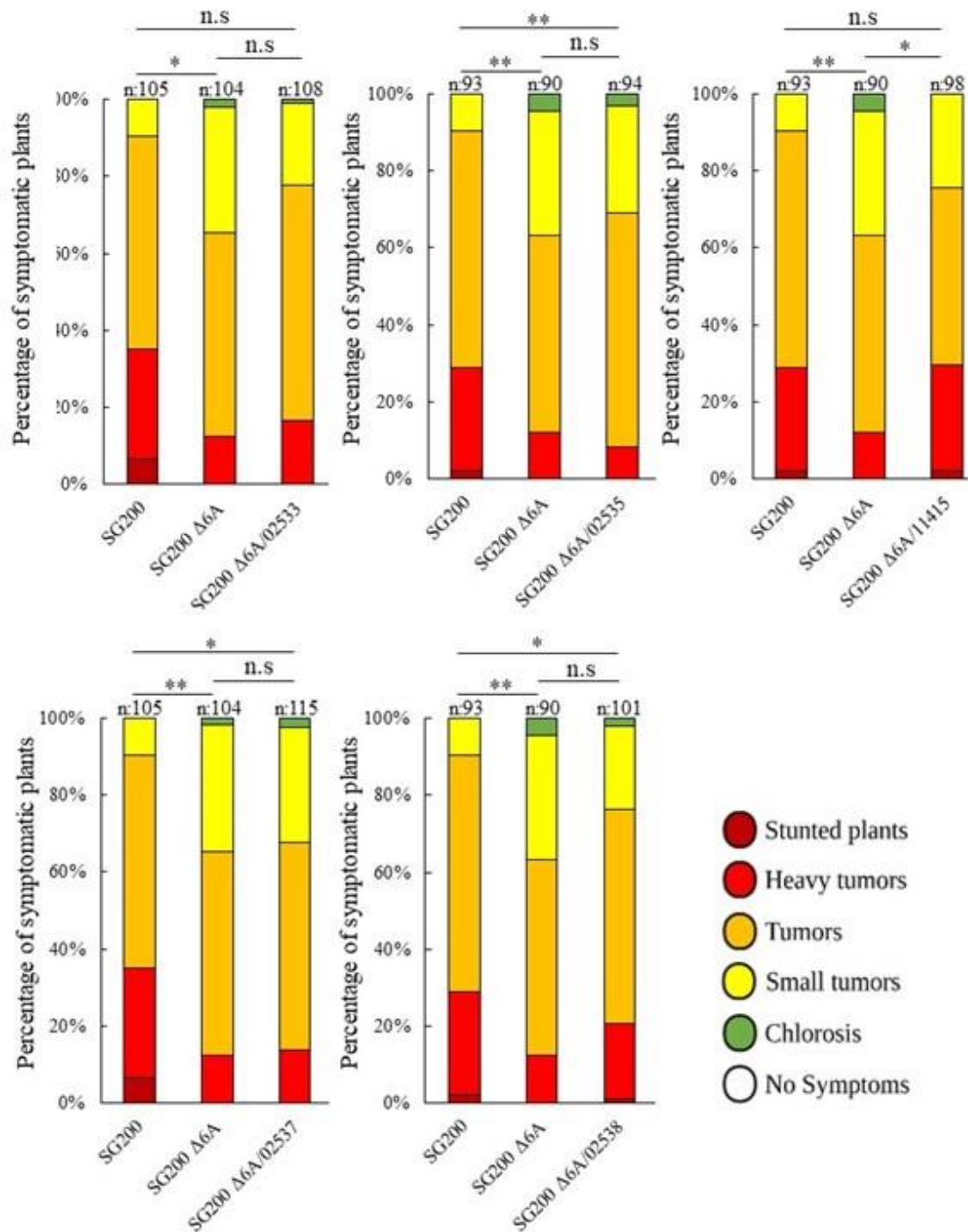


**Figure 13: Virulence assay of single gene cluster 6A complementation strains:** Virulence assay performed for the complementation of cluster 6A with transcript units generated with the MoRFunG toolkit. The strains SG200Δ6A/02533, SG200Δ6A/02535, SG200Δ6A/11415, SG200Δ6A/02537 and SG200Δ6A/02538 were evaluated and compared with the SG200 and SG200Δ6A. Disease rates are given as a percentage of the total number of infected plants. Three biological replicates were carried out. “n” represents the number of infected Golden Bantam maize seedlings. Significant differences between strains were analyzed by unpaired Student’s t-test analysis (\*:  $P \leq 0.05$ , \*\* $P \leq 0.01$ , n.s = no significance).

The virulence assay (Figure 13) revealed that the strains complemented with *umag\_02535*, *umag\_02537* or *umag:02538* in the SG200  $\Delta$ 6A genetic background were not able to revert the virulence defect of the cluster deletion. In the case of the complementation with *umag\_02533*, the mutant exhibited a similar phenotype than the SG200  $\Delta$ 6A, nevertheless the statistical results did not show significant differences either with SG200 or the cluster deletion strain. This intermediate phenotype could be attributed to a partial complementation with the effector gene *umag\_02533*. On the other hand, the strain SG200  $\Delta$ 6A/11415 fully complemented the virulence defect of the cluster deletion. Preliminary experimental data indicates that SG200 $\Delta$ 6A/11417 and SG200 $\Delta$ 6A/02540, are not capable of complementing the virulence phenotype of SG200 $\Delta$ 6A (data not shown), but additional biological replications need to be done to avoid statistical errors in the conclusions.

Complementing the SG200 $\Delta$ 6A strain with individual transcript units created using the MoRFunG toolkit provided valuable insights regarding the role in virulence of specific effector genes within the cluster 6A. These findings were particularly valuable given the presumed functional redundancy of these genes, making them challenging to assess through knockout approaches.

### **2.3 Endogenous promoters from *Ustilago maydis* included in the MoRFunG toolkit**

One of the greatest advantages of the MoRFunG toolkit, is the possibility to manipulate gene expression through the creation of tailor-made transcript units. These transcript units ideally exhibit a predictable expression pattern, achieved through the exchange of promoter regions. Endogenous promoters from effector genes of *U. maydis* were selected to be included in the MoRFunG toolkit. The selection criteria was based on the expression pattern of their effector genes (Lanver *et al.*, 2018b). The two main standards for selection were: The time of up-regulation and the presence of a peak of expression at a specific time point during the biotrophic stage of *U. maydis*. In this study, a peak of expression is understood as the accumulation of 30% or more of the total amount of reads in a single time point, concerning the total amount of reads across all the time points. Due to differences between the *U. maydis* strain and maize line used by Lanver *et al.*, (2018a) and this study, qRT-PCRs were performed to confirm that the expression patterns were the same under the experimental conditions of this study.

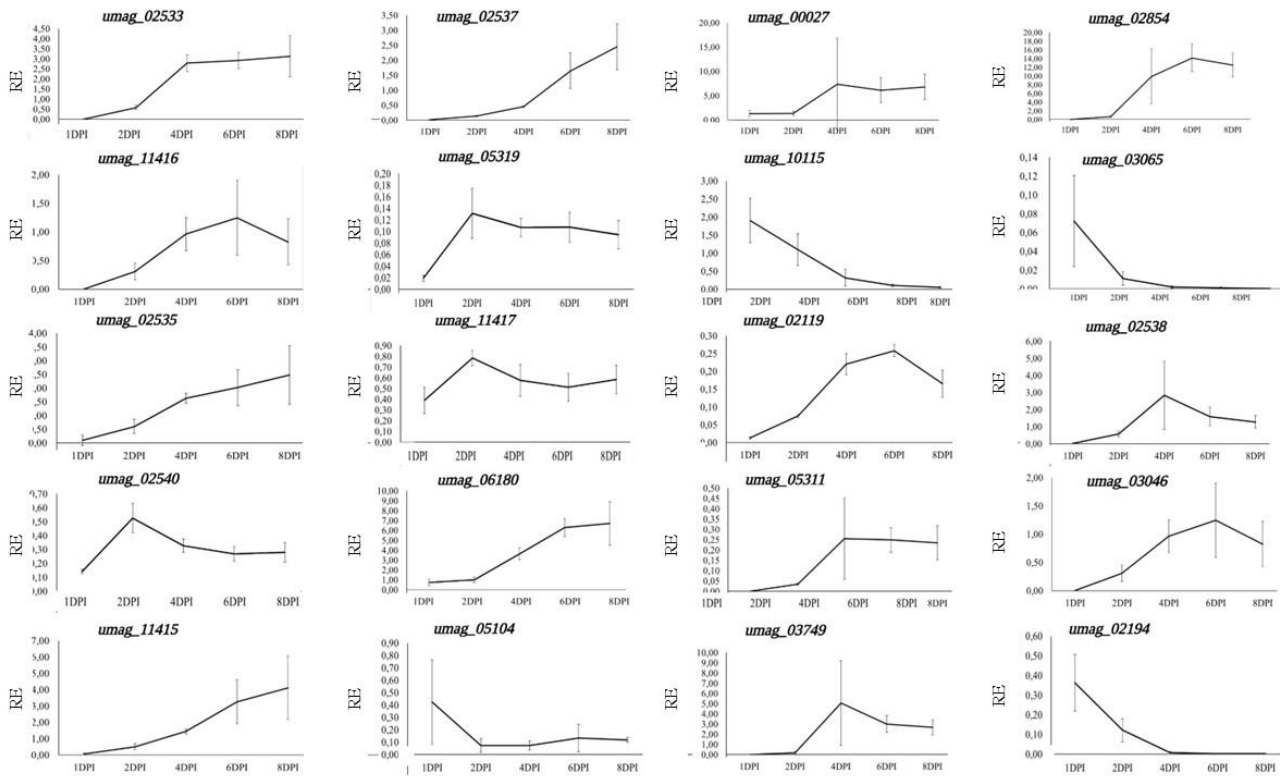


**Figure 14: qRT-PCR Native gene expression for promoter selection:** qRT-PCRs performed for most of the effector genes whose promoters were included in the MoRFunG toolkit. The samples were infected maize leaves with *U. maydis* SG200 (3<sup>th</sup> leaf, approximately 1 cm below the inoculation point, and approximately 4 cm long). The infections were performed at the stage of 3<sup>rd</sup> leaf. All the gene expression data was normalized against the housekeeping gene *ppi*. The “y” axis shows the relative expression (RE) of each gene in relation with *ppi*. The relative expression was quantified via qRT-PCR. Each time-point (1, 2, 4, 6 and 8 dpi) show the average expression of the genes from 3 independent biological replicates and two technical replicates, in ratio to *ppi* ( $2^{-\Delta C_t}$ ).

The selected effector gene’s promoters (Figure 14) were divided into 3 main categories based on their peak of expression: early promoters (peak between 0 and 2 dpi), middle promoters (peak at 4 dpi) and late promoters (peak at 6 dpi or later). Promoters that exhibited an expression pattern comparable to the ones from (Lanver *et al.*, 2018b), were cloned into MoRFunG level 0 modules. Promoter regions were defined as one Kb (Kilobase) upstream region (promoters of the cluster 6A were cloned with this criteria), or until the stop codon of the upstream adjacent gene. Promoters included in the MoRFunG toolkit are stated in Table 1 as modules of transcript units in level 0.

<b>Promoter</b>	<b>Category</b>	<b>Vector Level 0</b>
<i>umag_02533</i>	Middle	<i>pL0M-PU-umag_02533</i>
<i>umag_11416</i>	Middle	<i>pL0M-PU-umag_11416</i>
<i>umag_02540</i>	Early	<i>pL0M-PU- umag_02540</i>
<i>umag_11415</i>	Middle-late	<i>pL0M-PU- umag_11415</i>
<i>umag_02535</i>	Middle	<i>pL0M-PU- umag_02535</i>
<i>umag_02538</i>	Middle	<i>pL0M-PU- umag_02538</i>
<i>umag_02537</i>	Middle-late	<i>pL0M-PU- umag_02537</i>
<i>umag_05319</i>	Middle	<i>pL0M-PU- umag_05319</i>
<i>umag_11417</i>	Early-middle	<i>pL0M-PU- uma_11417</i>
<i>umag_06180</i>	Middle	<i>pL0M-PU-Uumag_06180</i>
<i>umag_05104</i>	Early	<i>pL0M-PU- umag_05104</i>
<i>umag_03046</i>	Late	<i>pL0M-PU- umag_03046</i>
<i>umag_00027</i>	Middle	<i>pL0M-PU- umag_00027</i>
<i>umag_10115</i>	Early	<i>pL0M-PU- umag_10115</i>
<i>umag_02119</i>	Middle	<i>pL0M-PU-umag_02119</i>
<i>umag_05311</i>	Middle	<i>pL0M-PU- umag_05311</i>
<i>umag_03749</i>	Middle-late	<i>pL0M-PU- umag_03749</i>
<i>umag_02194</i>	Early	<i>pL0M-PU- umag_02194</i>
<i>umag_02851</i>	Early	<i>pL0M_PU- umag_02851</i>
<i>otef Promoter</i>	Strong constitutive	<i>pL0M_PU_otef</i>
<i>umag_06065</i>	Early	<i>PL0M_PU- umag_03065</i>

**Table1: Promoters Level 0 Modules MoRFunG toolkit:** Promoters included in the MoRFunG.

### **2.3.1 Evaluation of endogenous promoter's activity in ectopic simultaneous multi-gene integration without insertion of resistance cassettes**

#### **2.3.1.1 *ip* locus Integration**

The MoRFunG toolkit aims to simplify and systematize the cloning process in *U. maydis*. As described previously, the cluster complementation done with this methodology was successfully achieved in the native locus. Nevertheless, this type of recombination event requires the generation of specific flanking regions depending on the genomic location.

In *U. maydis* the *ip* locus has been established as a well-defined ectopic integration site. The *ip* locus integration methodology uses the systemic inhibitor of fungal growth carboxin (cbx) as selection marker. The DNA fragments can be integrated in the *ip* locus through homologous recombination. The use of this selection marker was first described by (Broomfield & Hargreaves, 1992), who demonstrated how a single amino acid change in the iron-Sulphur subunit of the Complex II (succinate-ubiquinone reductase *umag\_00844*) involved in the respiratory electron transport in mitochondria, confers resistance to cbx. Since then, this locus is routinely used in heterologous gene expression and complementation studies in *U. maydis* (Loubradou *et al.*, 2001). For homologous recombination in the *ip* locus, the sequence of *umag\_00844* is used as flanking regions for the DNA to be inserted. The left flank is the second half of the coding sequence from *umag\_00844* presenting the two nucleotides change described by (Broomfield & Hargreaves, 1992). The right flank contains the first half of the “wild type” coding sequence of *umag\_00844*. After the recombination event, a duplication of the gene *umag\_00844* is generated, and one of the copies of *umag\_00844* contains the nucleotides change, making the transformant strains cbx resistant (Figure 15 A). The mutants created with this technique are easy to select and to confirm by southern blot analysis. The disadvantage for this methodology is the incorporation of resistance cassettes, and the possibility of unwanted multiple integrations.

With the aim of standardizing the MoRFunG toolkit, and to include modules that can be used for ectopic insertions in known locations, the recombination in the *ip* locus was adapted to the MoRFunG toolkit. Initially experiments combining CRISPR-Cas mediated double strand break together with homologous recombination with MoRFunG vectors (with appropriate flanks for the *ip* locus) were done to achieve ectopically insertions of constructs in this genetic location (scheme not shown). These experiments were not successful because all the strains



generated showed a genotype compatible to the wild type SG200 in southern blot analysis (Supplementary section 6.8.1 and supplementary Figure S6). The experimental evidence suggests an inefficient target of the sgRNA, with continues presence of the CRISPR vector that conferred resistance to cbx to the false positive transformants strains.

The second approach consisted of a single recombination event using only a MoRFunG level 2 vector to be inserted by homologous recombination into the *ip* locus. A difference than the conventional *ip* recombination, with the MoRFunG methodology, the succinate dehydrogenase gene *umag\_00844* is not duplicated (Figure 15B). The advantages of this homologous recombination alternative system are the low probabilities to generate unwanted multiple integrations, and the minimal modification of the genetic background at the insertion point. In contrast to *in-loci* complementation using MoRFunG toolkit, where the plasmids used as donor DNA were introduced in *U. maydis* without previous linearization, for the *ip* homologous recombination a digestion of the Level 2 vectors with the restriction enzyme *SspI* is required prior transformation.

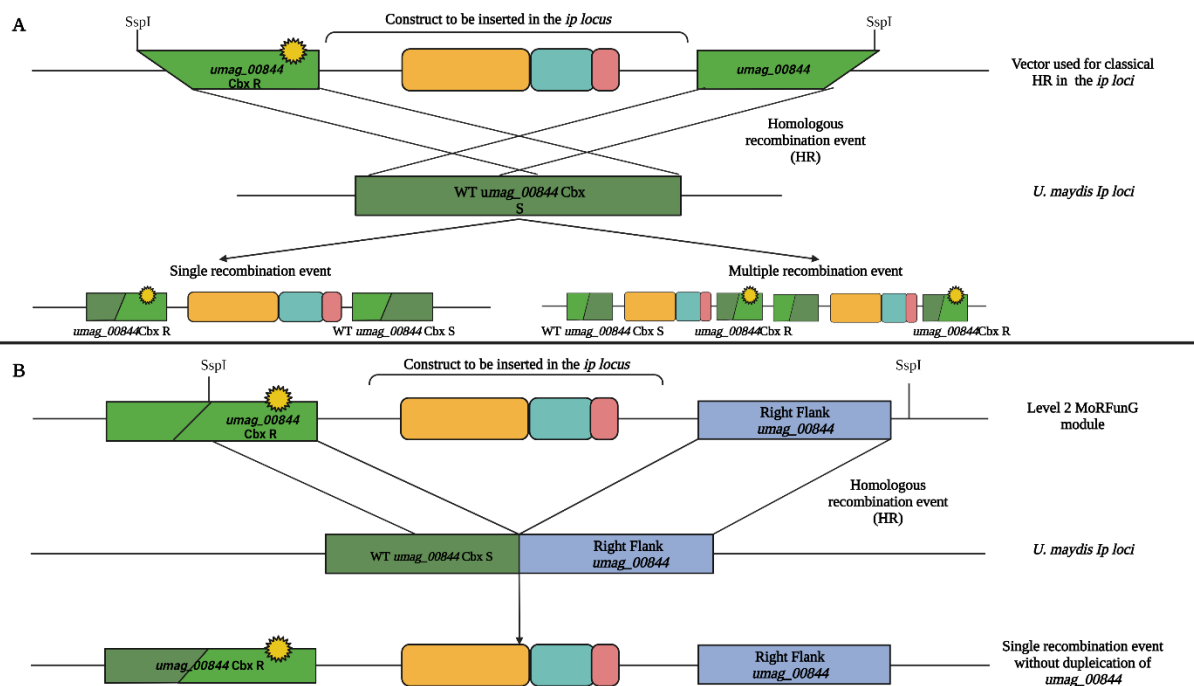


**Figure15: *ip* locus complementation:** **A.** Scheme of the conventional homologous recombination in the *ip* locus with gene duplication by incorporation of a resistance cassette. **B.** Homologous recombination in the *ip* locus generated with the MoRFunG toolkit L2 vector. Yellow circles represent the mutation point that gives cbx resistance (cbx R). Figure created with BioRender.com.

*U. maydis* transformations done using this method showed a lower number of transformants in contrast with the conventional ectopic integration in the *ip* locus (author's personal observations). I hypothesize that potentially, the large size of the vectors used could have a direct impact on the efficiency of the transformation. On the other hand, the system's advantages rely on the high probability of cbx resistant strains to contain the right DNA insertion. Except for the strains generated in the work frame of the cluster 6A experiments, all the other strains generated this study were done using this methodology.

### 2.3.2 Multi-tag ectopic integration

The first successful ectopic integration for combined gene expression in the *ip* locus done with the MoRFunG toolkit, consisted of a "Multi-tag" Level 2 construct. The level 2 plasmid included the left and right flanks for the *ip* locus (Figure 15 B), and three transcript units to be ectopically inserted. The strain named SG200 PU10115:*gfp*:NosT\_PU03749:*mCherry*:NosT\_PU03046:*cfp*\_NosT (shortly mentioned in this study as "multi-tag") consisted of three tailor made transcript units. Each transcript unit contained a promoter sequence (PU) of the genes *umag\_10115*, *umag\_03749* or *umag\_03046*, leading to the expression of the ORFs of *gfp*, *mCherry* and *cfp* respectively as schematized in Figure 16. Each transcript unit in level 1 also had a *Nos* terminator. The sequence from *umag\_00844* with the two base pairs modification for cbx resistance was used as left flank of the construct, and the genomic sequence downstream the *umag\_00844* as right flank.

The promoters used were selected based on their time of up-regulation in combination with their peak of expression. In this construct the *umag\_10115* is an early promoter, peaking at 1-2 dpi, the *umag\_03749* peaks at 4 dpi, and *umag\_03046* promoter has its peak of activity late (6-8 dpi) during the infection process. As mentioned previously, the pattern of expression of these genes was first selected based on RNAseq data (Lanver *et al.*, 2018a) and corroborated in qRT-PCRs with the solo-pathogenic strain SG200 (Figure 14).

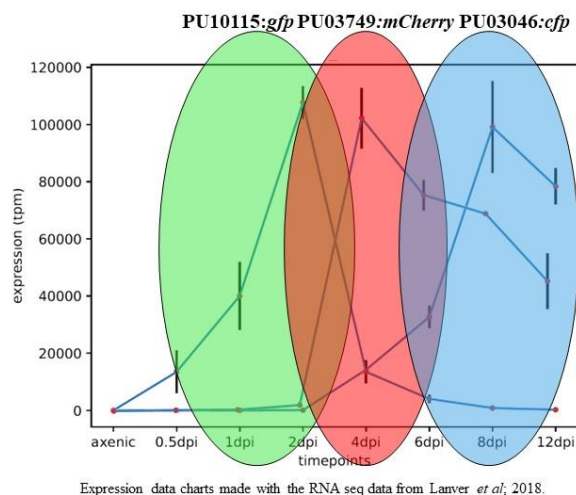


**Figure 16: Schematic representation of the pattern of activity of the early, middle, and late promoters for the multi-tag construct.** The green circle represents *gfp* under the control of the early promoter PU10115. The red circle represents *mCherry* under the control of the middle promoter PU030749. The blue circle represents *cfp* under the control of the late PU03046 promoter. Expression pattern from (Lanver *et al.*, 2018b).

After confirmation of the correct genomic insertion by southern blot (Supplementary Figure S7), one selected strain was evaluated in confocal microscopy to assess the production of the protein GFP under the control of the early promoter PU10115.

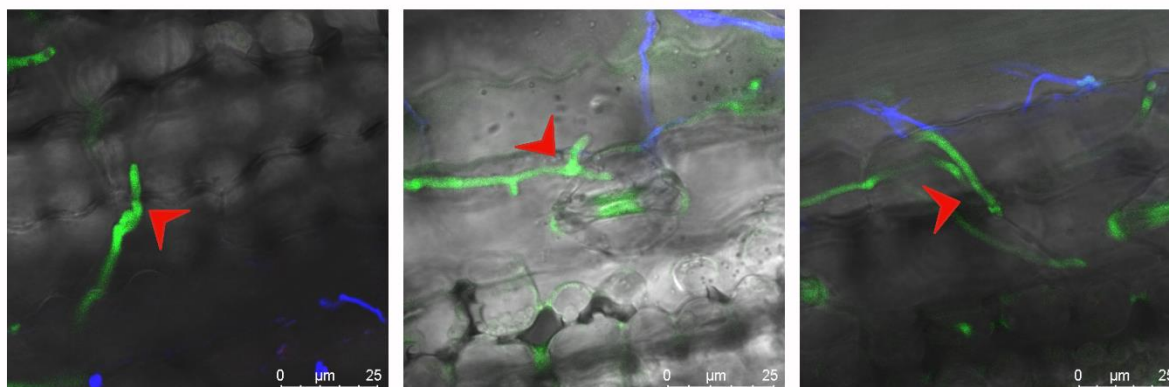


**Figure 17: Confocal microscopy of the “multi-tag *Ustilago maydis* strain: SG200 PU10115:*gfp*:NosT\_PU03749:*mCherry*:NosT\_PU03046:*cfp*\_NosT (SG200 Multi-tag)** Confocal microscopy images of maize leaves (3<sup>rd</sup> leaf) 1 cm below the infection site at 48 hpi. Example images show intracellular hyphae of the *U. maydis* multi-tag strain. Penetrating hyphae expressing GFP driven by the PU10115 are indicated with red arrows. The blue contrast was given by a calcofluor white staining of the hyphae located on the leaf surface. Figure created with BioRender.com.

In the microscopy images, it was possible to observe the fungal hyphae of the mutant being able to penetrate and proliferate in the plant tissue. The images also showed the expression of GFP at 48 hpi and the absence of mCherry and CFP (Figure 17). Although no virulence assay

was performed due to time constraints, in the maize infections done with this strain for sample collection, I could not see differences between the mutant strains and the SG200 in the leaves that I examined. The observation of fungal hyphae expressing GFP in infected plant material at 48 hpi suggests that the early promoter PU10115 is active in the *ip* locus. The results from this experiment are of a qualitative nature, not being possible to draw conclusions about the expression pattern during the whole infection process or the strength of up regulation of the promoter.

The expression of mCherry or CFP was not possible to confirm by confocal microscopy. The visualization of fungal hyphae in manual longitudinal cuts of maize leaves has technical limitations. With the progression of the disease, the fungus develops in deeper layers of tissue, being the resolution of the confocal microscopy not enough to detect fluorescence after 48 hpi. For the visualization of mCherry and CFP by confocal microscopy, additional studies need to be done.

In addition to the confocal imaging, qRT-PCRs were performed in these samples. The results were not conclusive (data not shown), probably due to a poor RNA quality, or sample interference due to the tandem arrangement of sequences with a high grade of similarity (*gfp*, *cfp* and *Nos* terminator). To show whether the *mCherry*'s ORF under the PU03749 was being transcribed, a screening PCR of the complete *mCherry* coding sequence using cDNA as a template was performed. This PCR evaluated the presence/absence of the translated *mCherry* sequence, at 1,2,4,6 and 8 dpi for the multi-tag samples, SG 200 (negative control) and an additional positive amplification control form a plasmid containing *mCherry*.

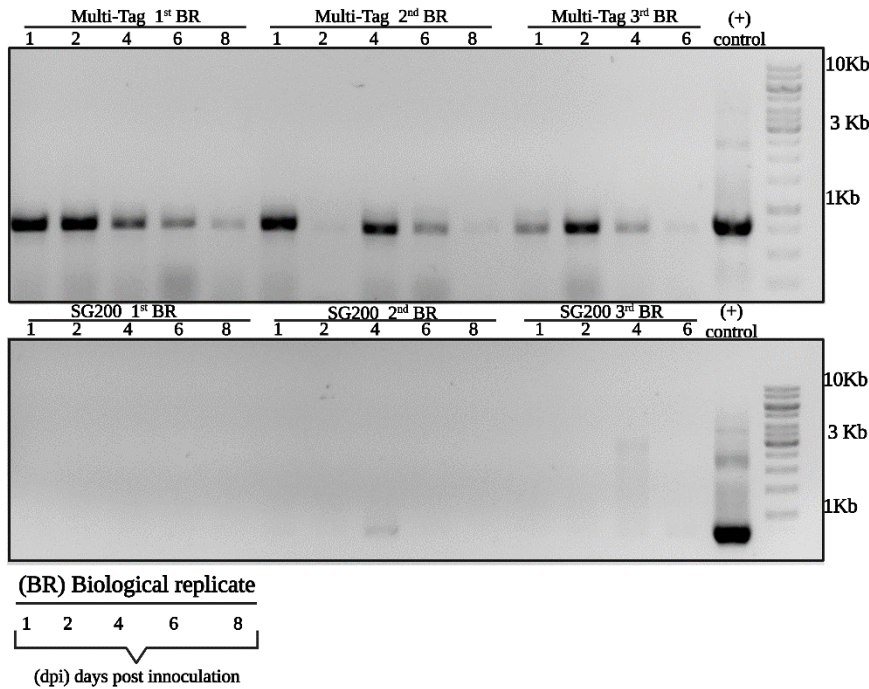


**Figure18: PCR from cDNA template to evaluate the translation of *mCherry* ORF:** PCR from cDNA obtained from infected plant material with SG 200 multi-tag and SG 200. The positive control is the L0 MoRFunG module plasmid pL0M-C-*mCherry*(FMTK38) containing the coding sequence of *mCherry*. The expected size for a positive amplification is 738 bp (base pairs).

Forward primer: TTTGAAGACAAAATGGTGAGCAAGGGCGAGG

Reverse primer: TTTGAAGACAAAAGCCTACTTGTACAGCTCGTCCATG

Figure created with BioRender.com.

The PCR's result showed amplification bands matching the size of the *mCherry*'s sequence for the multi-tag samples, also present in the positive control amplification. On the contrary, there was no amplification in the samples of the SG200 treatment (Figure 18). This result suggests that in the maize plants infected with the multi-tag construct, the *mCherry* ORF was translated to RNA, indicating that the promoter PU03749 was active in the *ip* locus. With this information it is not possible to conclude about the expression of *mCherry* at a protein level. Actually, in the samples corresponding to 1 and 2 dpi, amplification of the cDNA of *mCherry* was observed in all the early time-points in all the biological replicates for the mutant strain, although the fluorescence of the protein was not detected with confocal microscopy at that specific time-point, probably due to post-transcriptional regulations involving the UTRs.

In synthesis, this result suggests that *mCherry* can be translated under the control of the *umag\_03749*'s promoter in the *ip*-locus under the tested conditions. More experiments need to be done to draw conclusions about the expression of *mCherry* at a protein level. Concerning the expression of CFP, technical difficulties in the detection were experienced. The absence

of CFP in early stages of infection shown in the confocal microscopy pictures suggests that the promoter does not exhibit an early activation, but it was not possible to know if the promoter was active during later stages of the infection process. In contrast to *mCherry*, the sequence of *cfp* was impossible to distinguish from the sequence of *gfp* in PCR experiments.

In synthesis, the experimental data collected from the SG200 multi-tag strain (SG200 PU10115:*gfp*:NosT\_PU03749:*mCherry*:NosT\_PU03046:*cfp*\_NosT) indicates that two of the three promoters inserted ectopically were able to induce the transcription of the Tag's ORFs. Additional tests need to be conducted to complete the data set in this genomic location, including the quantitative characterization of the endogenous promoters when inserted ectopically, as well as their dynamic during the infection process. Some of these experiments are discussed in the outlook in the discussion section.

### 2.3.3 MoRFunG mediated $\Delta pep1$ combined complementation

Core effectors of *U. maydis* are essential for the disease establishment in the host. One of these effectors is the Pep1 protein, a host apoplastic peroxidase inhibitor. It was previously shown how *U. maydis*  $\Delta pep1$  was arrested upon penetration of the plant tissue, not producing any visible symptoms in infected maize plants (Doehlemann *et al.*, 2009), in that publication, the authors also explained the relevance of the Pep1 effector protein in the suppression of the host immune responses. The strain SG200  $\Delta pep1$  showed a massive induction of the plant's immune response, and arrestment of fungal proliferation in infected maize seedlings (Doehlemann *et al.*, 2009). To evaluate whether MoRFunG-mediated  $\Delta pep1$  complementation could rescue the impaired pathogenicity of SG200  $\Delta pep1$ , mutants with tailor-made transcript units, expressing *pep1* under the combined control of different endogenous promoters were created.

As structural level 0 modules, terminally tagged-*pep1* ORFs with *gfp* or *mCherry* were introduced to the MoRFunG system. As promoters, the endogenous promoters (PU) from *umag\_02851* and *umag\_11415* were used. These promoters were selected based on their expression patterns (Lanver *et al.*, 2018b). The gene *umag\_02851* shows early upregulation with a shutdown at approximately 2dpi, while the *umag\_11415* shows a later upregulation (starting at 2dpi) and it becomes progressively higher through the progression of the infection (Lanver *et al.*, 2018b). For this experiment three mutants were generated in the SG200  $\Delta pep1$  genetic background:

1.  $\Delta pep1/PU02851\_pep1:gfp:NosT -ip$
2.  $\Delta pep1/PU11415\_pep1:gfp:NosT -ip$
3.  $\Delta pep1/PU02851\_pep1:gfp:NosT\_PU11415\_pep1:mcherry:NosT-ip$

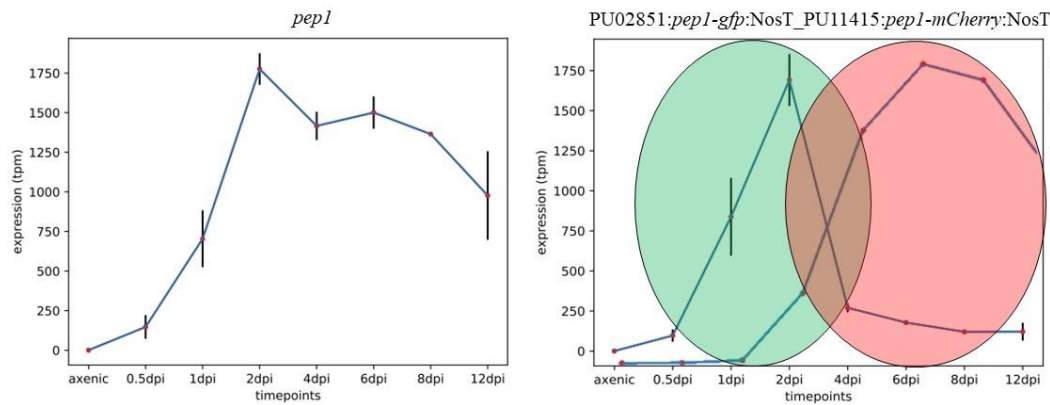


**Figure 19: Scheme of the dual expression pattern of *pep1* in the strain constructed with the MoreFunG toolkit:** In the left the expression pattern of *pep1* is visualized. In the right the combination in the expression pattern of the genes *umag\_02851* and *umag\_11415*. The promoters for those genes (*umag\_02851* and *umag\_11415*) were used to lead the expression of *pep1:gfp* and *pep1mCherry* respectively. The green and red circles are a graphical visualization of the experiment design, representing the expression of the different *pep1*-tagged genes. Between 2 and 4 dpi is expected that the expression level from both transcript units show an additive effect in the strain #3 that contains two copies of *pep1* under the control of two different endogenous promoters: SG200  $\Delta pep1/PU02851\_pep1:gfp:NosT\_PU11415\_pep1:mCherry:NosT-ip$ . The strain SG200  $\Delta pep1/PU02851\_pep1:gfp:NosT-ip$  is represented only with the green circle and the strain SG200  $\Delta pep1/PU11415\_pep1:mCherry:NosT-ip$  only with the red circle. Expression pattern data (Lanver *et al.*, 2018b). Data processed and graphics made by Dr. Jasper Depotter.

The tailor-made transcript units expressing *pep1* under the control of nonnative endogenous promoters were done with the MoRFunG toolkit and transformed into the SG200  $\Delta pep1$  genetic background as schematized in Figure 19. For the mutant #1 containing only one copy of *pep1* under the control of the early promoter PU 02851 ( $\Delta pep1/PU02851\_pep1:gfp:NosT -ip$ ) it was expected that the early upregulation of *pep1* allows penetration and early proliferation of *U. maydis*, lost in the  $\Delta pep1$  strain. It was assumed that the strain would not be able to fully complement the virulence defect due to the strong downregulation that the endogenous promoter shows after 2 dpi, considering the experimental evidence that suggest that Pep1 is required along the whole infection process (Doehlemann *et al.*, 2009). For the mutant #2, that contains a single copy of *pep1* under the control of the middle/late promoter PU 11415 ( $\Delta pep1/PU11415\_pep1:gfp:NosT ip$ ), none complementation was likely to occur, because the PU11415 starts its up-regulation slowly around 2 dpi. Since Pep1 is required in the establishment of biotrophy, the upregulation by the PU11415 is beyond the critical time limit for the *pep1* expression. For this reason, a non-virulent strain was expected. On the other

hand, for the combinatorial mutant #3 ( $\Delta pep1/PU02851\_pep1:gfp:NosT\_PU11415\_pep1:mCherry:NosT-ip$ ), it was assumed that the combination of the endogenous promoters PU02851 and PU11415 could potentially simulate the activity of the *pep1* promoter, complementing the virulence defect of the SG200  $\Delta pep1$ . All the generated strains were confirmed by southern blot analysis (Supplementary section 6.8.3).

Golden Bantam maize plants were infected at the stage of 3<sup>rd</sup> leaf with the goal of collecting leaves samples for total RNA extraction. Virulence assays were not performed for these strains. Nevertheless, in the 12 dpi plants that I observed, I was not able to detect tumor development in any of the mutants evaluated. The inability to form tumors was expected for mutants containing only one copy of *pep1* under the control of PU02851 or PU11415. The reason is that those promoters exhibited an expression pattern that individually does not meet the requirements for the expression of *pep1* through the whole infection process. Contrarily to what was expected, the complementation with *pep1* under the control of the combination of promoters ( $\Delta pep1/PU02851\_pep1:gfp:NosT\_PU11415\_pep1:mCherry:NosT-ip$ ) showed a virulence defect and no tumors were observed.

In order to evaluate if *pep1* was being expressed, and how far the infection progressed during early stages, plant material infected with the MoRFunG *pep1* complementation strains were evaluated with confocal microscopy.



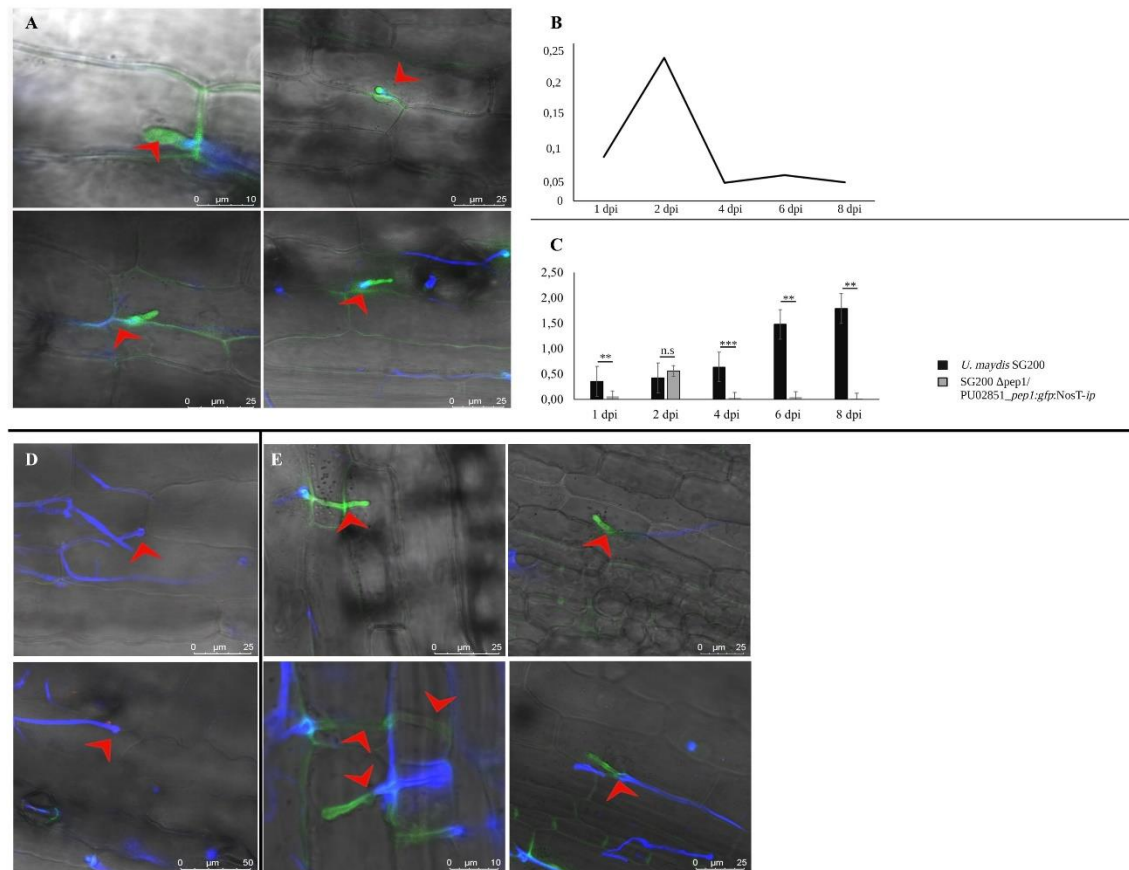


**Figure 20: SG200  $\Delta pep1/pep1$  MoRFunG complementation: microscopy images and qRT-PCR.** All samples for confocal microscopy were taken from the 3<sup>th</sup> infected maize leaf, 1 cm below the infection point, at 48 hpi and treated with calcofluor white staining solution for hyphae visualization. **A.** Confocal microscopy of SG200  $\Delta pep1/PU02851\_pep1:gfp:NosT$ . Red arrows indicate penetration events with GFP expression. **B.** qRT-PCR results of total cDNA obtained from infected maize plants with the strain SG200  $\Delta pep1/PU02851\_pep1:gfp:NosT-ip$  at different stages post infection. The relative expression of *pep1* was normalized against *ppi*. **C.** Comparison between the relative expression of *pep1* in the SG200 strain and in the SG200  $\Delta pep1/PU02851\_pep1:gfp:NosT-ip$  complementation strain. Significant differences between strains were analyzed by unpaired Student's t-test analysis (\*:  $P \leq 0.05$ , \*\* $P \leq 0.01$ ). **D.** Confocal microscopy SG200  $\Delta pep1/PU11415\_pep1:mCherry:NosT-ip$ . Red arrows indicate unsuccessful penetration events. **E.** Confocal microscopy SG200  $\Delta pep1/PU02851\_pep1:gfp:NosT-PU11415\_pep1:mCherry:NosT-ip$ . Red arrows indicate successful penetration events.

The confocal imaging results showed that the strain SG200  $\Delta pep1/PU02851\_pep1:gfp:NosT-ip$  (*pep1* under the control of the early endogenous promoter PU02851, with a strong downregulation at 2dpi) could penetrate the plant tissue, and express GFP (Figure 20A), which indicates that the promoter was active and in consequence that Pep1 was expressed. The comparison between the expression of *pep1* from SG200  $\Delta pep1/PU02851\_pep1:gfp:NosT-ip$ , and the *pep1* expression in SG200 in the qRT-PCR at different stages post infection showed that at 2 dpi there were not significant differences between the mutant strain and the SG200 control. Conversely, at 1 dpi significant differences were observed between the expression of *pep1:gfp* under the control of the promoter PU02851 and the SG200 (Figure 20C), being the

expression of *pep1* in the mutant strain significantly lower. Taking into consideration the relevance of Pep1 in early stages of infection, the disparity between the expression levels of *pep1* at 1 dpi between the SG200 and the mutant strain, could be a primary determinant for the success of the fungal proliferation inside the host. The differences observed in the RT-pPCR between the “wild type” *pep1* and the *pep1* under the control of the PU02851, could be attributed to either a weaker strength of up-regulation at 1 dpi, or to a later upregulation of the promoter. The analysis of the expression pattern of the *pep1* expressed under the PU02851 shows a comparable behavior the native effector of the promoter (*umag\_02851*) during the whole infection process (Figure 20B).

The confocal microscopy results for SG200  $\Delta pep1$ /PU11415\_ *pep1*:*mCherry*:NosT-*ip* (*pep1* under the control of the middle/late endogenous promoter PU11415), showed failed attempts of penetration of the fungal hyphae, and the expression of mCherry was not observed in confocal images (Figure 20D). These results were expected because the endogenous promoter PU11415 starts its upregulation slowly after 1dpi, peaking at 4 dpi and keeping the activity at a later stage of infection (Lanver et al., 2018a) which is past the critical time point for Pep1 to be able to fulfill its function. In consequence, the penetration was unsuccessful, and the infection process aborted.

The 3<sup>rd</sup> mutant containing *pep1* under the control of the endogenous promoters PU 02851 and PU11415 (SG200  $\Delta pep1$ /PU02851\_ *pep1*:*gfp*:NosT\_PU11415\_ *pep1*:*mCherry*:NosT-*ip*), was also unable to rescue the tumor formation under the mentioned conditions. Although the confocal images showed fungal penetration with expression of GFP (Figure 20E), and proliferation inside the host’s cell, the fungal development was weak. The inability of the mutant strain to recover the virulence of the  $\Delta pep1$  could be explained by the difference in expression of the first copy of *pep1* under the control of the *umag\_02851* promoter and the wild type *pep1*.

It was shown that Pep1 plays an essential role for the establishment of the biotrophy (Doehlemann *et al.*, 2009), reason for which even the smallest difference in the time of up regulation could have detrimental effects in the virulence performance of *U. maydis*. With the aim to increase the expression of *pep1* at the beginning of the infection process, an extra copy of *pep1-mCherry* under the control of the promoter from *umag\_03065* (PU03065) was added to the MoRFunG complementation construct. The selection of this promoter was based in the association of the *umag\_03065* with the formation of appressoria (Mendoza-Mendoza *et al.*,

2009). The new strain contained 3 copies of *pep1* under the control of three different promoters (SG200  $\Delta pep1$ /PU03065\_ *pep1*:*mCherry*:NosT:PU02851\_ *pep1*:*gfp*:NosT\_PU11415\_ *pep1*:*mCherry*:NosT-*ip* shortly mentioned in this study as SG200  $\Delta pep1$ /*pep1*). The same construct was transformed into SG200 as a positive control.

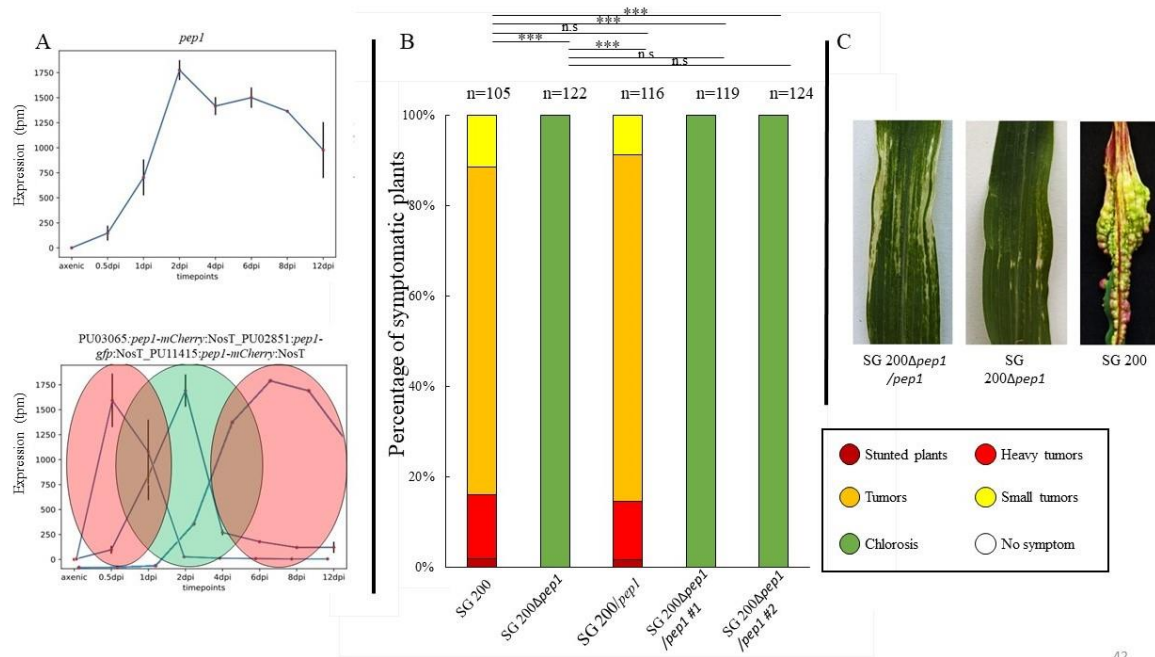


**Figure 21: Complementation of  $\Delta pep1$  with three endogenous promoters.** **A.** Expression pattern of *pep1* (up) and of the three effector genes whose promoters were used for expressing *pep1* with the MoRFunG toolkit (*umag\_03065*, *umag\_02851* and *umag\_11415*). The promoters PU03065, PU02851 and PU11415 were used to lead the expression of *pep1mCherry*, *pep1:gfp* and *pep1 mCherry* respectively. The green and red circles are a graphical visualization of the experiment design, representing the expression of the different tagged- *pep1*. Between 2 and 4 dpi was expected that the expression level from both transcript units show an additive effect **Strain name:** SG200 $\Delta pep1$ PU03065\_ *pep1*: *mCherry*:NosT /PU02851\_ *pep1*:*gfp*:NosT\_PU11415\_ *pep1*:*mCherry*:NosT-*ip* (shortened SG200 $\Delta pep1$ /*pep1*). Expression pattern data (Lanver *et al.*, 2018b). Data processed by Dr. Jasper Depotter. **B.** Virulence assay performed with the strains SG200, SG200 $\Delta pep1$ , SG200/*pep1* (MoRFunG *pep1* expression in wild type background), and SG200 $\Delta pep1$ PU03065\_ *pep1*:*mCherry*:NosT /PU02851\_ *pep1*:*gfp*:NosT\_PU11415\_ *pep1*: *mCherry*:NosT-*ip*). Disease rates are given as a percentage of the total number of infected plants. Three biological replicates were carried out. “n” represents the number of infected Golden Bantam maize seedlings. Significant differences between strains were analyzed by unpaired Student’s t-test analysis (\*:  $P \leq 0.05$ , \*\* $P \leq 0.01$ , n.s = no significance). **C.** Example of the symptoms presented with the MoRFunG *pep1* complementation. To the left the MoRFunG complementation of *pep1* under the control of three endogenous promoters, in the middle the  $\Delta pep1$  phenotype and to the right a typical symptomatology of the fully virulent *U. maydis* SG200 (SG200 figure courtesy of Dr. Bilal Ökmen).

After confirmation of the strain by southern blot analysis (Supplementary section 6.8.3), two independent mutants for the  $\Delta pep1$  triple complementation as well as the SG200 control were used for infection assays in maize plants. While the triple complementation construct in the SG200 genetic background showed a normal development regarding tumor formation, the triple complementation strains in the  $\Delta pep1$  genetic background were surprisingly not able to

complement the virulence defect of their progenitor strain (Figure 21B). The visible symptoms were mainly chlorosis, observed with more frequency in the complementation strain than in the plants infected with SG200  $\Delta pep1$ , although no tumor formation was present (Figure 21C). The fully virulent phenotype achieved by the strain containing the same construct in the SG200 genetic background suggests that the MoRFunG construct does not affect the biotrophy of *U. maydis*. In synthesis, these preliminary results imply that while the endogenous promoters can be active ectopically, they were not able to simulate the expression of the essential effector gene *pep1*.

## **2.4 New technologies for manipulation of gene expression, applied to *Ustilago maydis***

Gene expression and gene manipulation in *U. maydis* are of great interest to researchers. One promising advance in synthetic biology applied to gene manipulation is the use of light-regulated optogenetic approaches, enabling gene expression control through light impulses. In collaboration with Dr. Kung Tang (AG. Zurbriggen, HHU Düsseldorf) I set up a blue-on/blue-off optogenetic-system in the *U. maydis*-maize pathosystem.

The aim of the experiments carried out in this section were:

- To demonstrate proof of principle that optogenetic switches allow in *U. maydis* a stable light-regulated expression of the effector gene *see1* and its secretion in the absence of the host.
- Demonstrate that the implementation of the light switches in *U. maydis* does not affect the biotrophy.
- Demonstrate that the natural light-exposure of maize leaves, needed for efficient photosynthesis, does not affect the optogenetically light-regulated expression of the effector gene *see1* of *U. maydis* during the infection process.

### **2.4.1 Optogenetics blue-on and blue-off systems in *Ustilago maydis* strains**

The blue-on and blue-off optogenetic system for gene expression was originally optimized for *U. maydis* by the research led by Prof. Dr. Zurbriggen in Düsseldorf. Additionally, the quantitative characterization of a LOVpep/ePDZ-based blue light inducible gene expression system in *U. maydis* was described in the PhD dissertation of Dr. Lisa Cristin Hüsemann from AG Zurbriggen, University of Düsseldorf. With the aim to proof that the system can be utilized to manipulate gene expression through light stimulation in *U. maydis*, strains were generated for a light-inducible effector gene regulation during the infection process. To do this, the organ-specific effector *see1* (Seedling efficient effector 1 *umag\_02239*) required during tumor formation in maize seedlings (Redkar *et al.*, 2015) was selected to evaluate the performance of the light-inducible system in *U. maydis*. This effector gene was chosen because it has been previously shown that its ectopic overexpression did not increase the virulence of *U. maydis* in maize leaves (Redkar *et al.*, 2015). The vector system including the *see1* effector gene is schematized in Figure 3.

### **2.4.2 Stable light regulated *see1FLuc* expression and secretion of the See1FLuc complex in absence of the host**

To test if light stimulation can lead to the expression of genes of interest in absence of the host, the different *U. maydis* strains with light regulated switches were tested in axenic culture under different light conditions. The measurements were done by Dr. Kung Tang in the installation of AG Zurbriggen.

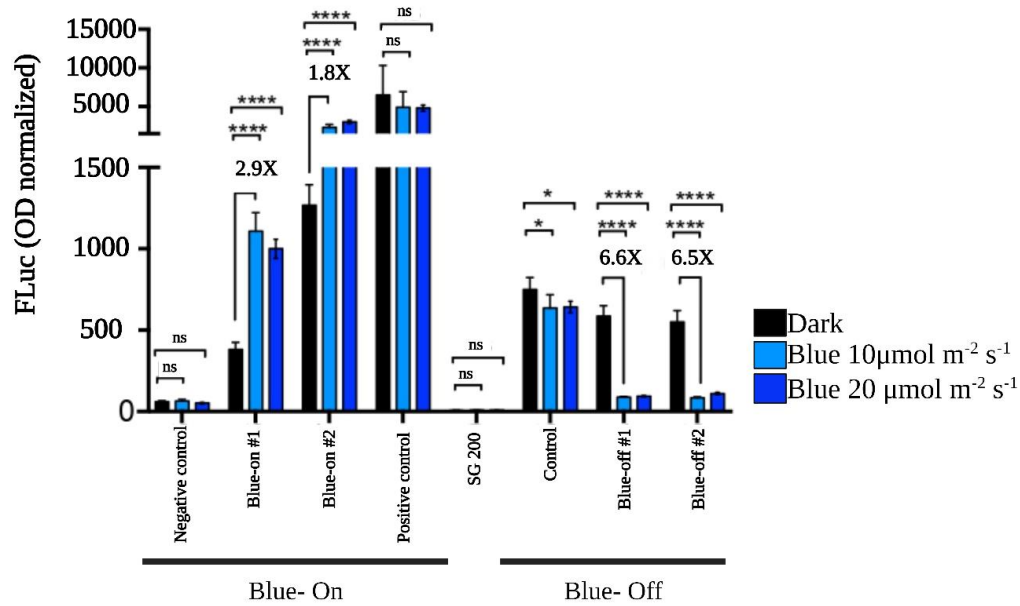
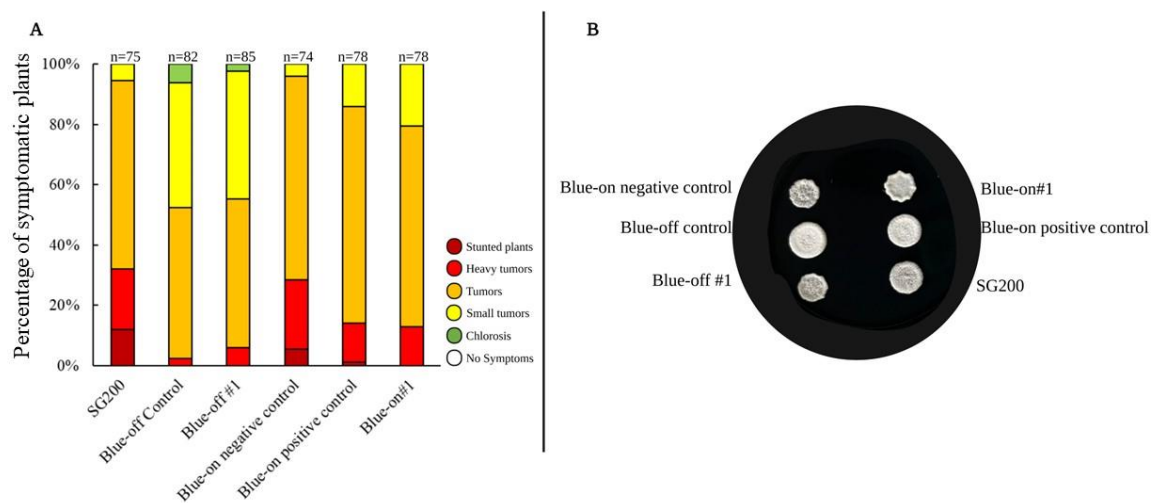


**Figure 22: FLuc expression of *U. maydis* in the blue-on and blue-off system, under different light conditions in YEPS<sub>light</sub> media:** The strains were inoculated in YEPS<sub>light</sub> medium and incubated overnight at 28 °C with shaking at 200 rpm. *U. maydis* precultures were placed into 24-well plates (OD<sub>600</sub> adjusted to 0.05 prior to the seeding) and incubated in light boxes at 10 or 20  $\mu\text{mol m}^{-2} \text{s}^{-1}$  blue light as well as in darkness. 80  $\mu\text{l}$  culture were taken from each well after 5 hours for FLuc measurement (method reference: Dr. Lisa Hüsemann PhD thesis). Bars are means  $\pm$ SEM of three biological replicates and four technical replicates. Statistics were performed via one-ANOVA. (\*\*\*\*, P value blue/dark < 0.0001; \*, P value blue/dark < 0.0332; ns = non-significant). This experiment, as well as the data analysis, was done by Dr. Kun Tang, group of Prof. Dr. Matias Zurbriggen, Institute of Synthetic Biology, Heinrich-Heine University of Düsseldorf. Figure modified with BioRender.com. Graphic done by Dr. Kun Tang.

The results show a significant level of detection of FLuc in the blue-on strains independently of the light intensity used, revealing substantial differences to their detection in dark incubation (Figure 22). The positive control (constitutive expression) on the other hand, showed similar levels of detection in all the conditions analyzed. The negative control in the blue-on system did not show significant activity in any of the light conditions evaluated in this experiment. For the blue-off strains, it was possible to observe a considerable activation in darkness, while the presence of blue light during this incubation period produced an inhibition in the expression *see1FLuc*. The preliminary experimental data suggest that optogenetic switches in *U. maydis* allow a stable light regulated gene expression in absence of the host under different light conditions.

### 2.4.3 *Ustilago maydis* optogenetic fungal strains and the maintenance of the biotrophic interaction with its host

To test if the fungal strains can maintain the biotrophy when the light switches are introduced into their genome, the fitness and virulence of the above-mentioned strains were assessed (Figure 23).



46

**Figure 23: Fitness evaluation of *U. maydis* optogenetic strains:** **A.** Preliminary virulence assay performed for the optogenetic *U. maydis* strains and the SG200 genetic background as control. Disease rates are given as a percentage of the total number of infected plants. Two biological replicates were carried out. “n” represents the number of infected Golden Bantam maize seedlings. **B** Filamentation assay on charcoal plate of all the optogenetic strains used for infection assays and the control/genetic background SG200.

All the strains used in this section were fully able to filament on charcoal plates, indicating their capability to form infectious filaments on the surface of maize leaves. The virulence assessment requires one additional biological replicate to provide statistically significant information. Nonetheless, the preliminary data showed that the 'blue-on' strains tended to have a phenotype like SG200, while the 'blue-off' strains exhibited a slightly reduced phenotype, possibly due to the constant expression of a repressor.

#### 2.4.4 Natural light exposure of maize leaves does not inadvertently affect the optogenetic light-regulated expression of *see1* in *U. maydis* during the infection process

To assess, whether natural light exposure of maize leaves affect the light-regulated expression of *see1* in the infection process, the expression of FLuc in maize seedlings infected with the different *U. maydis* strains included in the blue on and blue off optogenetic systems were evaluated under different light conditions (Figure 24).

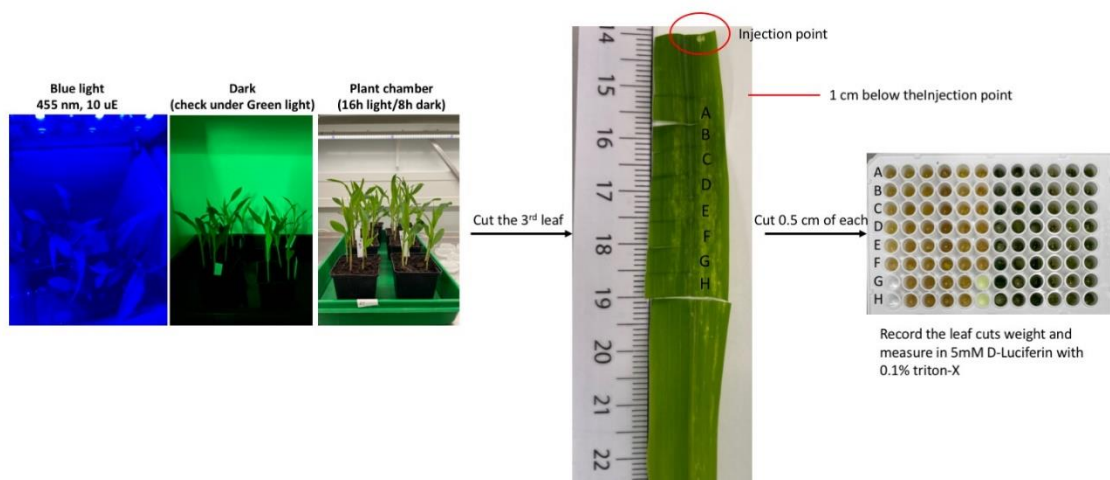
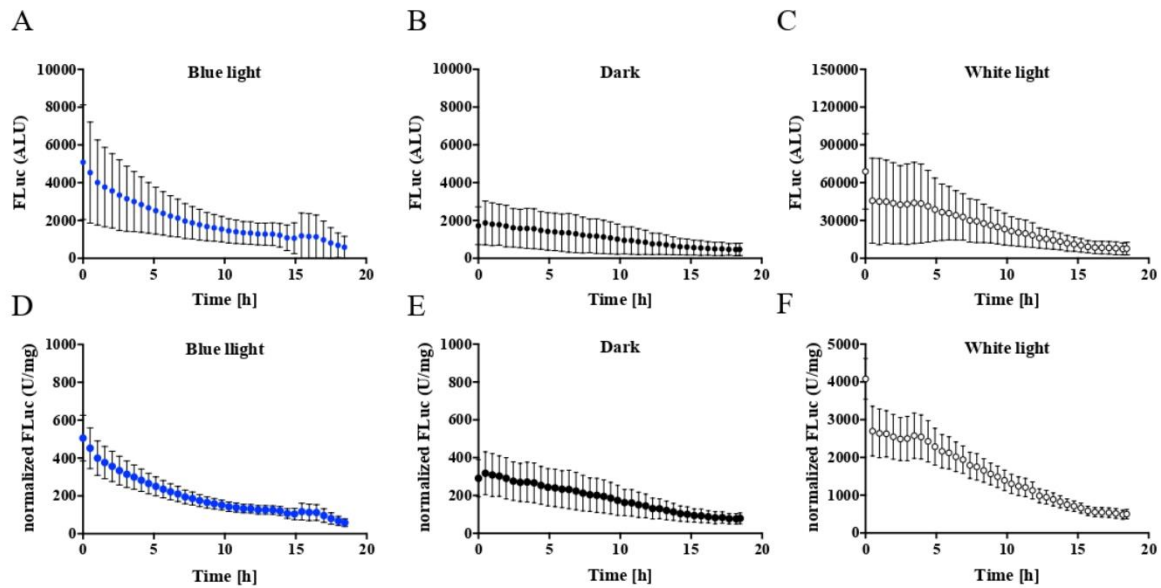


**Figure 24: Optogenetic experiment set-up in maize plants:** Seedling infections were done at the three leaves stage of Golden Bantam (7-days old, 4 plants per pot, 2-3 cm deep for seed, grow in greenhouse, actual temp. 22/20°C). The *U. maydis* SG200 strains pre-culture incubation, preparation, and injections are performed in dark or under green light. After injection, the plants are kept under three conditions: AG Zurbruggen\_plant chamber, dark or constantly 10 uE blue light illumination. In the case of SG200 successful infection, small tumors appeared after 4-6 dpi in the plant chamber. Figure courtesy of Dr. Kun Tang.

The results for this experiment were not conclusive. Only the positive control for the blue-on system with constitutive expression of *see1FLuc* exhibited expression in all the three conditions tested (white light, blue light, and darkness). This indicate that PIP-VP16 successfully binds to PIR3 in the promoter region activating the *see1FLuc* expression (Figure 25).





Positive control- Blue on system

**Figure 25: Establishment of FLuc kinetics on maize leaf.** (A-C) In 6 dpi, leaf samples of positive control of Blue-on system. Photo counts are recorded every 30 mins, sample **A** is under blue light illumination during the whole measurement; **B** and **C** are kept in dark during the whole measurement. Dots, indicate the mean of each measurement. (n=8 for blue and white, n=4 for dark) (D-F) the values in (A-C) are normalized to the weight of each leaf sample. Experiments carried out by Dr. Kun Tang, in the laboratory of Prof. Dr. Matias Zurbriggen, Institute of Synthetic Biology, Heinrich-Heine University of Düsseldorf. Infections were done by Ute Meyer. Original Figure Dr. Kung Tang, modified with Biorender.com

The strains containing the blue on switches did not show significant FLuc expression in any of the tested conditions. Prolonged exposure of the plants to constant blue illumination did not enhance the expression of FLuc (not shown). The same situation occurred for the strains containing the switches from the blue off system.

### 3 Discussion

#### 3.1 Proof of concept: the use of MoRFunG toolkit in *Ustilago maydis* and its ability to functionally complement large genomic deletions

Gene deletion assays for loss of functionality have been widely used in *U. maydis* to identify genes that encode for virulence factors. In order to confirm whether a deleted gene is responsible for an observed phenotype (in case of a virulence reduction), complementation assays are performed with the respective gene in the deletion strain. In the case of a successful complementation (recovery of the virulence defect), a specific genotype can be assigned to a given phenotype as a causal consequence and not because of unrelated secondary events. Although there are many techniques that allow efficient deletion of genomic regions, this is not always the case for complementation of large genomic fragments. In this PhD dissertation, a modular fungal toolkit for gene expression (MoRFunG toolkit) was constructed for *U. maydis*. The general aim was to systematize and facilitate gene expression with predictable expression patterns in this model organism, with the additional advantage of efficiently manipulating large genomic DNA fragments.

Proof of concept experiments were performed, to test the functionality of the MoRFunG toolkit in *U. maydis*. These experiments were conducted in the cluster 6A of *U. maydis*. This cluster was previously deleted (Kämper et al., 2006), and the deletion strains showed a clear reduction in the virulence. However, in that publication the authors were not able to complement such a deletion. In this study, the cluster 6A served as a template to show the efficiency of the MoRFunG toolkit being used as a high-throughput cloning approach. The successful reconstruction of the virulence cluster permitted not only to successfully complement the large genomic deletion at a sequence level, but also at a functional level.

For the cluster complementation, each transcript unit was defined as the combination of promoters, ORFs (open reading frame) and terminators. Each one of these modules was then introduced into level 0 vectors (modules of a transcript unit). Subsequently, these level 0 modules were assembled in a native arrangement in level 1 (transcript units) and later in level 2 modules with a clustered structure. The MoRFunG system was shown to be highly efficient during the cloning process in *E. coli*, regarding the complexity of the generated construct. This translated into an immediate reduction of the time required to assemble big DNA fragments in a single vector. Although it is theoretically possible to reconstruct clusters using other

techniques, they are expensive and time consuming.

Some of the advantages of the MoRFunG toolkit, when compared to other cloning approaches in a cluster context, include the rapid construction of vectors containing large genomic fragments. This is achieved through the combination of modules in a unidirectional and hierarchical manner. Additionally, the methodology used in the MoRFunG toolkit (Golden Gate and Molecular cloning) makes it possible to dispense with large overlapping sequences between the parts to be assembled. Moreover, the pre-determined set of vectors within the system contributes to making the overall cloning process user-friendly and efficient.

In relation to cluster 6A's experiments, its deletion resulted in a reduction of the virulence performance when compared to the wild type SG200 strain. The results confirmed the reduced virulence phenotype for the cluster 6A previously published (Kämper et al., 2006). Sequential complementation of the cluster deletion revealed that, the first half of the cluster (SG200  $\Delta$ 6A/C1), including the *umag\_02533*, *umag\_11415*, *umag\_02535* and *umag\_11416*, was enough to achieve a complementation in terms of virulence performance. Both the first half complementation strain (including *umag\_02533*, *umag\_11415*, *umag\_02535* and *umag\_11416*), and complete complementation strain SG200  $\Delta$ 6A/C2 (including *umag\_02533*, *umag\_11415*, *umag\_02535*, *umag\_11416\_umag\_02537*, *umag\_02538*, *umag\_11417* and *umag\_02540*) did not show significant differences with the SG200 positive control. These observations indicate that either one or a combination of the first four genes of the cluster suffice to achieve a full virulence performance.

Not only was the overall virulence deficiency in the SG200  $\Delta$ 6A recovered, but the individual MoRFunG transcript units of cluster 6A, used for complementation, also exhibited similar expression levels to the SG200 wild-type genes in the qRT-PCRs. These results demonstrated the possibility of the MoRFunG toolkit to recreate fully functional transcript units in *U. maydis*. Only *umag\_02535* from the complementation strains showed significant differences when compared to the expression of the gene in SG200 in the qRT-PCRs, under the specific experimental conditions used in this study. One possible explanation is that promoter elements were unavoidably modified during the cloning process, altering in consequence the strength of up regulation of this effector gene. It was however assumed, that the difference in gene expression did not influence the overall outcome of this experiment, because the expression level in the complementation strains was higher than in the SG200 control for *umag\_02535*, and the virulence defect of SG200  $\Delta$ 6A was not recovered when the modular *umag\_02535*

was used to complement the cluster deletion individually.

When comparing the qRT-PCR results between the genes in the first and second complementation mutants, and with the SG200 control, it was observed that the four genes introduced first (*umag\_02533*, *umag\_11415*, *umag\_02535* and *umag\_11416*) did not show significant variation in relation to the SG200 in the  $\Delta 6A/C1$  and  $\Delta 6A/C2$  mutants. This result indicates that the integration of 4 additional genes (*umag\_02537*, *umag\_02538*, *umag\_11417* and *umag\_02540*) in a second transformation step, did not induce variations concerning the activity of the genes that were introduced first. These observations suggest that individual transcript units of the MoRFunG, show genetic stability along successive cloning steps in *U. maydis*.

In summary, the experimental evidence shows that:

- *U. maydis* strains containing tailor made transcript units can infect maize plants and develop a normal infection process.
- The MoRFunG modules are functionally active in *U. maydis* during biotrophy.
- Level 0 modules (promoters, ORFs and terminators) are independent, and their combination generates functional transcript units.
- The MoRFunG toolkit can be successfully used in *U. maydis* as an efficient, fast, and user-friendly high throughput cloning approach.

### **3.2 Functional gene redundancy within the cluster 6A of *Ustilago maydis*, and the role of MoRFunG toolkit**

In order to elucidate links between genotypes and phenotypes, genetic engineering approaches are employed to generate targeted genetic modifications (Haimovich *et al.*, 2015). Gene deletion is one of the most frequently used experimental methodologies used by researchers, for example to identify genes associated with specific virulence phenotypes in pathogens of interest. In the model organism *U. maydis* gene replacement and more recently CRISPR-Cas mediated gene knockout has been widely used to identify effector genes with direct impact on the pathogen's virulence. However, the main challenge in gene knockout is the occurrence of functional redundancy. Functional redundancy is understood as the overlapping function of

one or more effector genes making them individually dispensable (Angot *et al.*, 2006; Birch *et al.*, 2009; Kvitko *et al.*, 2009; Stergiopoulos & De Wit, 2009; Khrunyk *et al.*, 2010). This phenomenon occurs as result of gene duplication caused by the arms race between PAMP-triggered immunity (pathogen-associated molecular patterns) and ETI (Effector triggered immunity) in plants, against effector genes from the pathogen side (Khrunyk *et al.*, 2010).

Although considerable research has been conducted in the virulence cluster 6A of *U. maydis*, the role in virulence of each effector of the cluster, or the relation among them, is still unclear. Previous studies were focused on the interaction of the genes included in cluster 6A of *U. maydis* and proteins of the host (Bindics *et al.*, 2022), additionally, in the PhD dissertation of Dr.Selma Schurack, several genes belonging to this cluster were shown to be differentially upregulated in different maize lines. In this study, the MoRFunG toolkit was used to successfully identify a gene of relevance within the virulence cluster 6A.

The analysis of single knockouts of the genes of the cluster did not show any virulence reduction when compared to the SG200 wild type. These results suggest that the genes of the cluster are dispensable for the virulence in the SG200 genetic background, concluding that the dysfunction of individual genes of cluster 6A does not affect the virulence when the rest of the genes are present. Previously published experimental data showed that some genes in cluster 6A are **Topless interacting proteins (Tips)**. The proteins UMAG\_11415 (Tip1), UMAG\_02535 (Tip2), UMAG\_02537 (Tip3), UMAG\_02538 (Tip4) and UMAG\_11417 (Tip5) were shown to be auxin signaling inducers in maize plants (Bindics *et al.*, 2022). All the “Tips” of cluster 6A, and the protein UMAG\_11416 exhibited between 28-30% of protein identity, but UMAG\_11416 did not show interaction with the maize Topless proteins under high stringency conditions, reason for which is not considered a “Tip” (Bindics *et al.*, 2022). Curiously, *umag\_11416* has been linked with a maize-line specific virulence function (Schurack *et al.*, 2021). Nevertheless, this gene did not show any specific experimental evidence that could identify it as relevant for the virulence of cluster 6A under the experimental conditions used in this study.

The two flanking genes of cluster 6A: *umag\_02533* and *umag\_02540* did not show auxin signaling, and they did exhibited a lack of identity in a protein level with the rest of the genes of the cluster (Bindics *et al.*, 2022). These effectors also did not exhibit a virulence reduction when knocked out individually, recovery of the virulence when used for single gene complementation of the cluster deletion, or reduction of the virulence performance when

knocked out simultaneously. All the experimental evidence implies that the flanking genes do not have a direct impact on the virulence of the cluster.

A comprehensive analysis of the multiple knockouts mentioned in this study showed that a mutant containing only the *umag\_02533*, *umag\_11416* and *umag\_02540* (Non Tips from the cluster 6A) and lacking all the effector genes of cluster 6A identified as Tips, exhibited a strong reduction in the virulence (Bindics *et al.*, 2022). This information supports the hypothesis that one or a combination of the Tips interactors (*umag\_02535*, *umag\_11415*, *umag\_02537*, *umag\_02538* and/or *umag\_11417*) are potentially responsible for the virulence of cluster 6A in concordance with the conclusions of Bindics *et al.*, (2022).

Considering the double knockouts (*umag\_02533\_02535* and *umag\_02533\_02540*), triple knockouts (*umag\_02533\_02535\_02540*) and adding the analysis the single gene complementation of SG200  $\Delta$ 6A, the likelihood of *umag\_02535* being relevant for the virulence of cluster 6A is rather low. The double KO including *umag\_02533* and *umag\_02535* did not show a reduced phenotype, and the in the single gene MoRFunG complementation of the cluster deletion, the strains SG200  $\Delta$ 6A/02535 was unable to recover the virulence. Surprisingly the triple KO of *umag\_02533\_02535\_02540* showed a reduced virulence phenotype. Although experimental data supports the theory that those genes are individually dispensable (KOs and single gene complementation of the cluster deletion), one potential explanation for these results is that an interaction among *umag\_02533*, *umag\_02535*, and *umag\_02540* is required for the normal development of the *U. maydis*. Contradictorily, in the two steps cluster complementation approach, it was shown that half a cluster complementation (*umag\_02533*, *umag\_11415*, *umag\_02535* and *umag\_11416*) did recover the virulence phenotype, although *umag\_02540* was not present.

Considering the results obtained from the  $\Delta$ 6A two steps complementation, particularly SG200  $\Delta$ 6A/C1 with *umag\_02533*, *umag\_02535*, *umag\_11415*, and *umag\_11416* successfully complementing the cluster deletion's virulence defect, and evidence suggesting the dispensability of genes *umag\_02533*, *umag\_02535*, and *umag\_11416*, I hypothesized that effector gene *umag\_11415* previously identified as one of the strongest interactions with Topless proteins within Cluster 6A Tips (Bindics *et al.*, 2022) might significantly contribute to Cluster 6A's virulence. This hypothesis was confirmed when the single gene complementation in the  $\Delta$ 6A genetic background showed that the effector gene *umag\_11415* generated with the MoRFunG toolkit was capable to fully recover the virulence defect of the

cluster 6A deletion.

These results provided an explanation of how half a cluster complementation fully restored the virulence defect. However, these findings also raise new questions to be addressed. For instance, why did the triple knockout (*umag\_02533*, *umag\_02535*, and *umag\_02540*) shows a reduced virulence performance, despite *umag\_11415*'s ability to complement the cluster deletion? Are *umag\_02535* and/or *umag\_02533* necessary regulator/s? Is this regulation dispensable when only *umag\_11415* is present? Is the reduced virulence in the cluster deletion and the phenotypic changes observed in the triple knockout caused by the same underlying factors?

To address these questions, future research could employ the MoRFunG toolkit for an easy and convenient elucidation of further interactions among the genes within the cluster and their intricate network. As a suggestion for future experiments, complementing the SG200  $\Delta$ 6A with *umag\_02533*, *umag\_02535*, and *umag\_02540* could be undertaken. This evaluation aims to determine whether the virulence phenotype can be restored, thus demonstrating that the interaction among these genes suffices *U. maydis* to exhibit wild-type behavior. Alternatively, it could investigate whether the virulence defect arises due to an imbalance in the co-regulation among these genes, and whether the presence of *umag\_11415* is essential for virulence.

The use of the MoRFunG toolkit as a genetic tool to investigate the role of effector genes within Cluster 6A marked a significant achievement. The complementation of *U. maydis*  $\Delta$ 6A through the single-gene complementation approach using the MoRFunG toolkit played a pivotal role in refining the questions surrounding the complex co-regulation between clustered effector genes. On one hand, the experimental evidence generated with the MoRFunG toolkit was of great value, as arriving at the same conclusion through the implementation of other methodologies would have been highly challenging, expensive, and time-consuming. On the other hand, this experiment exemplified the toolkit's versatility, highlighting the advantages of having a modular cloning system in *U. maydis*. The MoRFunG toolkit proves to be a valuable complement to the already excellent molecular instrumentarium of *U. maydis*.

### **3.3 MoRFunG's exchangeable modules, tailor-made transcript units and their activity in *Ustilago maydis***

MoRFunG is an abbreviation for “Modular Recombinant Fungal toolkit for Gene expression”. The terms “modular” and “recombinant” are key concepts to understand the advantages of this system. From an engineer’s point of view, the parts of a system are more efficient if they present an independent contribution to the whole. This “independency” allows the prediction of the system’s behavior (Benner & Sismour, 2005). The MoRFunG toolkit is defined as a cloning system in which its behavioral predictability is provided by the promoter modules. Its independence is determined by the capacity of the system’s modules (promoters, ORFs and terminators) to be combined unidirectionally, in hierarchical structure and in an unrestricted manner.

#### **3.3.1 Characterization of endogenous promoters using reporter genes: Multi-tag ectopic integration with the MoRFunG toolkit**

To date, the promoters included in the MoRFunG toolkit are of an endogenous nature. Some of these promoters were evaluated for their capacity to keep their expression patterns when inserted ectopically. In this dissertation, experiments were conducted to assess the possibility of simultaneously expressing three reporter genes (fluorescent proteins) under the control of three differentially upregulated endogenous promoters through a “Multi-tag” ectopic integration approach (Section 2.3.2). Preliminary experimental data suggests that the introduction of synthetic transcript units done with the MoRFunG toolkit did not affect the virulence performance of *U. maydis*.

The methodology used for visual detection of the reporter genes was confocal microscopy. This technique was effective for visualizing the reporter gene in early stages of infection. At 48 hpi, the GFP under the control of the early upregulated promoter (PU10115) was observed in penetrating hyphae, confirming the activity of the promoter inserted ectopically. However, as the infection advanced and fungal hyphae developed in deeper layers of the plant tissue, the reporter proteins were no longer visible in longitudinal sections of the samples. Suggestions for future experiments include performing cuts, for example with cryo-sectioning of the maize leaves at 4 dpi or later time-points. This approach could give access to deeper layers of tissue, avoiding chemical treatments of the leaves which can lead to loss of fluorescence.



The results of the PCRs whose template were cDNA (Section 2.3.2, Figure 18), showed that the second reporter gene *mCherry* (under the control of the middle promoter PU03749) was translated, and non-amplification band was observed in the SG200 control. These results also suggest the occurrence of potential post-transcriptional regulations, because although the PCR from cDNA exhibited a positive amplification band at 2dpi for the multi-tag treatment, at that specific time point that protein was not visualized with confocal microscopy. In combination these results show evidence that two out of three tailored-made transcript units done with the MoRFunG toolkit, inserted ectopically in the *ip* locus of *U. maydis* were active, the ORFs translated, and one of them confirmed to be transcribed. More experiments need to be done to draw conclusions about the activity of the third (late upregulated PU03046) promoter, the translation of the reporter genes into proteins, and the dynamic of the gene expression across the infection process.

Suggestions for the future characterization of endogenous promoters to be included into the MoRFunG toolkit, include quantitative analysis of the promoter's activity during the infection process. For a quantitative analysis of the promoters, novel synthetic biology tools could be implemented. Luciferases were customized and tested in *U. maydis* (Heucken *et al.*, 2023) showing that this markers don't affect the virulence performance of *U. maydis*. The use of (Photinus pyralis, firefly—FLuc) (Barletta *et al.*, 2000; Heucken *et al.*, 2023) sea pansy (Renilla reniformis, renilla—RLuc) (Srikantha *et al.*, 1996; Heucken *et al.*, 2023) , and *Gaussia princeps*, *gaussia*—GLuc (Wurdinger *et al.*, 2008; Heucken *et al.*, 2023) as tags proteins have the advantage of allowing a quantitative monitoring of the fungal growth and infection assays, by spraying the plants with luciferin and measuring the cumulative luminescence (Heucken *et al.*, 2023). Additionally, the authors described a ratio-metric way to monitor inducible gene expression using a dual reporter. Although in (Heucken *et al.*, 2023) the assay was done to evaluate inducible gene expression, the system could also be used for the evaluation of the profile of endogenous promoters into the MoRFunG toolkit.

### **3.3.2 *Ustilago maydis* $\Delta pep1$ tailored complementation using the MoRFunG toolkit**

The effector gene *pep1* has been demonstrated to play an essential role in the biotrophic development of *U. maydis* (Doehlemann *et al.*, 2009). Substantial experimental evidence supports the notion that Pep1 is indispensable throughout the entire infection process. However, due to its critical involvement in the establishment of biotrophy, the deletion of

*pep1* leads to the termination of the infection process, preventing researchers from investigating its impact during later stages of the fungal development inside its host. For instance, aspects such as the impact of a premature downregulation of *pep1* on the virulence performance of *U. maydis* cannot be assessed. In this study, we employed the MoRFunG toolkit to explore a differential up-regulation of *pep1*. This was achieved by co-expressing tagged *pep1* under the control of various endogenous promoters of *U. maydis*. The primary objective of this experiment was to demonstrate the applicability of the MoRFunG toolkit for achieving distinct expression levels of an essential effector gene.

The results from the MoRFunG *pep1* complementation (Section 2.3.3) in the SG200  $\Delta pep1$  genetic background were not conclusive. Confocal microscopy showed fungal expression of GFP (tagged to *pep1*), confirming the activity of the early promoter PU02851 in two mutants: a partial *pep1* complementation with the early promoter PU 02851 ( $\Delta pep1/PU02851\_pep1:gfp$ ), and a complete complementation ( $\Delta pep1/PU02851\_pep1:gfp:NosT\_PU11415\_pep1: mCherry:NosT-ip$ ) with *pep 1* under the control of two endogenous promoters. The microscopy images of the above-mentioned strains also revealed the ability of the mutants to penetrate the plant cells. Nevertheless, the fungal proliferation in both cases was weak, since a low number of penetrating hyphae was observed (authors' personal observations). Additionally, the progression of the infection did not advance as expected since not tumors were observed after 12 dpi in the strain with two copies of *pep1* under the control of two independent promoters ( $\Delta pep1/PU02851\_pep1:gfp:NosT\_PU11415\_pep1: mCherry:NosT-ip$ ) who was originally expected to fully recover the virulence performance. These findings indicate that although the mutant strains were likely able to establish an early biotrophy, the normal development of *U. maydis* was hindered by one or more yet-to-be-identified factors. To rule out that a late upregulation-time as the cause of the virulence defect, the promoter from *umag\_03065* appressoria related virulence factor (Mendoza-Mendoza *et al.*, 2009) was added to the construct. The complementation strains had both the PU02851 and the PU03065 promoters as early up-regulators together with the PU11415 promoter leading the expression of *pep1:gfp* or *pep1: mCherry*. The virulence assessment for this mutant showed a higher amount of chlorosis spots in infected maize plants but no tumors were observed, being the modular complementation of *pep1* using endogenous promoters of the MoRFunG toolkit not successful in terms of virulence recovery.

Previously, the *otef* promoter was used to complement the virulence defect of  $\Delta pep1$ , achieving only partial complementation (Doehlemann *et al.*, 2009). The *otef* promoter is known for its strong and constitutive expression in haploid sporidia, infecting filaments and in the early biotrophic stages (Doehlemann *et al.*, 2009). However, the gene *umag\_02146* (gene encoding translation elongation factor 1-alpha *tef1*) associated to the *otef* promoter, experiences a strong downregulation at 2 dpi based on the expression pattern (Lanver *et al.*, 2018a). In their study, Doehlemann *et al.*, (2009) attributed the partial recovery of virulence to this downregulation with symptoms like anthocyanin, chlorosis necrosis and small tumor formation. This suggests that although the virulence of the complementation of *pep1* with a foreign promoter was reduced, *pep1* was present, and the biotrophy was established, disregarding that the initial translation of *pep1* requires of specific promoter elements only present in the *pep1* promoter.

In this study, attempts to complement  $\Delta pep1$  using the MoRFunG toolkit were unable to restore the virulence defect. In contrast to the approach taken by Doehlemann *et al.* (2009), we employed endogenous promoters from a virulence factor associated with appressoria formation (*umag\_03065*) and an early upregulated effector gene (*umag\_02851*). These promoters are not activated before the penetration stages of *U. maydis*, since they promote the translation of virulent factors and effector genes. One hypothesis that explains the partial virulence recovery achieved by *otef* alone, as opposed to the endogenous promoters used in the MoRFunG toolkit, could be attributed to the already existence of Pep1 effector at the right moment for penetration due the constitutive nature of *Potef*. The well described *otef* promoter is active prior to filamentation, being Pep1 already strongly expressed even before the penetration stages. Although Pep1 is not expressed in axenic conditions for *U. maydis* SG200 (Doehlemann *et al.*, 2009), probably the endogenous promoters used in this study do not exactly meet the requirements regarding time and/or strength of upregulation to express sufficient Pep1 at the right time suppressing the host immune response and establishing the biotrophy.

One suggestion for future experiments, to prove that the MoRFunG can be used to fully restore the virulence defect of  $\Delta pep1$  is to substitute the PU03065 with the *otef* promoter to ensure that the biotrophy can be successfully established, while a full virulence phenotype will be completed by the expression of *pep1* under the promoters PU02851 at 2 dpi and for PU11415 during the rest of the infection process.

### **3.4 New technologies for gene expression and gene manipulation applied to *Ustilago maydis***

Several times this study has mentioned the importance of the development of new genetic tools for targeted gene manipulation. Experimental data that shows the benefits of new approaches for manipulation of large genomic fragments has been discussed. Adaptation of the MoRFunG toolkit to avoid the utilization of resistance cassettes for selection of mutants have been described, as well as its usage for combined gene expression.

Another challenge for researchers is to achieve spatiotemporal and quantitative control over the regulation of the gene expression (Ochoa-Fernandez *et al.*, 2020). Chemically inducible systems for targeted gene manipulation have been widely employed (Moore *et al.*, 2006; Andres *et al.*, 2019; Ochoa-Fernandez *et al.*, 2020). Nevertheless these systems present limitations regarding to the spatial resolution, diffusion effects, potential pleiotropic activity and toxicity (Ochoa-Fernandez *et al.*, 2020). Alternative methodologies consists on the modification of technologies that allow targeted gene manipulation with spatiotemporal precision, in a quantitative manner and with minimal toxicity and invasiveness (Ochoa-Fernandez *et al.*, 2020). Optogenetics is a novel development that is focused on the control of biological systems using light (Andres *et al.*, 2019), achieving a high level of spatial-temporal control with minimal invasiveness in the system.

Previous work with optogenetic tools done in the research group of Prof. Dr. Zurbriggen describes two blue-light regulated systems to control the expression of heterologous genes in *U. maydis*. In this study, these systems were adapted for the light-controllable expression of the effector gene *see1*. While the optogenetic switches in *U. maydis* allow a stable light regulated gene expression in absence of the host under different light conditions, it was not possible to detect gene activity for the light regulated promoter during the infection process (section 2.4.4). The reason could be that the inoculation points in the maize plants were exactly in the middle of the plant's stem, being surrounded by 3 leaves. This could partially limit the amount of light in contact with the pathogen. Another explanation could be that the growing parameters (especially temperature) were not optimized for the development of *U. maydis*, not being possible to formulate final conclusions for this experiment. It is required to optimize the conditions to use light regulated switches for gene expression during the *U. maydis* pathogenic development. Nevertheless, it has been proven that the incorporation of optogenetic regulatory elements in the genome of *U. maydis* did not modify the ability of the

organisms to establish a compatible biotrophic interaction with its host.

The use of optogenetics as a tool for targeted gene manipulation during the *U. maydis* pathogenic development, potentially including the optogenetic switches into the MoRFunG toolkit, offers a versatile, efficient, and flexible work tool. The goal of using optogenetic switches in *U. maydis* is to generate an inducible system that allows an orthogonal expression of entire synthesis pathways, by for example targeting transcription factors. Additionally, the use of a non-invasive-reversible system working in *U. maydis* could allow the expression of genes that compromise the fungus viability in a controlled manner, or to modify the expression pattern of effector genes in real time during the infection process with the utilization of different light wave lengths.

### 3.5 Overview and future perspectives

In the fields of genetic engineering and molecular biology, numerous methodologies and techniques have emerged over the past few decades. These advancements have yielded a diverse array of molecular tools tailored to a wide range of organisms. Well known model-organisms, used as metabolic factories for the overproduction of microbial compounds with industrial applications, have been the focus of attention in the development of genetically engineered systems. Availability of synthetic modular vectors that allow precise genetic manipulation are publicly available for *Escherichia coli* (Moore et al., 2016; Pohl et al., 2021), yeasts (Lee et al., 2015; Obst et al., 2017; Pohl et al., 2021), plants (Engler et al., 2014) mammalian cells lines (Martella et al., 2017), and some filamentous fungi such as *Aspergillus niger* (Sarkari et al., 2017), *Sordaria macrospora* and *Penicillium rubens* (Dahlmann et al., 2021).

While cutting edge technologies skyrocketed in some organisms, especially *Escherichia coli* and *Saccharomyces cerevisiae*, its development in other organisms has been considerable slower. Although *U. maydis* offers great potential for developing various molecular and synthetic biology techniques, including inducible promoters, fluorescent reporters, epitope tags, and polycistronic gene expression (Brachmann et al., 2004; Müntjes et al., 2020; Terfrüchte et al., 2014), artificially controlled gene expression techniques are less advanced compared to other eukaryotic model organisms. With the aim of enlarging the molecular toolbox available for *U. maydis*, a Modular Recombinant Fungal toolkit for gene expression (MoRFunG toolkit) was designed and tested in this study.

Existing gene expression toolkits for filamentous fungi and yeast rely on standardized and characterized collections of vectors designed to optimize the overproduction of specific microbial compounds. In contrast, the MoRFunG toolkit for *U. maydis* is uniquely focused on providing researchers with a versatile molecular tool that facilitates the rapid construction of genetic circuits, enabling predictable and dynamic gene expression patterns during biotrophic development. The predictability of gene expression dynamics, encompassing factors such as timing and strength of up-regulation, relies on promoter sequences. Promoters are regulatory elements controlling gene expression quantitatively and temporally (Scalcinati *et al.*, 2012; Latimer *et al.*, 2014; Tang *et al.*, 2020). The MoRFunG toolkit is composed of interchangeable modules, each containing the functional elements of a transcript unit, including at the moment endogenous promoters, open reading frames (ORFs), and terminators. The versatility that comes with the manipulation of the dynamics of effector gene expression provides valuable tools for various research goals. For instance, it enables the exploration of interplays between individual effectors at specific stages of the infection process, comprehension of intricate networks involving multiple effector genes, and assessment of how modifications in effector expression impact virulence, among other applications. Furthermore, an ambitious future goal for the MoRFunG toolkit is its utilization in the heterologous expression of genes from obligate maize pathogens. This could offer insights into their mechanisms of action, potentially aiding the scientific community in developing strategies such as resistant crops or biocontrol agents.

The MoRFunG toolkit, as well as others already published toolkits for gene expression in other organisms use Golden Gate Molecular cloning as cloning technique due to its flexible and efficient assembly of “essential ready to use” genetic parts, which uses the same MoClo language, allowing the assembly of numerous constructs simultaneously in one pot reaction with robust and reliable assembly rules and a high transformation and integration efficiency (Martella *et al.*, 2017; Sarkari *et al.*, 2017; Pohl *et al.*, 2021). While the controlled gene expression in *U. maydis* using the MoRFunG toolkit is promising, it requires further development. Fine genetic regulation is necessary to construct or manipulate pathways involving multiple genes, but endogenous promoters often do not meet the necessary requirements due to poor dynamic ranges, lack of well-defined characteristics, or not being orthogonal to endogenous regulations (Tang *et al.*, 2020). Designing genetically engineered promoters in *U. maydis* poses an even higher challenge as they need to be activated during the infection process, and the use of inducible promoters inside the plant is limited. Additionally,

fine-tuning the expression of effector genes requires complete independence from endogenous regulation and precise control over the timing of up regulation and strength of the promoters.

Further development of the MoRFunG toolkit to offer a highly sophisticated set of modules for controlling gene expression in *U. maydis* includes:

- The incorporation of artificial promoters with desirable properties based on the promoter motif, for example: specific binding sites, enhancer elements, or response elements, allowing them to modulate gene expression in response to environmental cues or specific signals.
- Addition of synthetic transcriptional activators or repressors.
- Increase in the options for delivery methods for example: self-replicating episomal AMA1 vectors for expression tests (Pohl *et al.*, 2021)
- Incorporation of detection systems that allow quantification of gene expression inside the plant host and in real time.
- Introduction of optogenetics promoter elements as modules of the MoRFunG toolkit, allowing light-inducible regulation of biological processes in an orthogonal manner with the aim to generate metabolic pathways independent of the effector's co-regulation.

In conclusion, the MoRFunG toolkit is a promising endeavor with great potential. This toolkit is set to become a valuable resource to the *Ustilago* scientific community, providing a standardized toolbox for precise genetic tuning, with the goal of detailed and predictable genetic manipulation of effector genes during the biotrophic development. Beyond this, utilizing the toolkit presents numerous additional advantages, such as its streamlined, rapid, and efficient cloning mechanisms, robustness, and remarkable versatility. As scientist, I predict that this cutting-edge methodology will open new paths for innovative research and contributes to a deeper understanding of the molecular mechanisms of the biotrophy of *U. maydis* as well as other relevant maize pathogens.

## 4 Materials and methodologies

The materials and methodologies applied in the experiments of this thesis are summarized in the following section.

### 4.1 Materials and suppliers

#### 4.1.1 Chemicals, media components, and additional materials

The chemicals, media components, solvents, enzymes, and reagents used in this study were acquired from the following companies unless stated differently: Roth, Ambion, BD, Gibco, Difco, Merck, GE Health Care Life Science, Honeywell Riedel-de Haen, Roche, Sigma-Aldrich and Invitrogen.

#### 4.1.2 Sterilization for buffers and solutions

Unless stated differently, all the buffers, media, and solutions were prepared with ddH<sub>2</sub>O and autoclaved for 5 min at 121°C. Heat-sensitive solutions were sterilized by filtration (0,2 µm pore). The respective methods section indicates the media, buffers, and solutions composition.

#### 4.1.3 Enzymes, antibiotics, and markers

Restriction enzymes from analytical digest and cloning were purchased from New England Biolabs (NEB). For high-fidelity DNA amplification, the polymerases used were Phusion® High Fidelity (NEB), Q5® High Fidelity (NEB,) or KOD (Merk). Golden Gate Molecular cloning reactions were used using *BpiI* Fast digest (Thermo Fisher Scientific) , *BsaI* (NEB,) and T4 ligase (NEB). For Gibson Assembly reactions, NEBuilder®HiFi DNA Assembly Master Mix from NEB was used. qRT-PCRs were done using qRT-PCR Master Mix (Promega). For digestion of the fungal cell wall Novozyme234 (Novo Nordisk) was utilized.

The antibiotics used in this study were: Carbenicillin (Roth), Kanamycin (Sigma Aldrich), Carboxin (Honeywell Riedel-de Haen), Hygromycin (Roche), Streptomycin (Roth) and Nourseothricin (Werner Bioreagents). The usage, as well as the working concentration for each antibiotic, can be found in Table 2.



Antibiotic	Microorganism	Working concentration µg/ml
Carbenicillin	<i>E. coli</i>	100
Kanamycin	<i>E. coli</i>	50
Streptomycin	<i>E. coli</i>	100
Carboxin	<i>U. maydis</i>	2
Hygromycin	<i>U. maydis</i>	200
Nourseothricin	<i>U. maydis</i>	150

**Table 2: Antibiotics for *E.coli* and *U. maydis*** Antibiotics used in this study with their respective concentration.

The markers used to determine DNA size in agarose electrophoresis are shown in Figure 26.

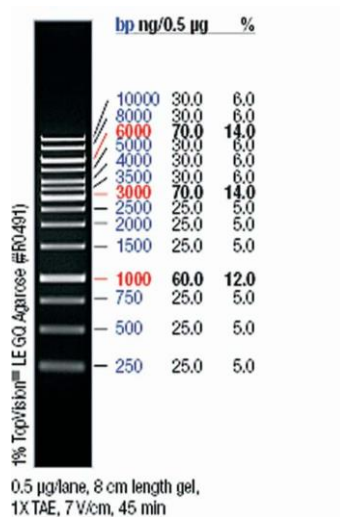


**Figure 26: Standard 1Kb marker used in this study:** Thermo Scientific GeneRuler 1 Kb DNA ladder used in this study for determination of DNA fragments size in agarose gel.

## 4.2 Commercial kits

For plasmid extractions of *E.coli* the NucleoSpin® PlasmidKit (Macherey- Nagel) was used. To purify DNA fragments (PCRs products and DNA from agarose gel), the NucleoSpin® gel and PCR Clean-up Kit (Macherey- Nagel) was employed. PCRs purifications for sequencing were done using SureClean Plus kit (Bioline). For enzymatic degradation of DNA, we used the TURBO DNA-free™ Kit ( Ambion®/ Thermo Fischer Scientific). Synthesis of cDNA was done by using RevertAid H Minus First Strand cDNA Synthesis Kit (Thermo Fischer Scientific).

In all the cases the commercial kits were used according to the manufacturer's instructions.

### 4.3 Media and growing conditions

The media composition of the cultures used for the cultivation of microorganisms used in this study is described below. All the media were autoclaved at 121°C before use unless the contrary is indicated.

#### 4.3.1 Media for *Escherichia coli*

**dYT liquid media:** (Sambrook et al. 1989) 1.6% (w/v) Tryptone, 1.0% (w/v) Yeast extract, 0.5% (w/v) NaCl.

**YT Agar:** 0.8% (w/v) Tryptone, 0.5% (w/v) Yeast extract 0.5% (w/v), NaCl 1.5% (w/v).

#### 4.3.2 Cultivation of *Escherichia coli*

*E.coli* was the organism used for plasmid replication. The cells were cultivated either on YT Agar or dYT liquid medium with the required antibiotics at 37°C with constant shaking at 200 rpm in the case of liquid cultures. For long-term storage of the *E.coli* strains, glycerol stocks were prepared by adding 60% sterile glycerol solution to an overnight culture in dYT in a 50% concentration (v/v) in a final volume of 1,5ml. The screw cap vials were then stored at -80°C. The antibiotics used are specified in Table 2.

#### 4.3.3 Media for *Ustilago maydis*

**Agar YEPSlight:** 1.0% (w/v) Yeast extract, 0.4% (w/v) Peptone.

**Sucrose Potato-Dextrose-Agar (PD):** 2.4% (w/v) Potato-Dextrose Broth, 2.0% (w/v) Agar.

**PD-Charcoal Agar:** addition of 1.0% (w/v) activated charcoal to the PD-Agar medium.

**Regeneration Agar:** (Schulz et al. 1990) 1 M Sorbitol, 1.0% (w/v) Yeast extract, 0.4% (w/v) Peptone, 0.4% (w/v) Sucrose, 1.5% (w/v) Agar.

#### 4.3.4 Cultivation of *Ustilago maydis*

In this study all the strain were generated in the genetic background of the *U. maydis* SG200 solo-pathogenic strain, able to filament without prior mating (Kämper *et al.*, 2006)

*U. maydis* strains were cultivated in YEPS<sub>light</sub> with constant shaking at 200rpm for liquid cultures, or Potato Dextrose (PD) Agar in case of solid cultures. In both cases, the incubation was carried out at 28°C. Glycerol stocks for long-term storage at -80°C were prepared in a 50% (v/v) solution with 60% glycerol solution and *U. maydis* liquid culture with an OD<sub>600</sub> between 0,6 and 1 in a total volume of 1,5 ml.

For growing *U. maydis* after transformation, the media used was Regeneration Agar, supplemented with 2µg/ml carboxin unless stated contrarily.

#### 4.3.5 Determination of cell density

When required, the cell density was determined by absorption at 600 nm (OD<sub>600</sub>) measured in a Genesis 10S VIS spectrophotometer (Thermo Fisher Scientific). The measurements were referenced with the liquid media required in each case. To ensure the linear co-dependency of the measurements, the cultures were diluted to absorption values below 0.8 for *U. maydis*.

Absorption of 1 OD<sub>600</sub> for *U. maydis* represents ~ 1,5x10<sup>7</sup> cells while for *E.coli* an absorption of 1 accounts for ~ 1x10<sup>9</sup> cells.

#### 4.3.6 Maize cultivation conditions

Maize seeds from the variety Golden Bantam were placed in pots with fresh soil (Einheitserde® VMV800) at about 5 cm deep. The plants were grown in a greenhouse or phytochambers at 28°C, over a long day period with 16h light with 80% humidity and an 8 h night at 22°C.

### 4.4 Virulence assay of *Ustilago maydis* in maize

The virulence performance of *U. maydis* strains was tested on maize plants infected for injection of *U. maydis* inoculum at the stage of 3rd leaf. The symptoms were scored at 12 or 9 dpi depending on external factors related to the greenhouse conditions. No difference in the

tumors were observed after 9 dpi. The symptoms were classified with a modification to the system published by (Redkar & Doehlemann, 2016) considering the size and frequency of tumors as shown in Figure 27. The disease rates are given as a percentage of the total amount of infected plants. The calculation of the disease index was done as mentioned by (Bindics et al., 2022).

All the strain tested in this study were also tested in charcoal plates showing complete normal filamentation indicating that in case of reduced virulence, the exhibited phenotype does not occur due to a defect in the filamentation.

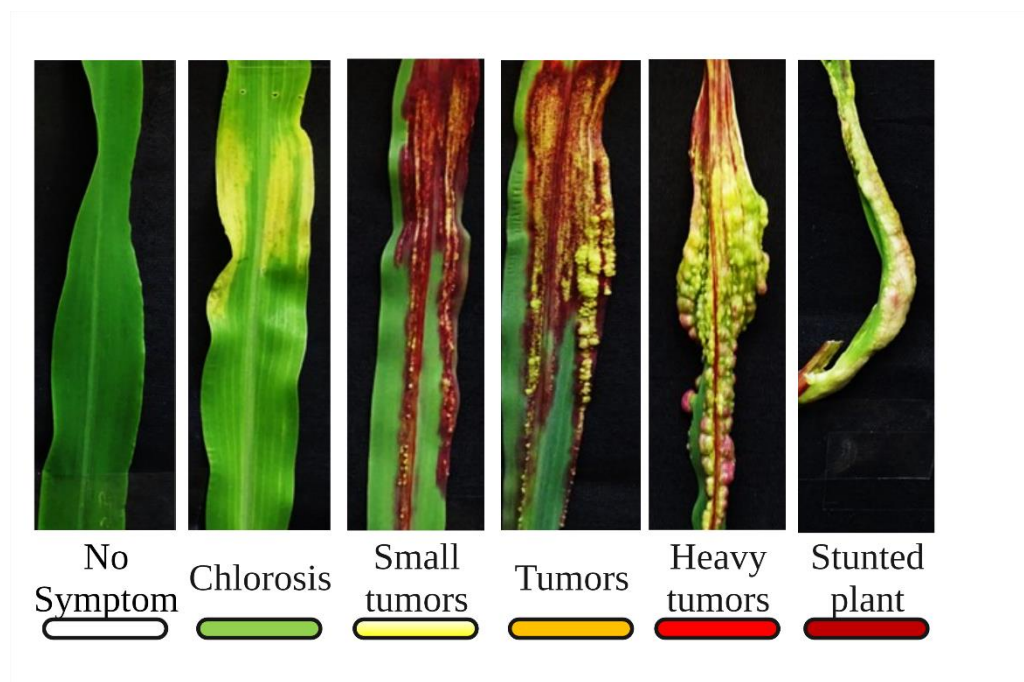


**Figure 27: Scoring system for *U. maydis* disease development in maize leaves.** Disease rating used for *U. maydis* virulence assays. The category of death plants is not shown in this picture or considered in the scoring of virulence assays. Plant pictures were courtesy of Dr. Bilal Ökmen. Figure created with Biorender.com.

## 4.5 Microbiological standard methods

### 4.5.1 Competent *Escherichia coli* cells production

The production of competent *E.coli* cells was conducted at 4°C, with all the solutions and equipment precooled at this temperature. The cell manipulation was done on ice in a cold room.

Pre-cultures of single *E.coli* colonies were grown in 15-20 ml of dYT medium at 37°C, with constant shaking at 200 rpm, until an OD<sub>600</sub> of ~ 0,6. The cells were then cooled on ice for 30

min and centrifuged for 8 min at 4°C at 1250 *xg*. After discarding the supernatant, the pellet was resuspended in RF1-solution with 1/3 of the initial culture volume followed by a 30 min incubation at 4°C. After incubation, the cells were centrifuged under the same conditions mentioned above, and the pellet was then resuspended in RF2-solution with 1/20 of the original culture volume. After incubating the cell suspension for 30 min at 4°C, the cells were aliquoted to 50 µl in pre-cooled reaction tubes, shock froze in liquid N<sub>2</sub>, and stored at -80°C.

**RF1 solution**

100 mM RbCl  
50 mM MnCl<sub>2</sub> x 4 H<sub>2</sub>O  
30 mM potassium acetate  
10 mM CaCl<sub>2</sub> x 2 H<sub>2</sub>O  
15% (w/v) Glycerol  
pH 5.8

**RF2 solution**

10 mM MOPS  
10 mM RbCl  
75 mM CaCl<sub>2</sub> x 2 H<sub>2</sub>O  
15% (w/v) Glycerol  
pH 5.8

**4.5.2 Heat-shock transformation of *Escherichia coli***

Chemically competent *E.coli* cells (TOP10 /DH5α) were used in this study for plasmid replication.

A concentration between 1 and 1,5 ng was added to 50 µl of competent cells and incubated on ice for 15 min followed by a heat shock of 42°C for 45 seconds. Immediately after the transformant cells were placed on ice for 2 min. For regeneration, 700 µl of dYT media were added, and the cells were incubated between 30 min to 1 hour at 37°C in constant shaking. After the regeneration period, the transformed cells were plated on YT Agar containing the specific antibiotic for selection and incubated overnight at 37°C.

### 4.5.3 *Ustilago maydis* protoplast

Overnight cultures of *U. maydis* were diluted to  $OD_{600}=0,2$  in 50 ml pf YEPS<sub>light</sub> medium and incubated at 200rpm at 28°C until  $OD_{600}=0,8-1$  was reached. The cultures were then centrifuged at 2000  $xg$  for 5 min. The pellets were resuspended in 10ml of SCS followed by a second centrifugation step under the same conditions. After discarding the supernatant, the pellets were then resuspended in 2ml of a filtered-sterile solution containing SCS with 7mg/ml Novozyme234 (Novo Nordik). The cells in SCS/Novozyme solution were incubated for 10-15 min at room temperature until ~30%-40% of the cells presented a protoplast morphology under the optic microscope (pinhead structure). When this stage was reached, the protoplast cells were placed on ice, and 10 ml of pre-cooled SCS was added to the suspension. The protoplast suspensions were centrifuged in a pre-cooled centrifuge at 4°C, 1300 $xg$  for 5 min. After carefully discarding the supernatant, a second resuspension with 10ml of STC was done, followed by a second cold centrifugation step under the same conditions mentioned before. In the last step, the pellet was resuspended in 500  $\mu$ l of cold STC and aliquot in 50  $\mu$ l in pre-cooled sterile reaction tubes. After aliquot them, the protoplast was either used for direct transformation or stored at -80°C until further use.

#### **SCS solution**

20 mM Na-Citrate, pH 5.8  
1 M Sorbitol  
sterile filtered

#### **STC solution**

10 mM Tris-HCl, pH 7.5  
100 mM CaCl<sub>2</sub>  
1 M Sorbitol  
sterile filtered

### 4.5.4 Transformation of *Ustilago maydis*

*U. maydis* protoplast were placed on iced and transformed or co-transformed with 1,5  $\mu$ g of plasmid/s in a maximal volume of 10  $\mu$ l together with 1 $\mu$ l heparin solution (1mg/ml) for every transformation. The transformation tubes were incubated for 10 min on ice before being suspended in 500  $\mu$ l of STC/PEG solution. After a second incubation on ice for 15 min, the transformation mix was carefully disposed on two layers of Regeneration Agar consisting of

a first 10ml layer of medium with an additional 2X selection agent, and a top 10ml layer of medium without selection agent. The transformant cells were then spread by gravity across the whole plate and incubated for 4-5 days at 28°C.

After the incubation period, colonies were passed to PD Agar containing the selection agent and incubated for 2 days at 28°C. In the last step, to remove the selection plasmid, colonies were selected and passed on PD Agar without selection (1 or 2 times) and incubated for 2 days at 28°C.

## **4.6 Molecular biology methods**

### **4.6.1 Plasmids**

All the plasmids in this study were isolated from *E. coli* strains using the NucleoSpin® Plasmid Kit from Machinerey-Nagel (REF 740588.250) according to the manufacturer's instructions.

### **4.6.2 Gibson Assembly**

For the construction of CRISPR and Optogenetic vectors, Gibson assembly cloning was done, using homologous recombination of small DNA fragments (Gibson et al., 2009). For this purpose, DNA fragments were designed to overlap with a minimum of 20 bp. The reaction was performed using NEBuilder®HiFi DNA Assembly Master Mix (NEB), according to the manufacturer's instructions.

### **4.6.3 CRISPR-CAS9 vectors**

The CRISPR-Cas9 single target as well as the multiplex were done using as a backbone the non-integrative, self-replicating pCas9HFI (Zuo et al., 2020). The sgRNA were designed either in the E-CRISP online software [www.e-crisp.org](http://www.e-crisp.org) (Heigwer et al., 2014) or CHOPCHOP online tool <https://chopchop.cbu.uib.no/>, targeting regions as close as possible to the ATG of the gene of interest.

In the case of multiplex CRISPR, the gRNAs targeting different genes were spaced by transfer RNA sequences as established by (Xie et al., 2015).

#### 4.6.4 P-MiniT cloning

Some sequences of DNA used in this study were introduced in p-MiniT 2.0 (NEB) according to the manufacturer's instructions.

#### 4.6.5 Golden Gate Molecular Cloning

All the modules included in the MoRFunG tool kit from this study were done by Golden Gate Molecular cloning.

Level 0,1 and 2 reactions were carried out in T100 Thermal cyclers from Bio-Rad Laboratories GmbH with the following protocol:

37°C	0:30 min
37°C	5:00 min
16°C	4:00 min
Go to Step #2 27 X	
80°C	20:00
4°C	∞

All the backbones used for the MorFunG modules were described by (Weber et al., 2011) except indicated contrary.

The level 0 Modules in this study were defined in 3 different categories: promoters, ORF and terminators, as “modules of a transcript unit”. Level 1 modules are defined by the combination of 3 level 0 modules (one from each category) independently if following the “like wild type sequence” or is a tailored made combination. Finally, level 2 modules represent combinations of 2 or more level 1 modules in a tandem arrangement. The system follows a hierarchical and unidirectional flow of cloning (Figure 28)



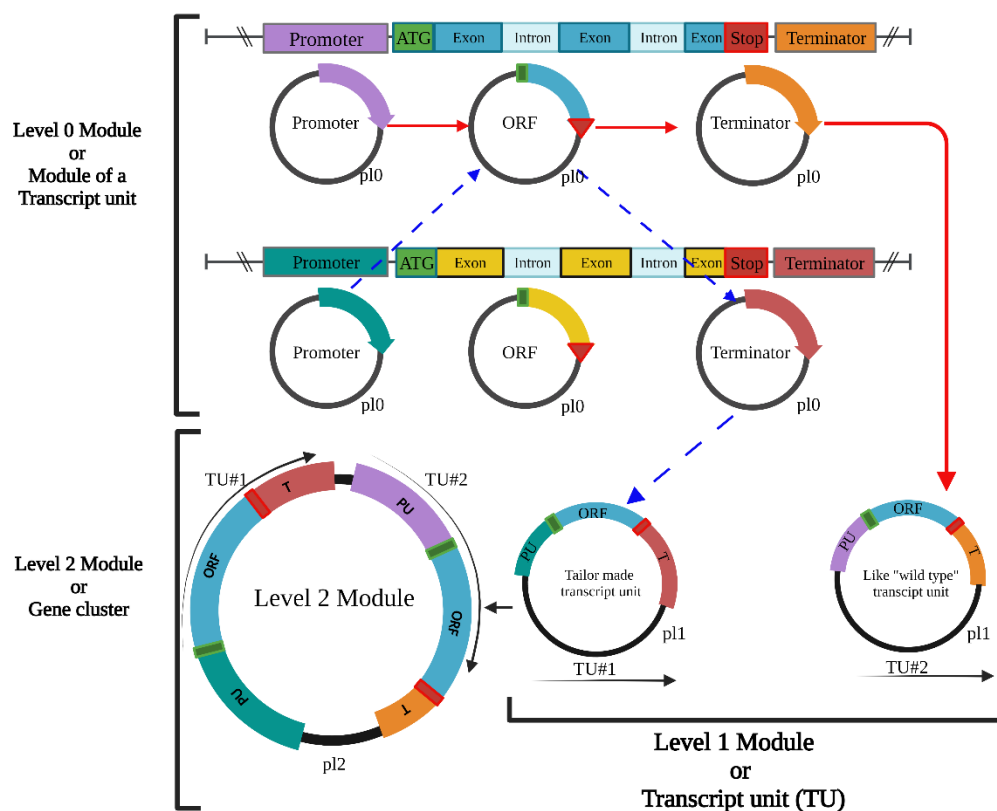


**Figure 28: Representation of the MoRFunG toolkit flow of cloning:**

p10: Plasmid level 0 is equivalent to a module of a transcript unit (promoter, ORF or terminator)

p11: Plasmid level1: Transcript unit. Combination of promoter, ORF and terminator in a specific vector

pL2: Plasmid level 2: tandemly arranged 2 or more level 1 vectors.

Figure created with Biorender.com

#### 4.6.5.1 Level 0 Modules

For all the level 0 modules (including domestication in level 0) the one tube reaction contained: 1  $\mu$ l T4 DNA ligase buffer (NEB), 0,5  $\mu$ l *BpiI* Fast digest (Thermo Fisher Scientific), 0,5  $\mu$ l T4 DNA ligase (NEB), 77-100 ng backbone, insert (1:2 ratio) and ddH<sub>2</sub>O when required to achieve a final volume of 10  $\mu$ l.

The backbones used for the level 0 modules are stated in Table 3.

Sequence to clone	Vector	Antibiotic for selection
Promoters	<i>pICH 41295</i>	Streptomycin
Open reading frames	<i>pICH 41308</i>	Streptomycin
Terminators	<i>pICH 41276</i>	Streptomycin

**Table 3: Level 0 Backbones from the MoClo system used in this study.**

#### 4.6.5.2 Primer design for level 0 modules and domestication in level 0

The primers used for cloning in level 0 modules had specific tails depending on the category of cloning (promoter, ORF and terminators). The sequences of the primer extensions can be found in Table 4.

Cloning category	Primer Orientation	Sequence
<b>Promoter</b>	Forward (vector ligation)	TTTGAAGACAAGGAG
	Reverse (vector ligation)	TTTGAAGACAACATT(NN)*
<b>Open reading frame</b>	Forward (vector ligation)	TTTGAAGACAATAATG**
	Reverse (vector ligation)	TTTGAAGACAAGAAGC
<b>Terminator</b>	Forward (vector ligation)	TTTGAAGACAAGCTT
	Reverse (vector ligation)	TTTGAAGACAAGCG

**Table 4: Primer extensions for cloning in level 0 modules:** The extensions are added to the overlapping region in the sequence of interest. \*(NN) two extra base pairs need to be considered to codify an extra amino acid (excluding methionine), to keep the reading frame correct. \*\*When the ATG is present in the primer extension, it should not be included in the ORF's overlapping region to not generate an amino acid duplication.

Independently of the category of cloning (promoters, ORF, or terminators) when necessary, domestication in level 0 was performed by generating PCR fragments with specific overlap to be included simultaneously in the level 0 reaction. For domestication, we refer to the elimination of *BpiI* and *BsaI* recognition sites from the sequence of interest. To this end, the sequence of interest was divided into 2 or more PCR fragments. For the 3' and 5' endings of the complete sequence, the extensions for vector ligation shown in Table 4 were used. For internal PCRs, the following overlaps were utilized:

**Forward primers for domestication:** TTTGAAGACAA plus last 4 nucleotides of the recognition site plus homology sequence.

**Reverse primers for domestication:** TTTGAAGACAA plus homology sequence.

An example of this process is shown in Figure 29.

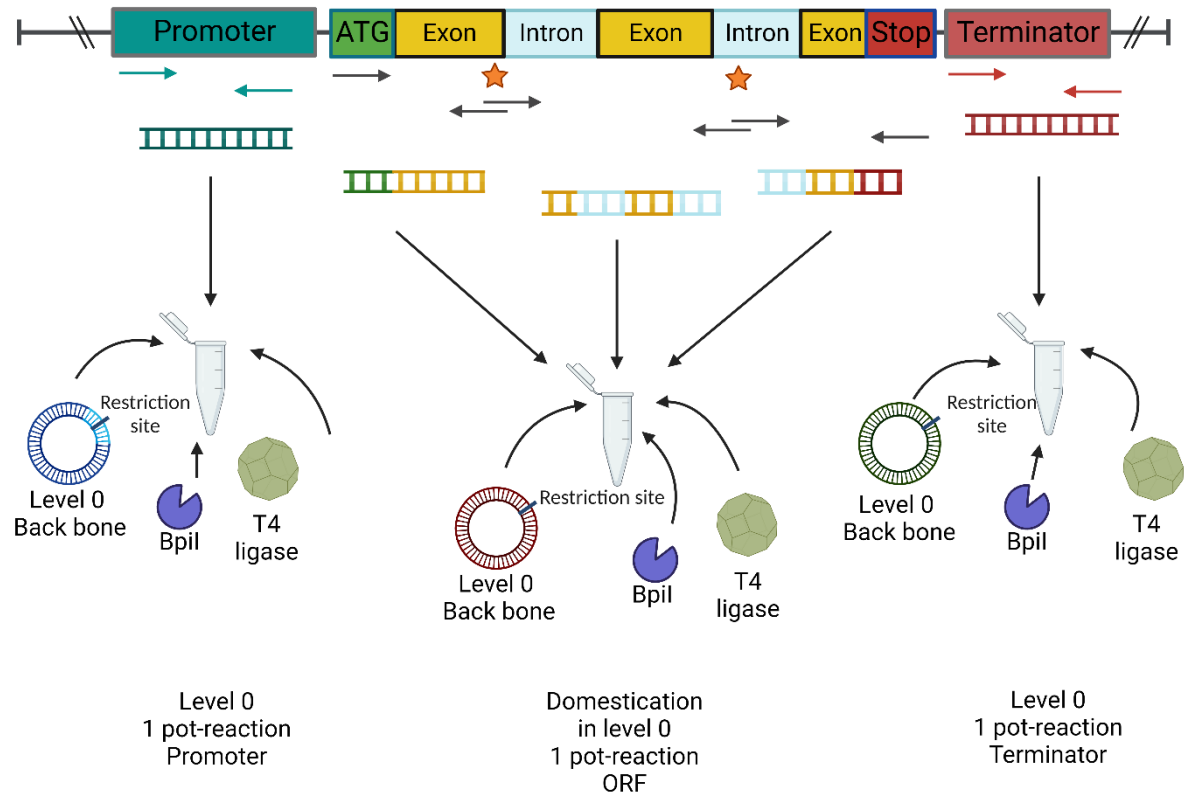


**Figure 29: Cloning reaction in level 0 without domestication (promoter and terminator) and with domestication in level 0 (ORF):** Stars represent recognition sites for the type IIS restriction enzymes *BpiI* or *BsaI*. Arrows oriented left to right represent forward primers. Arrows in orientation right to left represent reverse primers. Figure created with Biorender.com.

#### 4.6.5.3 Level 1 Modules

For all the level 1 modules, the one tube reaction contained: 1  $\mu$ l T4 DNA ligase buffer (NEB), 0,5  $\mu$ l *BsaI* HF (NEB), 0,5  $\mu$ l T4 DNA ligase (NEB), 77-100 ng backbone, insert (1:2 ratio) and ddH<sub>2</sub>O when required to achieve a final volume of 10  $\mu$ l.

The backbones used for level 1 are stated in Table 5.

<b>Position</b>	<b>Vector</b>	<b>Antibiotic for selection</b>
<b>Position 1 Forward</b>	<i>pICH47732</i>	Carbenicillin
<b>Position 2 Forward</b>	<i>pICH47742</i>	Carbenicillin
<b>Position 3 Forward</b>	<i>pICH47751</i>	Carbenicillin
<b>Position 4 Forward</b>	<i>pICH47761</i>	Carbenicillin
<b>Position 5 Forward</b>	<i>pICH47772</i>	Carbenicillin
<b>Position 1 Reverse</b>	<i>pICH47802</i>	Carbenicillin
<b>Position 3 Reverse</b>	<i>pICH47822</i>	Carbenicillin
<b>Position 5 Reverse</b>	<i>pICH47841</i>	Carbenicillin
<b>Position 6 Reverse</b>	<i>pICH47852</i>	Carbenicillin

**Table 5: Level 1 backbone vectors used in this study.**

#### **4.6.5.4 Level 2 Modules**

Level 2 reactions were done according to the following protocol: 1 µl T4 DNA ligase buffer (NEB), 0,5 µl *BpiI* Fast digest (Thermo Fisher Scientific), 0,5 µl T4 DNA ligase (NEB), 77-100 ng backbone, insert (1:2 ratio) and ddH<sub>2</sub>O when required to achieve a final volume of 10 µl.

In all cases the backbone Used was pAGM4673(Weber et al., 2011). The end linkers and/or dummies were used depending on the specific cases.

#### **4.6.6 *U. maydis* gDNA isolation protocol**

For the extraction of gDNA from *U. maydis* strains, a modified version of the protocol published by (Hoffman & Winston, 1987) was used. The pellets from 2ml overnight cultures from *U. maydis* strain were collected by centrifugation at 12000 *xg* in a 2 ml reaction tube. Between 0,2 and 0,3 g of glass beads (0,4-0,6 mm), together with 400 µl of Ustilago lysis buffer and 500 µl of phenol/chloroform were added to the pellet. The reaction tubes were incubated for 10 min at room temperature on a Vibrax-VXR shaker (IKA) at 2500 rpm. The samples were then centrifuged at 13300 *xg* for 10 min for separation of the phases. After

centrifugation, the upper aqueous phase containing the gDNA was transferred to a 1,5 ml reaction tube. The DNA was then precipitated by the addition of 1ml of 100% EtOH cold, inverted several times, and centrifuged at 13300  $xg$ , at 4°C for 10 min. Following the centrifugation, the supernatant was removed, and the pellet was resuspended in 200  $\mu$ l of 70% EtOH and centrifuged at 13300  $xg$  for 5 minutes. The supernatant was completely removed, and the pellets dissolved in 100  $\mu$ l of RNase and incubated at 37°C in a Thermomixer (Eppendorf) at 1200rpm for 30 min and stored at -20°C.

**Ustilago lysis buffer:** 50mM Tris-HCl (pH: 8.0)

50mM Na<sub>2</sub>-EDTA

1% (w/v) SDS

**Phenol/Chloroform:** 50% (v/v) Phenol (equilibrated in TE buffer)

50% (v/v) Chloroform

#### 4.6.7 Total RNA extraction from infected maize tissue

For the isolation of total RNA, samples from the infected leaf of maize plants were collected and frozen in liquid N<sub>2</sub>. A total of ten leaves per mutant, per time point per biological replicate, were taken and homogenized using a mortar and pestle, keeping the freezing conditions with liquid N<sub>2</sub>.

The samples were placed in previously cooled, RNase-free, 1,5  $\mu$ l reaction tubes and stored in -80°C until the RNA extraction procedure. TRIzol® reagent (Invitrogen) was used for the extraction of RNA according to the manufacturer's instructions. For each sample containing approximately 50-100mg of homogenized infected plant tissue, 1 ml of TRIzol® was immediately added and the samples were mixed in Vibrax-VXR shaker (IKA) at 2500 rpm for 5 min. To allow complete dissociation of the nucleoprotein complex the samples were incubated at room temperature for 5 minutes. After incubation, 0.2 ml of chloroform per ml of TRIzol® was added to the samples, and the tubes were then shaken vigorously by vortex for a few seconds, followed by a second incubation at room temperature for 2-3 min.

After centrifugation at 12000  $xg$  for 10 min at 4°C, the supernatants containing the RNA fraction (approx 50% of the total volume) were carefully transferred to a new reaction tube. For RNA precipitation, 400  $\mu$ l of 100% isopropanol per 1ml of TRIzol®, was added to the aqueous phase and the samples were then incubated at room temperature for 10 min, followed by centrifugation at 12000  $xg$  at 4°C for 10 min. After centrifugation, the supernatant was

removed leaving only the RNA pellet. The RNA was then washed by adding 1 ml of 75% ethanol per 1 ml of TRIzol®. The samples were then briefly vortex and centrifuged at maximum speed at 4°C for 5 min. The RNA pellet was then dried at room temperature for 10 min and resuspended in 50 µl of RNase free water, incubated in a hit block at 60°C for 15 minutes and immediately used for the DNase treatment.

#### **4.6.8 DNase treatment after RNA isolation from plant material**

For digestion of DNA contaminants after RNA isolation, the DNase treatment was performed using the Turbo DNA-Free™ commercial Kit from Ambion Life technologies™ according to the manufacturer's instructions. The total RNA samples were treated in a 50 µl reaction, containing 5 µl of 10X TURBO DNase Buffer and 1 µl of TURBO DNase enzyme and incubated at 37°C for 30 min followed by an inactivation step for the DNase by adding 5,5 µl of DNase Inactivation Reagent. After incubation at room temperature for 5 min with occasional mixing, the samples were centrifuged at 10000 *xg* for 2 min, and 44 µl of the supernatant were then transferred to a fresh reaction tube. For checking the quality of the RNA samples, 2 µl were run in 1% agarose gel run at 150 V for 30 min.

#### **4.6.9 cDNA synthesis**

From the RNA samples, the synthesis of cDNA was performed using the Thermo Scientific RevertAid H Minus First Strand cDNA Synthesis kit (Thermo Fisher Scientific) according to the manufacturer's instructions. The reaction consisted of 6 µl containing 1-5 µg of RNA template and 0,5 µl of oligo(dT)18 primer and the first incubation at 65°C for 5 min. Then, 2 µl of 5X Reaction Buffer, 0,5 µl of RiboLock RNase inhibitor, 1 µl of 10mM dNTP Mix, and 0,5 µl of RevertAid H Minus M-MuLV Reverse Transcriptase were added and the sample was then incubated at 42°C for 60min. The reaction was terminated by a 70°C, 5 min incubation. The cDNA was stored at -20°C until further use.

#### **4.6.10 Quantification of nucleic acids**

Quantification of cDNA, gDNA, plasmids, and RNA was performed using a NanoDrop ND\_1000 spectrophotometer (Thermo Fisher Scientific) according to the manufacturer's instructions. The concentration of nucleic acid was determined by µl using the appropriate

buffer as a blank control.

#### **4.6.11 Amplification of DNA by Polymerase chain reaction (PCR)**

For the amplification of DNA fragments, polymerase chain reactions were performed in T100 Thermal cyclers from Bio-Rad Laboratories GmbH. The polymerase used depended on the purpose of the experiment, and the reaction conditions were according to the manufacturer's instructions for each case. For analytical purposes GoTaq® green Master Mix (Promega) was used. For amplification of long fragments, or DNA fragments used for the construction of vector the enzymes Phusion® High Fidelity DNA Polymerase, Q5 ® High Fidelity DNA Polymerase (NEB) or KOD (Merk) were used.

#### **4.6.12 Quantitative real-time PCR (qRT-PCR)**

cDNA synthesized from RNA was used as a template for quantitative real-time PCR. For the qRT-PCR reactions, the GoTaq® qPCR Mastermix (Promega) was used according to the manufacturer's instructions in a final volume of 20 µl per reaction.

Each reaction contained 10 µl of GoTaq® qPCR Mastermix, 1 µl each primer (forward and reverse), 5 µl of cDNA (of a 5:195 dilution of cDNA) and 3 µl water.

All the primers for qRT-PCR in this study were optimized. The primer efficiency was analyzed in serial dilution; from  $10 \times 10^{-4}$  ng/µl to  $10 \times 10^{-7}$  ng/µl for plasmid templates or 4 serial dilutions from the 1:195 dilution from cDNA.

In all the cases the reactions were performed in an iCycler system (Bio-Rad) with the following program:

95°C	3 min
95°C	0:10 min
62°C	0:30 min
Repeat from step #2 45X	
65°C	0:05 min
95°C	0:05 min

#### **4.6.13 DNA digest**

The restriction digestion of DNA fragments was done by either New England Biolabs (NEB) enzymes or Thermo Fischer enzymes. The amount of digested DNA and the length of incubation times depended on the aim of the experiment.

For analytical digestion, a maximum amount of 1 µg of DNA was digested, using 0,25 µl of enzyme in a reaction volume of 50 µl, e incubated at the indicated temperature for a minimum amount of 2 hours.

For digestion of vectors with cloning purposes between 5 and 20 µg were digested in a final volume of reaction of 100 µl with 0,3 µl of the enzyme, overnight at the specific indicated temperature for each enzyme.

For Southern blot samples, 20 µl of the DNA suspension were digested in a final reaction volume of 200 µl, using 0,5 µl of enzyme overnight at the indicated temperature for the specific enzyme.

Either for checking analytical digest, or to control the quality of overnight digests with cloning purposes, 5 µl of reactions were run in 1 % agarose gel at 110V for 40 min.

#### **4.6.14 Agarose gel**

The visualization and separation of DNA fragments for PCRs, Southern blots, analytical digestions, and DNA purification, were done by agarose gel electrophoresis.

The samples were prepared by adding 1/5 of the ample volume of 6X loading dye (NEB) or TriTrack DNA loading dye (Thermo Fischer Scientific) except that indicated contrary.

For southern blots, the concentration of agarose in the gels was 0,9%(w/v), while for the other experiments was 1%(w/v). In the gels, 0,25 µg/ml of ethidium bromide in 1xTAE buffer.

To estimate the size of DNA fragments, a DNA marker of defined size was run in the first row of each gel.

The gels were run in electrophoresis chambers filled with 1X TAE- Buffer at 90-150 V for 20-120 min depending on the experiment. The DNA was then visualized by UV illumination using a gel documentation unit (Peqlab/VWR).



In the case that DNA fragment needed to be extracted from the gel, the band/s of interest was/were cut, and the DNA extracted using NucleoSpin® Gel and PCR Clean-up Kit (Macherey Nagel) according to the user manual.

#### **50x TAE-buffer**

2 M Tris-Base

2 M Acetic acid

50 mM EDTA pH 8.0

#### **4.6.15 Southern blot**

To identify specific genomic DNA integration and confirm genetically U. maydis mutants, Southern Blot experiments were done as described by (Southern, 1992)

The gDNA from the different strains was first digested with restriction enzymes (specific for each experiment) to generate a clear band pattern that distinguishes the mutant of interest concerning the genetic background in which it was generated.

For the restriction digest, 20 µl of DNA was digested in a final volume of 200 µl reaction using 1 µl of the respective restriction enzyme (or a combination of them when required in a 1:1 ratio). After completing overnight digestion to increase the DNA concentration and purity, 20 µl of 3 M sodium acetate was added to the samples followed by 150 µl of ice-cold 100% EtOH. The samples were then incubated for 30-60 min at -20°C and centrifuged for 20 min at 4°C at 12.000 *x g*. After centrifugation, the pellet was washed with 75% EtOH. After 15 min centrifugation (same condition as mentioned above) the EtOH was removed. The samples were then dissolved in 24 µl of a solution containing 20 µl of water and 4 µl of TriTrack DNA loading dye (Thermo Fischer Scientific). And dissolved at 37°C for 30 min.

The DNA samples were separated by gel electrophoresis (0,9% agarose) at 100V for 2 h. For depurination, the gels were incubated (slots down) in depurination solution for 15 min (or until the marker color was completely shifted from blue to bright yellow). Subsequently, the gels were neutralized with a transfer buffer for a minimum of 15 min until the marker was completely shifted from yellow to blue.

After neutralization, the gels were blotted (upward blotting). The DNA was transferred overnight using transfer buffer and Whatman papers for capillarity, to an Amersham Hybond-XL membrane (GE Health Care Life Sciences). After the transfer, the DNA was fixated to the

membrane by UV crosslinking (Amersham Biosciences) for 2 min. From this step on and until detection, the membranes were incubated in hybridization tubes with the downside of the membrane facing the inner side of the tubes. Immediately after crosslinking, the membranes were incubated with hybridization buffer (20ml) at 65°C for 30 min-2h in a hybridization oven (UVP HB-1000 Hybridizer, Ultra-violet products Ltd) in constant turning.

The probes for detection of nucleic acids were done using dioxigenin (DIG) labeled DNA fragments, synthesized by Phusion PCR (NEB) with the following conditions:

10 µl of 5x Phusion buffer  
 5 µl DIG labeling mix  
 0,5 µl forward primer  
 0,5 µl reverse primer  
 50 ng DNA template (preferentially plasmid)  
 1 µl Phusion polymerase  
 ddH2O up to 50 µl

The cycling conditions were:

98°C	30 sec		
98°C	10 sec		
60-72°C	10-30 sec		
72°C	30 sec per kb (60sec)	go to 2.:	35-40x
72°C	5-10 min		
12°C	∞		

The PCR product was mixed in 50ml of Southern-hybridization buffer. The Probe containing the hybridization buffer was then boiled for 10 min. The membranes were incubated at 65°C in the hybridization oven with the probe overnight and then washed 2 times for 15 min with southern wash buffer (20ml) at room temperature in a hybridization oven. The membranes were then incubated in DIG wash buffer (20ml) for 5 min. Next, the membranes were incubated for 30 min in 100 ml of DIG-buffer 2 (blocking solution) followed by a 30 min incubation in antibody solution at room temperature in a hybridization oven.

The membranes were then washed 2 times for 15 min with DIG-wash buffer and equilibrated for 5 min in 20 ml of DIG buffer 3.

Afterward, the membranes were placed in a transparent cut autoclaving bag and approximately

2,5 ml of CDP-star-solution was evenly spread across the membranes. After incubation at 37°C for 10-15 min in an incubation over, the southern blots were detected in a ChemiDoc™MP (Bio-Rad Laboratories GmbH).

**Depurination solution**

0.25 M HCl

**Transfer buffer**

0.5 M NaOH

1.5 M NaCl

**Southern hybridization buffer**

0,5 M NaPO<sub>4</sub> pH7

7% (w/v) SDS

**Southern wash buffer**

0,1M 1M NaPO<sub>4</sub> pH7

1%(w/v) SDS

**DIG buffer I**

0,1 M maleic acid

0,15M NaOH

Set to pH 7,5 with NaOH

Autoclave

**DIG buffer II**

1g skimmed milk powder

100ml DIG buffer 1

**DIG buffer III**

0,1 M Tris-HCL (pH9,5)

0,1M NaCl

0,05M MgCl<sub>2</sub>

#### **DIG wash buffer**

6ml Tween20  
2LDIG buffer 1

#### **Southern antibody solution**

2µl Anti- Dioxigenin-AP, Fab Fragmentes (Roche)  
20ml DIG Buffer 2

#### **CDP-star solution**

200 µl CDP-Star Solution (Roche)  
20 ml DIG Buffer 3

#### **4.6.16 DNA purification**

Nucleic acids were purified using the NucleoSpin® gel and PCR Clean-up kit (Macherey-Nagel) according to the manufacturer 's instructions.

#### **4.6.17 Sequencing**

Sequencing of DNA fragments was done by the company Eurofins. The DNA fragments for sequencing were either from a purified plasmid template or purified PCR products.

Sequencing DNA results were evaluated using the Clone Manager 9 Software or SnapGene Software.

### **4.7 Microscopy**

#### **4.7.1 Confocal laser-scanning microscopy**

For analysis of the presence/absence of Tag proteins (GFP or mCherry) associated or not to an effector gene, maize leaves infected with *U. maydis* mutant strains expressing the above-mentioned proteins were analyzed with a Leica TCS SP8 Confocal Laser Scanning Microscope.

The images were processed using the LEICA software LAS AFLite.

## 4.8 Optogenetics

The plasmids used for the Blue-on and Blue-off system adapted to *U. maydis* were a modification of plasmids designed in the working group of Prof. Dr. Matias Zurbringgen at the Heinrich Heine Universität Düsseldorf.

The incorporation of the ORF from the effector gene *see1* in frame with the *FLuc* gene was done by Gibson Assembly. The plasmids modified were pLH120 for the Blue-off system and pNH023 for the Blue-on system. In both cases, the coding sequence from *see1* was amplified using a proofreading enzyme with primers that contained overlaps designed for Gibson Assembly.

In the Table 6, a List of the *U. maydis* strains generated is listed together with the plasmid used in each case.

System	<i>U. maydis</i> strain	Plasmids
Blue-on	<i>U. maydis</i> Negative control Blue-on	<i>pNH023_see1</i>
	<i>U. maydis</i> Positive control Blue-on	<i>pNH023_see1</i> <i>pNH008</i>
	<i>U. maydis</i> Blue-on system	<i>pNH023_see1</i> <i>pNH047</i>
Blue-off	<i>U. maydis</i> Firefly reporter Blue-off	<i>pLH120_see1</i>
	<i>U. maydis</i> Blue-off system	<i>pLH120_see1</i> <i>pLH126</i>

**Table 6: Optogenetic *U. maydis* strains used in this study and the plasmids used for their generation.**

Technical information about the optogenetic plasmids can be found in the supplementary Table S3

### 4.8.1 Determination of FLuc expression in maize leaves

Maize infected plants infected with *U. maydis* strains included in the blue on and blue off optogenetic systems were kept under different light conditions in a growth chamber with white light, darkness or 10uE blue light. After 6dpi, the firefly luminescence was detected in 3-4 cm peace if the 3<sup>rd</sup> leaf of the infected plants. After recording the weight of each 0.5 cm width cut, the fresh samples were measured with 200 µl of 5 mM luciferin substrate with 0.1% triton-X in the Berthold plate reader.



## 5 Bibliography

**Ali S, Laurie JD, Linning R, Cervantes-Chávez JA, Gaudet D, Bakkeren G. 2014.** An Immunity-Triggering Effector from the Barley Smut Fungus *Ustilago hordei* Resides in an Ustilaginaceae-Specific Cluster Bearing Signs of Transposable Element-Assisted Evolution. *PLoS Pathogens* **10**.

**Anderson JC, Clarke EJ, Arkin AP, Voigt CA. 2006.** Environmentally controlled invasion of cancer cells by engineered bacteria. *Journal of Molecular Biology* **355**: 619–627.

**Andres J, Blomeier T, Zurbriggen MD. 2019.** Synthetic switches and regulatory circuits in plants. *Plant Physiology* **179**: 862–884.

**Angot A, Peeters N, Lechner E, Vaillau F, Baud C, Gentzbittel L, Sartorel E, Genschik P, Boucher C, Genin S. 2006.** *Ralstonia solanacearum* requires F-box-like domain-containing type III effectors to promote disease on several host plants. *Proceedings of the National Academy of Sciences of the United States of America* **103**: 14620–14625.

**Ashwini M, Murugan SB, Balamurugan S, Sathishkumar R. 2016.** Advances in molecular cloning. *Molecular Biology* **50**: 1–6.

**Banuett F, Herskowitz I. 1996.** Discrete developmental stages during teliospore formation in the corn smut fungus, *Ustilago maydis*. *Development* **122**: 2965–2976.

**Barletta RG, Udani R, Chan J, Kalkut G, Sosne G, Kieser T, Hatfull GF, Bloom BR, By S, Pazzagli M. 2000.** Gelmini, pinzani,. **305**.

**Barrangou R, Fremaux C, Deveau H, Richards M, Boyaval P, Moineau S, Romero DA, Horvath P. 2007.** CRISPR provides acquired resistance against viruses in prokaryotes. *Science* **315**: 1709–1712.

**Basse CW, Stumpferl S, Kahmann R. 2000.** Characterization of a *Ustilago maydis* Gene Specifically Induced during the Biotrophic Phase : Evidence for Negative as Well as Positive Regulation. **20**: 329–339.

**Begerow D, Stoll M, Bauer R. 2006.** A phylogenetic hypothesis of Ustilaginomycotina based on multiple gene analyses and morphological data. *Mycologia* **98**: 906–916.

- Benner SA, Sismour AM. 2005.** Synthetic biology. *Nature Reviews Genetics* **6**: 533–543.
- Bindics J, Khan M, Uhse S, Kogelmann B, Baggely L, Reumann D, Ingole KD, Stirnberg A, Rybecky A, Darino M, et al. 2022.** Many ways to TOPLESS – manipulation of plant auxin signalling by a cluster of fungal effectors.
- Birch PRJ, Armstrong M, Bos J, Boevink P, Gilroy EM, Taylor RM, Wawra S, Pritchard L, Conti L, Ewan R, et al. 2009.** Towards understanding the virulence functions of RXLR effectors of the oomycete plant pathogen *Phytophthora infestans*. *Journal of Experimental Botany* **60**: 1133–1140.
- Bölker M, Genin S, Lehmler C, Kahmann R. 1995.** Genetic regulation of mating and dimorphism in *Ustilago maydis*. *Canadian Journal of Botany* **73**: 320–325.
- Brachmann A, Weinzierl G. 2001.** Identification of genes in the bW / bE regulatory cascade in *Ustilago maydis*. **42**: 1047–1063.
- Braguy J, Zurbriggen MD. 2016.** Synthetic strategies for plant signalling studies: molecular toolbox and orthogonal platforms. *The Plant journal : for cell and molecular biology* **87**: 118–138.
- Brefort T, Doehlemann G, Mendoza-Mendoza A, Reissmann S, Djamei A, Kallmann R. 2009.** *Ustilago maydis* as a pathogen. *Annual Review of Phytopathology* **47**: 423–445.
- Broomfield PLE, Hargreaves JA. 1992.** A single amino-acid change in the iron-sulphur protein subunit of succinate dehydrogenase confers resistance to carboxin in *Ustilago maydis*. *Current Genetics* **22**: 117–121.
- Cameron DE, Bashor CJ, Collins JJ. 2014.** A brief history of synthetic biology. *Nature Reviews Microbiology* **12**: 381–390.
- Capecchi MR. 1989.** Capecchi1989. *Science* **244**: 1288–1292.
- Carreón-Anguiano KG, Islas-Flores I, Vega-Arreguín J, Sáenz-Carbonell L, Canto-Canché B. 2020.** Effhunter: A tool for prediction of effector protein candidates in fungal proteomic databases. *Biomolecules* **10**.
- Cohen-Tannoudji M, Robine S, Choulika A, Pinto D, El Marjou F, Babinet C, Louvard**



- D, Jaisser F. 1998.** I- Sce I-Induced Gene Replacement at a Natural Locus in Embryonic Stem Cells . *Molecular and Cellular Biology* **18**: 1444–1448.
- Dahlmann TA, Terfehr D, Becker K, Teichert I. 2021.** Golden Gate vectors for efficient gene fusion and gene deletion in diverse filamentous fungi. *Current Genetics* **67**: 317–330.
- Dean R, Van Kan JAL, Pretorius ZA, Hammond-Kosack KE, Di Pietro A, Spanu PD, Rudd JJ, Dickman M, Kahmann R, Ellis J, et al. 2012.** The Top 10 fungal pathogens in molecular plant pathology. *Molecular Plant Pathology* **13**: 414–430.
- Depotter JRL, Doehlemann G. 2020.** Target the core: durable plant resistance against filamentous plant pathogens through effector recognition. *Pest Management Science* **76**: 426–431.
- Depotter JRL, Zuo W, Hansen M, Zhang B, Xu M, Doehlemann G. 2021.** Effectors with different gears: Divergence of *Ustilago maydis* effector genes is associated with their temporal expression pattern during plant infection. *Journal of Fungi* **7**: 1–14.
- Djamei A, Depotter J, Saridis G, Prokchorchik M, Barghahn S, Sousa N De, Silva TE, Zuo W. 2023.** Modulation of Host Immunity and Development by *Ustilago maydis*. : 3–30.
- Djamei A, Kahmann R. 2012.** *Ustilago maydis*: Dissecting the Molecular Interface between Pathogen and Plant. *PLoS Pathogens* **8**: 11–14.
- Doehlemann G, Van Der Linde K, Aßmann D, Schwammbach D, Hof A, Mohanty A, Jackson D, Kahmann R. 2009.** Pep1, a secreted effector protein of *Ustilago maydis*, is required for successful invasion of plant cells. *PLoS Pathogens* **5**.
- Doehlemann G, Ökmen B, Zhu W, Sharon A. 2017.** Plant pathogenic fungi. *The Fungal Kingdom*: 703–726.
- Doehlemann G, Wahl R, Horst RJ, Voll LM, Usadel B, Poree F, Stitt M, Pons-Kühnemann J, Sonnewald U, Kahmann R, et al. 2008.** Reprogramming a maize plant: Transcriptional and metabolic changes induced by the fungal biotroph *Ustilago maydis*. *Plant Journal* **56**: 181–195.
- Dutheil JY, Mannhaupt G, Schweizer G, Sieber CMK, Münsterkötter M, Güldener U, Schirawski J, Kahmann R. 2016.** A tale of genome compartmentalization: The evolution of

virulence clusters in smut fungi. *Genome Biology and Evolution* **8**: 681–704.

**Engler C, Gruetzner R, Kandzia R, Marillonnet S. 2009.** Golden gate shuffling: A one-pot DNA shuffling method based on type IIS restriction enzymes. *PLoS ONE* **4**.

**Engler C, Kandzia R, Marillonnet S. 2008.** A one pot, one step, precision cloning method with high throughput capability. *PLoS ONE* **3**.

**Engler C, Marillonnet S. 2014.** Golden Gate cloning. *Methods in Molecular Biology* **1116**: 119–131.

**Engler C, Youles M, Gruetzner R, Ehnert TM, Werner S, Jones JDG, Patron NJ, Marillonnet S. 2014.** A Golden Gate modular cloning toolbox for plants. *ACS Synthetic Biology* **3**: 839–843.

**Feldbrügge M, Kämper J, Steinberg G, Kahmann R. 2004.** Regulation of mating and pathogenic development in *Ustilago maydis*. *Current Opinion in Microbiology* **7**: 666–672.

**Genet MG, Urban OM. 1996.** Identification of the pheromone response element in *Ustilago maydis*. : 31–37.

**Gibson DG. 2011.** Enzymatic assembly of overlapping DNA fragments. *Methods in Enzymology* **498**: 349–361.

**Gibson DG, Young L, Chuang RY, Venter JC, Hutchison CA, Smith HO. 2009.** Enzymatic assembly of DNA molecules up to several hundred kilobases. *Nature Methods* **6**: 343–345.

**Gilbert ES, Walker AW, Keasling JD. 2003.** A constructed microbial consortium for biodegradation of the organophosphorus insecticide parathion. *Applied Microbiology and Biotechnology* **61**: 77–81.

**Giraldo MC, Valent B. 2013.** Filamentous plant pathogen effectors in action. *Nature Reviews Microbiology* **11**: 800–814.

**Gisel K, Nicole J, Todd A, Chi-manzanero BH, Couoh-dzul OJ, Islas-flores I, Cantocanch B. 2022.** WideEffHunter: An Algorithm to Predict Canonical and Non-Canonical Effectors in Fungi and Oomycetes.

**Gold SE, Bakkerena G, Daviesb JE, Kronstada JW. 1994.** Three selectable markers for

transformation. **142**: 225–230.

**Haimovich AD, Muir P, Isaacs FJ. 2015.** Genomes by design. *Nature Reviews Genetics* **16**: 501–516.

**Hedges SB. 2002.** The origin and evolution of model organisms. *Nature Reviews Genetics* **3**: 838–849.

**Hemetsberger C, Herrberger C, Zechmann B, Hillmer M, Doehlemann G. 2012.** The *Ustilago maydis* effector Pep1 suppresses plant immunity by inhibition of host peroxidase activity. *PLoS Pathogens* **8**.

**Hemetsberger C, Mueller AN, Matei A, Herrberger C, Hensel G, Kumlehn J, Mishra B, Sharma R, Thines M, Hüchelhoven R, et al. 2015.** The fungal core effector Pep1 is conserved across smuts of dicots and monocots. *New Phytologist* **206**: 1116–1126.

**Heucken N, Tang K, Hüsemann L, Heßler N, Müntjes K, Feldbrügge M, Göhre V, Zurbriggen MD. 2023.** Engineering and Implementation of Synthetic Molecular Tools in the Basidiomycete Fungus *Ustilago maydis*. *Journal of Fungi* **9**.

**Hille F, Charpentier E. 2016.** CRISPR-cas: Biology, mechanisms and relevance. *Philosophical Transactions of the Royal Society B: Biological Sciences* **371**.

**Holliday R. 1964.** THE INDUCTION OF MITOTIC RECOMBINATION BY MITOMYCIN C IN *USTILAGO* AND *SACCHAROMYCES*1. : 323–335.

**Jones, J.D.G. DJL. 2006.** H E P L a N T Imm U N E S Y S T. *Nature* **444**: 323–329.

**Kämper J. 2004.** A PCR-based system for highly efficient generation of gene replacement mutants in *Ustilago maydis*. *Molecular Genetics and Genomics* **271**: 103–110.

**Kämper J, Kahmann R, Bölker M, Ma LJ, Brefort T, Saville BJ, Banuett F, Kronstad JW, Gold SE, Müller O, et al. 2006.** Insights from the genome of the biotrophic fungal plant pathogen *Ustilago maydis*. *Nature* **444**: 97–101.

**Keon JPR, White GA, Hargreaves JA. 1991.** Isolation , characterization and sequence of a gene conferring resistance to the systemic fungicide carboxin from the maize smut pathogen , *Ustilago maydis*. : 475–481.

**Khalil AS, Collins JJ. 2010.** Synthetic biology: Applications come of age. *Nature Reviews Genetics* **11**: 367–379.

**Khosla C, Keasling JD. 2003.** Metabolic-engineering-for-drug-discovery-and-development *Nature-Reviews-Drug-Discovery*. **2**.

**Khrunyk Y, Münch K, Schipper K, Lupas AN, Kahmann R. 2010.** The use of FLP-mediated recombination for the functional analysis of an effector gene family in the biotrophic smut fungus *Ustilago maydis*. *New Phytologist* **187**: 957–968.

**Kojic M, Holloman WK. 2000.** Shuttle vectors for genetic manipulations in *Ustilago maydis*. **338**: 333–338.

**Kuruma Y, Stano P, Ueda T, Luisi PL. 2009.** A synthetic biology approach to the construction of membrane proteins in semi-synthetic minimal cells. *Biochimica et Biophysica Acta - Biomembranes* **1788**: 567–574.

**Kvitko BH, Park DH, Velásquez AC, Wei CF, Russell AB, Martin GB, Schneider DJ, Collmer A. 2009.** Deletions in the repertoire of *Pseudomonas syringae* pv. *tomato* DC3000 type III secretion effector genes reveal functional overlap among effectors. *PLoS Pathogens* **5**.

**Lanver D, Müller AN, Happel P, Schweizer G, Haas FB, Franitza M, Pellegrin C, Reissmann S, Altmüller J, Rensing SA, et al. 2018a.** The biotrophic development of *Ustilago maydis* studied by RNA-seq analysis. *Plant Cell* **30**: 300–323.

**Lanver D, Müller AN, Happel P, Schweizer G, Haas FB, Franitza M, Pellegrin C, Reissmann S, Altmüller J, Rensing SA, et al. 2018b.** The biotrophic development of *Ustilago maydis* studied by RNA-seq analysis. *Plant Cell* **30**: 300–323.

**Lanver D, Tollot M, Schweizer G, Lo Presti L, Reissmann S, Ma LS, Schuster M, Tanaka S, Liang L, Ludwig N, et al. 2017.** *Ustilago maydis* effectors and their impact on virulence. *Nature Reviews Microbiology* **15**: 409–421.

**Latimer LN, Lee ME, Medina-Cleghorn D, Kohnz RA, Nomura DK, Dueber JE. 2014.** Employing a combinatorial expression approach to characterize xylose utilization in *Saccharomyces cerevisiae*. *Metabolic Engineering* **25**: 20–29.

**Lee ME, Deloache WC, Cervantes B, Dueber JE. 2015.** A Highly Characterized Yeast

Toolkit for Modular, Multipart Assembly.

**Leisen T, Bietz F, Werner J, Wegner A, Schaffrath U, Scheuring D, Willmund F, Mosbach A, Scalliet G, Hahn M. 2020.** *CRISPR/Cas with ribonucleoprotein complexes and transiently selected telomere vectors allows highly efficient marker-free and multiple genome editing in Botrytis cinerea.*

**Losi A. 2004.** The bacterial counterparts of plant phototropins. *Photochemical and Photobiological Sciences* **3**: 566–574.

**Loubradou G, Brachmann A, Feldbrügge M, Kahmann R. 2001.** A homologue of the transcriptional repressor Ssn6p antagonizes cAMP signalling in *Ustilago maydis*. *Molecular Microbiology* **40**: 719–730.

**Lu T. 1998.** Comparative QTL mapping of resistance to *Ustilago maydis* across four populations of European flint-maize.

**Makarova KS, Wolf YI, Alkhnbashi OS, Costa F, Shah SA, Saunders SJ, Barrangou R, Brouns SJJ, Charpentier E, Haft DH, et al. 2015.** An updated evolutionary classification of CRISPR-Cas systems. *Nature Reviews Microbiology* **13**: 722–736.

**Martella A, Matjusaitis M, Auxillos J, Pollard SM, Cai Y. 2017.** EMMA: An Extensible Mammalian Modular Assembly Toolkit for the Rapid Design and Production of Diverse Expression Vectors.

**Matei A, Doehlemann G. 2016.** Cell biology of corn smut disease — *Ustilago maydis* as a model for biotrophic interactions. *Current Opinion in Microbiology* **34**: 60–66.

**Matei A, Ernst C, Günl M, Thiele B, Altmüller J, Walbot V, Usadel B, Doehlemann G. 2018.** How to make a tumour: cell type specific dissection of *Ustilago maydis*-induced tumour development in maize leaves. *New Phytologist* **217**: 1681–1695.

**Mendoza-Mendoza A, Berndt P, Djamei A, Weise C, Linne U, Marahiel M, Vraneš M, Kämper J, Kahmann R. 2009.** Physical-chemical plant-derived signals induce differentiation in *Ustilago maydis*. *Molecular Microbiology* **71**: 895–911.

**Moore SJ, Lai H, Kelwick RJR, Chee SM, Bell DJ, Polizzi KM, Freemont PS. 2016.** EcoFlex: A Multifunctional MoClo Kit for *E. coli* Synthetic Biology.

- Moore I, Samalova M, Kurup S. 2006.** Transactivated and chemically inducible gene expression in plants. *Plant Journal* **45**: 651–683.
- Mueller AN, Ziemann S, Treitschke S, Aßmann D, Doehlemann G. 2013.** Compatibility in the *Ustilago maydis*-Maize Interaction Requires Inhibition of Host Cysteine Proteases by the Fungal Effector Pit2. *PLoS Pathogens* **9**.
- Mukherji S, Van Oudenaarden A. 2009.** Synthetic biology: Understanding biological design from synthetic circuits. *Nature Reviews Genetics* **10**: 859–871.
- Müller K, Weber W. 2013.** Optogenetic tools for mammalian systems. *Molecular BioSystems* **9**: 596–608.
- Obst U, Lu TK, Sieber V. 2017.** A Modular Toolkit for Generating *Pichia pastoris* Secretion Libraries.
- Ochoa-Fernandez R, Abel NB, Wieland FG, Schlegel J, Koch LA, Miller JB, Engesser R, Giuriani G, Brandl SM, Timmer J, et al. 2020.** Optogenetic control of gene expression in plants in the presence of ambient white light. *Nature Methods* **17**: 717–725.
- van der Oost J, Patinios C. 2020.** The genome editing revolution. *Trends in Biotechnology* **41**: 396–409.
- Osorio S, Tohge T, Fernie AR, Feussner I, Feussner K, Meinicke P, Stierhof Y, Schwarz H. 2011.** Metabolic priming by a secreted fungal effector. : 0–5.
- Perfect SE, O’Connell RJ, Green EF, Doering-Saad C, Green JR. 1998.** Expression cloning of a fungal proline-rich glycoprotein specific to the biotrophic interface formed in the *Colletotrichum*-bean interaction. *Plant Journal* **15**: 273–279.
- Pohl C, Meyer V, Bovenberg RAL, Nygård Y, Driessen AJM. 2021.** Modular Synthetic Biology Toolkit for Filamentous Fungi.
- Lo Presti L, Lanver D, Schweizer G, Tanaka S, Liang L, Tollot M, Zuccaro A, Reissmann S, Kahmann R. 2015.** Fungal effectors and plant susceptibility. *Annual Review of Plant Biology* **66**: 513–545.
- Purnick PEM, Weiss R. 2009.** The second wave of synthetic biology: From modules to

systems. *Nature Reviews Molecular Cell Biology* **10**: 410–422.

**Rajendran M, Ellington AD. 2008.** Selection of fluorescent aptamer beacons that light up in the presence of zinc. *Analytical and Bioanalytical Chemistry* **390**: 1067–1075.

**Redkar A, Hoser R, Schilling L, Zechmann B, Krzymowska M, Walbot V, Doehlemann G. 2015.** A secreted effector protein of *Ustilago maydis* guides maize leaf cells to form tumors. *Plant Cell* **27**: 1332–1351.

**Saitoh H, Fujisawa S, Mitsuoka C, Ito A, Hirabuchi A, Ikeda K, Irieda H, Yoshino K, Yoshida K, Matsumura H, et al. 2012.** Large-scale gene disruption in *Magnaporthe oryzae* identifies MC69, a secreted protein required for infection by monocot and dicot fungal pathogens. *PLoS Pathogens* **8**.

**Sarkari P, Marx H, Blumhoff ML, Mattanovich D, Sauer M, Steiger MG. 2017.** An efficient tool for metabolic pathway construction and gene integration for *Aspergillus niger*. *Bioresource Technology*.

**Scalcinati G, Knuf C, Partow S, Chen Y, Maury J, Schalk M, Daviet L, Nielsen J, Siewers V. 2012.** Dynamic control of gene expression in *Saccharomyces cerevisiae* engineered for the production of plant sesquiterpene  $\alpha$ -santalene in a fed-batch mode. *Metabolic Engineering* **14**: 91–103.

**Schilling L, Matei A, Redkar A, Walbot V, Doehlemann G. 2014.** Virulence of the maize smut *Ustilago maydis* is shaped by organ-specific effectors. *Molecular Plant Pathology* **15**: 780–789.

**Schirawski J, Mannhaupt G, Münch K, Brefort T, Schipper K, Doehlemann G, Di Stasio M, Rössel N, Mendoza-Mendoza A, Pester D, et al. 2010.** Pathogenicity determinants in smut fungi revealed by genome comparison. *Science* **330**: 1546–1548.

**Schurack S, Depotter JRL, Gupta D, Thines M, Doehlemann G. 2021.** Comparative transcriptome profiling identifies maize line specificity of fungal effectors in the maize–*Ustilago maydis* interaction. *Plant Journal* **106**: 733–752.

**Schuster M, Schweizer G, Kahmann R. 2018.** Comparative analyses of secreted proteins in plant pathogenic smut fungi and related basidiomycetes. *Fungal Genetics and Biology* **112**:

21–30.

**Schuster M, Schweizer G, Reissmann S, Kahmann R. 2016.** Genome editing in *Ustilago maydis* using the CRISPR-Cas system. *Fungal Genetics and Biology* **89**: 3–9.

**Shalem O, Sanjana NE, Zhang F. 2015.** High-throughput functional genomics using CRISPR-Cas9. *Nature Reviews Genetics* **16**: 299–311.

**Shmakov S, Abudayyeh OO, Makarova KS, Wolf YI, Gootenberg JS, Semenova E, Minakhin L, Joung J, Konermann S, Severinov K, et al. 2015.** Discovery and Functional Characterization of Diverse Class 2 CRISPR-Cas Systems. *Molecular Cell* **60**: 385–397.

**Skibbe SD, Doehlemann G, Fernandes J, Walbot V. 2010.** Maize Tumors Caused by *Ustilago* Genes in Host and Pathogen. *Science* **67**: 89–93.

**Southern EM. 1992.** Detection of specific sequences among DNA fragments separated by gel electrophoresis. 1975. *Biotechnology (Reading, Mass.)* **24**: 122–139.

**Spellig T, Bottin A. 1996.** Green fluorescent protein ( GFP ) as a new vital marker in the phytopathogenic fungus *Ustilago maydis*. **509**: 503–509.

**Sperschneider J, Dodds PN. 2022.** EffectorP 3 . 0 : Prediction of Apoplastic and Cytoplasmic Effectors in Fungi and Oomycetes. **35**: 146–156.

**Sperschneider J, Dodds PN, Gardiner DM, Singh KB, Taylor JM. 2018.** Improved prediction of fungal effector proteins from secretomes with EffectorP 2 . 0. **9**: 2094–2110.

**Sperschneider J, Gardiner DM, Dodds PN, Tini F, Covarelli L, Singh KB, Manners JM, Taylor JM. 2016.** EffectorP: Predicting fungal effector proteins from secretomes using machine learning. *New Phytologist* **210**: 743–761.

**Srikantha T, Klapach A, Lorenz WW, Tsai LK, Laughlin LA, Gorman JA, Soll DR. 1996.** The Sea Pansy *Renilla reniformis* Luciferase Serves as a Sensitive Bioluminescent Reporter for Differential Gene Expression in *Candida albicans*. **178**: 121–129.

**Steen EJ, Chan R, Prasad N, Myers S, Petzold CJ, Redding A, Ouellet M, Keasling JD. 2008.** Metabolic engineering of *Saccharomyces cerevisiae* for the production of n-butanol. *Microbial Cell Factories* **7**: 1–8.



- Steinberg CWB and G. 2004.** Ustilago maydis , model system for analysis of the molecular basis of fungal pathogenicity U S T I L A G O M A Y D I S , A N I N T E R E S T I N G M O D E L . **5**: 83–92.
- Steinberg G, Perez-martin J. 2007.** Ustilago maydis , a new fungal model system for cell biology. : 61–67.
- Stergiopoulos I, De Wit PJGM. 2009.** Fungal effector proteins. *Annual Review of Phytopathology* **47**: 233–263.
- Sternberg SH, Redding S, Jinek M, Greene EC, Doudna JA. 2014.** DNA interrogation by the CRISPR RNA-guided endonuclease Cas9. *Nature* **507**: 62–67.
- Stotz HU, Mitroussia GK, de Wit PJGM, Fitt BDL. 2014.** Effector-triggered defence against apoplastic fungal pathogens. *Trends in Plant Science* **19**: 491–500.
- Straube A, Enard W, Berner A, Wedlich- R. 2001.** A split motor domain in a cytoplasmic dynein. **20**: 5091–5100.
- Tanaka S, Brefort T, Neidig N, Djamei A, Kahnt J, Vermerris W, Koenig S, Feussner K, Feussner I, Kahmann R. 2014.** A secreted Ustilago maydis effector promotes virulence by targeting anthocyanin biosynthesis in maize. *eLife* **3**: 1–27.
- Tang H, Wu Y, Deng J, Chen N, Zheng Z. 2020.** Promoter Architecture and Promoter Engineering in Saccharomyces cerevisiae.
- Waks Z, Silver PA. 2009.** Engineering a synthetic dual-organism system for hydrogen production. *Applied and Environmental Microbiology* **75**: 1867–1875.
- Wang JUN, Holden DW, Leongtt SA. 1988.** phytopathogenic fungus. **85**: 865–869.
- Weber E, Engler C, Gruetzner R, Werner S, Marillonnet S. 2011.** A modular cloning system for standardized assembly of multigene constructs. *PLoS ONE* **6**.
- Win J, Chaparro-Garcia A, Belhaj K, Saunders DGO, Yoshida K, Dong S, Schornack S, Zipfel C, Robatzek S, Hogenhout SA, et al. 2012.** Effector biology of plant-associated organisms: Concepts and perspectives. *Cold Spring Harbor Symposia on Quantitative Biology* **77**: 235–247.

**Wright A V., Nuñez JK, Doudna JA. 2016.** Biology and Applications of CRISPR Systems: Harnessing Nature's Toolbox for Genome Engineering. *Cell* **164**: 29–44.

**Wurdinger T, Badr C, Pike L, Kleine R De, Weissleder R, Breakefield XO, Tannous BA. 2008.** A secreted luciferase for ex vivo monitoring of in vivo processes. **5**: 171–173.

**Yi M, Valent B. 2013.** Communication between filamentous pathogens and plants at the biotrophic interface. *Annual Review of Phytopathology* **51**: 587–611.

**Zuo W, Depotter JR, Doehlemann G. 2020.** Cas9HF1 enhanced specificity in *Ustilago maydis*. *Fungal Biology*.

## 6 Supplementary

### 6.1 Bacterial strains used in this study

Backbone	Construct
pGAM1311	#2305-pGAM1311Lb-Rb6A
pCas9HFI	#2306-pCas9HfI_02533_02535
pCas9HFI	#2307- pCas9HfI_02533_02535_02540
pICH47811	#2362-pL1M-R2:umag_02533
pICH47761	#2363-pL1M-F4:umag_02535
pICH47772	#2364-pL1M-F5:umag_11416
pCas9HFI	#2406-pCas_9HfI: umag_11417
pCas9HFI	#2407-pCas_9HfI: umag_02538
pCas9HFI	#2408-pCas_9HfI: umag_02537
pCas9HFI	#2443-pCas_9HfI: umag_11415 c#3
pAGM4673	#2452-pL2-R1:R6RBlong
pAGM4673	#2453-pL2-F1:R6R2 <sup>nd</sup> comp 6A
pICH47742	#3094- p11:p2F_PU10115_gfp_NosT#4
pICH47751	#3114-pL1_P3F_PU03749_cfp_NosT #3
pICH47761	#3115- pL1_P4F_PU03046_mCherry_NosT#

	4
<b>pICH47751</b>	#3207- P11_3F_PU03749_mCherry_NosT
<b>pICH47761</b>	#3209-pL1_4F_PU03046_cfp_NosT
<b>pICH47802</b>	#3210-pL1_1R_CbxNosT
<b>pAGM4301</b>	#3214- pL2_PU10115gfp_PU03749mCherry _PU03046cfp-Cbx
<b>pAGM4301</b>	#3229- pL2_PU10115gfp_PU03749mCherry _PU03046cfp-Cbx #7
<b>pCas9HFI</b>	#3277-PcasHFI_Pam173free #5
<b>pAGM4673</b>	#3373- pL2_PU10115gfp_PU03749mCherry _PU03046cfp-Cbx D4
<b>pAGM4673</b>	#3377- pL2_1R:3R_PU11415_pep1mCherryN osT_Cbx locus (A3)
<b>pAGM4673</b>	#3378- pL2_1R:3R_PU02851_pep1gfpNosT_ Cbxlocus (B3)
<b>pNH023</b>	#3379-pNH023_See1 Optogenetic
<b>pLH120</b>	#3380-pLH120_See1 Optogenetic
<b>pCas9HFI</b>	#3382- pCas9HFI_sg200_PAM200deletion

<b>pUMa260</b>	#163-Plasmid for Cbx probe
<b>pAGM4673</b>	#3384- P11_P2F_PU02851_pep1gfp_NosT
<b>pAGM4673</b>	#3385- pL1_P2F_PU11415_pep1mCherry_NosT
<b>pAGM4673</b>	#3393- pI2_1R:5R_PU02851:pep1mCherry_PU11415:pep1GFP
<b>pAGM4674</b>	#3393- pI2_1R:5R_PU02851:pep1mCherry_PU11415:pep1GFP
<b>pAGM4675</b>	#3394- pL2_PU10115gfp_PU03749mCherry_PU03046cfpCbx D4 CbxRMod
<b>pAGM4678</b>	#3397-pI2_PU11415_gfp_NosT Cbxlocus (G2) CbxRMod
<b>pAGM4679</b>	#3398- pI2_1R:3R_PU11415_pep1mCherryNosT_Cbx locus (A3) CbxRMod
<b>pAGM4680</b>	#3399pI2_1R:3R_PU02851_pep1mCherryNosT_Cbxlocus (B3) CbxRMod
<b>pAGM4681</b>	#3400- pI2_1R:5R_PU02851:pep1gfp_PU11415:pep1mCherry CbxRMod
<b>P1Rev</b>	#3402-pL1_1R_CbxNosT CbxRMod

<b>pAGM4680</b>	#3448- pI1_P4F_PU03065_mCherryep1_NosT
<b>pAGM4680</b>	#3455- pI2_1R:5R_PU02851_11415_03065_mCherryep1-GFP:pep1-mCherry:pep1_NosT
<b>#3302 pNH047</b>	
<b>#3303 pNH023</b>	
<b>#3304 pNH008</b>	
<b>#3305 pLH120</b>	
<b>#3306 pLH126</b>	
<b>pCas9HFI</b>	#2456-pCas_9HfI_1 <sup>st</sup> C6A.
<b>pCas9HFI</b>	#2457-pCas_9HfI_2 <sup>nd</sup> C6A.
<b>pAGM4680</b>	#2511-pL2M <sup>1/2</sup> 6A::_R1:R6Short

**Table S1: *Escherichia coli* strains generated during this doctoral research.** Level 0 modules from the MoRfunG toolkit are not included in this table.

## 6.2 Bacterial strains containing MoRFunG modules

Code	Plasmid name	Plasmid backbone	Gene/insert
<b>FMTK 1</b>	pL0M-PU-umag_02533	pICH41295	Promoter <i>umag_02533</i>
<b>FMTK 2</b>	pL0M-C-umag_02533	pICH41308	ORF <i>umag_02533</i>
<b>FMTK 3</b>	pL0M-UT-umag_02533	pICH41276	Terminator <i>umag_02533</i>

<b>FMTK 4</b>	pL0M-UT- umag_02535	pICH41276	Terminator <i>umag_02535</i>
<b>FMTK 5</b>	pL0M-C-umag_11415	pICH41308	ORF <i>umag_11415</i>
<b>FMTK 6</b>	pL0M-PU-umag_11416	pICH41295	Promoter <i>umag_1116</i>
<b>FMTK 7</b>	pL0M-UT-umag_02537	pICH41276	Terminator <i>umag_02537</i>
<b>FMTK 8</b>	pL0M-UT-umag_02538	pICH41276	Terminator <i>umag_02538</i>
<b>FMTK 9</b>	pL0M-UT-umag_11417	pICH41276	Terminator <i>umag_11417</i>
<b>FMTK 10</b>	pL0M-PU-umag_02540	pICH41295	Promoter <i>umag_02540</i>
<b>FMTK 11</b>	pL0M-UT-umag_02540	pICH41276	Terminator <i>umag_02540</i>
<b>FMTK 12</b>	pL0M-PU-umag_11415	pICH41295	Promoter <i>umag_11415</i>
<b>FMTK 13</b>	pL0M-PU-umag_02535	pICH41295	Promoter <i>umag_02535</i>
<b>FMTK 14</b>	pL0M-UT-umag_11416	pICH41276	Terminator <i>umag_11416</i>
<b>FMTK 15</b>	pL0M-C-umag_11417	pICH41308	ORF <i>umag_11417</i>
<b>FMTK 16</b>	pL0M-C-umag_02540	pICH41308	ORF <i>umag_02540</i>
<b>FMTK 17</b>	pL0M-C-umag_02537	pICH41308	ORF <i>umag_02537</i>
<b>FMTK 18</b>	pL0M-C-umag_11416	pICH41308	ORF <i>umag_11416</i>
<b>FMTK 19</b>	pL0M-C-umag_02538	pICH41308	ORF <i>umag_02538</i>
<b>FMTK 20</b>	pL0M-PU-umag_02538	pICH41295	Promoter <i>umag_02538</i>
<b>FMTK 21</b>	pL0M-C-umag_02535	pICH41308	ORF <i>umag_02535</i>
<b>FMTK 22</b>	pL0M-PU-umag_02537	pICH41295	Promoter <i>umag_02537</i>
<b>FMTK 23</b>	pL0M-PU-umag_11417	pICH41295	Promoter <i>umag_11417</i>
<b>FMTK 24</b>	pL0M-UT-umag_11415	pICH41276	Terminator <i>umag_11415</i>

<b>FMTK 25</b>	pL0M-PU-umag_05319	pICH41295	Promoter umag_05319
<b>FMTK 26</b>	pL0M-PU-umag_06180	pICH41295	Promoter umag_06180
<b>FMTK 27</b>	pL0M-PUumag_05104	pICH41295	Promoter umag_05104
<b>FMTK 28</b>	pL0M-PU-umag_03046	pICH41295	Promoter umag_03046
<b>FMTK 29</b>	pL0M-PU-umag_00027	pICH41295	Promoter umag_00027
<b>FMTK 30</b>	pL0M-PU-umag_10115	pICH41295	Promoter umag_10115
<b>FMTK 31</b>	pL0M-PU-umag_02119	pICH41295	Promoter umag_02119
<b>FMTK 32</b>	pL0M-PU-umag_05311	pICH41295	Promoter umag_05311
<b>FMTK 33</b>	pL0M-PU-umag_03749	pICH41295	Promoter umag_03749
<b>FMTK 34</b>	pL0M-PU-umag_02194	pICH41295	Promoter umag_02194
<b>FMTK 35</b>	pL0M-C-gfp	pICH41308	ORF <i>gfp</i>
<b>FMTK 36</b>	pL0M-UT-NOST-	pICH41276	<i>Nos</i> Terminator
<b>FMTK 37</b>	pL0M-C-cfp	pICH41308	ORF <i>cfp</i>
<b>FMTK 38</b>	pL0M-C-mCherry	pICH41308	ORF <i>mCherry</i> Stop codon added
<b>FMTK 39</b>	pL0M_PU-umag_02851	pICH41295	Promoter <i>umag_02851</i>
<b>FMTK 40</b>	Pl0M_C_pep1MCherry	pICH41308	ORF umag_01987:mCherry
<b>FMTK 41</b>	Pl0M_C_pep1gfp	pICH41308	ORF umag_01987gfp
<b>FMTK 42</b>	pL0M_PU_Potef	pICH41295	<i>otef</i> constitutive promoter
<b>FMTK 43</b>	pL0M_C_FLuc	pICH41308	ORF <i>Fluciferase</i>



Optogenetics			
<b>FMTK 44</b>	pL0M_PU-umag_03065	pICH41295	Promoter umag_03065

**Table S2: *Escherichia coli* strains generated for this study containing the level 0 for the MorFunG toolkit.** FMTK stands for Fungal Modules ToolKit. **pL0M**: plasmid level zero module. **PU**: Promoter and untranslated regions. **C**: ORF. **TU**: Terminator and untranslated regions.

### 6.3 Technical information of the optogenetic plasmids

Optogenetic Plasmid	Description
<i>pLH120_see1</i>	<i>Upp3-(C120)5-PCMV-FLuc_see1</i>
<i>pLH126</i>	<i>Cco1-Po2tef-NLS-Sql1-EL222</i>
<i>pNH023_see1</i>	<i>Upp3-PIR3-PCMVmin-FLuc_see1</i>
<i>pNH008</i>	<i>Cco1-PO2tef-PIP-VP16ff</i>
<i>pNH047</i>	<i>Cco1-nosT-AsLOV2pep-PIP- P<sub>hCMVmin</sub>-CMVenhacer(5'-3')- P<sub>hCMVmine</sub>PDZb-VP16ff-nosT</i>

**Table S3:** Description of optogenetic plasmids.

## 6.4 Fungal strains used in this study

<b>Ustilago maydis strain</b>	<b>Usage</b>
#1332 SG200 Δ6A #4	Cluster Deletion
#1333 SG200 Δ6A #9	Cluster Deletion
#1334 SG200Δ6A #11	Cluster Deletion
#1390 SG200 KO: <i>umag_11417</i> c#4	CRISPR frameshift KO
#2406 SG200.KO. <i>umag_11417</i> c#2	CRISPR frameshift KO
#1392 SG200.KO. <i>umag_02538</i> c#1	CRISPR frameshift KO
#1393 SG200.KO. <i>umag_02538</i> c#2	CRISPR frameshift KO
#1394 SG200KO <i>umag_02537</i> c#1	CRISPR frameshift KO
#1395 SG200 KO <i>umag_02535</i> c#3	CRISPR frameshift KO
#1396 SG200 KO <i>umag_02535</i> c#4	CRISPR frameshift KO
#1397 SG200 KO <i>umag_11416</i> c#4	CRISPR frameshift KO
#1398 SG200 KO <i>umag_11416</i> c#8	CRISPR frameshift KO
#1399 SG200.KO <i>umag_02540</i> c#5	CRISPR frameshift KO
#1431 SG200 KO: <i>umag_02537</i> c#3	CRISPR frameshift KO
#1432 SG200 KO: <i>umag_02540</i> c#1	CRISPR frameshift KO
#1433 SG200 KO: <i>umag_02540</i> c#3	CRISPR frameshift KO
#1450 SG200 KO: <i>umag_02533</i> #4	CRISPR frameshift KO
#1451 SG200 KO: <i>umag_02533</i> #7	CRISPR frameshift KO

#1627 SG200 KO <i>umag_11417</i> Cl2.4	CRISPR frameshift KO
#1654 SG200 $\Delta$ 6A:: <i>umag_02533_11415_02535_11416</i> 1C#53 (SG 200 $\Delta$ 6A/C1)	Cluster 6A half complementation MoClo MoRFunG
#1655 SG200 $\Delta$ 6A:: <i>umag_02533_11415_02535_11416</i> 1C#46(SG 200 $\Delta$ 6A/C1)	Cluster 6A half complementation MoClo MoRFunG
#1656 SG200 $\Delta$ 6A/C1:: <i>umag_11416_02537:02538:11417:02540</i> #53D8(SG 200 $\Delta$ 6A/C2)	$\Delta$ 6A_1C53:: <i>11416_02537_02538_11417_02540</i> MoRFunG
1657: SG200 $\Delta$ 6A/C1 :: <i>umag_11416_02537:02538:11417:02540</i> #53D9 (SG 200 $\Delta$ 6A/C2)	$\Delta$ 6A_1C53:: <i>11416_02537_02538_11417_02540</i> MoRFunG
#1658 SG200 $\Delta$ 6A/C1:: <i>umag_11416_02537:02538:11417:02540</i> #46A15 (SG200 $\Delta$ 6A/C2)	$\Delta$ 6A_1C46:: <i>11416_02537_02538_11417_02540</i> MoRFunG
1659: SG200 $\Delta$ 6A/C1:: <i>umag_11416_02537:02538:11417:02540</i> $\Delta$ 6A/C2) #46AD7(SG200	$\Delta$ 6A_1C46:: <i>11416_02537_02538_11417_02540</i> MoRFunG
#1665 SG200 $\Delta$ 6A:: <i>umag_02533</i> MoClo Cl#2	$\Delta$ 6A single gene complementation
#1666 SG200 $\Delta$ 6A:: <i>umag_02533</i> MoClo Cl#3	$\Delta$ 6A single gene complementation
#1667 SG200 $\Delta$ 6A:: <i>umag_02533</i> MoClo Cl#4	$\Delta$ 6A single gene complementation
#1668 SG200 $\Delta$ 6A:: <i>umag_02537</i> MoClo Cl#2	$\Delta$ 6A single gene complementation

#1669 SG200 $\Delta$ 6A:: <i>umag_02537</i> MoClo Cl#3	$\Delta$	6A	single	gene complementation
#1670 SG200 $\Delta$ 6A:: <i>umag_02537</i> MoClo Cl#6	$\Delta$	6A	single	gene complementation
#1671 SG200 $\Delta$ 6A:: <i>umag_11415</i> MoClo Cl#1	$\Delta$	6A	single	gene complementation
#1672 SG200 $\Delta$ 6A:: <i>umag_11415</i> MoClo Cl#2	$\Delta$	6A	single	gene complementation
#1673 SG200 $\Delta$ 6A:: <i>umag_11415</i> MoClo Cl#8	$\Delta$	6A	single	gene complementation
#1674 SG200 $\Delta$ 6A:: <i>umag_02540</i> MoClo Cl#3	$\Delta$	6A	single	gene complementation
#1675 SG200 $\Delta$ 6A:: <i>umag_02540</i> MoClo Cl#6	$\Delta$	6A	single	gene complementation
#1676 SG200 $\Delta$ 6A:: <i>umag_02535</i> MoClo Cl#4	$\Delta$	6A	single	gene complementation
#1677 SG200 $\Delta$ 6A:: <i>umag_02535</i> MoClo Cl#6	$\Delta$	6A	single	gene complementation
#1678 SG200 $\Delta$ 6A:: <i>umag_02535</i> MoClo Cl#8	$\Delta$	6A	single	gene complementation
#1679 SG200 $\Delta$ 6A:: <i>umag_02535</i> MoClo Cl#11	$\Delta$	6A	single	gene complementation
#1680 SG200 $\Delta$ 6A:: <i>umag_02535</i> MoClo Cl#12	$\Delta$	6A	single	gene complementation
#1681 SG200 $\Delta$ 6A:: <i>umag_02538</i> MoClo Cl#6	$\Delta$	6A	single	gene

	complementation
<b>#1682 SG200: <math>\Delta</math>6A:<i>umag_02538</i> MoClo Cl#7</b>	$\Delta$ 6A single gene complementation
<b>#1683 SG200 <math>\Delta</math>6A::<i>umag_02538</i> MoClo Cl#8</b>	$\Delta$ 6A single gene complementation
<b>#1684 SG200<math>\Delta</math>6A::<i>umag_02538</i> MoClo Cl#9</b>	$\Delta$ 6A single gene complementation
<b>#1685 SG200 <math>\Delta</math>6A::<i>umag_11417</i> MoClo Cl#12</b>	$\Delta$ 6A single gene complementation
<b>#1686 SG200 <math>\Delta</math>6A::<i>umag_11417</i> MoClo Cl#10</b>	$\Delta$ 6A single gene complementation
<b>#1687 SG200 <math>\Delta</math>6A::<i>umag_11417</i> MoClo Cl#8</b>	$\Delta$ 6A single gene complementation
<b>#1688 SG200<math>\Delta</math>6A::<i>umag_11417</i> MoClo Cl#6</b>	$\Delta$ 6A single gene complementation
<b>#1849SG200_Multitag_gfp:<i>mCherry:cfp</i>PU10115_03749_03046</b>	Cbx integration without duplication of succinate dehydrogenase gene. MoClo
<b>#1858 SG200_PU11415:<i>pep1mCherry:NosT</i> (Cbx)#5.7</b>	Cbx integration without duplication of succinate dehydrogenase gene. MoClo
<b>#1859 SG200PU11415:<i>pep1mCherry:NosT</i> (Cbx)#5.9</b>	Cbx integration without duplication of succinate dehydrogenase gene. MoClo
<b>#1860 SG200_PU02851:<i>pep1gfp:NosT</i> (Cbx)#6.3</b>	Cbx integration without duplication of succinate

	dehydrogenase gene. MoClo
<b>#1861 SG200_PU02851:<i>Pep1gfp</i>:NosT (Cbx)#6.4</b>	Cbx integration without duplication of succinate dehydrogenase gene. MoClo
<b>#1862S SG200_PU02851:<i>Pep1gfp</i>:NosT (Cbx)#6.5</b>	Cbx integration without duplication of succinate dehydrogenase gene. MoClo
<b>#1863SG200_PU02851:<i>pep1gfp</i>:NosT_PU11415:<i>pep1m Cherry</i>:NosT (Cbx)# 7.1</b>	Cbx integration without duplication of succinate dehydrogenase gene. MoClo
<b>#1864SG200_PU02851:<i>pep1gfp</i>:NosT_PU11415:<i>pep1m Cherry</i>:NosT (Cbx)# 7.3</b>	Cbx integration without duplication of succinate dehydrogenase gene. MoClo
<b>#1865SG200_PU02851:<i>pep1gfp</i>:NosT_PU11415:<i>pep1m Cherry</i>:NosT (Cbx)# 7.6</b>	Cbx integration without duplication of succinate dehydrogenase gene. MoClo
<b>#1874 SG200 blue off_see1 #1</b>	upp3-(C120)5-PCMV-FLuc-cco1-Potef-NLS-Sql1-EL222
<b>#1875 SG200 blue off_see1 #3</b>	upp3-(C120)5-PCMV-Fluc-cco1-Potef-NLS-Sql1-EL222
<b>#1876 SG200 blue onn_see1 # 9</b>	upp3-PiR3-PCVMmin-FLuc_see1-cco1-nosT-AsLOV2pep-PIP-PhCMVmin-CMVenhacer5'>3'PhCMVminePDZb-VP16ff-nosT

#1877 SG200 blue onn_see1 # 11	upp3-PiR3-PCVMmin- Fluc_see1-cco1-nosT- AsLOV2pep-PIP- PhCMVmin- CMVenhacer5'>3'PhCMV minePDZb-VP16ff-nosT
SG200_PU02851:pep1gfp:NosT_PU11415:pep1mCherry :NosT_PU03065pep1mCherryNosT	Cbx integration without duplication of succinate dehydrogenase gene. MoClo
SG200_Δpep1_PU02851:pep1gfp:NosT_PU11415:pep1m Cherry:NosT_PU03065pep1mCherryNosT #5	Cbx integration without duplication of succinate dehydrogenase gene. MoClo
SG200_Δpep1_PU02851:pep1gfp:NosT_PU11415:pep1 mCherry:NosT_PU03065pep1mCherryNosT #7	Cbx integration without duplication of succinate dehydrogenase gene. MoClo

Table S4: *Ustilago maydis* strains generated during this study.

## 6.5 *Ustilago maydis* strains belonging to the optogenetic system

System	<i>U. maydis</i> strain	Plasmids
Blue-on	<i>U. maydis</i> Negative control Blue-on	<i>pNH023_see1</i>
	<i>U. maydis</i> Positive control Blue-on	<i>pNH023_see1</i> <i>pNH008</i>
	<i>U. maydis</i> Blue-on system	<i>pNH023_see1</i> <i>pNH047</i>
Blue-off	<i>U. maydis</i> Firefly reporter Blue-off	<i>pLH120_see1</i>
	<i>U. maydis</i> Blue-off system	<i>pLH120_see1</i> <i>pLH126</i>

**Table S5: *Ustilago maydis* blue-on and blue-off strains and the vectors used for cloning.** *Ustilago maydis* strains generated using the blue on and off light inducible system for the control of the effector See1 and the plasmids used for the construction of each strain.

The blue-on system counts with a total of three *U. maydis* strains including one positive and one negative control strain.

The blue-off system counts with two *U. maydis* strains.

## 6.6 Cluster 6A deletion and complementation: genetic confirmation

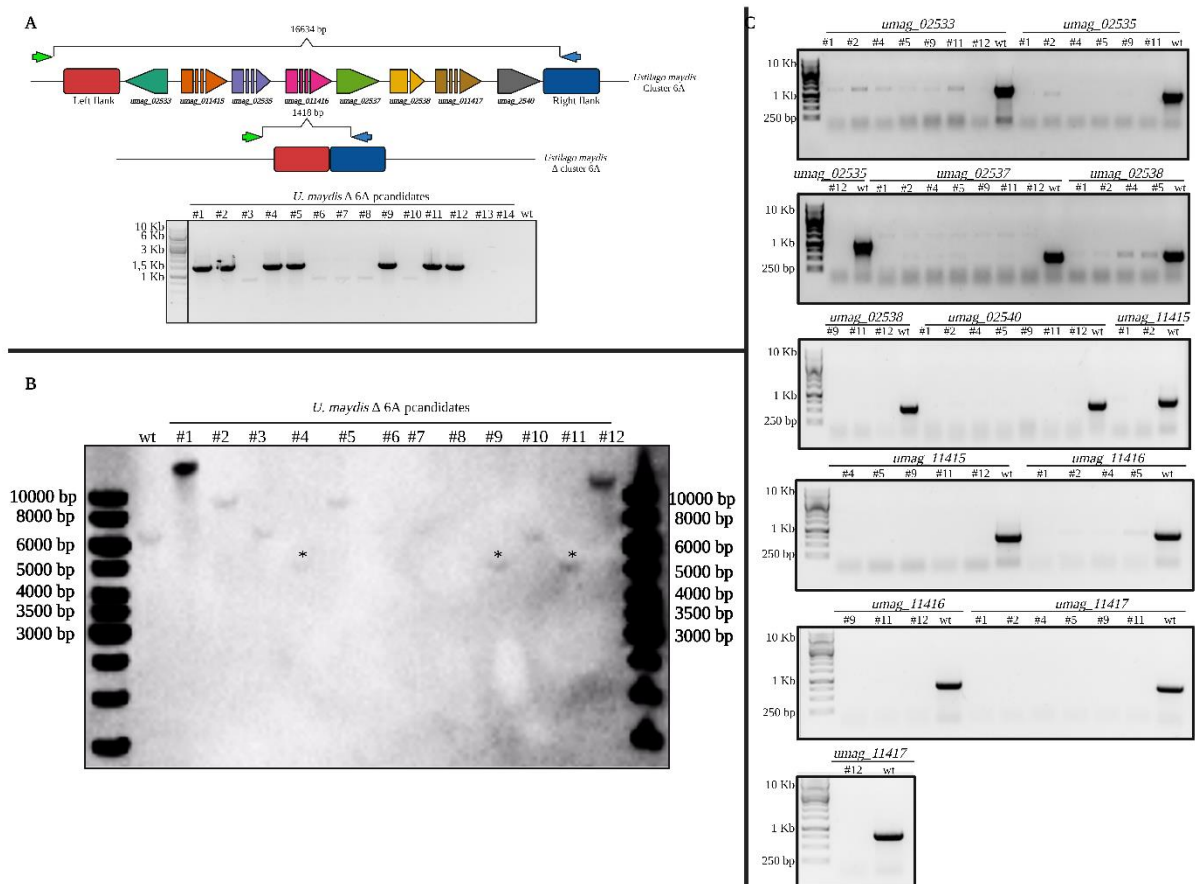


**Figure S1: Genetic confirmation of the cluster 6A deletion strains**

**A.** Screening PCR done to determine which putative mutants contained the flanking regions forming a genetic scar. Green arrows represent the forward primer (TCACAGAGCGTTCGTGCAG) and blue arrows represent the reverse primer (GTGATGCCGTCAATCTTGTC). The SG200 was used as a non-amplification control since the complete amplicon (16634 bp) had a size outside the amplification capability of the polymerase used (go-Tac). **B.** Southern blot of the putative strains for the cluster 6A deletion. The gDNA was digested with the enzyme *NcoI*. The expected size for the wild type was 7500bp and for positive strains containing the genetic scar and cluster deletion 5500bp. The probe was done using as template the plasmid #2305 pGAM1311Lb-Rb2020 and amplified with the forward primer: TAAGACATCCCGATCCGTG and reverse primer: GTATTCGGCGTCGTTAC. **C.** Screening PCR for amplification of the genes of the cluster in selected mutants with the wild type SG200 as positive control. Strains indicate with \* were positive.

*umag\_02533*: forward primer: ATGCGAACGCTTCAGCAC, reverse primer: TCAATGGACGTGCTCAAGAC

*umag\_02535*: forward primer: ATGATCCTCATCCAATTTTCG, reverse primer: TCAGCTTGAGCCACCTATTG

*umag\_02537*: forward primer: ATGAGGATGACGCTAACC, reverse primer: TCACGAGCGTGGACGCTTG

*umag\_02538*: forward primer: ATGCACGCCTCACGTATTTTG, reverse primer: TCATCCATGGCTGCTTTTCG

*umag\_02540*: forward primer: ATGACAAAGATGCTCAACCTAATCAC, reverse primer: TCAGGACTGGTTTCTGCGGGAAG

*umag\_11415*: forward primer: ATGCGTTATCTCGCCTTGG, reverse primer: CTAGCTTCCACTTGTGCCG

*umag\_11416*: forward primer: ATGATGCTCTTGAACGTCTCC, reverse primer: TACTTTGGTGGGCGTC

*umag\_11417*: forward primer: ATGATTTTTTCAGATATCCTTGTTTC, reverse primer: CTAAGATTCCGAAACAGCGTC.



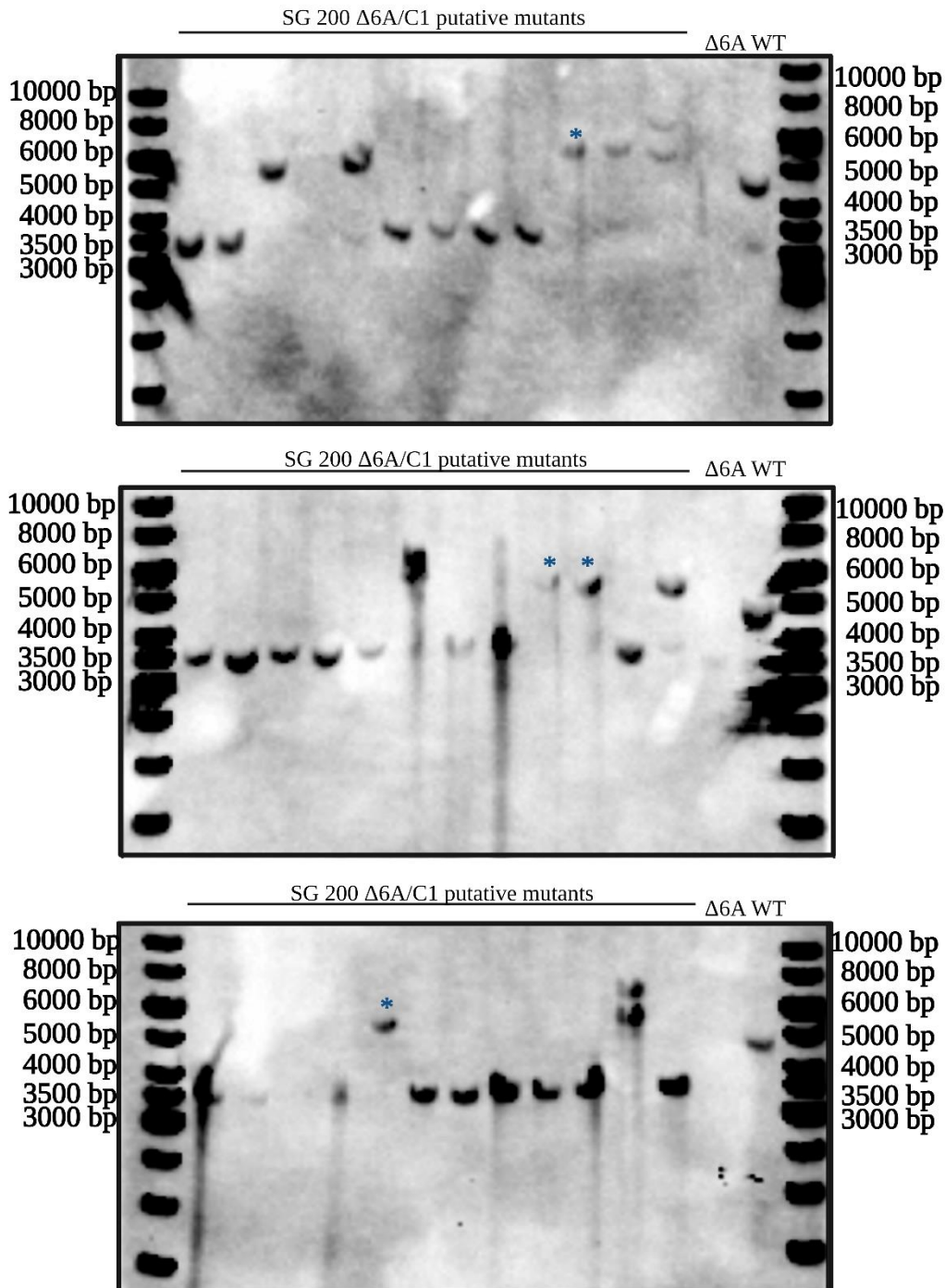


**Figure S2: Southern blot of the  $\Delta 6A/IC$  (First complementation)**

The Figure shows the southern blot of the putative mutants for the first half cluster complementation containing the genes *umag\_02533*, *umag\_02535*, *umag\_11415* and *umag\_11416*. The gDNA was digested with NcoI and EcoRV. The expected sizes for a positive mutant was 6186bp,  $\Delta 6A$ : 3767 bp and SG200: 5068 bp. The probe was done using as template the plasmid #2305 pGAM1311Lb-Rb2020 and amplified with the forward primer: TAAGACATCCCGATCCGTG and reverse primer: GTATTTTCGGCGTCGTTAC. Strains indicated with a blue \* were considered positive. Figure created with Biorender.com

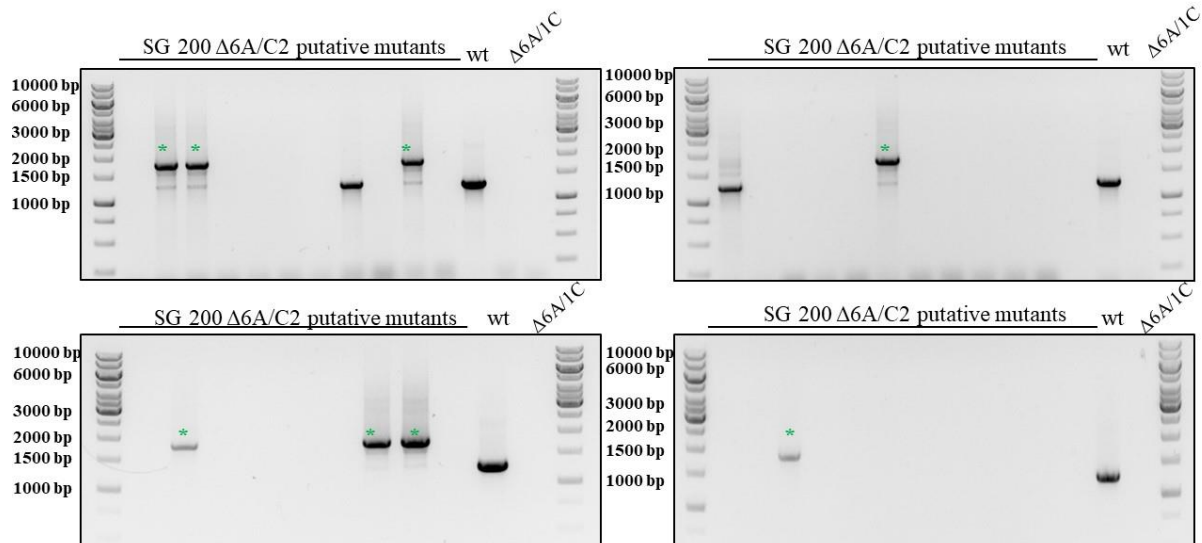
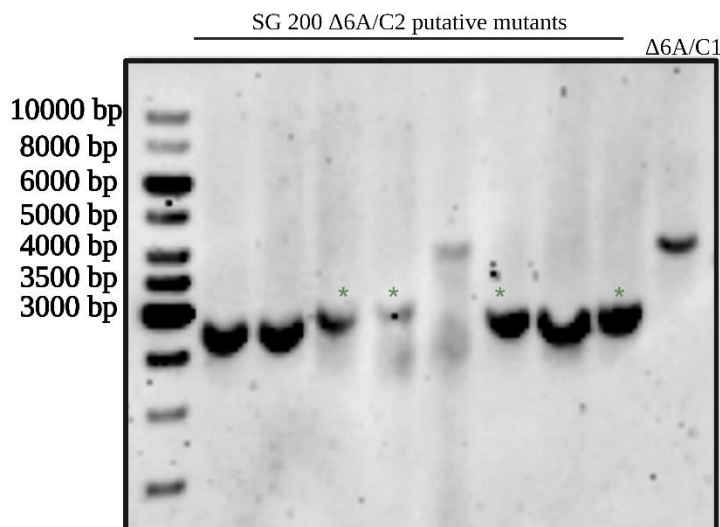


**Figure S3: Screening PCR for putative mutants for  $\Delta 6A/2C$  (second complementation)**

The Figure shows the screening PCR of the putative mutants for the second half cluster complementation containing the genes *umag\_02533*, *umag\_02535*, *umag\_11415* and *umag\_02537*, *umag\_02538*, *umag\_11416*, *umag\_11417* and *umag\_02540*. The amplification product contain sequences from the last part of the MoRFunG construct to the genome. Forward primer: TATGAGCGGAAGCGAGGAAG; reverse primer: TGATGGGAGTCGTGATTCG. Expected sizes: **SG200 (wt)**: 1261 bp,  $\Delta 6A/1C$  (genetic background, first complementation): no amplification, positive insertion  $\Delta 6A/2C$ : 1789 bp. Bands indicated with a green \* were analysed by southern blot.



**FigureS4: Southern blot of the  $\Delta 6A/2C$  (second complementation)**

The Figure shows the southern blot of the putative mutants for the second half cluster complementation containing the genes *umag\_02533*, *umag\_02535*, *umag\_11415* and *umag\_02537*, *umag\_02538*, *umag\_11416*, *umag\_11417* and *umag\_02540*. The gDNA was digested with PvuI and EcoRV. The expected sizes for a positive mutant was 3106bp, and for  $\Delta 6A/1C$  control: 4242. The probe was done using as template the plasmid #2305 pGAM1311Lb-Rb2020 and amplified with the forward primer: TAAGACATCCCGATCCGTG and reverse primer: GTATTTTCGGCGTCGTTCAC. Strains indicated with a green\* were considered positive. Figure crated with Biorender.com

## 6.7 Expression pattern of effector genes of the cluster 6A

The expression pattern shown in the supplementary figure S5 were obtain from the RNA seq Data from (Lanver *et al.*, 2018a). The data was processed by Dr. Deppoter.

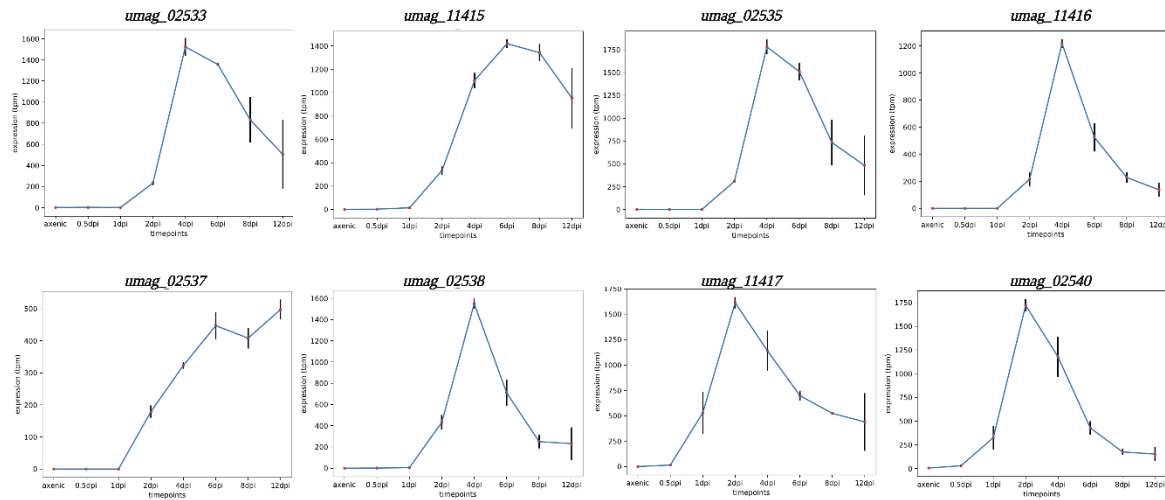


**Figure S5: Expression gene from the genes of the cluster 6A.** The expression pattern were obtain from the RNA seq Data from (Lanver *et al.*, 2018a). The data was processed by Dr. Jasper Deppoter. Figure created with Biorender.com.

## 6.8 Supporting experimental data for ectopic simultaneous multi-gene integration without insertion of resistance cassettes.

### 6.8.1 CRISPR mediated integration of a multi-gene construct.

In the section 2.3.1.1 was mentioned that a CRISPR mediated integration for inserting a multi-gene construct in the *ip* locus of *U. maydis* was not possible. Here is stated the experimental data of the experiment.

Co-transformation of SG200 was done following the standard protocol. The vectors used were the CRISPR vector #3277 and the DNA donor vector # 3377 (see Table S1). The CRISPR vector backbone counts with the *cbx* resistance gene, being homologous sequence with the SG200 *umag\_00844* (sequence targeted for the sgRNA used in this experiment). To avoid linearization of the CRISPR vector, the plasmid # 3277 was mutagenized using site directed mutagenesis to delete the PAM motif that was recognized for the sgRNA.

sgRNA: GGTTTGTTGTTTCAGTGAGAG

Mutagenesis primer forward:  
GCTTGTGGTTTGTTCAGTGAGAgtttAAACGCTACGGGCAAGATGAGG

Mutagenesis primer reverse:  
CCTCATCTTGCCCGTAGCGTTTaaacTCTCACTGAACAACAAACCACAAGC

Transformants were selected and isolated using the standard protocol. The mutants were analyzed by southern blot.

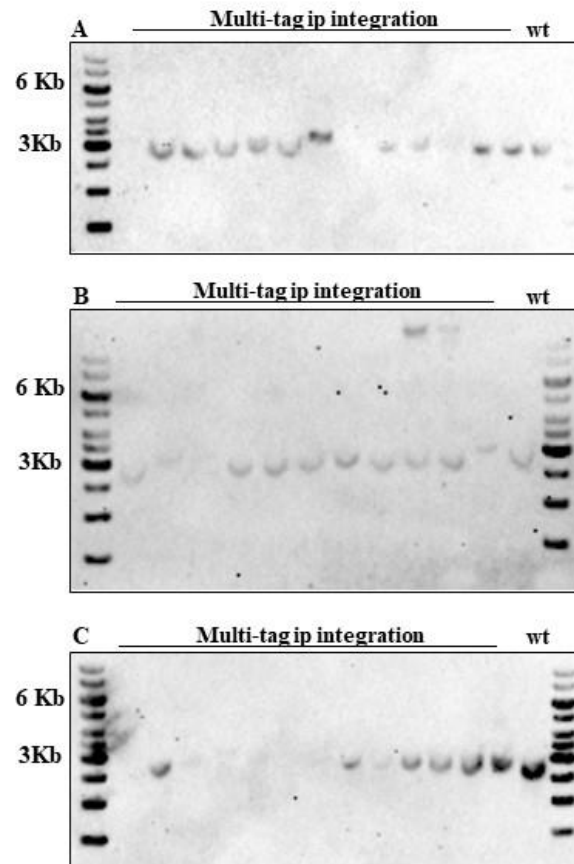


**Figure S6: Southern blot of the unsuccessful multi-gene integration strains that showed *cbx* resistance done with MoRFunG and CRISPR.** The expected sizes were 3255 bp for SG200 and 5266 bp for the multi gene integration. DNA samples for southern blot analysis were digested with the restriction enzyme *Nco*I (NEB). The probe used was amplified using as template the plasmid # 3210 (Table S1) using the following primers:  
 Forward primer: TTTGGTCTCAAGCGATGTCGCTATTCAACGTCAG  
 Reverse primer:CAAATGTTTGAACGATCTGCAGCCGGGCGGCCGCTTACGACGAAGCCATGATAGGG

## 6.8.2 Multi-Tag ectopic integration using the MoRFunG toolkit and homologous recombination

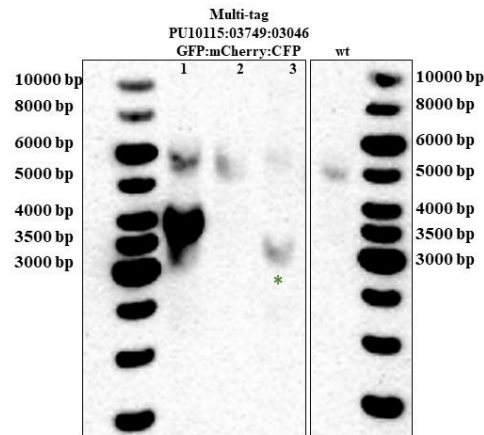


**Figure S7: Southern blot of the multi-gene integration strains that showed *cbx* resistance done with MoRFunG through homologous recombination.** Green \* represents strains containing the expected band. The strains were generated in the SG200 genetic background using the plasmid #3373 pL2\_PU10115*gfp*\_PU03749*mCherry*\_PU03046*cfp*-Cbx. The samples were digested with HindIII HF (NEB). The expected sizes were: Positive integration: 3560 bp and SG200: 5688 bp.

The probe used was amplified using the following primers in the plasmid template #163 (Table S1).

Forward primer: TTCACACAGGAAACAGCTATGACC.

Reverse primer: ACGACGTTGTAACGACGGCCAG.

### 6.8.3 Complementation of $\Delta pep1$ using MoRFunG toolkit under the control of different promoters

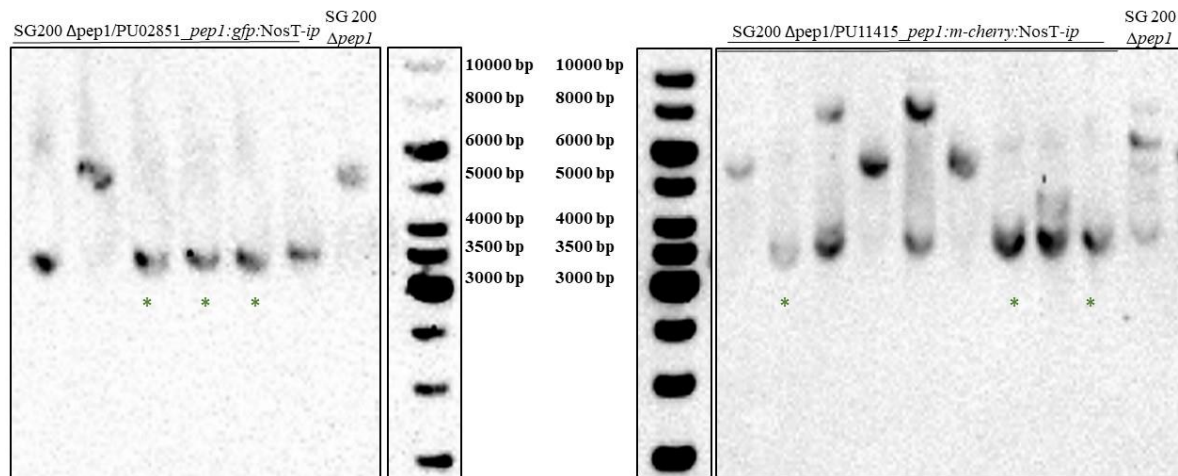


**Figure S8: Southern blot of the *U. maydis* strains containing a single copy of *pep1* tagged with GFP or mCherry that showed *cbx* resistance done with MoRFunG through homologous recombination.** Green \* represent strains containing the expected band. Genetic background: SG200  $\Delta pep1$ . The strains SG200  $\Delta pep1$ ./PU02851\_ *pep1:gfp:NosT-ip* were done using the plasmid #3378 P12\_1R:3R\_PU02851\_ *pep1gfpNosT\_Cbx*locus. The strains  $\Delta pep1$ ./PU11415\_ *pep1:mCherry:NosT-ip* were generated using the plasmid #3377 P12\_1R:3R\_PU11415\_ *pep1CherryNosT\_Cbx* loci. The samples were digested with HindIII HF (NEB). The expected sizes were: Positive integration: 3560 bp and SG200: 5688 bp.

The probe used was amplified using the following primers in the plasmid template #163 (Table S1)

Forward primer: TTCACACAGGAAACAGCTATGACC

Reverse primer: ACGACGTTGTAAAACGACGGCCAG

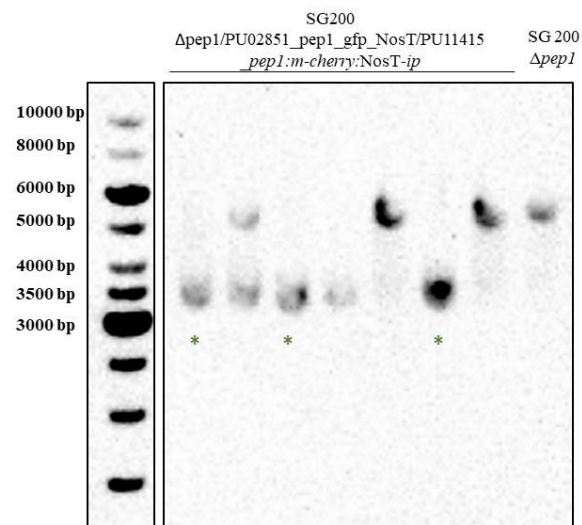


**Figure S9: Southern blot of the *U. maydis* strains containing a two copies of *pep1* tagged with GFP and mCherry under the control of the promoters PU02851 and PU11415 that showed cbx resistance done with MoRFunG through homologous recombination.** Green \* represents strains containing the expected band. The strains were generated in SG200  $\Delta pep1$  genetic background using the plasmid #3400 P12\_1R:5R\_PU02851:*pep1**gfp*\_PU11415:*pep1**mCherry* CbxRMod. The samples were digested with HindIII HF (NEB). The expected sizes were: Positive integration: 3560 bp and SG200: 5688 bp.

The probe used was amplified using the following primers in the plasmid template #163 (Table S1)

Forward primer: TTCACACAGGAAACAGCTATGACC

Reverse primer: ACGACGTTGTAAAACGACGGCCAG



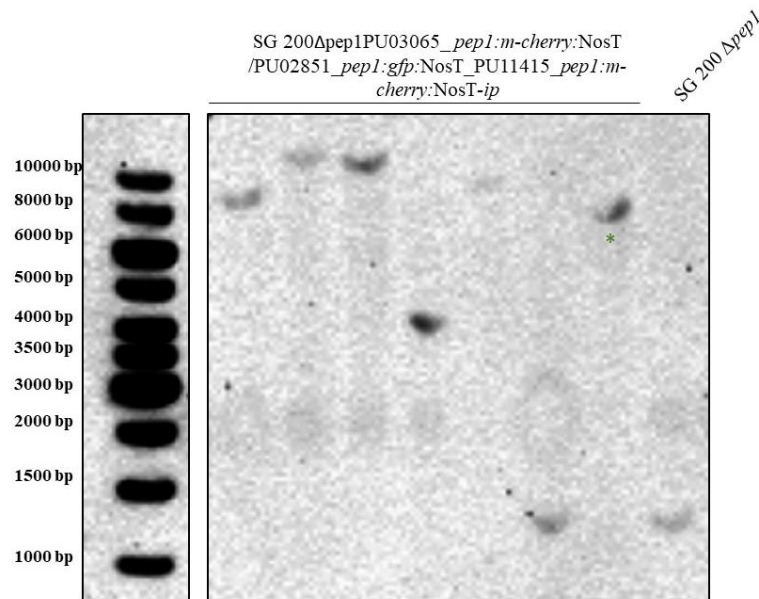


**Figure S10: Southern blot of the *U. maydis* strains containing a three copies of *pep1* tagged with GFP and mCherry under the control of the promoters PU 03065, PU02851 and PU11415 that showed *cbx* resistance done with MoRFunG trough homologous recombination. Green \* represent strains containing the expected band. The strains were generated in SG200  $\Delta$ pep1 genetic background using the plasmid #3455 P12\_1R:5R\_PU02851\_11415\_03065\_mCherry*pep1*-GFP:*pep1*-mCherry:*pep1*\_NosT.**

The samples were digested with EcoRV and SacII. The expected size for positive DNA insertion was 9964 bp and for the SG200  $\Delta$ pep1 genetic background 1926 bp

The probe used was amplified using the following primers in the plasmid template #163 (Table S 1)

Forward primer: TTCACACAGGAAACAGCTATGACC

Reverse primer: ACGACGTTGTAAAACGACGGCCAG

The positive strain band is lower than the expected size but considering that the band in the negative control is also lower it is assumed that the strain contains the positive insertion and that the difference in sizes is due to an artefact of the methodology.

## 6.9 Technical supporting information for the Optogenetic experiments

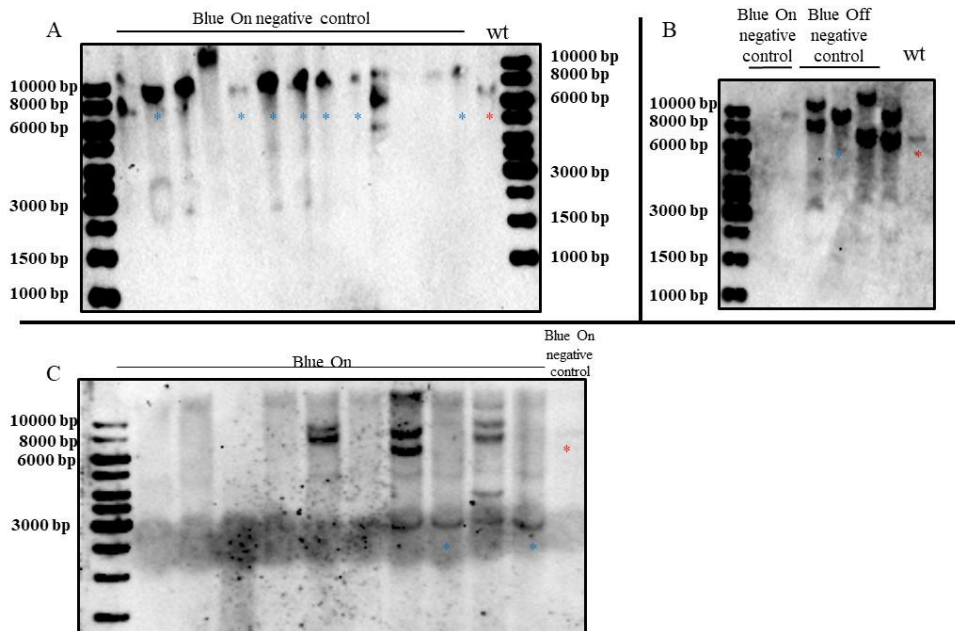


**Figure S11: Southern blot of the *U. maydis* optogenetic strains**

**A.** Southern blot for the Blue On negative control: SG200 pNH023 :upp3-PIR3-PCMVmin-*FLuc\_see1*. Samples digested with *Bam*HI-*Ssp*I. Positive insertion: 9600 bp (\*). Wt: *U. maydis* SG200: 7292 bp (\*). Probe amplification from the plasmid: Upp3-(C120)5-PCMV-*FLuc\_see1*. Forward primer: TTCACACAGGAAACAGCTATGACC. Reverse primer: GCCGCATTAATAGGCCTGAGTGG.

**B.** Southern blot for the Blue Off negative control: SG200 pLH120: upp3-(C120)5-PCMV-*FLuc\_see1*. Samples digested with *Bam*HI-*Ssp*I. Positive insertion: 9665 bp (\*). Wt: *U. maydis* SG200: 7292 bp (\*). Probe amplification from the plasmid: Upp3-(C120)5-PCMV-*FLuc\_see1*. Forward primer: TTCACACAGGAAACAGCTATGACC. Reverse primer: GCCGCATTAATAGGCCTGAGTGG.

**C.** Southern blot for the Blue On strain: SG200 pNH023 :upp3-PIR3-PCMVmin-*FLuc\_see1*// pNH047 Cco1-nosT-AsLOV2pep-PIP-PhCMVmin-CMVenhacer(5'-3')-PhCMVminePDZb-VP16ff-nosT. Samples digested with *Nco*I. Positive insertion: 2878 bp (\*). Control: SG200 pNH023 :upp3-PIR3-PCMVmin-*FLuc\_see1* 7712 bp (\*). Probe amplification from the plasmid: pNH008 Cco1-PO2tef-PIP-VP16ff Forward primer: CATATAACGTTAGAACGTGATTGCA. Reverse primer: AAATGCCTATCGAGGATGTTG.

(\*\*\*) The strains for the constitutive expression of *FLuc\_see1* were confirmed by the constitutive production of F-Luciferine.

Southern blots for the constitutive expression of FLuc in the Blue-On system, and the Switch off in the Blue Off system did not work with the enzyme/probe used. Due to time reason the genetic confirmation could not be done in this study and remain to be confirmed in the future.

## 6.10 Oligonucleotides

### 6.10.1 Primers

Primer Name	Sequence	Use
Fp a Cluster 6a test	GCAGAAGAGGATCCGATCTTCTCAG	PCR check cluster 6A
Anna Rp a	CTGACCTCCTCACTACTAAG	PCR check cluster 6A
Anna Fp b	CTCTCCTTCTTCGCGTGTAG	PCR check cluster 6A
Anna reverse 1	ACTAGAGCCTAGCTGCAAAG	PCR check cluster 6A
Anna Fp 2	ACATGAGCCGAGAGCGAGAG	PCR check cluster 6A
Anna RP3	TGGCAACGGAATTCGATGTC	PCR check cluster 6A
Anna Fp4	CATACGAAGCAGGCCAAATC	PCR check cluster 6A
Anna RP5	GATGGCATCTTCGCCCTCTG	PCR check cluster 6A
Anna FP6	TCATCTCCTTCGCGATCCAC	PCR check cluster 6A
Anna Rp7	GAGCCTCTGACAGGCTTGTG	PCR check cluster 6A
Anna Fp8	GTATCCAGCAGCCTCATGAC	PCR check cluster 6A
Anna Rp9	ACGCTTTCTGGAGCCTCTGAC	PCR check cluster 6A
Anna Fp10	GGGCTTCTAGCTGATTCTTG	PCR check cluster 6A
Anna Primer d	CGAGCTGAGACAAGCTGTAG	PCR check cluster 6A
Anna Fp11	GCTCGAAAGGCGATGTAGTG	PCR check cluster 6A
Anna rp12	GTCTCCAGCTCATGGTTTCG	PCR check cluster 6A
Anna Fp13	ACGTCTCCGAGCCTCTTTAG	PCR check cluster 6A
Anna Rp14	ACCGGCTTCTTAACGAACAG	PCR check cluster 6A
Anna Fp15	TGCAGGTAAAGGTCGCTCTC	PCR check cluster 6A
AnnaRp16	AGTGCGGAAGCCAAGAGTCG	PCR check cluster 6A
Anna Fp17	TGTCGCCTGCGACAACCAAC	PCR check cluster 6A
Anna Rp18	TCGACCAACGGATCATCTAC	PCR check cluster 6A
Anna Fp 19	CTAGACGTGACCAGTTGAC	PCR check cluster 6A
Anna Rp20	CCCAAGCGTTCTCAAATGTG	PCR check cluster 6A
Anna Fp21	GGACGTCACCAACTGTATG	PCR check cluster 6A
Anna Rp22	CCTTTCGGACGTCGACATTG	PCR check cluster 6A
Anna Fp23	CAAACAGGCCAAACAGTGTG	PCR check cluster 6A
Anna Rp24	GTGATGCCGTCAATCTTGGTC	PCR check cluster 6A
p.Fp1_02533	TTTGAAGACAAGGAGGTCATGTAGGGAGG TGGGAGGGCCACAAGTTAG	MoClo
p.Rp2_02533	TTTGAAGACAACGTCTCGTTGATCCGCGTC CCG	MoClo
p.Fp3_02533	TTTGAAGACAAGACGACTTCTCTCGCTCTC GGCTCATGTACC	MoClo
p.Rp4_02533	TTTGAAGACAAAGTCTCGACCAGGCGGCCA TCC	MoClo
p.Fp5_02533	TTTGAAGACAAGACTTATTTAGAGCGCATA TTTG	MoClo
p.Rp6_02533	TTTGAAGACAACATTCAAAGTGCTGTAGGA AAGGGATGTTG	MoClo
c.Fp1_02533	TTTGAAGACAAAATGCGAACGCTTCAGCAC TTC	MoClo
C.RP2_02533	TTTGAAGACAAGGCTCGTATGAGGAAGTG CAATC	MoClo
c.Fp3_02533	TTTGAAGACAAGGCCTGACAAGACGATCG GTACAC	MoClo
c.Rp4_02533	TTTGAAGACAAAAGACCCAACGCACATCT TGTGGC	MoClo
c.Fp5_02533	TTTGAAGACAACCTTGTCTATTTCGCACTAC CG	MoClo

c.Rp6_02533	TTTGAAGACAAGCAGACTGCTGTGCTGAAT G	MoClo
c.Fp7_02533	TTTGAAGACAAGTCCGCAAAAAGCTG	MoClo
c.Rp8_02533	TTTGAAGACAAAAGCTCAATGGACGTGCTC AAGAC	MoClo
t.FP1_02533	TTTGAAGACAAGCTTTTCTGCATCCGTTCATC AC	MoClo
t.Rp2_02533	TTTGAAGACAAAAGCGGCTGAACTTGCCCA AAC	MoClo
Fp tRNA anna	CGGTGCTTTTTTTGTGGTACTGCATTGGTAG TGTAAG	PCR amplification
Rp tRNA anna	CTGCATCGACGGGGAAT	PCR amplification
Fp Scar check LB	ACCAAAGATGCGCTCCAG	PCR amplification
Rp scar check LB	CAACATCGCTGCTGCCAAC	PCR amplification
FP scar check RB	GTTATGAGCGGAAGCGAGGAAG	PCR amplification
Rp scar check RB	GAAGGCTTGAGCTTCTCGACAAACG	PCR amplification
02533.fp check	ATGCGAACGCTTCAGCAC	PCR amplification
02533rp check	TCAATGGACGTGCTCAAGAC	PCR amplification
02535 FP.Check	ATGATCCTCATCCAATTCG	PCR amplification
02535 Rp.check	TCAGCTTGAGCCACCTATTG	PCR amplification
02537 FP.check	ATGAGGATGACGCTAACC	PCR amplification
02537 Rp.check	TCACGAGCGTGGACGCTTG	PCR amplification
02538 FP Check	ATGCACGCCTCACGATTTTTG	PCR amplification
02538 RP.check	TCATCCATGGCTGCTTTTCG	PCR amplification
02540 Fp.check	ATGACAAAGATGCTCAACCTAATCAC	PCR amplification
02540 Rp.check	TCAGGACTGGTTTCTGCGGGAAG	PCR amplification
11415 Fp. Check	ATGCGTTATCTCGCCTTGG	PCR amplification
11415 RP.check	CTAGCTTCCACTTGTGCCG	PCR amplification
11416 FP.check	ATGATGCTCTTGAACGTCTCC	PCR amplification
11416 Rp.check	TACTTTGGTGGGGCGTC	PCR amplification
11417 Fp.check	ATGATTTTTAGATATCCTTGTTT	PCR amplification
11417.RP check	CTAAGATCCGAAACAGCGTC	
p.Fp#1_11415	TTTGAAGACAAGGAGGACGCGTTCATGCCT TGTC	MoClo
p.Rp#2_11415	TTTGAAGACAACAGACCACTTCTCTCGCTC TC	MoClo
p.Fp#3_11415	TTTGAAGACAATCTGGTTGATCCGCGTCCC G	MoClo
p.Rp#4_11415	TTTGAAGACAACATTCCTTGTAAGCTTTTCT TGGCTAAG	MoClo
C.FP1_11415	TTTGAAGACAAAATGCGTTATCTCGCCTTG GCTTC	MoClo
c.Rp2_11415	TTTGAAGACAAGTCCTCGCCGCTCGTTCTG AGG	MoClo
c.Fp3_11415	TTTGAAGACAAGGACATCGTCAGGACCTTC TAC	MoClo
d.Rp4_11415	TTTGAAGACAAAAGCCTAGCTTCCACTTGT GCCG	MoClo
T.Fp1_11415	TTTGAAGACAAGCTTTATGCCTCGTGATAA CTCCACGTC	MoClo
T.Rp2_11415	TTTGAAGACAAGGCTCTACTCGGTGACG	MoClo
T.Fp3_11415	TTTGAAGACAAGGCCGAGATTAACATCGTC ATACG	MoClo
T.Rp4_11415	TTTGAAGACAAAAGCGCCAGCTTCTAGCCAA GTCTTGC	MoClo
p.Fp1_02535	TTTGAAGACAAGGAGATATGAAGTCAGGCT CAGACTGGC	MoClo

p.Rp2_02535	TTTGAAGACAAGGTTTCTACTCGGTGACGA GGT	MoClo
p.Fp3_02535	TTTGAAGACAAAACCGAGATTAACATCGTC ATAC	MoClo
p.Rp4_02535	TTTGAAGACAACATTGGGGCTAACATGCAGA AAGCTGAAG	MoClo
c.Fp1_02535	TTTGAAGACAAAATGATCCTCATCCAATTT CGTTGC	MoClo
C.RP2_02535	TTTGAAGACAAAAGCTCAGCTTGAGCCACC TATTG	MoClo
T.Fp#1_02535	TTTGAAGACAAGCTTTCATCTCCTTCGCGAT CCAC	MoClo
t.Rp#2_02535	TTTGAAGACAAGACACCTGTGAACGCAGTT CC	MoClo
T.Fp#3_02535	TTTGAAGACAATGTCCCGCCCTCTCGCAAG	MoClo
T.Rp#4_02535	TTTGAAGACAAAAGCGAGCTGCCGTTCTACT GAGGG	MoClo
Fp#1Lbb	TTTGAAGACAAGGAGTGAGCGGTAGCCCA GATG	MoClo
Rp#2Lbb	TTTGAAGACAAAAGCGGACGTGATACCGAC AAGAATG	MoClo
Fp1Rbb	TTTGAAGACAAGGAGTCTGGAACACTGTGA CTAAC	MoClo
Rp2RBb	TTTGAAGACAAAAGCGAAAACGACGGCCAG TG	MoClo
p.Fp1_11416	TTTGAAGACAAGGAGAGGAATGGGGGCGA CAAC	MoClo
p.Rp2_11416	TTTGAAGACAAGAAACCTGTGAACGCAGTT CC	MoClo
p.FP3_11416	TTTGAAGACAATTTCCCGCCCTCTCGCAAG	MoClo
p.Rp4_11416	TTTGAAGACAACATTGCCAAGAATCAGCTA GAAGCCC	MoClo
Quick change	GCGTCCGGCTTGATTTGCGGCTGGGTTTGC AGACTC	MoClo
Cds. FP#1_11416	TTTGAAGACAAAATGATGCTCTTGAACGTC TCC	MoClo
Cds.Rp#2_11416	TTTGAAGACAAAAGCCTACTTTGGTGGGGC GTC	MoClo
T.Fp#1_11416	TTTGAAGACAAGCTTCCATACACTGTTC AACGTC	MoClo
t.Rp#2_11416	TTTGAAGACAAAAGCGTCACTACATCGCCTT TCG	MoClo
p.Fp1_02537	TTTGAAGACAAGGAGCTAACTTATGTAGCA GGCCGGAG	MoClo
p.Rp2_02537	TTTGAAGACAACATTGCTTTGAATCTTTTCC CGCAAGG	MoClo
p.Qch#1_02537	AATGCTCGATTTTCAGTGTCCGCAGAGATG TAGAGCTGTG	Mutagenesis
p.qch#2_02537	TTTCGAACACCTATATGCGACCCGTTGTAG CCTTTTCCAC	Mutagenesis
Cds.Qch#1_02537	TCGGGCTGGTGAAAGGCGAGGACCAATTCT C	Mutagenesis
Cds.Qch#2_02537	GGGTCGTGACCTCAGCCTGGGTATAGAAAG C	Mutagenesis
Cds.Fp#1_02537	GGGTCGTGACCTCAGCCTGGGTATAGAAAG C	MoClo
Cds.RP#2_02537	TTTGAAGACAAAAGCTCACGAGCGTGGAC GCTTG	MoClo
T.Fp#1_02537	TTTGAAGACAAGCTTAAAGTGGTTGCGTTC TCTGAAG	MoClo

t.Rp#2_02537	TTTGAAGACAAAGCGGGCGTCACAAACCCG ACTGG	MoClo
p.Fp1_02538	TTTGAAGACAAGGAGACCTTTTTGTAGCTC AAATTCCGGC	MoClo
p.Rp2_02538	CATTTGAAGACAACATTCCCTTGAAACCCC GCTGAGG	MoClo
Quick change Cds_02538	GATGCTGGTGGAGGACTTTGCTCGC	Mutagenesis
Cds.Fp#1	TTTGAAGACAAAATGCACGCCTCACGTATT TTG	MoClo
Cds.Rp#2	TTTGAAGACAAAAGCTCATCCATGGCTGCT TTC	MoClo
T.Fp#1_02538	TTTGAAGACAAGCTTCTACGTTTCGTGATTT GCATCTC	MoClo
t.Rp#2_02538	TTTGAAGACAAAGCGGGAAAAGAGAACAT GGTTCC	MoClo
P.Quickch#1	GAGTGACGGTAAAGGGGCTCGGGCAAGC	MoClo
p.Fp#1_11417	TTTGAAGACAAGGAGTGCTCGCCGCAAGA AAGATG	MoClo
p.Rp#1_11417	TTTGAAGACAACATTGTTCTCAAGCACTT TCGTTGAC	MoClo
Qch#1 Cds.11417	AGGAAGTTTCAAGAAACCTTAGACTTATG	MoClo
Cds.Fp#1_11417	TTTGAAGACAAAATGATTTTTTCAGATATCC TTGTTTCATCAC	MoClo
Cds.Rp#2_11417	TTTGAAGACAAAAGCCTAAGATTCCGAAAC AGCGTCTC	MoClo
T.FP#1_11417	TTTGAAGACAAGCTTACAGCTCCAATAAG GAGTG	MoClo
T.Rp#2_11417	TTTGAAGACAAAGCGTTTGAATGTTGAGAG ATGAGTC	MoClo
p.Fp#1_02540	TTTGAAGACAAGGAGGCTCCATTTGCGACC AAAG	MoClo
p.Rp#2_02540	TTTGAAGACAAGAGCCCGAACGATTCATGA AGG	MoClo
p.Fp#3_02540	TTTGAAGACAAGCTCAATGCGTCTATCGCG G	MoClo
p.Rp#4_02540	TTTGAAGACAACATTTTTTGATGCTGACGAT TGTCCTG	MoClo
Qch#1 Cds.02540	GACCACAATGCAGGACGACTCTGGAACAC	Mutagenesis
Cds.Fp#1_02540	TTTGAAGACAAAATGACAAAGATGCTCAAC CTAATCAC	MoClo
Cds.Rp#2_02540	TTTGAAGACAAAAGCTCAGGACTGGTTTCT GCG	MoClo
T.FP#1_02540	TTTGAAGACAAGCTTTAAGACATCCCGATC CGTG	MoClo
T.Rp#2_02540	TTTGAAGACAAAGCGGACTCAACCCGAACC CG	MoClo
c.Fp3_02535	TTTGAAGACAACGTGCTGTCGTGTGAAC	MoClo
C.RP2_02535	TTTGAAGACAAGACGACCGATTGGGTATTG AG	MoClo
FpLBnew#1	TCACAGAGCGGTTTCGTGCAG	PCR amplification flanks cluster 6A
RpLBnew#2	CTATTGCGTTGAACGGAGAG	PCR amplification flanks cluster 6A
FP.LbpAGM1311 ovv	AGCCTCCATCCTCACGTTAC	PCR amplification flanks cluster 6A
Rp.LB short#4	TGCATGCCTGCAGGTGCGACTAGCCTCCATC CTCACGTTAC	Gibson assembly flanks cluster 6A
Fp.RB new def #3	CCACGGATCGGGATGTCTTACTGCATCCGT TCATCAC	Gibson assembly flanks cluster 6A

Rp.RbpAGM1311 ovv	TAAGACATCCCGATCCGTG	PCR amplification flanks cluster 6A
Rp.RB new def #4	AAAACGACGGCCAGTGAATTGTATTTTCGGC GTCGTTACGATTG	PCR amplification flanks cluster 6A
Fp.P.02533 Cbx	GTATTTCCGGCGTCGTTAC	PCR amplification
Rp.P.02533 Cbx	GAAGCTTGTCATGTAGGGAGGTGGGAG	PCR amplification
Fp.P.02535 Cbx	GAAGCTTGCCTCGTGATAACTCCACGTCTT G	PCR amplification
Rp.P.02535 Cbx	GCCATGGGCTAACATGCAGAAAGCTGAAG	PCR amplification
Fp.P.02538 Cbx	GAAGCTTGCTAGCCTAGACTGAAACTC	PCR amplification
Rp.P.02538 Cbx	GCCATGGCTTGAAACCCCGCTGAGG	PCR amplification
Qcp.P.02538 Cbx	CAAGGTGAATTGTTTCATGGCCTAAATGCA GGTAAAG	PCR amplification
Fp.P.11416 Cbx	GAAGCTTTCATCTCCTTCGCGATCCAC	PCR amplification
Rp.P.11416 Cbx	GCCATGGCAAGAATCAGCTAGAAGCCC	PCR amplification
UMAG_04040_F	GGCATGCGAGAAGTGACGATTGCTAAGCTA GTG	PCR amplification
UMAG_04040_R	GCCATGGTGCTGCTGCAACCACCCTAC	PCR amplification
UMAG_05928_F	GGCATGCTCGAGGACACCAGCTTCA	PCR amplification
UMAG_05928_R	GCCATGGCTTGGTGAAGCTTTTGCTCG	PCR amplification
UMAG_03751_F	GAAGCTTGTCGCCAACATTTCCC	PCR amplification
UMAG_03751_R	GCCATGGGTCGATGCTGAAGAGGACCTCAA	PCR amplification
UMAG_05311_F	GAAGCTTATTGTGAGCCCGTGCTG	PCR amplification
UMAG_05311_R	GAAGCTTATTGTGAGCCCGTGCTG	PCR amplification
Fp.qPCR02533 #2	CGGATCCAGCACTAGCACTC	qRT-PCR
Rp.qPCR02533 #2	GCGAAGACCCAACGCACATC	qRT-PCR
Fp.qPCR_02535	CTTCAGAAGGCATGGGAAC	qRT-PCR
Rp.qPCR_02535	TTAGCGCCATTTGTGCTTC	qRT-PCR
Fp.qPCR_03751	CAAGCAGGTGTCGGAACAAC	qRT-PCR
Rp.qPCR_03751	GTGTTTGGCTGACGGGTAGTG	qRT-PCR
Rp.qPCR_04040	CCAGCTCTTGAAGGAGTC	qRT-PCR
Fp.qPCR_04040#2	CCTACCTCGTCCCCTTTCC	qRT-PCR
Fp.qPCR_05311#2	TTGAATACCGACACGGTCTC	qRT-PCR
Rp.qPCR_05311#2	AGATTCTCGACGCTCCTCTC	qRT-PCR
Fp.qPCR_05928#2	CCGCCTGTCGAAATTACAAG	qRT-PCR
Rp.qPCR_05928#2	AGGATGTGTCGGACCTGATG	qRT-PCR
Fp.qPCR_11416	CCAAAGCGGAGCCTATCATC	qRT-PCR
Rp.qPCR_11416#2	GATCGTGCATCACGGTTGTTCTAC	qRT-PCR
Fp1.Domest LV1 LB	TTTGGTCTCAAGCGAGCCTCCATCCTCACG TTAC	MoClo
Rp1 Domst LV1 LB	TTTGGTCTCACAGACCAAATGCATCGTAGA AA	MoClo
Fp2. Domest LV1 LB	TTTGGTCTCATCTGAAACTGGCCAACAATA AAG	MoClo
Rp2 Domest LV1 LB	TTTGGTCTCAGGAGCCACGGATCGGGATGT CTTAC	MoClo
FP. RB L1	TTTGGTCTCAAGCGTAAGACATCCCGATCC GTGG	MoClo
Rp RB L1	TTTGGTCTCAGGAGGTATTTCCGGCGTCGTTT AC	MoClo
p.Qch#2_11416	ACAGGTGCATTGAGGACGTTGCTCTTACTT CATCG	Mutagenesis
p.Qch#2_02535	GTCATACGACTTCACGGCTGTTTTTGCGCTT G	Mutagenesis
p.Qch#2_11415	TCAAAGCGTTCGCTGTCTTCTTTTCTCGAA AGA	Mutagenesis

Qch XL 1_11416	GGAACTGCGTTCACAAGTCTCCCGCCCTC	Mutagenesis
Qch XL 1C_11417	GAGGGCGGGAGACTTGTGAACGCAGTTCC	Mutagenesis
Qch XL 2_11415	CAAAAGCGTCGCTGCCTTCTTTCTCGAA AG	Mutagenesis
Qch XL 2C_11416	CTTTCGAGAAAAGGAAGGCAGCGACGCTTT TG	Mutagenesis
FP RB 1st compl	TTTGGTCTCAAGCGAGGCACAGACCAAGAT TGAC	PCR amplification
FP New Probe 6A	TTGGGTTGGCTCGACGACAG	PCR amplification
Rp New Probe 6A	GCGTGTGACAAGGCTGCTTC	PCR amplification
UMAG_11415 RP check	ACCGCTCGGAGAAATCTGTG	PCR amplification
FP11415_02535 1st complement check	GAGGTGGTCGAATTCCTCAG	PCR amplification
End RB short RP Check	TCACGAGACTCACGACTTTG	PCR amplification
Anna U_11415 Fp	GCAAGGTATGTTTCGCTGGTTC	PCR amplification
Fp.L1 T.02537 Left Flank. MoClo	TTTGGTCTCAAGCGAAAGTGGTTGCGTTCT CTG	MoClo
Rp.L1 T.02537 Left Flank. MoClo	TTTGGTCTCAGGAGGCGTCACAAACCCGAC TGGT	MoClo
Fp.p02473 L0 Moclo	TTTGAAGACAACATTCTTGATGGAATTCGA GTTTCTG	MoClo
Rp.p02473 L0 Moclo	TTTGAAGACAAGGAGGGTCTGAAGCAGTC GAGTCTC	MoClo
Quick change p02473 BpiI correction	CTGTGCGAGTTAGTCGAACACTACGCCTTT TAAG	Mutagenesis
Fp1_p02826 MoClo	TTTGAAGACAAGGAGGCGATCCACTCATGT ATCCG	MoClo
Rp2_p02826 MoClo	TTTGAAGACAAAAGACACCTGATGCGTAA G	MoClo
Fp2_p02826 MoClo	TTTGAAGACAACTTTTCAATGTACTGTTCGC TTC	MoClo
Rp4_p02826 MoClo	TTTGAAGACAACATTGGTGTGCTTGATTTT GCCTCG	MoClo
Qck Chng#1 P_05295	GTTCTCGACGTGGAAGTTCGTCTTTTCAGCA TTGATTC	Mutagenesis
Qck Chng#2P_05295	GCTGAGTAGCTGAAGGCGGGCTCTGATAGA GTAGGAAAGC	Mutagenesis
Fp1P_05295 MoClo	TTTGAAGACAAGGAGAGTGTTCACGTCGTC ATCTG	MoClo
Rp2P_05295 MoClo	TTTGAAGACAACATTCCTGCCGATTGTGC GTGTAG	MoClo
Fp1P_05319 MoClo	TTTGAAGACAAGGAGTCAGCACCAATTGCT CGTAGTA	MoClo
Rp2P_05319 MoClo	TTTGAAGACAACATTCCTTGAAGGTATC AGAGTAAG	MoClo
Fp1P_06180 MoClo	TTTGAAGACAAGGAGGGCTCAATAGCGACT AATAAAG	MoClo
Rp2P_06180 MoClo	TTTGAAGACAACATTGGTTTGTCTCGCAGT GTG	MoClo
Fp-qPCR_02535	GGCAGGAATCTAGCGCATCA	qRT-PCR
Rp-qPCR_02535	TATCGGTAGCTGTGTCTCTGC	qRT-PCR
Fp-qPCR_02538	ACGGAACTTCGCCTTACGAT	qRT-PCR
Rp-qPCR_02538	GTCAGCATCTTTCTTGCGGC	qRT-PCR
Fp-qPCR_11416	CAGGAGAGTTACAGCCGTGG	qRT-PCR
Rp-qPCR_11416	TTGATTTGCGGCTGGGTTT	qRT-PCR
Fp-qPCR_02537	GGAGAGAGTTCATCGGGCTG	qRT-PCR
Rp-qPCR_02537	TCGGAGACGTTGTTGTCGTT	qRT-PCR
Fp-qPCR_11415	ACATGATCGCGTTTCGTCCA	qRT-PCR



Rp-qPCR_11415	GGCTCAGTTCCTTTCCCCAA	qRT-PCR
Fp-qPCR_02540	ACACCTGGCAACAGCATCAT	qRT-PCR
Rp-qPCR_02540	CGTTGCGGTATCCCTTCTT	qRT-PCR
Fp-qPCR_11417	TCAATCGAAAGCGAAGCCGA	qRT-PCR
Rp-qPCR_11417	TGCACGACTCTTCTGCACAT	qRT-PCR
Fp-qPCR_02826	AGCCATACAGTGCGATCCAG	qRT-PCR
Rp-qPCR_02826	ATCTCTCTGCTTATGCGCCC	qRT-PCR
Fp-qPCR_02826 B	AATCCCGAAGCCGAAGTGTT	qRT-PCR
Rp-qPCR_02826 B	ACCAGAACGGGTCTTGCATC	qRT-PCR
Fp-qPCR_02473 B	GCGCAGAAGGTACAGGAAGT	qRT-PCR
Rp-qPCR_02473 B	AGCCATCAAGGTTTCTCGGG	qRT-PCR
Fp-qPCR_05295	CCTCGTCCGCAAGGTAATCA	qRT-PCR
Rp-qPCR_05295	AGCTCGAAAGTCTCTGCAC	qRT-PCR
Fp-qPCR_05295 B	ATATGCGACCTTCGAGCCTG	qRT-PCR
Rp-qPCR_05295 B	AGTCGGTGGGACTGAAGGAT	qRT-PCR
Fp-qPCR_06180	CGGGACTTTGACTGATGCCA	qRT-PCR
Rp-qPCR_06180	GGGATGGCTCTTACCACCTG	qRT-PCR
Fp-qPCR_05319	CTGGGCACTGTCTCCTCATC	qRT-PCR
Rp-qPCR_05319	GTTTCTCTCGGCCCTCAACA	qRT-PCR
RP.U_11415	GAACAACAAGACGTGGAGTTATC	PCR amplification
FP.Outside prom 02473	CTAGAATTGTTTGGCGCACGAG	PCR amplification
RP.Outside prom 02473	TAGTGGGACAGAAGGTAGG	PCR amplification
FP.Outside prom 02826	CAACAACCGACGTGAGATG	PCR amplification
RP.Outside prom 02826	CAAATGCTACCGCGGCTTTG	PCR amplification
Fp-qPCR_05295 C	TTTCATCCGCCCCAGTGAAT	qRT-PCR
Rp-qPCR_05295 c	TCCACATGCACGTTAGGGAC	qRT-PCR
Fp.L1 Cds_02537 MoClo	TTTGGTCTCAAGCGATGAGGATGACGCTAA CC	MoClo
Rp-L1_Cds_02537 MoClo	TTTGGTCTCAGGAGTACGAGCGTGGACGC TTG	MoClo
Fp-qPCR_10115	CTCCTAGTGGCTCCTCGTCT	qRT-PCR
Rp-qPCR_10115	TGATACTTGGAGCCGAACCG	qRT-PCR
10115 B	GTGCCAAGCAACCTGAAACA	qRT-PCR
10115 B	CGAACCGGAAGGCACTTTTC	qRT-PCR
Fp-qPCR_02194	AGGCTATGAGCAGACTCCCA	qRT-PCR
Rp-qPCR_02194	TCGAGAGGTTGACTGGACT	qRT-PCR
02194 B	CGTTCTTGGGCGTTGTTCTG	qRT-PCR
02194 B	TGGGAGTCTGCTCATAGCCT	qRT-PCR
Fp-qPCR_05104	CAACGATGGCGCTCTTAACG	qRT-PCR
Rp-qPCR_05104	AGCCAGTGTGGAGTTACCG	qRT-PCR
05104 B	CCAATGTTGGTGGTGGCAAG	qRT-PCR
05104 B	TTCCGGGAAGACCAATGTCG	qRT-PCR
Fp-qPCR_04557	ACCGAGGTCAACGTCAAGTC	qRT-PCR
Rp-qPCR_04557	CAGCGTTGAACTTGTCAGCC	qRT-PCR
04557 B	AACTATTTCTCGGCGCTCGG	qRT-PCR
R04557 B	CAAAGTTGCAATGGTGCCT	qRT-PCR
Fp-qPCR_02192	CTATGGCCTCGTCAGCAGAG	qRT-PCR
Rp-qPCR_02192	TGCTGGGATCCTTGCTCTTG	qRT-PCR
_02192 B	GAATCCGGGCTTGTGGAAGA	qRT-PCR
02192 B	TACGGAAGTCTGCGTTGACC	qRT-PCR
Fp-qPCR_03046	TGCACTTACAGCTACGGTCG	qRT-PCR
Rp-qPCR_03046	AAAGCCTTGGTCTTCACGCT	qRT-PCR
03046 B	TGGACGCGGTTCTCAAACT	qRT-PCR

03046 B	TGTCTACGCAGAAGTGGTGC	qRT-PCR
Fp-qPCR_12217	CACCATCGTATTGTCCGCCT	qRT-PCR
Rp-qPCR_12217	AGCCAAAAGGACAACCAGCA	qRT-PCR
12217 B	TGCATGCAGTGTGATGTTCG	qRT-PCR
12217 B	CCGTGGATGGCTGGATCATA	qRT-PCR
Fp-qPCR_03749	GCTTCTTTGAGCCTGACCCT	qRT-PCR
Rp-qPCR_03749	TTGCTGTCTAGAGAACGACC	qRT-PCR
03749 B	GATGCCGTTTTAGCCACGTC	qRT-PCR
03749 B	CGCTGCATTCTTTCAGGTT	qRT-PCR
Fp-qPCR_01375	GCTCAGCCTTTGTTCTGCTC	qRT-PCR
Rp-qPCR_01375	GAGCTCATTGAGGCATCGGT	qRT-PCR
01375 B	AAGCTCAACCGGAGATGGTG	qRT-PCR
01375 B	TTGGCAGGCGGATTCTTGAT	qRT-PCR
Fp-qPCR_00027	ACATCATCTCTGTGCGACGCC	qRT-PCR
Rp-qPCR_00027	ATTGCGACAGTCAGTACCCG	qRT-PCR
00027B	CACCTGTGCCGTTTCAGAGAT	qRT-PCR
00027B	ACCAACAACAGGAGAGAGCG	qRT-PCR
Fp-qPCR_02854	AGCAGCTCAGAGTGCAAGAG	qRT-PCR
Rp-qPCR_02854	CGAACGCGTTTGTGGTTCTT	qRT-PCR
02854 B	AGCTTGGAGCACTGACACTT	qRT-PCR
02854 B	TGCAGTGTAAGCGAGGTTGA	qRT-PCR
Fp-qPCR_01236	TGTCTGGACCCTCGGGTAAT	qRT-PCR
Rp-qPCR_01236	AAGATGCAGCTGCTTTTGGC	qRT-PCR
01236 B	GTGAACTTCGTGCGCAACAT	qRT-PCR
01236 B	ATCGTGACGTTTTCTGGGCT	qRT-PCR
Fp-qPCR_02119	CTCACACCTGGTCGTGCTCA	qRT-PCR
Rp-qPCR_02119	AACACTACGCTTGTGCTCCA	qRT-PCR
02119 B	CACTTATTCGGGCAACCGA	qRT-PCR
02119 B	GCGCCCCCTTCTATCGATCTT	qRT-PCR
Fp-qPCR_05311	CGCACACTGGTATCCCAACA	qRT-PCR
Rp-qPCR_05311	CCAGCTTCATTGCGAGGAGA	qRT-PCR
05311 B	CTCGCATGAAGAGCCAGAGT	qRT-PCR
05311 B	TGCTTTCCAGATCGCTTTGC	qRT-PCR
RP 1 PCR clust 6A	GTGCGAGACAAGTCTTTCGAG	PCR amplification cluster 6A check
FP 2 PCR clust 6 A	CAAAAGCGTCGCTGTCTTCC	PCR amplification cluster 6A check
rp 2 pcr CLUST 6A	GAAGCCCGCCTCGTTTACAG	PCR amplification cluster 6A check
FP 3 PCR clust 6 A	TGTGGCCAAGTCCATCATT	PCR amplification cluster 6A check
RP 3 PCR clust 6A	GGATATGCACGCAGGATTTG	PCR amplification cluster 6A check
FP 4 PCR clust 6A	CCCGCATCCCAATCAAGACC	PCR amplification cluster 6A check
RP 4 PCR clust 6A	TGATCGTCCAGCTTGGGAAGG	PCR amplification cluster 6A check
FP 5 PCR clust 6A	CGACCCAGTTGATCATACAG	PCR amplification cluster 6A check
RP 5 PCR clust 6A	TCAGGACTGGTTTTCTGCGGGAAG	PCR amplification cluster 6A check
FP Nos T	GCTGGCCCTTCCCAGAAACCAGTCTGA GCGCCCGCCCGGCTGCAG	PCR amplification
RP NosT	ACCGTCACAGCAAGTGGTGACATCGATGA ATTCTCATGTTTAC	PCR amplification

FP PCR 6 clust 6A	AACATGAGAATTCATCGATGTCACCACTTG CGTGTGAC	PCR amplification
FP1 Pl0M 10115	TTTGAAGACAAGGAGAGCGACTCTTTGGCC TCGAA	MoClo
Rp 1 10115 Domest	TTTGAAGACAAaTCTTCGAACGAACTTCCC AG	MoClo
Fp 2 Domest. 10115	TTTGAAGACAAAGaIGGTTAGTGACGCCTT C	MoClo
Rp 2 L0m 10115	TTTGAAGACAACATTggGTTGGTTTTGCGAA TGCCGAG	MoClo
Mutagenesis BsaI P_10115	GAATCTTTACATTACGAaACCATCTCAATTG CTCATTC	Mutagenesis
Rp Mutagenesis BsaI prom 10115	GAATGAGCAATTGAGATGGTTCGTAATGT AAAGATTC	Mutagenesis
Fp c02537for Gibson pGAM int.	CAAGCTTGCATGCCTGCAGGTCGACTATGA GGATGACCGTAACCCAG	Gibson assembly
Rp_Cds_02537 NosT ovv	TGTTTTGAACGATCTGCAGCCGGGCGGCCGC TCACGAGCGTGGACGCTTGCT	Gibson assembly
Fp NosT fpr Gibson	GCGGCCGCCCGGCTGCAG	PCR amplification
RP NosT pGAM ovv	TCACGACGTTGTAAAACGACGGCCAGTGAA TTTCATCGATGAATTCTCATGT	Gibson assembly
FP Cds_02537 L1 ovv	TTTGGTCTCAGGAGATGAGGATGACGCTAA CCCAG	MoClo
RP NosT ovv Pl1R	TTGGTCTCAAGCGTCATCGATGAATTCTCA TGT	MoClo
Mutageneses 1 BpiI 02194	GGGAAAGAGTTTGAAGaGTGCGAAGTGAT GAAAGCGGAAG	Mutagenesis
Primer mutagenesis 2 prom 02194	GCGTCCAGTAGACTGAAGgCTTCATTTTATT TCAAG	Mutagenesis
FP.02194Moclo L0	TTTGAAGACAAGGAGcGCAGACTAAGGTCA GGTCAGGGC	MoClo
"RP fow orient.p_02194=Primer 1"	TTTGAAGACAACATTggGGTTGTATTCGAAA CAGAGA	MoClo
FP PU05104	TTTGAAGACAAGGAGCTTTCCCACTCCGAC TTCGG	MoClo
RP Pl0M Fow orient PU05104	TTTGAAGACAACAttggCTCCGTTGCGAAAG GCGTAG	MoClo
Mutagenesis BpiI 02192 Fow	GCGGACCATCCATCTGCTAAGaTCTTCATCT CTTTCTTC	Mutagenesis
Primer mutagenesis 02192 rever orientation	GAAGAAAAGAGATGAAGaICTTAGCAGATG GATGGTCGCC	Mutagenesis
FP with Rev overlap PU02192	TTTGAAGACAACATTggTCTGGGACATGGG CCGAGGG	Mutagenesis
Rp with fow ovv PU02194	TTTGAAGACAAGGAGACTTATCAGCGTGTG CTCTC	MoClo
Fp rev ovv_PU 03046	TTTGAAGACAACATTggGGCGATTGCCGGA TAGAAGT	MoClo
Rp PU03046 fow ovv	TTTGAAGACAAGGAGAAAATGGCTCTGAC GAGTCG	MoClo
Mutagenesis1 BpiI 03749	GCAACTACTCCGGCTAGACTCAGCTGcCTTC AAGGAGGACCCAAGCG	Mutagenesis
Mutagenesis#2 BpiI 03749	GCCCCGTGGGAGCTGAGTGAAGgCTGTATGG ATCGATTGATG	Mutagenesis
Fp with Rev ovv PU 03749	TTTGAAGACAACATTggCCTGTTGCTCTCGC CTGTTTT	Mutagenesis
Rp with fow ovv PU 03749	TTTGAAGACAAGGAGTGATGCAAGGCCGG TACTTG	MoClo
FP Prom 00027	TTTGAAGACAAGGAGTCCATGACAGATGG ACTGAA	MoClo
Rp prom_00027	TTTGAAGACAACATTggCACGGGCAATGGA	MoClo

	TTTTGAAAA	
Mutagenesis 02119 BpiI fow	CCGGTCTGTTTTGTGTGGGAaACAACAAC ATGTGTGAGC	Mutagenesis
Mutagenesis 1 BpiI 02119 reverse	GCTCACACATGTTGTTGTtTTCCACACAAA ACAGACCGG	Mutagenesis
Fp PU 02119	TTTGAAGACAAGGAGAGGGATGGGATGGA AGCACGA	PCR amplification
RP Pu 02119	TTTGAAGACAACATTggCCCGTCTGCTCAGA ACGCGG	PCR amplification
Mutagenesis1 BpiI P.05311	CAGCTCATCTGAAGGGGCGAaACCGTGTTG CAACTCGTTT	Mutagenesis
Mutagenesis 2 Prom 05311	GATTCGAGCGCCAAAACCGAAGAgGCATAT ATCGTGTCGCAAGGG	Mutagenesis
Mutagenesis 3 P05311	GGAGAGATTTTCGTCTACACAaGTCTCAAAA ACGGTTGTTC	Mutagenesis
Fp PU 05311	TTTGAAGACAAGGAGATTCTTTGACGTGCT TCATT	MoClo
Rp Pu05311	TTTGAAGACAACATTggCGTTGGTGCAAGA CTCTCTGT	MoClo
Fp KO 11415 chopchop	AATCTGCAAGGTATGTTTCGCT	PCR
RpKo 11415 chopchop	GAAGCTTGTCCCCACAGATACT	PCR
FpKO 11417 chopchop	TCAAAGATTCACAAAGCCTCAA	PCR
Rp KO 11417 chopchop	GGTGTGTTGGTGAAAGGGTTAT	PCR
Fp probe southern 11415	GAATCAAGCAGTAGCCAAATCC	PCR
Rp probe southern 11415	CGAGGCATGAGAGGAAAGCG	PCR
LeftFlank_Cbx_Fw_AIR	AAAAAGAAAATTCGTCAGGAGGGCGTTGC	PCR
LeftFlank_Cbx_Rv_AIR	GGGCGACTGAAGATGTTACCCTC	PCR
RightFlank_Cbx_Fw_AIR	CGGTCTGTACGAGTGCATTCTGTG	PCR
RightFlank_Cbx_Rv_AIR	GCCGACTTCTCAACTGCTCCTAC	PCR
Mutagenesis StopCbx AIR Fw	CATCCACACCGACCATGTAATCGCTATTCA ACTAAGTCAGCAACGGTCTT	Mutagenesis
Mutagenesis Stop Cbx_Rv_AIR	AAGACCGTTGCTGACTTAGTTGAATAGCGA TTACATGGTCGGTGTGGATG	Mutagenesis
A>G_RflankCbx BpiIFree multi 1X AIR Fw	TTTGGTGAGGAGCGAAGgCAGAAGCTCGAG AACACCTTTTCG	Mutagenesis
A>G_RflankCbx BpiIFree multi 1X AIR Rv	CGAAAAGGTGTTCTCGAGCTTCTGcCTTCGC TCCTCACAAA	Mutagenesis
Mutagenesis 1 Left flank	GAGTCTTGAACCTGAGAGTGTGCGTcTCTTC TGACGCTTG	Mutagenesis
Mutagenesis 2 left flank	TTCAACTAAGTCAGCAACGcTCTTCGTACCG CTCTCCGAC	Mutagenesis
LeftFlank_Cbx_Fw_AIR MoClo	TTTGGTCTCAAGCGAAGAAAATTCGTCAGG AGGGCGTTGC	MoClo
LeftFlank_Cbx_Rv_AIR MoClo	TTTGGTCTCAGGAGGGGCGACTGAAGATGT TCACCCTC	MoClo
RightFlank_Cbx_Fw_AIR MoClo	TTTGGTCTCAAGCGCGGTCTGTACGAGTGC ATTCTGTG	MoClo
RightFlank_Cbx_Rv_AIR MoClo	TTTGGTCTCAGGAGCCGTGAGCATTGTCAT CGGTTTTTTG	MoClo
Fp_GFP_L0_AIR	TTTGAAGACAAAATGGTGAGCAAGGGCGA GGAGCT	MoClo
Rp_GFP_L0_AIR	TTTGAAGACAAAAGCTTACTTGTACAGCTC GTCCATG	MoClo
Fp_NosT_L0_AIR	TTTGAAGACAAGCTTTCGGCCGCCCGGCTG CAGAT	MoClo
Rp_NosT_L0_AIR	TTTGAAGACAAAGCGCATCGATGAATTCTC ATGTT	MoClo
Fp_L1ovv Cbx_Nost	TTTGGTCTCAAGCGATGTCGCTATTCAACG	MoClo

TCAG		
Rp_Cbx_NosT Ovv	CAAATGTTTGAACGATCTGCAGCCGGGCGG CCGCTTACGACGAAGCCATGATAGGG	MoClo
Fp NosT_GA ovv Cbx	CTTCCGAGCGCCCTATCATGGCTTCGTCGT AAGCGGCCGCCCCGGCTGCAGATCGTTC	MoClo
Rp_NosT_GACbx_NosT L1 ovv	TTTGGTCTCAGGAGTCATCGATGAATTCTC ATGTTTG	MoClo
Mutagenesis Saring cbx	TCGCTATTCAACGTCAGCAACGgcCTTCGTA CCGCTCTCCGAC	Mutagenesis
2nd Mutagenesis Cbx	GCGTGACGACTTTGGTGAGGAGCGgAGACA GAAGCTCG	Mutagenesis
Mutagenesis Right Flank	GACAATGCTGACGGAAGGgCTCTATGAGAT TGCAAGG	Mutagenesis
Fp_Right Flank	TTTGGTCTCAAGCGGGAAACGCTACGGGCA AGATGAG	MoClo
Rp_Right Flank	TTTGGTCTCAGGAGCAAATTCCGAGCTTCC GAAG	MoClo
FP CFP AIR MoClo L0 L0 Cds	TTTGAAGACAAAATGGCCGTGAGCAAGGG CGAG	MoClo
RP+Stop CFP AIR L0Cds	TTTGAAGACAAAAGCTCACTTGTACAGCTC GTCCATGC	MoClo
Fp mCherry lo Anna Moclo Cds	TTTGAAGACAAAATGGTGAGCAAGGGCGA GG	MoClo
RP mCherry lo Anna Moclo Cds	TTTGAAGACAAAAGCctaCTTGTACAGCTCG TCCATG	MoClo
Check mCherry Fow 1	CTGAAGGGCGAGATCAAGCA	qRT-PCR
Check mCherry Rev 1	TAGTCCTCGTTGTGGGAGGT	qRT-PCR
Check mCherry Fow 2	GAAGGGCGAGATCAAGCAGA	qRT-PCR
Check mCherry Rev 2	TCGTTGTGGGAGGTGATGTC	qRT-PCR
Check CFP Fow 1	GCAGAAGAACGGCATCAAGG	qRT-PCR
Check CFPRev 1	TGCTCAGGTAGTGGTTGTCTG	qRT-PCR
Check CFP Fow 2	ACGACGGCAACTACAAGACC	qRT-PCR
Check CFP Rev 2	GCCTTGATGCCGTTCTTCTG	qRT-PCR
Check GFP Fow 1	CCGACCACTACCAGCAGAAC	qRT-PCR
Check GFP Rev 1	CTCGTTGGGGTCTTTGCTCA	qRT-PCR
Check GFP Fow 2	GCAGAAGAACGGCATCAAGG	qRT-PCR
Check GFP Rev 2	TGCTCAGGTAGTGGTTGTCTG	qRT-PCR
AIR 8094 Mut PAM cbx	GCTTGTGGTTTGTGTTTCAGTGAGAgttAAAC GCTACGGGCAAGATGAGG	Mutagenesis
AIR 8120 Fow PAMCbx_b	GCTTGTGGTTTGTGTTTCAGTGAGAgtttAAA CGCTACGGGCAAGATGAGG	Mutagenesis
AIR 8121 Rev PAMCbx_b	CCTCATCTTGCCCGTAGCGTTTaaacTCTCAC TGAACAACAAACCACAAGC	Mutagenesis
Fp-P10 02851	TTTGAAGACAAGGAGCCCATTTCCATTTCC ATTCTG	MoClo
Rp-P10 02851	TTTGAAGACAACATTggGATGAAAGAAAAA AGACTACCGAG	MoClo
Fp pep1 Lo ovv	TTTGAAGACAAAATGATGACCACACTGGTG CAAACC	MoClo
Rp pep1 mCherry ovv	CATGGCGGTGGCGATCGAGCGCATG	MoClo
Fp mCherry-pep1 ovv	CGGTAGCATGTTTGGCATGCGCTCGATCGC CACCGCCATGGTGAGCAAGGGCGAGG	Gibson assembly
FP pep1GFP AIR	TTTGAAGACAAAATGATGACCACACTGGTG CAAAC	MoClo
Rp pep1 GFP AIR	TTTGAAGACAAAAGCTTACTTGTACAGCTC GTCCATGC	MoClo
Fp-qPCR02851 A	TCGCTCAAGAAGGCTGACTG	qRT-PCR
Rp-qPCR02851 A	AGGTGGAGACAGAGCGAGAT	qRT-PCR

Fp-qPCR02851 B	GCCAAGCAGACTTTTGTCCG	qRT-PCR
Rp-qPCR02851 B	GGTGTTCGGGAAGAAACCAC	qRT-PCR
Fp_see1pLH120	gaagacaccgggaccgatccagcctcATGCTCTTCACCA CCTTCGTTTC	Optogenetics
RpSee1Fluc	cttgatgttcttggcgtcctccatcaattCGTCGTCGGCCCA AATTTATAC	Optogenetics
Fp_see1pNH023 ovv	caccgggaccgatccagcctcATGCTCTTCACCACCTT CGTTTC	Optogenetics
Fow Mut 200	GATATATCATATCGTTCTTTtTCAGCACTTC TTTTGTCAATTT	Mutagenesis
Rev Mut 200	AAATTGACAAAAGAAGTGCTGAaaAAAGAA CGATATGATATATC	Mutagenesis
FP L0 Potef AIR	TTTGAAGACAAGGAGGCATGCCTGCAGGTC GAAATTC	MoClo
Rp Potef L0 AIR	TTTGAAGACAACATTGGGGATCGAATTCCT GCAGCCC	MoClo
Fp Check optogenetic vector blue on/off	gtattggcatcaacattctgaatc	PCR check
Fp PCR 1st position PvuII Ovv	GATTTAGGTGACACTATAGAACTCGAGCAG AGCGACTCTTTGGCCTCGAA	Gibson assembly
Rp NosT	CATCGATGAATTCTCATGTTTGACAGC	PCR
Fp PCR 2nd position	GATAAGCTGTCAAACATGAGAATTCATCGA TGTGATGCAAGGCCGACTTG	PCR
Rp NosT	CATCGATGAATTCTCATGTTTGACAGC	PCR
Fp PCR 3 position	GATAAGCTGTCAAACATGAGAATTCATCGA TGAAAATGGCTCTGACGAGTCG	PCR
Rp NosT EcoRv ovv	GACTCACTATAGGGAGACCGGCAGATCTGA TCATCGATGAATTCTCATGTTTGACAGC	PCR
Fp Mut Cbx Resist	CTTTTCGCTCTACCGGATGCCttACCATCATGA ACTGCTCCAG	Mutagenesis
Rp Mut Cbx Resist	CTGGAGCAGTTCATGATGGTaaGGCATCGGT AGAGCGAAAAG	Mutagenesis
Fp Multitag const	GCTTTACGAATTCCCATGGGGAG	PCR control
Rp Multitag const	GCTTCAACTGGCGCTCAAATTCC	PCR control
Fp internal Moclo multitag	TCCGCAAGAATTCAAGCTTGGA	PCR control
Rp Internal Moclo multitag	TCCGAGCTCGAATTCTAGTAG	PCR control
Rp from genomic to Moclo	TCCAAGCTTGAATTCTTGCGGAG	PCR control
AIR 8610 FP coolprobe	CATATAACGTTAGAACGTGATTGCA	PCR
AIR8611 Rp coolprobe	AAATGCCTATCGAGGATGTTG	PCR
FP Prom 03065	TTTGAAGACAAGGAGCGGTTTCTGAGCAC CGAGC	MoClo
RP Prom 03065	TTTGAAGACAACATTccCGCGAAATAGGAA AAATGAGGTG	MoClo
Change BPiI 03065 fow	CACAAAGCACAACCAGAAGgCAGCGCTTTC CTTCCGAGG	Mutagenesis
Change BPiI 03065 rev	CCTCGGAAGGAAAGCGCTGcCTTCTGGTTG TGCTTTGTG	Mutagenesis
qPCR FP mCherry New	TCGTTGTGGGAGGTGATGTC	qRT-PCR
qPCR RP mCherry New	TGCTTGATCTCGCCCTTCAG	qRT-PCR
qPCR Fow 2 mCherry	AAGAAAACGATGGGCTGGGA	qRT-PCR
qPCR Rev 2mCherry	TTGACCTCAGCGTCGTAGTG	qRT-PCR
qPCR Fow 3 mCherry	ACTTGAAGCTGTCCTTCCCC	qRT-PCR
qPCR Rev 3 mCherry	TGTAGATGAACTCGCCGTCC	qRT-PCR
qPCR mCherry pep1 F1	GCCCCAGACTCTAACGACC	qRT-PCR
qPCRmCherry pep1 R1	TGAAGCGCATGAACTCCTTGA	qRT-PCR
qPCR mCherry pep1 F2	CCCAGACTCTAACGACCAGGA	qRT-PCR
qPCRmCherry pep1 R2	CTTGAAGCGCATGAACTCCTT	qRT-PCR

qPCR mCherry pep1 F3	CCCAGACTCTAACGACCAGG	qRT-PCR
qPCRmCherry pep1 R3	CCATGTTATCCTCCTCGCCC	qRT-PCR
qPCR pep1 GFP Fow1	CTGCTAGGAGGAATCGGTAGC	qRT-PCR
qPCR pep1 GFP Rev1	GCTGAACTTGTGGCCGTTTA	qRT-PCR
qPCR pep1 GFP Fow2	GGAATCGGTAGCATGTTTGGC	qRT-PCR
qPCR pep1 GFP Rev2	GACACGCTGAACTTGTGGC	qRT-PCR
qPCR pep1 GFP Fow3	GCCTGCTAGGAGGAATCGG	qRT-PCR
qPCR pep1 GFP Rev3	CTTGTGGCCGTTTACGTCC	qRT-PCR
Fp GFP new 1	ACGACTTCTTCAAGTCCGCC	qRT-PCR
Rp GFP new1	TCTTGTAGTTGCCGTCGTCC	qRT-PCR
Fp GFP new 2	CACTACCAGCAGAACACCCC	qRT-PCR
Rp GFP new2	ATGTGATCGCGCTTCTCGTT	qRT-PCR
Fp GFP new 3	GAGCAAAGACCCCAACGAGA	qRT-PCR

**Table S6:** Primers designed and/or primers used in this study.

### 6.10.2 sgRNAs

Name	Sequence	Use
<b>sgRNA 02533</b>	CAAAATTCCATTCTACAACGCTGCAAGT GAGTTGAGCGAGTTTTAGAGCTAGAAA TAGC	Multiplex 6A
<b>sgRNA 02535</b>	TCGATTCCCCGTCGATGCAGATTTTC GAACTTGAAGTGGTTTTAGAGCT AGAAATAGC	Multiplex 6A
<b>sgRNA 02540</b>	TCGATTCCCCGTCGATGCAGTATCA CGTCGCTCGTATCGTTTTAGAGCT AGAAATAGC	Multiplex 6A
<b>sgRNA 11416</b>	TCGATTCCCCGTCGATGCAGTTTCT CTGGCAAAAAGTGC GTTT TAGAGCTAGAAATAGC	Single KO
<b>sgRNA 02533</b>	CAAAATTCCATTCTACAACGCTCTC GCCACTAAATCCAT GTTTTAGAGCTAGAAATAGC	Single KO
<b>sgRNA 02535</b>	CAAAATTCCATTCTACAACGTTCTGA GAAGCGTCTGATGGTTT TAGAGCTAGAAATAGC	Single KO

<b>sgRNA 02537</b>	CAAAATTCCATTCTACAACGTTTGC CACGATGGGTGTCAGTTTTAGAGCT AGAAATAGC	Single KO
<b>sgRNA 11415</b>	CAAAATTCCATTCTACAACGTCAAC TTCTTACATGCCGGGTTTTAGAGCT AGAAATAGC	Single KO
<b>sgRNA 02538</b>	CAAAATTCCATTCTACAACGTACCT GAAACGGCCGGCTTGTTTTAGAGCT AGAAATAGC	Single KO
<b>sgRNA 11415</b>	CAAAATTCCATTCTACAACGCTTCC GTTTCAGCACTCCTGTTTTAGAGCT AGAAATAGC	Single KO
<b>SgRNA 02540</b>	TCGATTCCCCGTCGATGCAG GTATCACGTCGCTCGTATC GTTTTAGAGCTAGAAATAGC	Single KO
<b>sgRNA11417</b>	CAAAATTCCATTCTACAACGAAGCA CTAGGCCTATCGTCGTTTTAGAGCT AGAAATAGC	Single KO
<b>sgRNA 1st complementation</b>	CAAAATTCCATTCTACAACGATGGT ATATAGGCATCGAAGTTTTAGAGCT AGAAATAGC	cluster 6A complementation
<b>sgRNA 2nd complementation</b>	CAAAATTCCATTCTACAACGAGGCG ATGTAGTGACGCTTGGTTTTAGAGC TAGAAATAGC	cluster 6A complementation
<b>sgRNA Cbx</b>	CAAAATTCCATTCTACAACGGTTTG TTGTTTCAGTGAGAGGTTTTAGA	Target UMAG_00844
<b>sgRNA Cbx#2</b>	CAAAATTCCATTCTACAACGAATTG ACAAAAGAAGTGCTGGTTTTAGAG CTAGAAATAGC	Target UMAG_00844



---

<b>sgRNA Cbx#3</b>	CAAAATTCCATTCTACAACGAGGAG CGTCGTCGACTCGAGTTTTAGAGCT AGAAATAGC	Target UMAG_00844
<b>sgRNA PAM Pcas9Cbx</b>	AAGCTAATACGACTCACTATAGAAT TGACAAAAGAAGTGCTGGTTTTAGA GCTAGAAATAGCAAG	Target Pam motif in pCas9Hfi Cbx

---

**Table S7:** sgRNAs designed and/or primers used in this study.

## 6.11 Figure licenses



49 Spadina Ave. Suite 200  
Toronto ON M5V 2J1 Canada  
www.biorender.com

### Confirmation of Publication and Licensing Rights

February 19th, 2023  
Science Suite Inc.

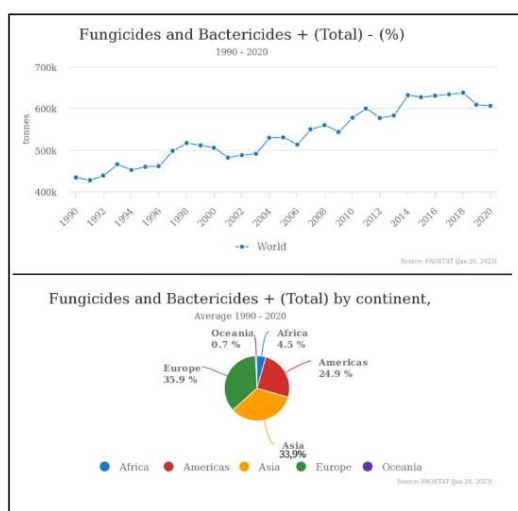
**Subscription:** Student Plan  
**Agreement number:** YJ25167AKX  
**Journal name:** PhD thesis

To whom this may concern,

This document is to confirm that Anna Rybecky has been granted a license to use the BioRender content, including icons, templates and other original artwork, appearing in the attached completed graphic pursuant to BioRender's [Academic License Terms](#). This license permits BioRender content to be sublicensed for use in journal publications.

All rights and ownership of BioRender content are reserved by BioRender. All completed graphics must be accompanied by the following citation: "Created with BioRender.com".

BioRender content included in the completed graphic is not licensed for any commercial uses beyond publication in a journal. For any commercial use of this figure, users may, if allowed, recreate it in BioRender under an Industry BioRender Plan.



For any questions regarding this document, or other questions about publishing with BioRender refer to our [BioRender Publication Guide](#), or contact BioRender Support at [support@biorender.com](mailto:support@biorender.com).



49 Spadina Ave. Suite 200  
Toronto ON M5V 2J1 Canada  
www.biorender.com

## Confirmation of Publication and Licensing Rights

February 19th, 2023  
Science Suite Inc.

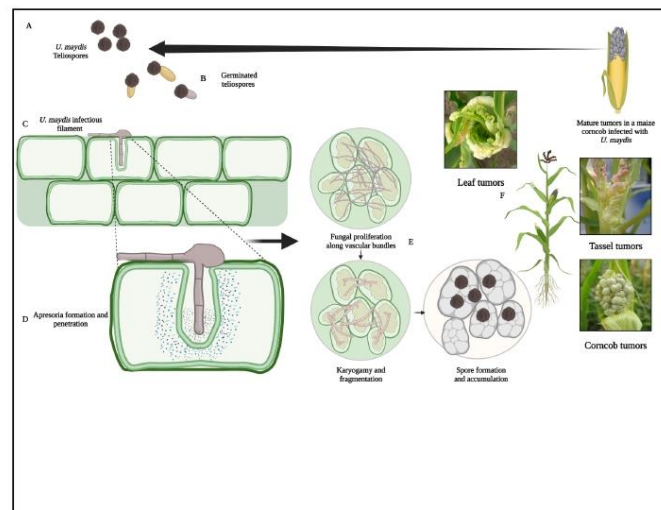
**Subscription:** Student Plan  
**Agreement number:** XW25166ZRB  
**Journal name:** PhD thesis

To whom this may concern,

This document is to confirm that Anna Rybecky has been granted a license to use the BioRender content, including icons, templates and other original artwork, appearing in the attached completed graphic pursuant to BioRender's [Academic License Terms](#). This license permits BioRender content to be sublicensed for use in journal publications.

All rights and ownership of BioRender content are reserved by BioRender. All completed graphics must be accompanied by the following citation: "Created with BioRender.com".

BioRender content included in the completed graphic is not licensed for any commercial uses beyond publication in a journal. For any commercial use of this figure, users may, if allowed, recreate it in BioRender under an Industry BioRender Plan.



For any questions regarding this document, or other questions about publishing with BioRender refer to our [BioRender Publication Guide](#), or contact BioRender Support at [support@biorender.com](mailto:support@biorender.com).



49 Spadina Ave. Suite 200  
Toronto ON M5V 2J1 Canada  
www.biorender.com

## Confirmation of Publication and Licensing Rights

February 19th, 2023  
Science Suite Inc.

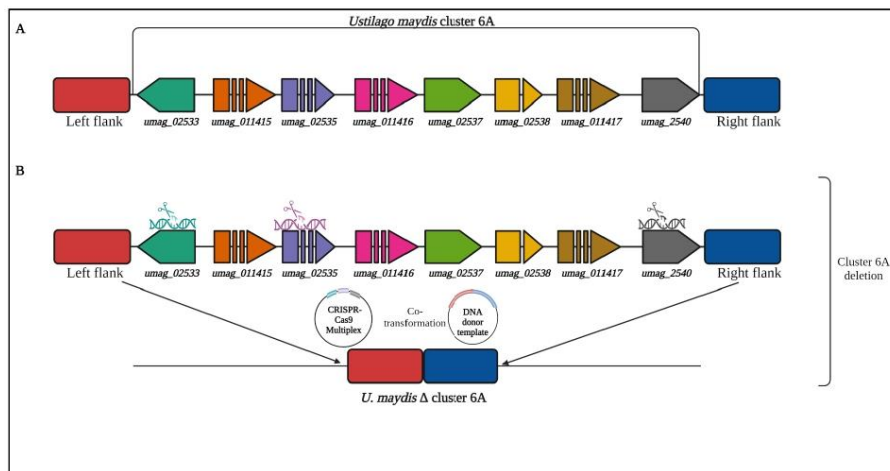
**Subscription:** Student Plan  
**Agreement number:** NY25165P8R  
**Journal name:** PhD thesis

To whom this may concern,

This document is to confirm that Anna Rybecky has been granted a license to use the BioRender content, including icons, templates and other original artwork, appearing in the attached completed graphic pursuant to BioRender's [Academic License Terms](#). This license permits BioRender content to be sublicensed for use in journal publications.

All rights and ownership of BioRender content are reserved by BioRender. All completed graphics must be accompanied by the following citation: "Created with BioRender.com".

BioRender content included in the completed graphic is not licensed for any commercial uses beyond publication in a journal. For any commercial use of this figure, users may, if allowed, recreate it in BioRender under an Industry BioRender Plan.



For any questions regarding this document, or other questions about publishing with BioRender refer to our [BioRender Publication Guide](#), or contact BioRender Support at [support@biorender.com](mailto:support@biorender.com).



49 Spadina Ave. Suite 200  
 Toronto ON M5V 2J1 Canada  
 www.biorender.com

## Confirmation of Publication and Licensing Rights

February 19th, 2023  
 Science Suite Inc.

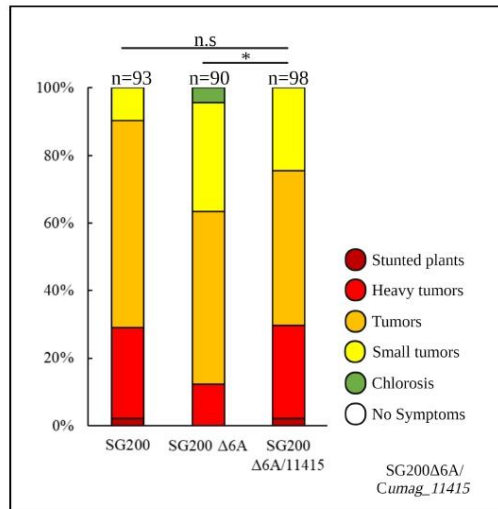
**Subscription:** Student Plan  
**Agreement number:** W125165VZU  
**Journal name:** PhD thesis

To whom this may concern,

This document is to confirm that Anna Rybecky has been granted a license to use the BioRender content, including icons, templates and other original artwork, appearing in the attached completed graphic pursuant to BioRender's [Academic License Terms](#). This license permits BioRender content to be sublicensed for use in journal publications.

All rights and ownership of BioRender content are reserved by BioRender. All completed graphics must be accompanied by the following citation: "Created with BioRender.com".

BioRender content included in the completed graphic is not licensed for any commercial uses beyond publication in a journal. For any commercial use of this figure, users may, if allowed, recreate it in BioRender under an Industry BioRender Plan.



For any questions regarding this document, or other questions about publishing with BioRender refer to our [BioRender Publication Guide](#), or contact BioRender Support at [support@biorender.com](mailto:support@biorender.com).



49 Spadina Ave. Suite 200  
 Toronto ON M5V 2J1 Canada  
 www.biorender.com

## Confirmation of Publication and Licensing Rights

February 19th, 2023  
 Science Suite Inc.

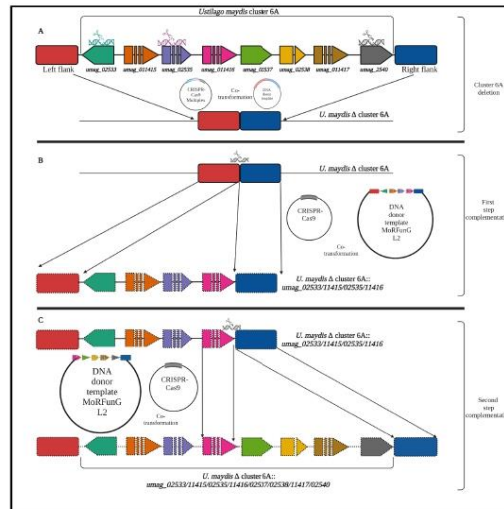
**Subscription:** Student Plan  
**Agreement number:** YO25165RXR  
**Journal name:** PhD thesis

To whom this may concern,

This document is to confirm that Anna Rybecky has been granted a license to use the BioRender content, including icons, templates and other original artwork, appearing in the attached completed graphic pursuant to BioRender's [Academic License Terms](#). This license permits BioRender content to be sublicensed for use in journal publications.

All rights and ownership of BioRender content are reserved by BioRender. All completed graphics must be accompanied by the following citation: "Created with BioRender.com".

BioRender content included in the completed graphic is not licensed for any commercial uses beyond publication in a journal. For any commercial use of this figure, users may, if allowed, recreate it in BioRender under an Industry BioRender Plan.



For any questions regarding this document, or other questions about publishing with BioRender refer to our [BioRender Publication Guide](#), or contact BioRender Support at [support@biorender.com](mailto:support@biorender.com).



49 Spadina Ave. Suite 200  
Toronto ON M5V 2J1 Canada  
www.biorender.com

## Confirmation of Publication and Licensing Rights

February 19th, 2023  
Science Suite Inc.

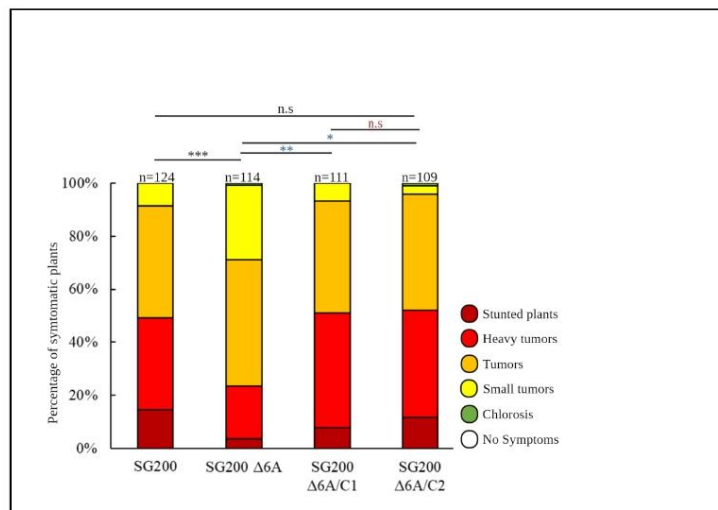
**Subscription:** Student Plan  
**Agreement number:** KB25167M3X  
**Journal name:** PhD thesis

To whom this may concern,

This document is to confirm that Anna Rybecky has been granted a license to use the BioRender content, including icons, templates and other original artwork, appearing in the attached completed graphic pursuant to BioRender's [Academic License Terms](#). This license permits BioRender content to be sublicensed for use in journal publications.

All rights and ownership of BioRender content are reserved by BioRender. All completed graphics must be accompanied by the following citation: "Created with BioRender.com".

BioRender content included in the completed graphic is not licensed for any commercial uses beyond publication in a journal. For any commercial use of this figure, users may, if allowed, recreate it in BioRender under an Industry BioRender Plan.



For any questions regarding this document, or other questions about publishing with BioRender refer to our [BioRender Publication Guide](#), or contact BioRender Support at [support@biorender.com](mailto:support@biorender.com).



49 Spadina Ave. Suite 200  
 Toronto ON M5V 2J1 Canada  
 www.biorender.com

## Confirmation of Publication and Licensing Rights

February 19th, 2023  
 Science Suite Inc.

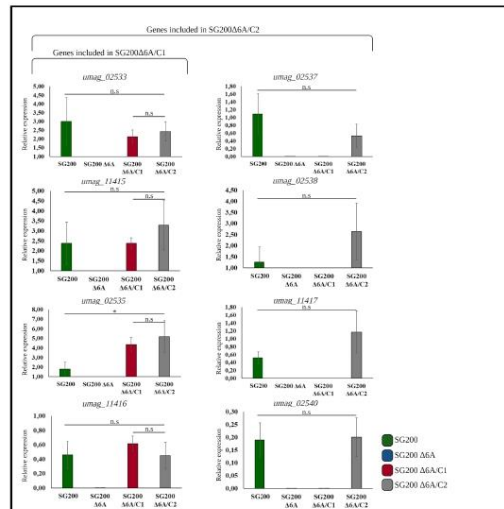
**Subscription:** Student Plan  
**Agreement number:** PZ25166LAV  
**Journal name:** PhD thesis

To whom this may concern,

This document is to confirm that Anna Rybecky has been granted a license to use the BioRender content, including icons, templates and other original artwork, appearing in the attached completed graphic pursuant to BioRender's [Academic License Terms](#). This license permits BioRender content to be sublicensed for use in journal publications.

All rights and ownership of BioRender content are reserved by BioRender. All completed graphics must be accompanied by the following citation: "Created with BioRender.com".

BioRender content included in the completed graphic is not licensed for any commercial uses beyond publication in a journal. For any commercial use of this figure, users may, if allowed, recreate it in BioRender under an Industry BioRender Plan.



For any questions regarding this document, or other questions about publishing with BioRender refer to our [BioRender Publication Guide](#), or contact BioRender Support at [support@biorender.com](mailto:support@biorender.com).





49 Spadina Ave. Suite 200  
 Toronto ON M5V 2J1 Canada  
 www.biorender.com

## Confirmation of Publication and Licensing Rights

February 19th, 2023  
 Science Suite Inc.

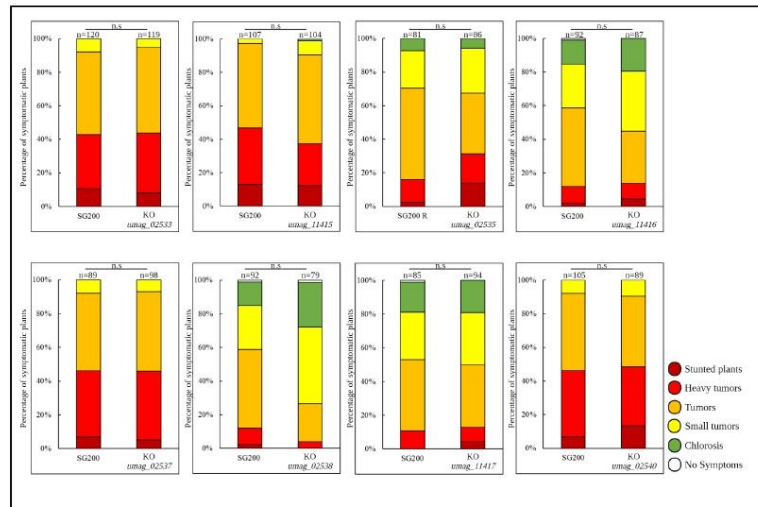
**Subscription:** Student Plan  
**Agreement number:** LJ25165Y8L  
**Journal name:** PhD thesis

To whom this may concern,

This document is to confirm that Anna Rybecky has been granted a license to use the BioRender content, including icons, templates and other original artwork, appearing in the attached completed graphic pursuant to BioRender's [Academic License Terms](#). This license permits BioRender content to be sublicensed for use in journal publications.

All rights and ownership of BioRender content are reserved by BioRender. All completed graphics must be accompanied by the following citation: "Created with BioRender.com".

BioRender content included in the completed graphic is not licensed for any commercial uses beyond publication in a journal. For any commercial use of this figure, users may, if allowed, recreate it in BioRender under an Industry BioRender Plan.



For any questions regarding this document, or other questions about publishing with BioRender refer to our [BioRender Publication Guide](#), or contact BioRender Support at [support@biorender.com](mailto:support@biorender.com).



49 Spadina Ave. Suite 200  
 Toronto ON M5V 2J1 Canada  
 www.biorender.com

## Confirmation of Publication and Licensing Rights

February 19th, 2023  
 Science Suite Inc.

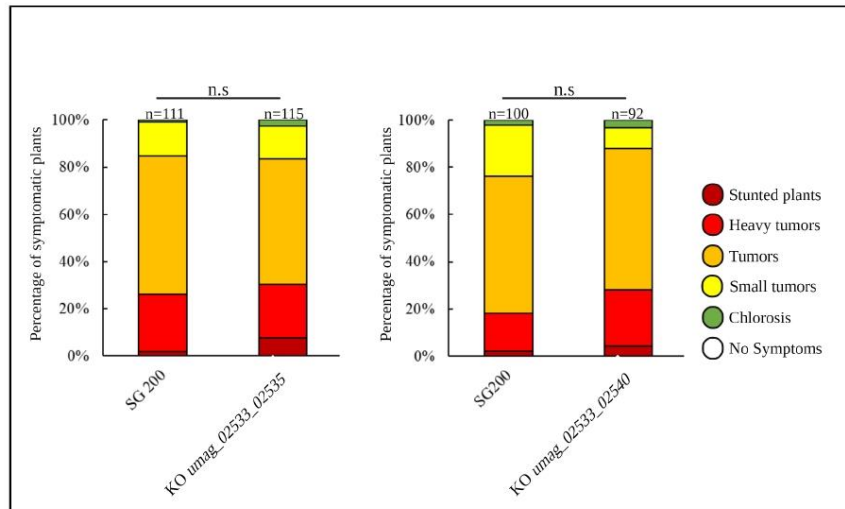
**Subscription:** Student Plan  
**Agreement number:** HS251661DU  
**Journal name:** PhD thesis

To whom this may concern,

This document is to confirm that Anna Rybecky has been granted a license to use the BioRender content, including icons, templates and other original artwork, appearing in the attached completed graphic pursuant to BioRender's [Academic License Terms](#). This license permits BioRender content to be sublicensed for use in journal publications.

All rights and ownership of BioRender content are reserved by BioRender. All completed graphics must be accompanied by the following citation: "Created with BioRender.com".

BioRender content included in the completed graphic is not licensed for any commercial uses beyond publication in a journal. For any commercial use of this figure, users may, if allowed, recreate it in BioRender under an Industry BioRender Plan.



For any questions regarding this document, or other questions about publishing with BioRender refer to our [BioRender Publication Guide](#), or contact BioRender Support at [support@biorender.com](mailto:support@biorender.com).



49 Spadina Ave. Suite 200  
Toronto ON M5V 2J1 Canada  
www.biorender.com

## Confirmation of Publication and Licensing Rights

February 19th, 2023  
Science Suite Inc.

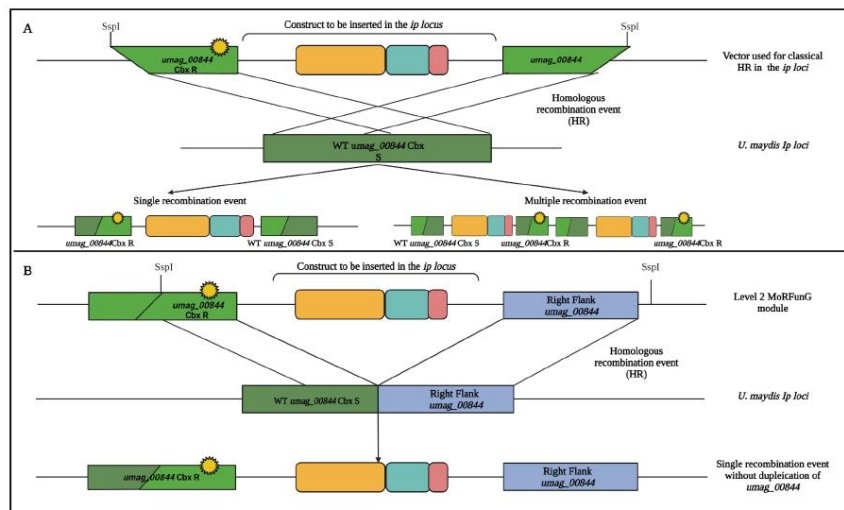
**Subscription:** Student Plan  
**Agreement number:** XU25166HP2  
**Journal name:** PhD thesis

To whom this may concern,

This document is to confirm that Anna Rybecky has been granted a license to use the BioRender content, including icons, templates and other original artwork, appearing in the attached completed graphic pursuant to BioRender's [Academic License Terms](#). This license permits BioRender content to be sublicensed for use in journal publications.

All rights and ownership of BioRender content are reserved by BioRender. All completed graphics must be accompanied by the following citation: "Created with BioRender.com".

BioRender content included in the completed graphic is not licensed for any commercial uses beyond publication in a journal. For any commercial use of this figure, users may, if allowed, recreate it in BioRender under an Industry BioRender Plan.



For any questions regarding this document, or other questions about publishing with BioRender refer to our [BioRender Publication Guide](#), or contact BioRender Support at [support@biorender.com](mailto:support@biorender.com).



49 Spadina Ave. Suite 200  
Toronto ON M5V 2J1 Canada  
www.biorender.com

## Confirmation of Publication and Licensing Rights

February 19th, 2023  
Science Suite Inc.

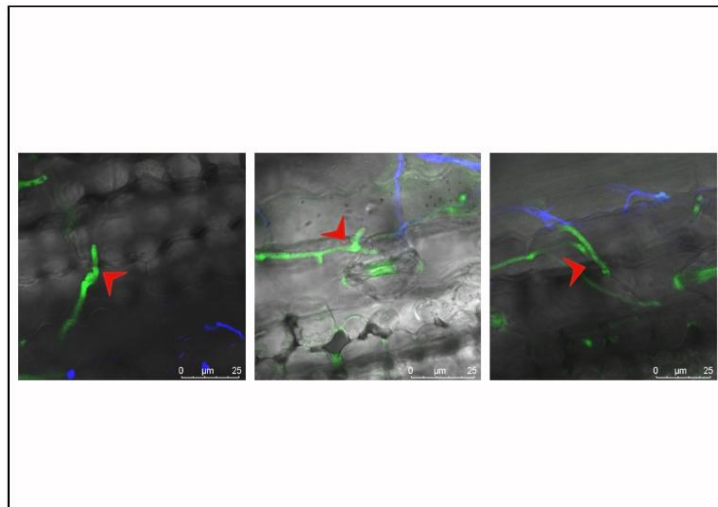
**Subscription:** Student Plan  
**Agreement number:** UN2516EV07  
**Journal name:** PhD thesis

To whom this may concern,

This document is to confirm that Anna Rybecky has been granted a license to use the BioRender content, including icons, templates and other original artwork, appearing in the attached completed graphic pursuant to BioRender's [Academic License Terms](#). This license permits BioRender content to be sublicensed for use in journal publications.

All rights and ownership of BioRender content are reserved by BioRender. All completed graphics must be accompanied by the following citation: "Created with BioRender.com".

BioRender content included in the completed graphic is not licensed for any commercial uses beyond publication in a journal. For any commercial use of this figure, users may, if allowed, recreate it in BioRender under an Industry BioRender Plan.



For any questions regarding this document, or other questions about publishing with BioRender refer to our [BioRender Publication Guide](#), or contact BioRender Support at [support@biorender.com](mailto:support@biorender.com).



49 Spadina Ave. Suite 200  
Toronto ON M5V 2J1 Canada  
www.biorender.com

## Confirmation of Publication and Licensing Rights

February 19th, 2023  
Science Suite Inc.

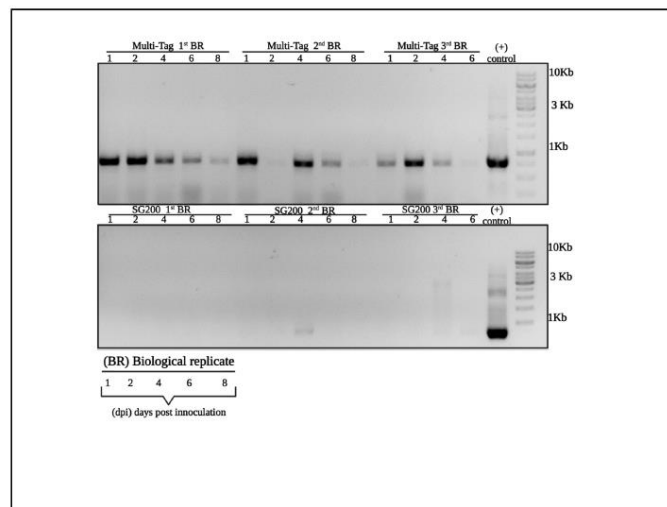
**Subscription:** Student Plan  
**Agreement number:** SF2516824C  
**Journal name:** PhD thesis

To whom this may concern,

This document is to confirm that Anna Rybecky has been granted a license to use the BioRender content, including icons, templates and other original artwork, appearing in the attached completed graphic pursuant to BioRender's [Academic License Terms](#). This license permits BioRender content to be sublicensed for use in journal publications.

All rights and ownership of BioRender content are reserved by BioRender. All completed graphics must be accompanied by the following citation: "Created with BioRender.com".

BioRender content included in the completed graphic is not licensed for any commercial uses beyond publication in a journal. For any commercial use of this figure, users may, if allowed, recreate it in BioRender under an Industry BioRender Plan.



For any questions regarding this document, or other questions about publishing with BioRender refer to our [BioRender Publication Guide](#), or contact BioRender Support at [support@biorender.com](mailto:support@biorender.com).



49 Spadina Ave. Suite 200  
 Toronto ON M5V 2J1 Canada  
 www.biorender.com

## Confirmation of Publication and Licensing Rights

February 19th, 2023  
 Science Suite Inc.

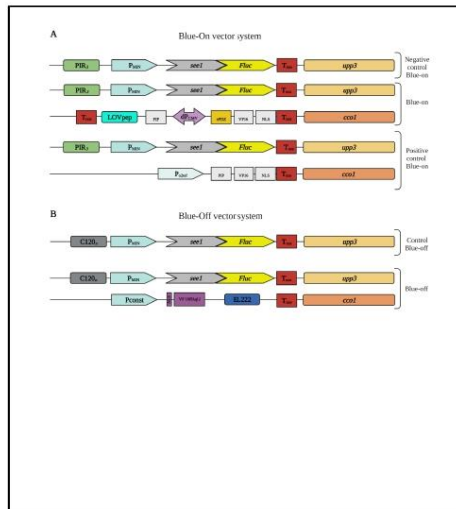
**Subscription:** Student Plan  
**Agreement number:** SQ2516DMF8  
**Journal name:** PhD thesis

To whom this may concern,

This document is to confirm that Anna Rybecky has been granted a license to use the BioRender content, including icons, templates and other original artwork, appearing in the attached completed graphic pursuant to BioRender's [Academic License Terms](#). This license permits BioRender content to be sublicensed for use in journal publications.

All rights and ownership of BioRender content are reserved by BioRender. All completed graphics must be accompanied by the following citation: "Created with BioRender.com".

BioRender content included in the completed graphic is not licensed for any commercial uses beyond publication in a journal. For any commercial use of this figure, users may, if allowed, recreate it in BioRender under an Industry BioRender Plan.



For any questions regarding this document, or other questions about publishing with BioRender refer to our [BioRender Publication Guide](#), or contact BioRender Support at [support@biorender.com](mailto:support@biorender.com).



49 Spadina Ave. Suite 200  
Toronto ON M5V 2J1 Canada  
www.biorender.com

## Confirmation of Publication and Licensing Rights

February 19th, 2023  
Science Suite Inc.

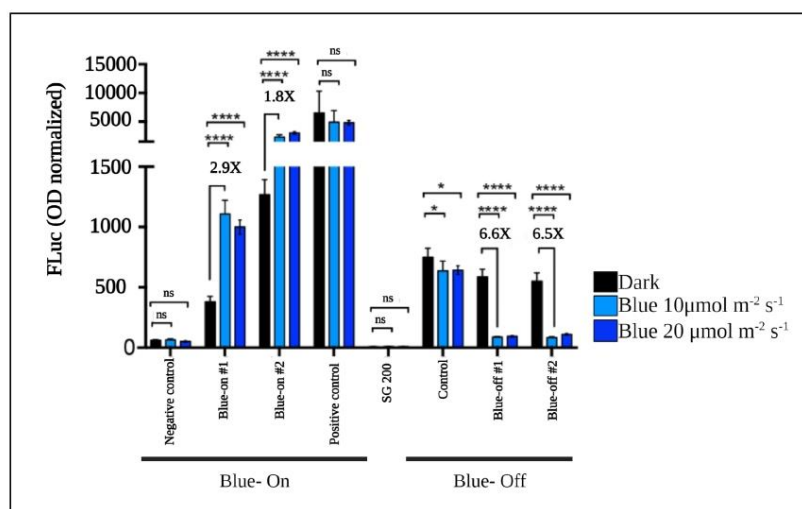
**Subscription:** Student Plan  
**Agreement number:** VF25167DQI  
**Journal name:** PhD thesis

To whom this may concern,

This document is to confirm that Anna Rybecky has been granted a license to use the BioRender content, including icons, templates and other original artwork, appearing in the attached completed graphic pursuant to BioRender's [Academic License Terms](#). This license permits BioRender content to be sublicensed for use in journal publications.

All rights and ownership of BioRender content are reserved by BioRender. All completed graphics must be accompanied by the following citation: "Created with BioRender.com".

BioRender content included in the completed graphic is not licensed for any commercial uses beyond publication in a journal. For any commercial use of this figure, users may, if allowed, recreate it in BioRender under an Industry BioRender Plan.



For any questions regarding this document, or other questions about publishing with BioRender refer to our [BioRender Publication Guide](#), or contact BioRender Support at [support@biorender.com](mailto:support@biorender.com).



49 Spadina Ave. Suite 200  
Toronto ON M5V 2J1 Canada  
www.biorender.com

## Confirmation of Publication and Licensing Rights

February 19th, 2023  
Science Suite Inc.

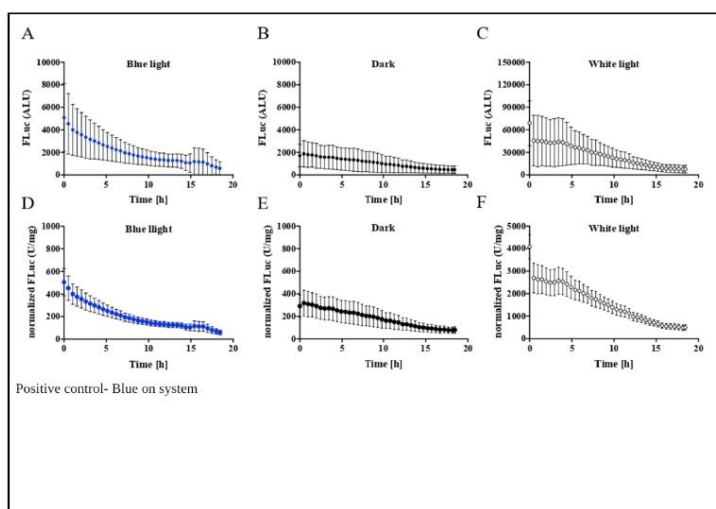
**Subscription:** Student Plan  
**Agreement number:** KW2516761W  
**Journal name:** PhD thesis

To whom this may concern,

This document is to confirm that Anna Rybecky has been granted a license to use the BioRender content, including icons, templates and other original artwork, appearing in the attached completed graphic pursuant to BioRender's [Academic License Terms](#). This license permits BioRender content to be sublicensed for use in journal publications.

All rights and ownership of BioRender content are reserved by BioRender. All completed graphics must be accompanied by the following citation: "Created with BioRender.com".

BioRender content included in the completed graphic is not licensed for any commercial uses beyond publication in a journal. For any commercial use of this figure, users may, if allowed, recreate it in BioRender under an Industry BioRender Plan.



For any questions regarding this document, or other questions about publishing with BioRender refer to our [BioRender Publication Guide](#), or contact BioRender Support at [support@biorender.com](mailto:support@biorender.com).





49 Spadina Ave. Suite 200  
Toronto ON M5V 2J1 Canada  
www.biorender.com

## Confirmation of Publication and Licensing Rights

February 19th, 2023  
Science Suite Inc.

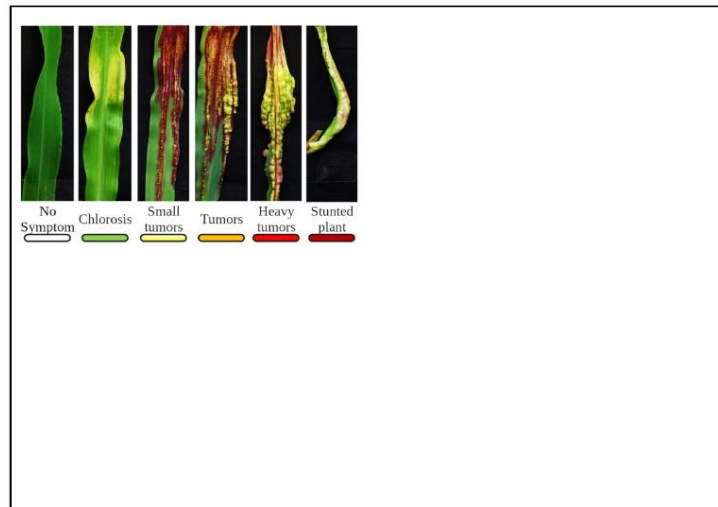
**Subscription:** Student Plan  
**Agreement number:** LF25167HS0  
**Journal name:** PhD thesis

To whom this may concern,

This document is to confirm that Anna Rybecky has been granted a license to use the BioRender content, including icons, templates and other original artwork, appearing in the attached completed graphic pursuant to BioRender's [Academic License Terms](#). This license permits BioRender content to be sublicensed for use in journal publications.

All rights and ownership of BioRender content are reserved by BioRender. All completed graphics must be accompanied by the following citation: "Created with BioRender.com".

BioRender content included in the completed graphic is not licensed for any commercial uses beyond publication in a journal. For any commercial use of this figure, users may, if allowed, recreate it in BioRender under an Industry BioRender Plan.



For any questions regarding this document, or other questions about publishing with BioRender refer to our [BioRender Publication Guide](#), or contact BioRender Support at [support@biorender.com](mailto:support@biorender.com).



49 Spadina Ave. Suite 200  
 Toronto ON M5V 2J1 Canada  
 www.biorender.com

## Confirmation of Publication and Licensing Rights

February 19th, 2023  
 Science Suite Inc.

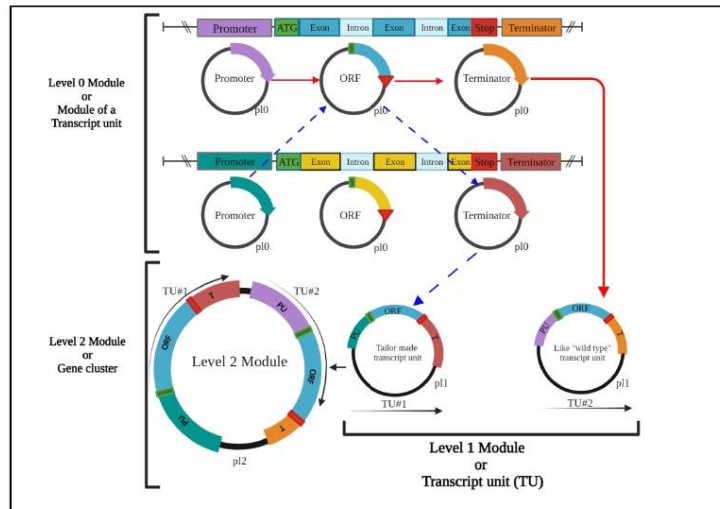
**Subscription:** Student Plan  
**Agreement number:** CZ2516EQCH  
**Journal name:** PhD thesis

To whom this may concern,

This document is to confirm that Anna Rybecky has been granted a license to use the BioRender content, including icons, templates and other original artwork, appearing in the attached completed graphic pursuant to BioRender's [Academic License Terms](#). This license permits BioRender content to be sublicensed for use in journal publications.

All rights and ownership of BioRender content are reserved by BioRender. All completed graphics must be accompanied by the following citation: "Created with BioRender.com".

BioRender content included in the completed graphic is not licensed for any commercial uses beyond publication in a journal. For any commercial use of this figure, users may, if allowed, recreate it in BioRender under an Industry BioRender Plan.



For any questions regarding this document, or other questions about publishing with BioRender refer to our [BioRender Publication Guide](#), or contact BioRender Support at [support@biorender.com](mailto:support@biorender.com).



49 Spadina Ave. Suite 200  
 Toronto ON M5V 2J1 Canada  
 www.biorender.com

## Confirmation of Publication and Licensing Rights

February 19th, 2023  
 Science Suite Inc.

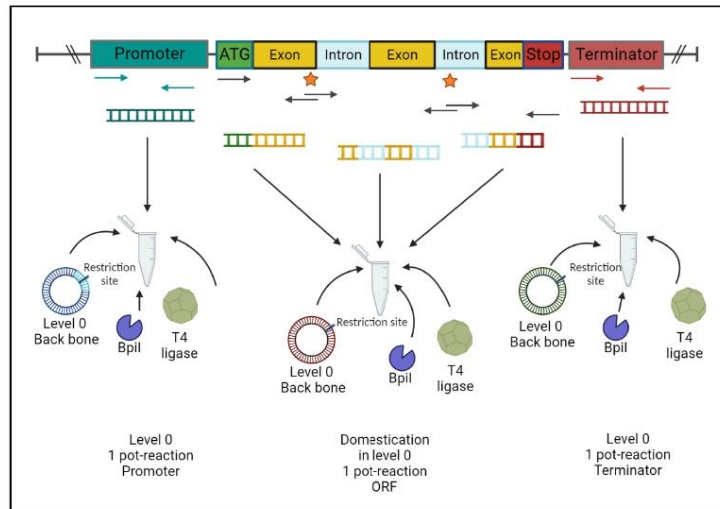
**Subscription:** Student Plan  
**Agreement number:** TA2516F2TP  
**Journal name:** PhD thesis

To whom this may concern,

This document is to confirm that Anna Rybecky has been granted a license to use the BioRender content, including icons, templates and other original artwork, appearing in the attached completed graphic pursuant to BioRender's [Academic License Terms](#). This license permits BioRender content to be sublicensed for use in journal publications.

All rights and ownership of BioRender content are reserved by BioRender. All completed graphics must be accompanied by the following citation: "Created with BioRender.com".

BioRender content included in the completed graphic is not licensed for any commercial uses beyond publication in a journal. For any commercial use of this figure, users may, if allowed, recreate it in BioRender under an Industry BioRender Plan.



For any questions regarding this document, or other questions about publishing with BioRender refer to our [BioRender Publication Guide](#), or contact BioRender Support at [support@biorender.com](mailto:support@biorender.com).



49 Spadina Ave. Suite 200  
Toronto ON M5V 2J1 Canada  
www.biorender.com

## Confirmation of Publication and Licensing Rights

February 19th, 2023  
Science Suite Inc.

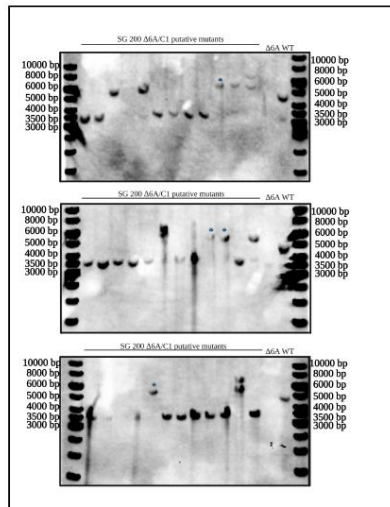
**Subscription:** Student Plan  
**Agreement number:** VP25165LF6  
**Journal name:** PhD thesis

To whom this may concern,

This document is to confirm that Anna Rybecky has been granted a license to use the BioRender content, including icons, templates and other original artwork, appearing in the attached completed graphic pursuant to BioRender's [Academic License Terms](#). This license permits BioRender content to be sublicensed for use in journal publications.

All rights and ownership of BioRender content are reserved by BioRender. All completed graphics must be accompanied by the following citation: "Created with BioRender.com".

BioRender content included in the completed graphic is not licensed for any commercial uses beyond publication in a journal. For any commercial use of this figure, users may, if allowed, recreate it in BioRender under an Industry BioRender Plan.



For any questions regarding this document, or other questions about publishing with BioRender refer to our [BioRender Publication Guide](#), or contact BioRender Support at [support@biorender.com](mailto:support@biorender.com).



49 Spadina Ave. Suite 200  
Toronto ON M5V 2J1 Canada  
www.biorender.com

## Confirmation of Publication and Licensing Rights

February 19th, 2023  
Science Suite Inc.

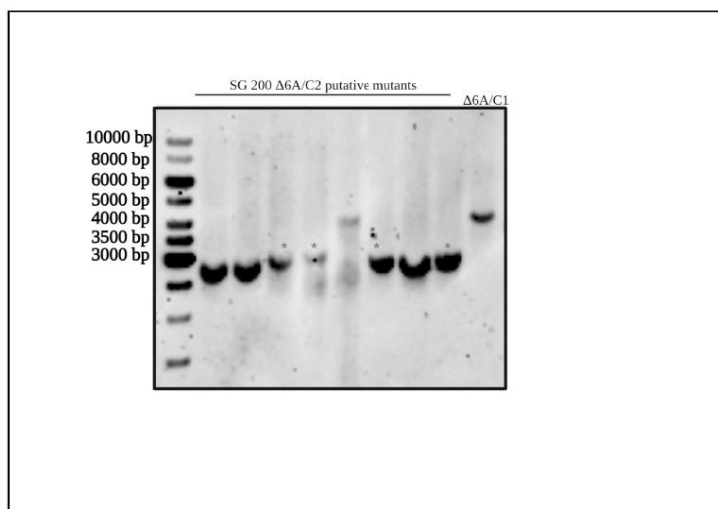
**Subscription:** Student Plan  
**Agreement number:** IE25162KWM  
**Journal name:** Thesis

To whom this may concern,

This document is to confirm that Anna Rybecky has been granted a license to use the BioRender content, including icons, templates and other original artwork, appearing in the attached completed graphic pursuant to BioRender's [Academic License Terms](#). This license permits BioRender content to be sublicensed for use in journal publications.

All rights and ownership of BioRender content are reserved by BioRender. All completed graphics must be accompanied by the following citation: "Created with BioRender.com".

BioRender content included in the completed graphic is not licensed for any commercial uses beyond publication in a journal. For any commercial use of this figure, users may, if allowed, recreate it in BioRender under an Industry BioRender Plan.



For any questions regarding this document, or other questions about publishing with BioRender refer to our [BioRender Publication Guide](#), or contact BioRender Support at [support@biorender.com](mailto:support@biorender.com).



49 Spadina Ave. Suite 200  
Toronto ON M5V 2J1 Canada  
www.biorender.com

## Confirmation of Publication and Licensing Rights

February 19th, 2023  
Science Suite Inc.

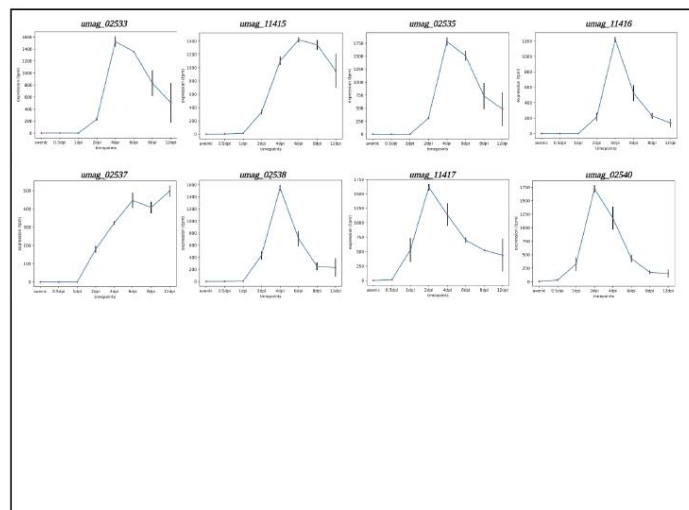
**Subscription:** Student Plan  
**Agreement number:** RO2516LX0U  
**Journal name:** PhD license

To whom this may concern,

This document is to confirm that Anna Rybecky has been granted a license to use the BioRender content, including icons, templates and other original artwork, appearing in the attached completed graphic pursuant to BioRender's [Academic License Terms](#). This license permits BioRender content to be sublicensed for use in journal publications.

All rights and ownership of BioRender content are reserved by BioRender. All completed graphics must be accompanied by the following citation: "Created with BioRender.com".

BioRender content included in the completed graphic is not licensed for any commercial uses beyond publication in a journal. For any commercial use of this figure, users may, if allowed, recreate it in BioRender under an Industry BioRender Plan.



For any questions regarding this document, or other questions about publishing with BioRender refer to our [BioRender Publication Guide](#), or contact BioRender Support at [support@biorender.com](mailto:support@biorender.com).



## Eidesstattliche Erklärung

Hiermit versichere ich an Eides statt, dass ich die vorliegende Dissertation selbstständig und ohne die Benutzung anderer als der angegebenen Hilfsmittel und Literatur angefertigt habe. Alle Stellen, die wörtlich oder sinngemäß aus veröffentlichten und nicht veröffentlichten Werken dem Wortlaut oder dem Sinn nach entnommen wurden, sind als solche kenntlich gemacht. Ich versichere an Eides statt, dass diese Dissertation noch keiner anderen Fakultät oder Universität zur Prüfung vorgelegen hat; dass sie - abgesehen von unten angegebenen Teilpublikationen und eingebundenen Artikeln und Manuskripten - noch nicht veröffentlicht worden ist sowie, dass ich eine Veröffentlichung der Dissertation vor Abschluss der Promotion nicht ohne Genehmigung des Promotionsausschusses vornehmen werde. Die Bestimmungen dieser Ordnung sind mir bekannt. Darüber hinaus erkläre ich hiermit, dass ich die Ordnung zur Sicherung guter wissenschaftlicher Praxis und zum Umgang mit wissenschaftlichem Fehlverhalten der Universität zu Köln gelesen und sie bei der Durchführung der Dissertation zugrundeliegenden Arbeiten und der schriftlich verfassten Dissertation beachtet habe und verpflichte mich hiermit, die dort genannten Vorgaben bei allen wissenschaftlichen Tätigkeiten zu beachten und umzusetzen. Ich versichere, dass die eingereichte elektronische Fassung der eingereichten Druckfassung vollständig entspricht."

Teilpublikationen:

- Bindics, Janos; Khan, Mamoona; Uhse, Simon; Kogelmann, Benjamin; Baggely, Laura; Reumann, Daniel; D. Ingole, Kishor; Stirnberg, Alexandra; Rybecky, Anna; Darino, Martin; Navarrete, Fernando; Doehlemann, Gunther; Djamei, Armin. (2022) "Many ways to TOPLESS – manipulation of plant auxin signaling by a cluster of fungal effectors". New Phytologist. <https://doi.org/10.1111/nph.18315>.

Datum, Name und Unterschrift

22.09.2023.

Anna Ines Hempel geb. Rybecky





## **Delimitations of own contribution**

The results presented in this study were acquired by me independently and without other assistance than stated here. The complete project was directed by Prof. Dr. Guther Doehlemann with a continues feedback about the experiments to be done. People who contributed to experiments done for this dissertation are stated below.

### **Janina Werner**

Experiments that required manipulation of solvents and chemicals that were of risk during my pregnancy, including procedures such as DNA extraction, experiments requiring ethidium bromide, handling of compounds such as hygromycin from July to December 2022. Genetic confirmation for the  $\Delta pep1$  complementation strains as well as the southern blot confirmation of the optogenetic strains.

### **Jan Mülhöfer**

RNA extraction from the  $\Delta pep1$  complementation experiments and multi-tag (Sections 2.3.2 and 2.3.3). Maize sampling and qRT-PCRs in December 2022 for the same experiments.

### **Dr. Jasper Depotter**

Bioinformatic analysis of the effector genes and their expression pattern.

### **Dr. Selma Schurack**

Generation of the KO strains for the double knockouts (*umag\_02533/02535* and *umag\_02533/02540*) and triple KO (*umag\_02533/02535/02540*).

### **Prof. Dr. Matias Zurbriggen**

Plasmids for the optogenetic system (without *see1*) were provided for the group of Prf. Dr. Zurbriggen.

### **Dr. Kun Tang**

Detection of luciferase in infected maize plants at the Heinrich-Heine University in Düsseldorf in the group of Prof. Dr. Matias Zurbriggen. Data process and visualization of optogenetic experiments in maize and in absence of the host.

### **Prof. Dr. Armin Djamei /Dr. Mamoona Kahn**

Generation of the “tips” deletion mutant.

### **Ute Meyer**

Infection of maize plants with the optogenetic *U. maydis* strains in Düsseldorf.

### **Marco Campano**

Introduction of the *otef* promoter and the *FLuc* ORF into the MoRFunG toolkit (level 0) inside the framework of his master module.

## Acknowledgments

In this space I would like to acknowledge all the people that helped me in the completion of my PhD. Undertaking this doctorate was not only a professional learning process for me, but also a personal challenge that included moving to a new country, learning a new language, and unexpectedly living through a pandemic. It was an amazing time, and it would not have been the same without all the people that supported me.

First, I would like to mention the AG Doehlemann as a team. I enjoyed immensely to be part of this group. Every single person in there taught me something that has great value to me.

Many thanks to Prof. Dr. Gunther Doehlemann. Personally, I would like to thank you Gunther for the opportunity to perform this PhD in your group. Thank you for your help and support every time I needed it. Even before I arrived in Germany, you helped me organize an apartment in the Studentenwohnheim on very short notice. You supported me until the very end of the PhD with your advice. Thank you for trusting in all of us in the lab, and for creating a good working atmosphere. I learned a lot from you, and I am immensely thankful for your supervision.

A special thanks to two PhDs that forever will occupy a special place in my memory: Janina and Andrea. Thank you for every little interaction we had, Girls. I am fortuitous to have made friends like you during my PhD.

Thank you, Janina, for being the best lab mate ever, it was a pleasure to share every (work) day in the last three years with you and to share very important personal moments together. You are a great person to work with. Thank you for all the things you did for me in the lab (specially plating my *E.coli* last minute transformations when I left for German course).

A big thanks to Johanna, Rapha, Ute and Jan and Gudrun for being the lifesavers of the Lab, organizing everything around us and making sure that we have everything we need. Jan gets special thanks for his help during my pregnancy. It was a lot of work and you did it great. Gracias Johanna, my South American carnival-companion, I always appreciated having someone with home vibes to talk to.

I want to mention all the postdocs that shared work-life with me: Malaika, Jasper, Giorgios, Sina, Weiliang and Wei for sharing the day-to-day life in the lab and for helping me in with your experience.

I would like to give a special thanks to Bilal, the person with the driest sense of humor and at the same time one of the funniest people I had the pleasure to meet in the lab, thank you for your honest and direct feedback (even though not easy to hear, it was most valuable and welcome).

A big thanks to all the PhD students that I met along the way. The old generation, (Jan, Selma, Kathi) who set up the tone for the beginning of the PhD. My generation of PhDs (Priya, Luyao, Yoon Joo, Maurice, Phillip, Daniel, Namarta, Janina and Andrea), for making every lunch, coffee break, ice, or whatever thing we could do before/during and after corona funny and enjoyable.

To the new generation of PhDs, I am sure you will perpetuate the good traditions and

make your own in the AG Doehlemann. Good luck in this amazing professional step you are taking.

A big thanks to my family. It would have been impossible for me to do anything without their support. Thank you, mom and dad, for giving me the gift of education, thank you for trusting in me without questions asked and for encouraging me to be a better person. Thank you, mom, for coming here at the moment I needed you the most. I could not have asked to have a better mom than you. I love you. Thank you to the two friends I did not have to make myself, but life gifted them to me, Juancho and Kathi, my siblings. Even younger than me, they taught me always to be bmCgetter. I miss you two a lot. I would also like to mention my German family. Ulla and Volker. Since I have been here, they took me as their own daughter and were there for me all the time, I never felt so welcomed, thank you a lot.

The last paragraph of my dissertation goes to the two people that make me the happiest person in this world: Stefan and Madeleine. Stefan, during my PhD you were my biggest support in easy and hard times. Thank you for inspiring me to be the best version of myself, personally and professionally. The patience you always had for me is remarkable, especially when writing this dissertation 24/7 with pregnancy hormones, while preparing everything for our little Madeleine. It couldn't have been easy, but you managed. Little one, thank you for not kicking that hard all the hours that I spent sitting in that chair during your last months in my belly while I was writing this dissertation. Thank you for giving me the most amazing title I could ask for: "your mom". I hope one day you read this and use it as motivation to do whatever you decide that you want to do in life with determination and resilience. I am sure you will 😊.

## *Curriculum vitae*

### **EDUCATION**

**DOCTORAL DEGREE**, Universität zu Köln. 03.2019-06.12.2023

Development of genetic tools for gene manipulation in *Ustilago maydis*.

**DIPLOMA IN MICROBIOLOGY**, Universidad Nacional de Rio Cuarto-Argentina. 2012-2017

Source of inoculum and mechanisms of penetration of species from the *Fusarium graminearum* spp. complex in soybean.

### **WORK EXPERIENCE**

**03.2019-Present:** Doctoral degree in genetics, Universität zu Köln.

**06.2018-08.2018:** Research exchange, Wageningen UR.

Research collaboration in the research project “Integrated and innovative key actions for mycotoxins management in the food and feed chains”.

**2017-2018:** Diploma thesis: Source of inoculum and mechanisms of penetration of species from the *Fusarium graminearum* spp. complex in soybean.

**2017-2018:** Science communication: dissemination of knowledge as a teaching proposal in virology, Universidad Nacional de Rio Cuarto.

**07.2017-03.2018:** Detection and quantification of mycotoxins in cereal grains and derivate products, Universidad Nacional de Rio Cuarto.

**07.2017-03.2018:** Postgraduate laboratory assistant. Isolation of fungal pathogens from cereal crops, morphological identification, mycotoxins production, and isolation.

**07.2017-03.2018:** Laboratory assistant in the Biology Department, Universidad Nacional de Rio Cuarto.

## LANGUAGES

Spanish: mother language.

English: fluent written and spoken.

German: B2 with certificate.

## FURTHER TRAINING

Skills for Project Leaders/Managers by Sabine Lerch M.A., February 08 – 10, 2021.

Conflict Management by Sabine Lerch M.A., June 28 – 29, 2021.

Scientific Writing and Publishing. Nature masterclasses. August 25, 2020.

Good Scientific Conduct: Biases in Science by Prof. Niels Gehring. October – 9, 2020.

## PUBLICATIONS

→**Rybecky, Anna**; Chulze, Sofia; Chiotta, Maria(2018). “Effect of water activity and temperature on growth and trichothecene production by *Fusarium meridionale*”. International Journal of Food Microbiology, 285(February), 69–73. <https://doi.org/10.1016/j.ijfoodmicro.2018.07.028>.

→Bindics, Janos; Khan, Mamoona; Uhse, Simon; Kogelmann, Benjamin; Baggely, Laura; Reumann, Daniel; D. Ingole, Kishor; Stirnberg, Alexandra; **Rybecky, Anna**; Darino, Martin; Navarrete, Fernando; Doehlemann, Gunther; Djamei, Armin. (2022) “Many ways to TOPLESS – manipulation of plant auxin signaling by a cluster of fungal effectors”. New Phytologist. <https://doi.org/10.1111/nph.18315>.

## References

Prof. Dr. Gunther Döhlemann. Universität zu Köln. [g.doehlemann@uni-koeln.de](mailto:g.doehlemann@uni-koeln.de)